MIXED-INTEGER PROGRAMMING MODELS FOR SHALE GAS DEVELOPMENT

Submitted in partial fulfillment of the

requirements for the degree of

DOCTOR OF PHILOSOPHY

at

CARNEGIE MELLON UNIVERSITY

Department of Chemical Engineering

Pittsburgh, Pennsylvania

by

MARKUS G. DROUVEN

B.Sc., Mechanical Engineering, RWTH Aachen University, Germany

M.Sc., Chemical Engineering, RWTH Aachen University, Germany

April 2017

ABSTRACT

Shale gas development is transforming the energy landscape in the United States. Advances in production technologies, notably the dual application of horizontal drilling and hydraulic fracturing, allow the extraction of vast deposits of trapped natural gas that, until recently, were uneconomic to produce. The objective of this work is to develop mixed-integer programming models to support upstream operators in making faster and better decisions that ensure low-cost and responsible natural gas production from shale formations.

We propose a multiperiod mixed-integer nonlinear programming (MINLP) model along with a tailored solution strategy for strategic, quality-sensitive shale gas development planning. The presented model coordinates planning and design decisions to maximize the net present value of a field-wide development project. By performing a lookback analysis based on data from a shale gas producer in the Appalachian Basin, we find that return-to-pad operations are the key to cost-effective shale gas development strategies.

We address impaired water management challenges in active development areas through a multiperiod mixed-integer linear programming (MILP) model. This model is designed to schedule the sequence of fracturing jobs and coordinate impaired- and freshwater deliveries to minimize water management expenses, while simultaneously maximizing revenues from gas sales. Based on the results of a real-world case study, we conclude that rigorous optimization can support upstream operators in cost-effectively

reducing freshwater consumption significantly, while also achieving effective impaired water disposal rates of less than one percent.

We also propose a multiperiod MINLP model and a tailor-designed solution strategy for line pressure optimization in shale gas gathering systems. The presented model determines when prospective wells should be turned in-line, and how the pressure profile within a gathering network needs to be managed to maximize the net present value of a development project. We find that backoff effects associated with turn-in line operations can be mitigated through preventive line pressure manipulations.

Finally, we develop deterministic and stochastic MILP models for refracturing planning. These models are designed to determine whether or not a shale well should be restimulated, and when exactly to refracture it. The stochastic refracturing planning model explicitly considers exogenous price forecast uncertainty and endogenous well performance uncertainty. Our results suggest that refracturing is a promising strategy for combatting the characteristically steep decline curves of shale gas wells.

ACKNOWLEDGMENTS

First, I would like to thank my advisor, Professor Ignacio E. Grossmann, for being a true inspiration and a role model. Over the past four years I have learned a lot about mathematical programming, shale gas development and research in general, but it almost fades in comparison to what Ignacio has taught me about leadership and integrity. I want to thank Ignacio especially for encouraging me to pursue my very own research path and for sharing my excitement for a truly fascinating project. It has been a real pleasure working with Ignacio and I am very grateful to call him my *Doktorvater*.

I would also like to thank my thesis committee members, Meagan Mauter, Diego Cafaro, Nikolaos Sahinidis and Erik Ydstie for their guidance and advice over the past four years.

At CMU, I was fortunate enough to meet countless wonderful people: fellow graduate students, visiting researchers, undergraduate students, staff and faculty members from all over the world. The interactions with all of them shaped my fabulous graduate student experience. In particular, I would like to thank Sumit Mitra, Francisco Trespalacios and Pablo Garcia-Herreros for encouraging me to join the Ph.D. program at CMU. I would also like to thank my fellow group members and all other graduate students in the CAPD for their friendship. I greatly enjoyed our conversations, working with you, learning from you, and all the fun we have had together.

Over the past four years I have had the opportunity to collaborate with Professor Diego Cafaro at INTEC (UNL – CONICET) in Argentina as part of my research. It has been an absolutely wonderful experience working with Diego and I am truly grateful for his guidance and support as a mentor and a friend.

In many ways, the intent of this work is to bridge the gap between the mathematical programming community in academia and decision-makers in the shale industry. Due to some very kind and supportive individuals at EQT, I was given the extraordinary opportunity to apply nearly all of my theoretical contributions to practical problems in industry. Specifically, Lisa Lubchansky and Joseph Sinnott helped me really understand the challenges that decision-makers in the shale industry face and they motivated me to address “real”, i.e., practically relevant problems. I am very grateful for all their support and I truly appreciate their sincere interest in my work.

On a personal note, I want to thank my parents, Brenda and Bernd Drouven, as well as my brother, Carsten Drouven, for their unconditional love and endless support. Even though they were an ocean away, I always felt close to my family and I knew that I could count on them.

Finally, I am eternally grateful to my wife, Svenja Drouven, who has supported me since day one of this venture. This work would not have been possible without you. Thank you for always believing in me, Svenja.

Financial support from the National Science Foundation under grant CBET-1437669, the Scott Energy Institute at Carnegie Mellon University and the Eastman Chemical Company is gratefully appreciated.

TABLE OF CONTENTS

LIST OF FIGURES

LIST OF TABLES

CHAPTER 1

Introduction

Shale gas development is reshaping the United States' energy future. The Energy Information Administration (EIA) assumes that shale gas will account for more than half of all natural gas production in the U.S. by 2040 (EIA, 2014). This is a remarkable development considering the fact that as of 2005 the U.S. were producing hardly any natural gas from shale formations. Given the projected production increase, virtually all stages of the existing natural gas supply chain will need new, expanded, and/or upgraded infrastructure: gas gathering pipelines, processing facilities, transmission pipelines, storage facilities and many more (Goellner, 2012).

Shale gas extraction involves a combination of vertical drilling, horizontal drilling and hydraulic fracturing. Hydraulic fracturing refers to the injection of water into a geologically tight formation under high pressure of up to 70 MPa. This well stimulation creates fractures in the sub-surface reservoir that locally increase the permeability of the formation which allows trapped gas to flow into the wellbore and up to the surface. Hydraulic fracturing requires large amounts of water, oftentimes more than 20 million liters of water per well. In addition, operators add proppant and special additives into the water to keep fractures open and enhance the gas flow into the wellbore. The typical composition of the fracturing fluid is 90% water, 9% proppant and 1% chemical additives.

Nowadays, upstream operators have the ability to drill as many as 40 horizontal wells from a single well pad. Fig. 1.1 illustrates a well pad with eight wells. These multi-well pads allow operators to recover large quantities of gas from a single location while reducing the surface disruption to a minimum. By developing several wells in parallel, operators can also take advantage of economies of scale that lower the unit cost for drilling a single well.

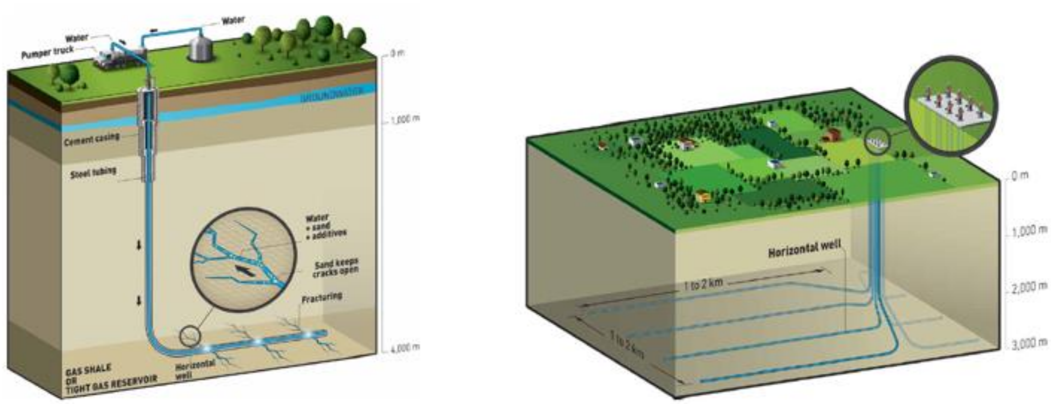

Fig. 1.1: Cross section through a typical shale gas well (left) and a multi-well pad configuration (right)

A single well pad is typically developed as follows: initially, operators construct a temporary well site. For this purpose the pad is levelled, water impoundments and pits are excavated, and an access ramp is built to the site itself. As soon as the pad construction is concluded, a drilling rig is moved on site and assembled. Drilling may take several months depending on how many wells are drilled, how deep they reach vertically, and how far they extend horizontally. Next, completion operations begin, which involve the actual fracturing of the formation. Commonly, the lateral sections of the wells are stimulated in stages which are sealed off temporarily and treated individually. During this development phase the operators need to have large quantities of water stored on site. Once completed, the wells are ready for production and they can be turned “in-line”, which means they are connected to the local gathering system. Today it is expected that shale wells will produce gas for up to 15-30 years.

Fig. 1.2 summarizes the sequence of development operations that need to be completed in order to produce natural gas from a shale reservoir. It is important to recognize that each development operation requires certain resources and is oftentimes characterized by unique challenges. At the same time, shale gas producers can leverage a number of degrees of freedom in each development operation. This flexibility provides the industry with opportunities to adapt to market conditions, price environments and/or environmental challenges. Since the coordination of these development operations lies at the foundation of this thesis, we examine their inherent challenges and opportunities in some more detail.

Fig. 1.2: Sequence of shale gas development operations

For instance, the construction of a gathering system is necessary to deliver natural gas to major demand hubs. This development operation involves the installation of pipelines and compressor stations. Economies of scale play a key role in deciding what size pipelines or compressors are necessary and cost-effective for a particular gathering system. Moreover, pipeline diameters and compressor configurations are standardized in the oil and gas industry. Therefore, upstream operators can only select from a limited set of equipment sizes. On the other hand, shale gas producers oftentimes have ample flexibility in designing and sizing their gathering networks. They can choose from a superstructure of options to maximize the utilization of their equipment.

Building a well pad is another important operation that is part of the development process. Upstream operators need to size these pads carefully, while evaluating how many horizontal wells they choose to drill, and how much water storage capacity they wish to provide for fracturing operations. Constrained acreage positions often prevent producers from placing a large number of wells at a given location.

Vertical and horizontal drilling operations are crucial for the success of any shale gas development project. Upstream operators rely on drilling rigs and crews for this step, and the logistical coordination of both can be very challenging. At the same time, drilling schedules can be rearranged on relatively short notice. This can be exploited to implement return-to-pad operations or “split” pad development.

Hydraulic fracturing of shale wells is directly linked to serious water management challenges. Producers need to make a number of important decisions when performing fracturing jobs: a) whether to use freshwater or impaired water, b) where to obtain the water from, c) how to deliver it on-site (trucking vs. piping), d) which storage options to select (water pits or above-ground storage tanks), e) how to blend different water qualities, and f) whether or not to treat the water prior to reuse. The primary degree of freedom here is the rearrangement of the fracturing schedule. By advancing or delaying certain fracturing operations, operators can maximize recycle rates for impaired water and reduce disposal as much as possible.

Once completed, shale wells are ready to be turned in-line. At this point in the development process, producers mostly struggle with bottlenecks in their gathering systems. Oftentimes the installed pipelines do not have sufficient capacity to take in the produced gas, or the opening of new wells would result in undesirable line pressure increases (leading to production “backoffs”). However, shale companies have the opportunity to adjust their turn in-line schedules to avoid these situations. Active line pressure management gives the industry another degree of freedom to improve the utilization of available gathering capacity.

Even once shale wells are actively producing natural gas, upstream operators continue to face operational challenges. Shale companies are responsible for meeting downstream gas quality specifications when feeding into transmission pipelines. This can be difficult to accomplish since their assets frequently produce a variety of different gas qualities. Producers can either enter into midstream agreements with processing companies to have their gas purified, or they can implement gas blending strategies to avoid processing entirely. It is also important to note that shale wells produce impaired water along with raw natural gas. These water volumes need to be dealt with by either treating, recycling or disposing of them – leading to additional challenges and opportunities for water management.

In this work we also recognize that shale wells can be fractured more than once. These refracturing opportunities allow upstream operators to reinvigorate their assets and thereby improve the economics of mature wells. However, planning refracture treatments of shale wells faces two critical obstacles: price forecast uncertainty and well performance uncertainty. Shale companies want to ensure that the cost of a well restimulation is justified over a wide range of price scenarios. Moreover, they want to account for the possibility that the post-refracturing production performance may not be as good as expected. In light of these uncertainties, optimizing the timing and frequency of refracture treatments presents both an opportunity and a challenge.

Across all development operations described above, it is important to emphasize that shale gas wells are characterized by steep production decline curves. Initially, wells may produce at very high rates of up to 280,000 m^3/day. However, this initial phase is followed by drastic declines as high as 65-85% within the first year. In fact, as seen in Fig. 1.3 some shale wells produce more than half their total estimated ultimate recovery (EUR) within the first year of operation. The initial peak in production is due to the sudden release of trapped gas after the well stimulation. Eventually though, the production decline is driven by pressure depletion and the inherently low permeability of the reservoir.

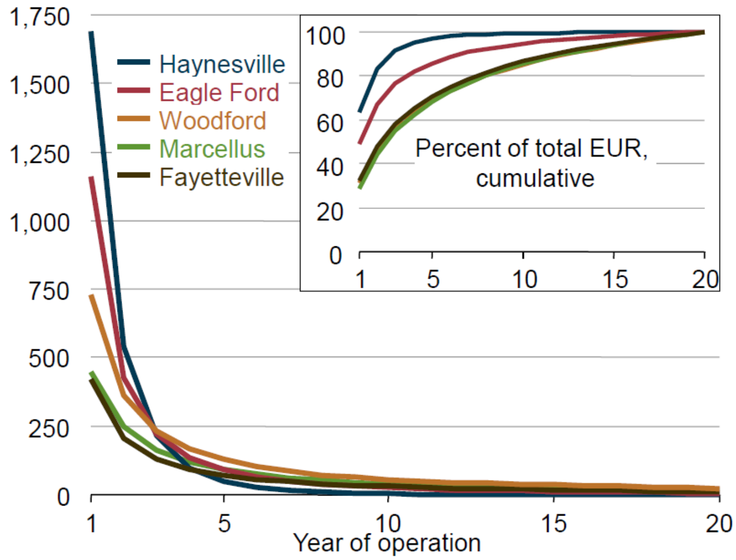

Fig. 1.3: Production profiles in million cubic feet per year for shale gas wells in major U.S. shale plays

1.1 Quality-Sensitive Shale Gas Development Planning

Shale wells produce a variety of different gas qualities. Operators traditionally distinguish between dry gas and wet gas. The primary component of both gas qualities is methane. The key difference between them is that dry gas contains very few so-called natural gas liquids (NGLs). These NGLs are light hydrocarbons that include ethane, propane, pentane, butane and natural gasoline. In wet gas, on the other hand, these components can account for up to 15% of the total gas. In addition, the extracted gas may also contain impurities such as nitrogen, carbon dioxide or hydrogen sulfide. The distinction between different gas qualities is important for a number of reasons.

For one, gas that is delivered to interstate transmission pipelines must be within a specific heating value range (approximately 0.9 kJ/kmol), and it may contain no more than trace components of hydrogen sulfide or carbon dioxide, for example. A gas stream that meets these specifications is considered pipeline-quality gas (Tobin et al., 2006). In order to meet these specifications the produced raw gas generally needs to be treated, i.e., purified at dedicated processing plants. The primary purpose of these processing plants is to separate natural gas liquids and undesirable components from the raw gas stream and return pipeline-quality gas to the operators. This processing service is typically not performed by the operators themselves, but rather provided by midstream processors as an independent, contract based business.

Generally, dry gas – which contains mostly methane (heating value: 889 kJ/mol) – can be marketed as pipeline-quality gas and operators do not have to pay for processing. The NGL components contained in wet gas, however, increase the heating value of the gas mixture significantly above pipeline specifications (ethane: 1,560 kJ/mol, propane: 2,220 kJ/mol, pentane: 3,507 kJ/mol). Therefore, wet gas always has to be purified prior to its delivery which results in non-negligible processing expenses to the upstream operator. The intriguing tradeoff, though, is that the NGLs contained in wet gas oftentimes trade at a premium to pipeline-quality gas, i.e., their sales prices are significantly higher. Hence, the distinction between dry gas and wet gas is very important in terms of the shale gas development problem.

The quality issue of shale gas development is further complicated by the fact that the composition of the extracted gas may vary spatially within a particular gathering system. Therefore, it is oftentimes problematic to classify a development area as distinctively wet or dry. Since individual wells will be feeding different gas qualities into one and the same gathering system at varying production rates, it may be non-obvious for the decision-makers to determine: a) which wells to develop over time with respect to a given gas and liquids price forecast, b) when and how to blend gas streams to meet quality specifications, or c) when and how much processing capacity to procure from a midstream processor. Hence, we postulate in this work that the shale gas development problem is truly quality-sensitive, i.e., the quality of the extracted gas determines decisively which development strategies are profitable for the operator, and which ones may not be feasible.

1.2 Impaired Water Management in Shale Gas Development Areas

It is well-known that shale gas development – which involves hydraulic fracturing – requires significant quantities of water; often several million gallons of water for a single well. However, it is fairly common that a portion of the injected water is recovered after the respective well is turned in-line. The shale industry distinguishes between so-called *flowback water* during the early phase of a well's production life cycle (typically 10-30% of the injected water) and *produced water* further into the lifetime of a well. Both, flowback water and produced water are referred to as *impaired water*, since the water is contaminated. Minerals and organic constituents present in the formation dissolve into the water, creating a brine solution that includes high concentrations of salts, metals, oils, greases, and soluble organic compounds (Gregory et al., 2011). Initially, the shale industry disposed of impaired water in class-II injection wells. However, this practice is both costly and may also have resulted in undesirable, injection-induced seismic activity in certain areas of the U.S. (Folger & Tiemann, 2014).

Rather than disposing of the impaired water, operators nowadays are increasingly re-using the recovered water to reduce the freshwater demand for fracturing new shale gas wells (Mauter et al., 2013). Companies are proactively blending freshwater and impaired water, and thereby reducing the water volumes that have to be sent to disposal wells (Mauter et al., 2014). That said, when oil and gas prices are low and development activity is reduced, the shale industry has fewer opportunities to reuse impaired water. More impaired water has to be disposed of, and consequently operational water management expenses – which operators are trying to decrease in low-price environments – are actually increasing. However, while reduced development activity strains water management operations, it also provides producers with more flexibility to re-organize the timing of fracturing operations. Since companies are drilling, fracturing and completing fewer wells, fracturing jobs may be delayed, interrupted or simply extended without negatively affecting business objectives. In other words, the fracturing schedule becomes a true degree of freedom in low-price environments.

Hence, the objective here is to explore whether and how impaired water disposal expenses can be lowered, while simultaneously taking advantage of any available flexibility in fracturing operations. One option that appears intriguing are so-called return-to-pad operations (Drouven and Grossmann, 2016), i.e., to intentionally delay individual fracturing jobs on a multi-well pad until an increasing amount of impaired water can be reused, rather than sent to disposal. In essence, our goal is to evaluate whether water operations should have a bigger impact on the fracturing schedule, i.e., whether water operations should possibly even “drive” the fracturing schedule.

1.3 Line Pressure Optimization in Shale Gas Gathering Systems

Fig. 1.4 shows a simplified illustration of a typical shale gas gathering system. The gathering network is characterized by a few key elements, namely: existent and prospective well pads, existent and prospective gathering pipelines of varying sizes, one or several compressors and a coupling link to a large-diameter, long-distance transmission pipeline. On every existent pad one or more shale wells actively produce natural gas which is then fed into gathering lines at varying rates over time. The shale gas gathering system itself is typically operated at relatively low pressures, ranging from 50 to 200 psi. Low line pressures allow producers to extract the most gas from their shale wells, since they create a large differential between the reservoir pressure and the wellhead pressure. In other words, as the line pressure in a gathering system increases, overall production typically decreases (Lee & Wattenberger, 1996; Boyan & Ghalambor, 2014). Since the reverse statement is true as well, upstream producers generally prefer to operate their gathering systems at the lowest possible line pressure.

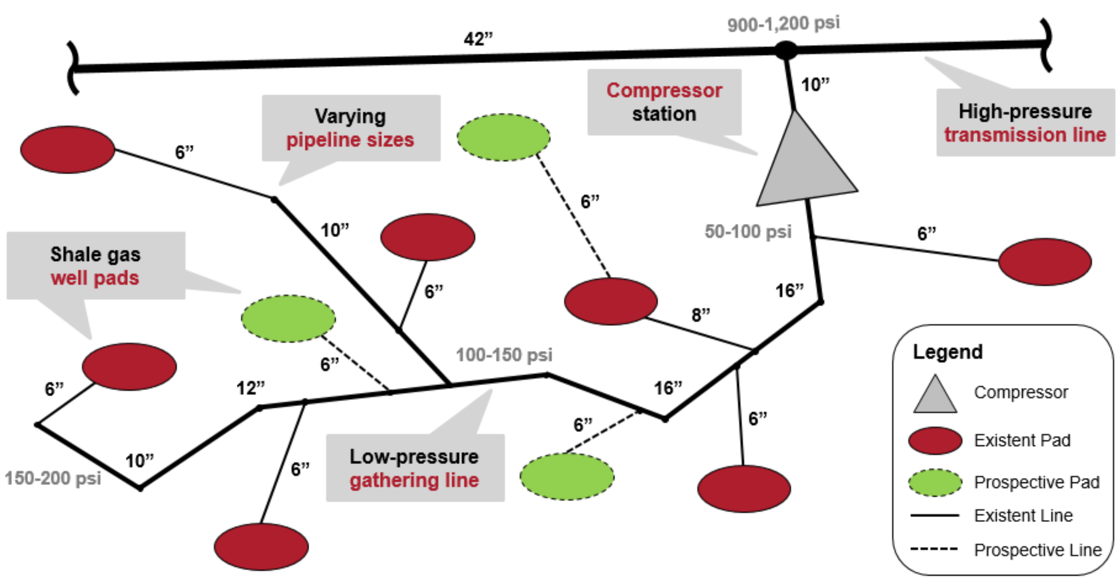

Fig. 1.4: Illustration of a shale gas gathering system with key network elements

However, eventually the produced gas needs to be delivered to a transmission pipeline which will move the gas to major demand hubs. These transmission lines are operated by midstream companies at very high pressures between 900-1,200 psi in order to transport large quantities of natural gas over long distances. Therefore, it is up to the shale gas producer to overcome the pressure differential between the low-pressure gathering system and the high-pressure transmission line. This is typically accomplished through one or several compressors. Compressor stations allow upstream operators to produce the gas at low pressures, on the one hand, but still meet the transmission line's pressure delivery requirements on the other hand. Due to the significant pressure differential that needs to be overcome by the compressor, and the considerable volumes of gas that are processed, compression expenses can be a major cost factor in the operation of shale gas gathering systems. Consequently, upstream producers struggle to balance two conflicting objectives: a) operating their gathering systems at low pressures and thereby increasing gas production, and b) raising line pressures so as to minimize compression expenses.

1.4 Planning of Shale Gas Well Refracture Treatments

Shale wells are known for their rapid production declines. Upstream operators struggle with these characteristically steep production decline curves. For one, they are contractually obligated to providing steady gas deliveries to midstream distributors over time – which is difficult to accomplish given that shale well production rates decline by as much as 65-85% within the first year after turning wells in line. Moreover, as Cafaro and Grossmann (2014) suggest and Drouven and Grossmann (2016) confirm, operators need to maximize the utilization of production and gathering equipment – such as pipelines and compressors – in order to stay profitable. In reality, however, production and gathering equipment is usually sized based on the initially high production rates. This means that within a matter of months shale gas wells feed into oversized pipelines and compressor stations, and equipment utilization drops. Even worse, in order to satisfy contractual gas delivery agreements, operators are forced to open up new wells continuously to honor their obligations, and hence the process is repeated over and over again.

However, it turns out that shale wells can be fractured more than once. And there is increasing evidence suggesting that many mature shale wells still contain large volumes of oil and gas that can be recovered through the process of *refracturing* or *well restimulation* (Fear, 2016). Kotov & Freitag (2015) argue that the steep decline curves in unconventional reservoirs after the initial fracturing operation typically result in 10 percent or less recovery of the available reserves. This implies that refracturing theoretically has the potential to recover 90 percent of remaining hydrocarbons in the shale formation. More importantly, well restimulations could serve as an ideal countermeasure against the inherently steep production declines experienced by shale wells. By reinvigorating the gas production of their assets, operators can improve the utilization of their gathering equipment and might be able to refrain from developing new wells continuously just to make up for production offsets.

1.5 Overview of the Thesis and Research Objectives

In this thesis we propose a number of mixed-integer programming models to address various challenges associated with shale gas development. Fig. 1.5 provides an overview of the topics addressed in this work. We review previous, related work in each chapter individually. However, it should be noted that chapter 2 – which focuses on shale gas blending strategies and the arrangement of midstream processing agreements – is motivated by the work of Cafaro & Grossmann (2014) who present a multiperiod MINLP for strategic shale gas development planning. The model we propose in chapter

3 to optimize water operations compares to the work by Yang et al. (2014), Yang et al. (2015) and Bartholomew & Mauter (2016) who also focus on water management challenges in active development areas. To the best of our knowledge, we are the first to address rigorous line pressure optimization in shale gas gathering systems, as discussed in chapter 5. With the exception of Knudsen & Foss (2013, (2015), previous work in this domain neglects how pressure variations in pipeline networks affect the production of shale wells, individually and collectively. The aforementioned authors primarily focus on developing dynamic shale well reservoir models, whereas our work is intended to support upstream operators in making tactical field development decisions. Finally, it is interesting to note that, to date, the refracturing planning problem we address in chapters 5 and 6 has received fairly little attention in academia. A report by Sharma (2013) is one of the few contributions that discusses the challenges and opportunities of well restimulations in greater detail.

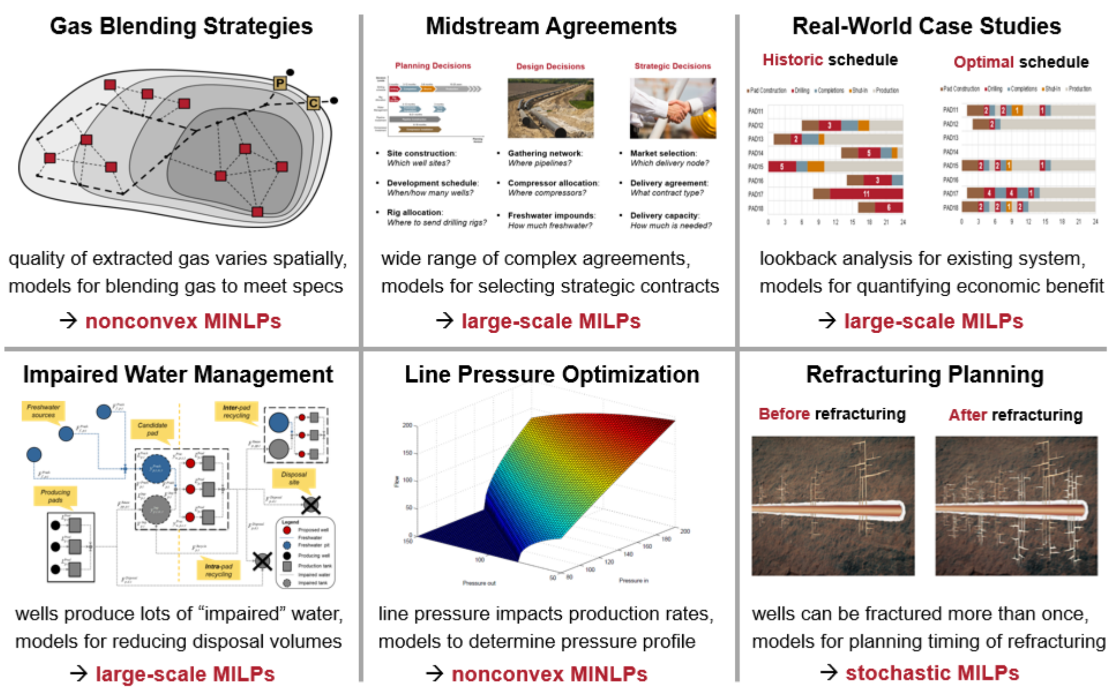

Figure 1.5: Overview of research topics addressed in this thesis

The objectives of this thesis are as follows:

- Develop MINLP models to address the long-term, quality-sensitive shale gas development planning problem and investigate effective solution strategies
- Propose MILP models for water management in shale gas development areas with a particular focus on rearranging fracturing schedules to maximize impaired water recycle rates and minimize water disposal
- Address the line pressure optimization problem in shale gas gathering systems by developing MINLP models and investigating effective solution strategies
- Develop MILP models to address the refracturing planning problem
- Extend the previously proposed models for refracturing planning to account for uncertain price forecasts and uncertain well performance
- Apply the proposed models to real-world case studies and attempt to quantify the economic potential of rigorous, mathematical optimization in this domain

1.5.1 Chapter 2: Planning Models for Strategic Field Development

In chapter 2, we address the long-term, quality-sensitive shale gas development problem. This problem involves planning, design and strategic decisions such as where, when and how many shale gas wells to drill, where to lay out gathering pipelines, as well as which delivery agreements to arrange. Our objective is to use computational models to identify the most profitable shale gas development strategies. For this purpose we propose a large-scale, nonconvex, mixed-integer nonlinear programming (MINLP) model. We rely on generalized disjunctive programming (GDP) to systematically derive the building blocks of this model. Based on a tailor-designed solution strategy we identify near-global solutions to the resulting large-scale problems. Finally, we apply the proposed modeling framework to two case studies based on real data to quantify the value of optimization models for shale gas development. Our results suggest that the proposed models can increase profitability by several million U.S. dollars.

1.5.2 Chapter 3: Scheduling Models for Impaired Water Management

In chapter 3, we present a mixed-integer linear programming model to support upstream operators in identifying optimal strategies for impaired water management in active shale gas development areas. The proposed model is designed to coordinate three key development decisions such that the net present value is maximized: a) the fracturing schedule, b) the water supply sourcing and distribution strategy, and c) the selection of appropriate water storage solutions. We specifically allow return-to-pad operations in the fracturing schedule, and assume that water blending ratios for fracturing jobs are unrestricted, i.e., companies may use only impaired water to meet the completions water demand. Moreover, we explicitly consider the sizing and timing of water storage solutions. By applying the optimization model to a real-world case study, we find that impaired water disposal volumes can be reduced drastically if operators manage to coordinate their fracturing schedule with impaired water availability.

1.5.3 Chapter 4: Scheduling Models for Pressure Management

In chapter 4, we propose a mixed-integer nonlinear programming model to address the line pressure optimization problem for shale gas gathering systems. This model is designed to determine: a) the optimal timing for turning prospective wells in-line, b) the optimal pressure profile within a gathering network, and c) the necessary compression power for delivering produced gas to long-distance transmission lines. We rely on a pressure-normalized decline curve model to quantify how line pressure variations impact the gas production of individual wells. The reservoir model itself is incorporated in a gas transmission optimization framework, which rigorously evaluates pressure drops along pipeline segments throughout the gathering network. Moreover, we explicitly consider compression requirements to lift line pressure from gas gathering levels to setpoints dictated by transmission pipeline companies. Since the resulting optimization models are large-scale, nonlinear and nonconvex, we propose a solution procedure based on an efficient initialization strategy. Finally, we present a detailed case study, and we show that the proposed optimization framework can be used effectively to manage line pressures in shale gas gathering systems by properly scheduling when, and how many, new wells are brought online.

1.5.4 Chapter 5: Deterministic Models for Refracturing Planning

In chapter 5, we propose two optimization models to address the refracturing planning problem. First, we present a continuous-time nonlinear programming (NLP) model based on a novel forecast function that predicts pre- and post-treatment productivity declines. Next, we propose a discrete-time, multi-period mixed-integer linear programming (MILP) model that explicitly accounts for the possibility of multiple refracture treatments over the lifespan of a well. In an attempt to reduce solution times to a minimum, we compare three alternative formulations against each other (big-M formulation, disjunctive formulation using Standard and Compact Hull-Reformulations) and find that the disjunctive models yield the best computational performance. Finally, we apply the proposed MILP model to two case studies to demonstrate how refracturing can increase the expected recovery of a well and improve its profitability by several hundred thousand USD.

1.5.5 Chapter 6: Stochastic Models for Refracturing Planning

In chapter 6, we present a comprehensive optimization framework to address the shale gas well development and refracturing planning problem. At its core, this problem is concerned with, if and when, a new shale gas well should be drilled at a prospective location, and whether or not it should be refractured eventually over its lifespan. Within the optimization framework we account for two major sources of uncertainty: exogenous gas price uncertainty and endogenous well performance uncertainty. We propose a mixed-integer linear, two-stage stochastic programming model embedded in a moving horizon strategy to dynamically solve the practical planning problem under exogenous and endogenous uncertainties. The framework is based on a novel, generalized production estimate function that predicts the gas production over time depending on how often a well has been refractured, and when exactly it was restimulated last. Based on a detailed case study we conclude that early in the life of an active shale well, refracturing makes economic sense even in low-price environments, whereas additional restimulations only appear to be justified if prices are elevated.

1.5.5 Chapter 7: Conclusions and Directions for Future Work

In chapter 7, we summarize the main findings of this thesis and we outline directions for future work. In particular we discuss: a) global optimization strategies for quality-sensitive shale gas development, b) quality-sensitive impaired water management, c) global optimization strategies for line pressure management, d) refracturing opportunities in field-wide development planning, e) multi-stage stochastic programming for refracturing planning, and f) multi-level shale gas development planning.

CHAPTER 2

Mixed-Integer Nonlinear Programming Models for Strategic Shale Gas Development Planning

In this chapter, we present an optimization framework to address the long-term, quality-sensitive shale gas development problem. After presenting a brief literature review on related publications, we summarize the scope of our work in terms of a general problem statement and list the modeling assumptions. In the following section we present the proposed models for the long-term shale gas development problem: one addresses the development project with only one delivery node, and the other model captures the general, multiple delivery node development problem. While the former can be solved to global optimality with an MILP model, the general formulation yields a nonconvex MINLP for which we describe a solution strategy that is designed to identify near-global and optimal solutions. Finally, we apply the models to two case studies that demonstrate and quantify the value of rigorous optimization models for long-term shale gas development planning.

2.1 Literature Review

To date, the long-term shale gas development problem has received little attention in literature. Previous work has been focused primarily on conventional on- and offshore oil and gas field development planning, and the body of literature on this topic is extensive. For instance, Iyer and Grossmann (1998) propose a discrete-time, multi-period mixed-integer linear programming (MILP) model for the design and planning of offshore oilfield infrastructure. The design decisions consider the well drilling schedule, the installation of well and production platforms, and fluid production rates in every time period to maximize the net present value. Van den Heever and Grossmann (2000) address the same problem as Iyer and Grossmann, but include the nonlinear reservoir performance in the formulation, rendering the model a mixed-integer nonlinear programming (MINLP). Van den Heever et al. (2001) extend the oil field development problem by considering complex economic objectives, such as fiscal rules and royalty payments. Goel and Grossmann (2004) consider the offshore gas field development planning problem under uncertainty in reservoir reserves, for which they propose a stochastic programming approach.

Selot et al. (2008) specifically address natural gas production systems with multiple gas qualities. The authors develop a single-period model for a limited planning horizon of one week and consider gas quality specifications at delivery nodes. Tavallali et al. (2013) integrate critical elements of upstream oil production and spatiotemporal subsurface dynamics in a multi-period mathematical programming approach. Knudsen and Foss (2013) consider late-life shale gas wells producing at low erratic rates due to reservoir depletion and liquid loading. The authors present a shale gas well reservoir proxy model and a production scheduling model formulated as a generalized disjunctive program (GDP) that allow for enhanced gas production through cyclic shut-in based production strategies. In order to address field-wide multi-pad shale gas systems Knudsen et al. (2014a) propose a Lagrangean relaxation based decomposition scheme to deal with the dimensionality of the resulting large-scale MILPs. Furthermore, Knudsen et al. (2014b) make use of the proposed well scheduling models to argue that shale gas wells could be used for natural gas supply in electric power plants. Yang et al. (2014) focus on optimization models for shale gas water management. Given an uncertain water availability the authors propose a two-stage stochastic MILP model based on the State-Task Network (STN) representation to minimize the expected water related expenses for transportation, treatment, storage and disposal, while accounting for natural gas sales revenues. Also, Yang et al. (2015) extended their modeling framework to optimize longer-term investment decisions using a deterministic MILP model for determining the location and capacity of water impoundments, piping options, treatment technologies and facility locations, as well as the optimal fracturing schedule.

To the best of our knowledge, Cafaro and Grossmann (2014) are the first to have addressed the long-term shale gas development problem from a strategic perspective. The authors propose a large-scale, nonconvex MINLP model to identify the optimal shale gas supply chain. In the proposed model, nonlinearities arise from concave power law expressions to represent economies of scale. A major restriction is that the shale gas composition is assumed to be independent of well pad locations. Recently, Gao and You (2015) examine the well-to-wire life cycle of electricity generated from shale gas. In this context, the authors present a multi-objective, nonconvex MINLP model to optimize the design and operation of shale gas supply chain networks considering economic and environmental factors.

The models proposed in this work are important extensions of the previous work by Cafaro and Grossmann (2014). The following paragraphs summarize the major new developments.

1) We present a novel superstructure for the shale gas development problem that is motivated by real-world gathering systems. This superstructure captures the distinctive “tree”-structure of typical gas gathering systems. These systems are characterized by trunk lines that “branch” out into the development area and eventually “ramify” to the well pads through a tight grid of flow pipelines. In addition, the superstructure explicitly distinguishes between different delivery options in real-world shale gas development areas, namely processing sales routes and direct delivery sales arcs.

2) As part of the shale gas development problem upstream operators need to size gathering pipelines and transmission compressors. Oftentimes the corresponding design variables are treated as continuous decision variables to simplify the synthesis problem. In this work we consider discrete sizes of pipeline diameters and compressors, which allows us to use mixed-integer linear constraints for equipment sizing purposes. More importantly, by restricting the design variables to discrete values, we can capture economies of scale without dealing with continuous concave cost functions.

3) In this work we also extend the scope of the shale gas development problem to explicitly consider strategic development decisions, which to the best of our knowledge have not been addressed before. The aforementioned strategic decisions include: a) the selection of delivery nodes, b) the arrangement of delivery agreements, and c) the procurement of delivery capacity. These downstream decisions have a major impact on the upstream development of a particular shale gas gathering system and add to the complexity of the overall development problem.

4) Lastly, we specifically address the general shale gas development problem with multiple delivery nodes while explicitly considering spatial gas composition variations.

These composition variations are common in real-world gas gathering systems and complicate shale gas development in practice. On the one hand, upstream operators target different gas qualities depending on prevailing price forecasts. On the other hand, the operators need to ensure that their gas deliveries satisfy gas quality specifications at the delivery nodes. The consideration of spatial gas quality variations within multiple delivery node gathering systems yields a nonconvex MINLP for which we propose a tailor-designed solution strategy.

2.2 General Problem Statement

The problem addressed in this chaper can be stated as follows. Within a potential shale gas development area as depicted in Fig. 2.1, an upstream operator has identified a set of candidate wells pads from which shale gas may or may not be extracted. Long-term production and gas quality forecasts are given for every candidate pad. To extract the gas the operator can develop, i.e., drill and fracture, a limited number of wells at every pad. For the purpose of development, a finite number of drilling rigs and completion crews are available to the operator. Ultimately, the operator wishes to sell extracted gas at a set of downstream delivery nodes, which are typically located along interstate transmission pipelines. For this purpose, a gathering system superstructure has been identified. This superstructure specifies all feasible and competitive options for laying out gathering pipelines to connect candidate well pads to the given set of delivery nodes. In addition, the superstructure indicates candidate locations for compressor stations, as well as the location of existing processing plants within reach of the gathering network. Finally, the superstructure also reveals available freshwater sources within and outside of the development area (note that in general the proposed superstructure may also include existing well pads, pipelines, and compressor stations).

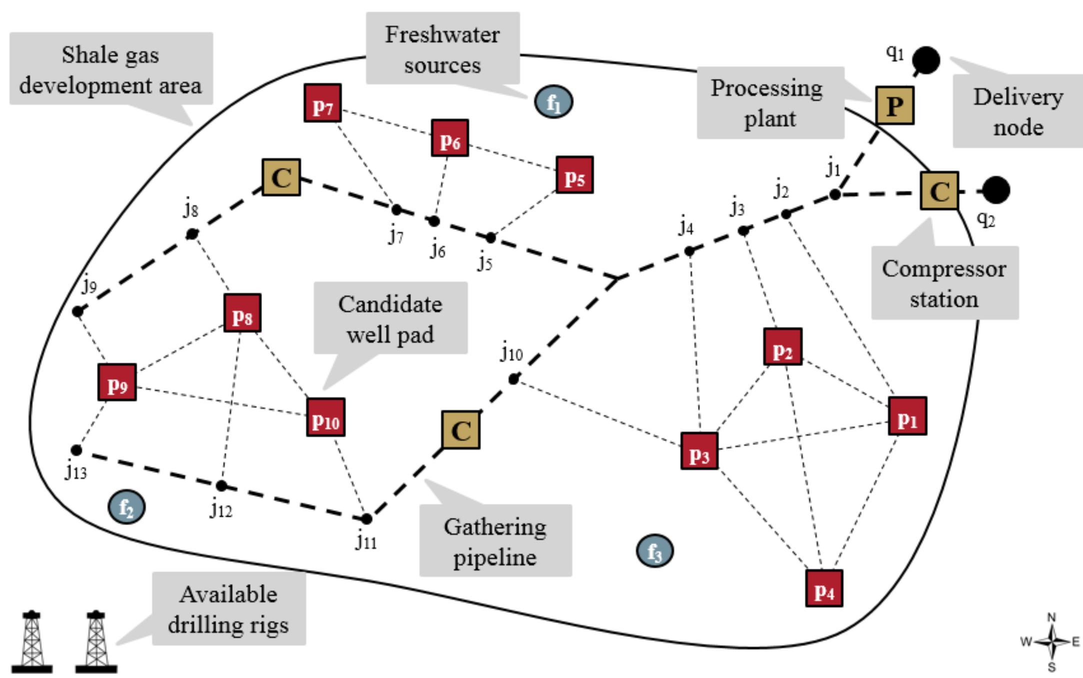

Fig. 2.1 Proposed shale gas development superstructure

The long-term shale gas development problem involves planning, design and strategic decisions. In terms of planning decisions the operator needs to decide: a) where and when to construct well pads, b) where, when and how many wells to drill at every candidate well pad, c) whether selected wells should be shut-in and if so for how long, d) how to allocate drilling rigs and completion crews over time, and e) how much freshwater to obtain from the available set of water sources. The design decisions involve: a) where to lay out gathering pipelines, b) what size pipelines to install, c) where to construct compressor stations, and d) how much compression power to provide. Finally, we consider strategic decisions that include: a) the selection of preferred downstream delivery nodes, b) the arrangement of delivery agreements, and c) the procurement of take-away capacity. The upstream operator's objective is to determine the optimal development strategy by making the right planning, design and strategic decisions such that the net present value is maximized for an extended planning horizon.

2.3 Novel Superstructure

The novel superstructure that we rely on in this work is motivated by real-world shale gas gathering systems. As depicted in Fig. 2.1 this superstructure consists of a given set of candidate well pads $p \in \mathcal{P}$ that are connected to a potential gathering system through candidate pipelines, i.e., the dashed lines in Fig. 2.1 represent alternative, feasible options for laying out pipelines in the development area. The individual pipeline segments are distinguished by the purpose they serve in the network. *Well pipelines* connect neighboring well pads with each other along *well arcs* $(p, \hat{p}) \in \mathcal{PPA}$. These connections are very common in practice since several well pads are often clustered in certain areas of a gathering system. *Flow pipelines* originate at the well pads $p \in \mathcal{P}$ and lead to junctions $j \in \mathcal{J}$ in the gathering system along *flow arcs* $(p, j) \in \mathcal{PJA}$. The candidate junctions are interconnected through so-called *gathering pipelines* along *gathering arcs* $(j, \hat{j}) \in \mathcal{JJA}$. These gathering pipelines reach far into a development area and collect all the extracted gas within a particular gathering system. Typically, all the gas that is gathered within a regional development area is fed to a network hub that serves as a *splitting node* within a particular gathering system. In Fig. 2.1 the node $j_1 \in \mathcal{J}$ serves as such an intermediate splitting node. Here, the gas flows can be directed to one or more *delivery nodes* $q \in \mathcal{Q}$ along *delivery arcs* $(j, q) \in \mathcal{JQA}$. These delivery nodes are typically located along interstate transmission pipelines that gather extracted gas from multiple development areas within states or national regions and transmit it to major gas consuming hubs throughout the nation.

In terms of delivery arcs we differentiate between two particular sales options in this work: *processing sales routes* $(j,q) \in \mathcal{PSR}$ and *direct sales routes* $(j,q) \in \mathcal{DSR}$. By default, gas that is extracted from unconventional reservoirs needs to be purified before it can be sold to transmission pipelines. For this purpose, operators will generally deliver extracted raw gas to processing plants. These processing plants then separate natural gas liquids and undesirable components from the gas stream and return pipeline-quality gas to the upstream operators. Direct sales routes, on the other hand, allow operators to sell the extracted raw gas directly to transmission pipelines without intermediate processing. However, in order to qualify for direct deliveries, the gas must meet strict quality specifications and the operators are responsible for compressing the gas prior to its delivery.

2.4 Modeling Assumptions

The major assumptions in this work are:

1) The planning horizon is discretized into a set of time periods, i.e., commonly months or annual quarters. A long-term natural gas and NGLs price forecast is given for the entire planning horizon.

2) Shale gas is a mixture of ideal gases. However, the composition of the extracted shale gas may vary spatially within the development area. It is assumed that the composition is known at every candidate well pad.

3) Long-term production forecasts, i.e., static type-curves, are available for all candidate well pads. Due to leasing and permitting restrictions, upstream operators can only drill

a limited number of wells at candidate well pads at any point in time. In addition, due to technological constraints and space limitations, no more than a maximum number of total wells can be drilled at every candidate well pad. The layout of the individual wells at candidate well pads (total vertical depth, lateral length, number of stages, etc.) is assumed to be fixed in advance depending on how many wells are to be drilled. Finally, freshwater demand for hydraulic fracturing is a given total volume for every well.

4) Flow directions within the proposed pipeline superstructure are specified in advance. Wellhead outlet pressures as well as compressor suction and discharge pressures are fixed. As such fixed pressure drops are assumed throughout the gathering system. Pipelines are sized based on a given gas velocity and compression power is determined for a fixed pressure ratio.

5) Investment costs related to well development, pipeline constructions, and compressor installations are subject to economies of scale. No uncertainty is assumed in any model parameters.

2.5 Model Formulations

In this section we describe the proposed mixed-integer programming models for the multi-period, long-term shale gas development problem. We distinguish between two variations of the development problem in this work:

1) The *single delivery node* development problem: the decision-maker is restricted to choose just one delivery node among a given set of candidate take-away options.

2) The *multiple delivery node* development problem: the extracted gas may be sent to several delivery nodes, i.e., “splitting” is explicitly permitted.

Fig. 2.2 shows a comparison of the two different problems. The key distinction between them is that in the single delivery node problem (left) all flows converge to no more than one delivery node, whereas the multiple delivery node problem (right) allows the gas to be directed to more than one sales point. The differences are most visible at the splitting node (highlighted in orange in Fig. 2.2).

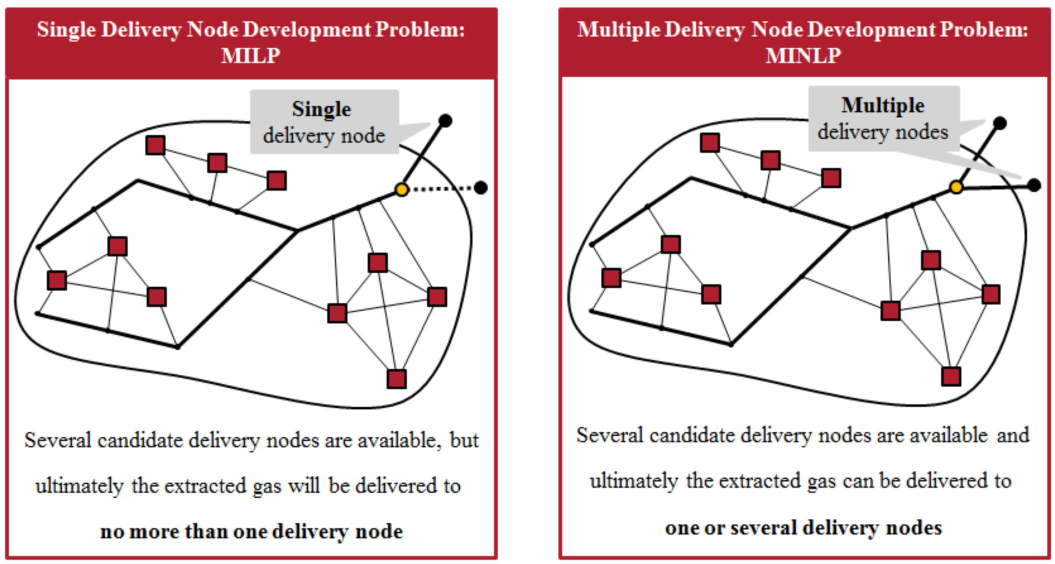

Fig. 2.2: Comparison of the single delivery problem (left) and the multiple delivery node problem (right)

We address the single delivery node problem first and show that it can be formulated as a mixed-integer linear program (MILP), which can therefore be solved to global optimality. Thereafter, we extend the proposed model to capture the more general multiple delivery node problem which involves a large number of bilinear terms that render the optimization problem a nonconvex mixed-integer nonlinear program (MINLP) for which a method is proposed that yields near optimal solutions.

2.5.1 Model Formulation: Single Delivery Node Problem

In this section we describe the set of constraints for the single delivery node development problem.

Production constraints

To determine how many horizontal wells $n \in \mathcal{N}$ should be developed at every candidate pad $p \in \mathcal{CP}$ in any time period $t \in \mathcal{T}$ we introduce the binary decision variable $y_{n,p,t}^{DRILL}$. Since the development process involves drilling, fracturing and completions operations, it will generally take several months after the beginning of drilling operations until the wells have been completed and are ready for production. Hence, we define the parameter τ_n^{WD} as the development lead time that increases with the number of wells being developed in parallel. This parameter allows us to formulate Eq. (2.1), which states that the number of wells that have been completed at a pad $p \in \mathcal{CP}$ in time period $t \in \mathcal{T}$, represented by the integer variable $NWD_{p,t}$, depends on how many wells were drilled $t - \tau_n^{WD}$ time periods in advance, denoted by the binary variable $y_{n,p,t-\tau_n^{WD}}^{DRILL}$. It is important to note here that the number of wells $n \in \mathcal{N}_0$ that can be drilled at a particular pad location includes the *zero-element* n_0. Hence, the enforced multiple-choice constraint (2.2) can be satisfied even when no wells are drilled.

$$NWD_{p,t} = \sum_{n \in \mathcal{N}_0} n \cdot y_{n,p,t-\tau_n^{WD}}^{DRILL} \qquad \forall p \in \mathcal{CP}, t \in \mathcal{T} \tag{2.1}$$

$$\sum_{n \in \mathcal{N}_0} y_{n,p,t}^{DRILL} = 1 \qquad \forall p \in \mathcal{CP}, t \in \mathcal{T} \tag{2.2}$$

In practice the drilling and fracturing processes require different resources and cannot be performed simultaneously. During the drilling phase, operators rely on tophole and horizontal rigs to drill the vertical and lateral sections of the well. In preparation of the fracturing process, however, these rigs need to be moved off the pad to free up space for roughly 12-18 tractor trailers equipped with high-power water pumps that are eventually circled around each wellhead to fracture the wells. Hence, due to space limitations, wells cannot be fractured while other wells are still being drilled and vice versa. This practical constraint is expressed in Eq. (2.3) which states that as long any number of wells that have been drilled, have not been completed yet – captured by the development lead time parameter τ_n^{WD} – no new set of wells can be drilled.

$$\sum_{n \in \mathcal{N}} \sum_{\tau = t - \tau_n^{WD} + 1}^{t-1} y_{n,p,\tau}^{DRILL} \leq 1 \qquad \forall p \in \mathcal{CP}, t \in \mathcal{T} \tag{2.3}$$

The total number of wells that can be drilled and developed at every candidate location throughout the planning horizon is generally constrained by the operator's acreage position, permitting constraints, and/or lease commencement and expiration dates. In the proposed formulation the parameter $n_{p,t}^{max}$ in Eq. (2.4) limits how many wells can be developed at every candidate pad location at any point in time.

$$\sum_{\tau=1}^{t} \sum_{n \in \mathcal{N}} n \cdot y_{n,p,\tau}^{DRILL} \leq n_{p,t}^{\max} \qquad \forall p \in \mathcal{CP}, t \in \mathcal{T} \tag{2.4}$$

Upstream operators generally prefer to develop as many wells as possible at a particular well pad to take advantage of economies of scale. To quickly recover their development expenses, the operators will usually turn all completed wells in line as soon as possible, i.e., the extracted gas is fed into the gathering system to downstream delivery nodes. However, given the characteristic shale well production profiles, operators are increasingly exploring the option of keeping a subset of the developed wells shut-in temporarily. The motivation for this strategy is as follows. Initially, shale well production rates are very high, at times up to 280,000 m^3/day. Turning all developed wells in line at the same time requires substantial downstream capacity in terms of pipeline sizes and compression power. Such investments are very costly, i.e., in the range of several million U.S. dollars, and within a matter of months the wells' production rates will decline rapidly, often by as much as 65-85% within the first year after production begin. At this time the previously installed downstream equipment is over-sized and under-utilized. To avoid poor equipment utilization, operators may choose to keep a subset of the developed wells shut-in temporarily and only produce from the remaining set of wells. In Eq. (2.5) we distinguish between the number of wells that have been completed at a particular well pad, $NWD_{p,t}$, and the number of wells that are actively producing, $NWP_{p,t}$, thus allowing for temporary shut-ins.

$$\sum_{\tau=1}^{t} NWP_{p,\tau} \leq \sum_{\tau=1}^{t} NWD_{p,\tau} \qquad \forall p \in \mathcal{CP}, t \in \mathcal{T} \tag{2.5}$$

The implication of Eq. (2.5) is that the number of (active) wells producing raw gas is indeed an additional degree of freedom to the optimization. The optimizer can choose to keep a subset of the developed wells shut-in for any period of time to maximize equipment utilization, i.e., the available pipeline and compressor capacity.

Based on how many wells are producing, we can calculate the amount of gas $F^0_{p,t}$ that can be extracted at every well pad at any point in time. This flow rate is obtained by multiplying the number of wells producing at a particular pad, $NWP_{p,t}$, with the corresponding long-term, static production forecast, i.e., the type-curve parameter $\gamma_{p,t}$.

$$F^0_{p,t} \leq \sum_{\tau=1}^{t-1} NWP_{p,\tau} \cdot \gamma_{p,t-\tau} \qquad \forall p \in \mathcal{CP}, t \in \mathcal{T} \tag{2.6}$$

Since the operator can always choose to choke the wells and produce less gas, Eq. (2.6) is expressed as an inequality constraint. It is important to note, however, that in reality choking leads to a production delay that is not captured by Eq. (2.6). As such, the proposed formulation represents a minor simplification that is justified by the fact that intermediate, temporary shut-ins are fairly rare and they are usually concluded as quickly as possible.

The proposed formulation can easily be extended to account for existing wells that are already feeding into the gathering system at the beginning of the planning horizon. We introduce the set of producing pads $p \in \mathcal{PP}$ to identify pads that have already been turned in line. Based on the forecasted production rate for these well pads, $f^0_{p,t}$, we simply impose the inequality in Eq. (2.7).

$$F^0_{p,t} \le f^0_{p,t} \qquad \forall p \in \mathcal{PP}, t \in \mathcal{T} \tag{2.7}$$

Prior to well development at any candidate pad, a well site needs to be constructed. We introduce a binary decision variable $y^{CON}_{p,t}$ that denotes the beginning of the site construction process. Eq. (2.8) ensures that no well is developed before the construction process with lead time τ^S_p has been completed.

$$y^{DRILL}_{n,p,t} \le \sum_{\tau=1}^{t-\tau^S_p} y^{CON}_{n,p,\tau} \qquad \forall\, \mathrm{n} \in \mathcal{N}, p \in \mathcal{CP}, t \in \mathcal{T} \tag{2.8}$$

Flow balances

Flow balances are imposed at all well pads and gathering junctions within the proposed gathering superstructure. Eq. (2.9) represents the flow balances at all well pads $p \in \mathcal{P}$ – candidate and producing –and involves pad production flow rates $F^0_{p,t}$, flows from and to neighboring well pads $F^{PP}_{p,\hat{p},t}$, as wells as flows from pads to gathering junctions $F^{PJ}_{p,j,t}$. Eq. (2.10) ensures that flows to neighboring well pads $F^{PP}_{p,\hat{p},t}$ are constrained by the actual production rates at the originating pads.

$$F^{0}_{p,t} + \sum_{(\hat{p},p)\in \mathcal{PPA}} F^{PP}_{\hat{p},p,t} = \sum_{(p,\hat{p})\in \mathcal{PPA}} F^{PP}_{p,\hat{p},t} + \sum_{(p,j)\in \mathcal{PJA}} F^{PJ}_{p,j,t} \qquad \forall p \in \mathcal{P}, t \in \mathcal{T} \quad (2.9)$$

$$\sum_{(p,\hat{p})\in \mathcal{PPA}} F^{PP}_{p,\hat{p},t} \le F^{0}_{p,t} \qquad \forall p \in \mathcal{P}, t \in \mathcal{T} \quad (2.10)$$

Eq. (2.11) balances incoming and outgoing flows at gathering junctions $j \in \mathcal{J}$, which includes flows from pads to gathering junctions $F^{PJ}_{p,j,t}$, flows between neighboring junctions $F^{JJ}_{j,\hat{j},t}$, and flows from gathering junctions to delivery nodes $F^{JQ}_{j,q,t}$.

$$\sum_{(p,j)\in \mathcal{PJA}} F^{PJ}_{p,j,t} + \sum_{(\tilde{j},j)\in \mathcal{JJA}} F^{JJ}_{\tilde{j},j,t} = \sum_{(j,\hat{j})\in \mathcal{JJA}} F^{JJ}_{j,\hat{j},t} + \sum_{(j,q)\in \mathcal{JQA}} F^{JQ}_{j,q,t} \qquad \forall j \in \mathcal{J}, t \in \mathcal{T} \quad (2.11)$$

Equipment sizing constraints

The shale gas development problem requires operators to size necessary equipment such as pipelines and compressors. In order to simplify the optimization problem the corresponding design variables are often treated as continuous decision variables[15]. In practice, however, pipelines and compressors are standardized in the oil and gas industry. Hence, we enforce discrete equipment sizes throughout this work, i.e., we assume that only a finite set of pipeline diameters and compressor sizes are commercially available. Moreover, for modeling purposes we take advantage of discrete equipment sizes by systematically deriving disjunctive models based on Generalized Disjunctive Programming (GDP) that generally yield tight continuous relaxations (Grossmann & Trespalacios, 2013). Lastly, in section 2.5.2 Model Formulation:

Objective Function we show that by only considering discrete equipment sizes we can capture economies of scale without explicitly having to introduce nonlinear, concave cost expressions into the objective function. We illustrate the general equipment sizing framework proposed in this work with two examples, namely delivery pipelines and gathering compressors.

Delivery pipelines are intended to connect gathering junctions $j \in \mathcal{J}$ with delivery nodes $q \in \mathcal{Q}$, and they are a crucial part of any shale gas gathering system. Based on the proposed superstructure, the length of candidate delivery pipelines, $l_{j,q}$, is known. Hence, the only remaining degree of freedom for sizing purposes is the pipeline's diameter. The more gas $F_{j,q,t}^{JQ}$ flows through a delivery pipeline segment, the larger the respective pipeline diameter δ_d needs to be to provide the right amount of flow capacity. In this work we size pipelines based on fluid velocity, since pressure drops are relatively small in typical gas gathering systems given that the pipeline segments are relatively short (< 15 km) and the operating pressure is relatively low (< 2.5 MPa). In addition, gas velocity itself is an important design criterion that is commonly used for preliminary sizing purposes. Operators need to bound the maximum gas velocity to reduce noise emissions and prevent pipeline corrosion. Based on a pre-specified, maximum gas velocity, we can calculate a sizing coefficient k^P that allows us to determine the necessary pipeline diameter with sufficient accuracy. Details regarding the calculation of the sizing coefficient k^P are provided in Appendix A: Pipeline Sizing Guidelines.

Within the proposed model we use disjunction (2.12) to size delivery pipelines (we note that all disjunctions in this work are exclusive).

$$\bigvee_{d \in \mathcal{D}_0} \left[\begin{array}{c} Z_{d,j,q,t}^{PIPE} \\ k^P \cdot F_{j,q,t}^{JQ} \leq \left(\delta_{j,q}^0\right)^2 + \delta_d^2 \end{array} \right] \qquad \forall (j,q) \in \mathcal{JQA}, t \in \mathcal{T} \quad (2.12)$$

This disjunction states that at any point in time, a particular pipeline diameter $d \in \mathcal{D}_0$ must be selected along every candidate pipeline segment, i.e., precisely one Boolean variable $Z_{d,j,q,t}^{PIPE}$ has to be true in every time period $t \in \mathcal{T}$ along every arc $(j,q) \in \mathcal{JQA}$. Since the lengths of all candidate arcs are fixed and given, the diameter selection will determine precisely how much flow capacity needs to be available along every candidate pipeline segment $(j,q) \in \mathcal{JQA}$, i.e., how much gas $F_{j,q,t}^{JQ}$ can flow along the respective arc. It is important to note here that the set of commercially available pipeline diameters $d \in \mathcal{D}_0$ explicitly includes the *zero-diameter* d_0. Hence, it is possible to select no flow capacity along an arc which corresponds to the design decision of excluding that arc from the eventual gathering system. In this case no gas may flow along that arc.

It is also important to note that the disjunction (2.12) accounts for pre-installed pipeline capacity $\delta_{j,q}^0$. If a pipeline has already been laid out along a delivery arc $(j,q) \in \mathcal{JQA}$, then the corresponding flow capacity is available and must not be installed. In this sense, the proposed formulation does allow for *looping* of existing pipelines which is the common practice of designing parallel pipeline segments.

Evidently, additional flow capacity along any pipeline segment is only available if a pipeline with the corresponding diameter has been installed previously. Since the construction of a gathering pipeline typically involves several annual quarters, we define the parameter τ^P as the lead time for installing any pipeline segment and we impose the logic constraint (2.13). This constraint states that the flow capacity associated with the Boolean variable $Z_{d,j,q,t}^{PIPE}$ is only available if a pipeline installation was initiated τ^{P} time periods in advance, denoted by the Boolean variable $Y_{d,j,q,t}^{PIPE}$. This Boolean variable in turn incurs the respective capital expenses as expressed in the objective function in section 2.5.2 Model Formulation: Objective Function.

$$\bigvee_{\tau=1}^{t-\tau^{P}} Y_{d,j,q,\tau}^{PIPE} \Leftrightarrow Z_{d,j,q,t}^{PIPE} \qquad \forall d \in \mathcal{D}, (j,q) \in \mathcal{JQA}, t \in \mathcal{T} \qquad (2.13)$$

In general terms, the disjunction (2.12) can be transformed into a set of mixed-integer linear constraints by using either a Big-M (BM) or a Hull-Reformulation (HR). While the HR involves more constraints and variables than the BM, its continuous relaxation is at least as tight as, and generally tighter, than the Big-M. Therefore, we favor the HR. To reformulate disjunction (2.12) we introduce the binary variables $y_{d,j,q,t}^{PIPE}$ and $z_{d,j,q,t}^{PIPE}$ that correspond directly to their counterpart Boolean variables $Y_{d,j,q,t}^{PIPE}$ and $Z_{d,j,q,t}^{PIPE}$. Technically, we would also need to disaggregate the continuous decision variables $F_{j,q,t}^{JQ}$ for every disjunctive term. However, in this particular case we can derive the *compact* Hull Reformulation of disjunction (2.12), which does not require disaggregated variables as shown in Appendix B: Compact Hull Reformulation. The result is shown in Eq. (2.14).

Since disjunction (2.12) is exclusive, we add Eq. (2.15) and transform the logic constraint (2.13) into the mixed-integer linear constraint (2.16) using propositional logic. Due to the structure of Eq. (2.16), either $y_{d,j,q,t}^{PIPE}$ or $z_{d,j,q,t}^{PIPE}$ may be specified as continuous decision variables. In the authors' experience, however, this does not yield noticeable computational speed-ups.

$$k^P \cdot F^{JQ}_{j,q,t} \le \left(\delta^0_{j,q}\right)^2 + \sum_{d\in\mathcal{D}_0} \delta_d^2 \cdot z^{PIPE}_{d,j,q,t} \qquad \forall \left(j,q\right)\in\mathcal{JQA}, t\in\mathcal{T} \quad (2.14)$$

$$\sum_{d\in\mathcal{D}_0} z^{PIPE}_{d,j,q,t} = 1 \qquad \forall (j,q)\in\mathcal{JQA}, t\in\mathcal{T} \quad (2.15)$$

$$\sum_{\tau=1}^{t-\tau^P} y^{PIPE}_{d,j,q,\tau} = z^{PIPE}_{d,j,q,t} \qquad \forall d\in\mathcal{D}, \left(j,q\right)\in\mathcal{JQA}, t\in\mathcal{T} \quad (2.16)$$

The pipeline sizing formulation for delivery pipelines represented by Eqs. (2.14) -(2.16) is adapted for all candidate gathering pipelines $\left(j,\hat{j}\right)\in\mathcal{JJA}$, flow pipelines $\left(\mathrm{p},j\right)\in\mathcal{PJA}$ and well pipelines $\left(\mathrm{p},\hat{p}\right)\in\mathcal{PPA}$ that are considered in the gathering superstructure. In addition, Eqs. (2.17) and (2.18) are redundant constraints that strengthen the pipeline sizing formulation.

$$\delta^0_{p,j} + \sum_{d\in\mathcal{D}} y^{PIPE}_{d,p,j,t} \cdot \delta_d \le \delta^0_{j,\tilde{j}} + \sum_{d\in\mathcal{D}} y^{PIPE}_{d,j,\tilde{j},t} \cdot \delta_d \qquad \forall (p,j,\tilde{j})\in\mathcal{NDA}, t\in\mathcal{T}$$

(2.17)

$$\delta^0_{j,\tilde{j}} + \sum_{d\in\mathcal{D}} y^{PIPE}_{d,j,\tilde{j},t} \cdot \delta_d \le \delta^0_{\tilde{j},\hat{j}} + \sum_{d\in\mathcal{D}} y^{PIPE}_{d,\tilde{j},\hat{j},t} \cdot \delta_d \qquad \forall (j,\tilde{j},\hat{j})\in\mathcal{NDA}, t\in\mathcal{T}$$

(2.18)

The underlying logic is that prior to solving the shale gas development problem, operators can easily identify *non-decreasing pipeline capacity arcs* $\left(p,j,\hat{j}\right)\in\mathcal{NDA}$ and $\left(j,\tilde{j},\hat{j}\right)\in\mathcal{NDA}$ within the gathering superstructure. Along these neighboring arcs, the flow capacity – represented by the installed pipeline capacity – is not allowed to decrease, i.e., a decrease in flow capacity would indicate that the preceding pipeline segment is over-sized. If two pipelines merge into one segment, for example, it is clear that the subsequent pipeline may not decrease in terms of flow capacity. In practice, similar constraints are oftentimes imposed as part of the design problem to allow for “pigging” in gathering pipelines, i.e., the practice of using so-called “pigs” to clean operational pipelines in regular intervals.

The proposed sizing formulation for pipelines can easily be extended to size gathering compressors. These compressors need to be installed between regional shale gas gathering systems and interstate transmission pipelines. Typically, the line pressure of shale gas gathering systems is in the range of 2 MPa, whereas interstate transmission pipelines are generally operated at well above 7 MPa. Operators are only responsible for installing gathering compressors along direct delivery sales routes, i.e., when gas processing is not necessary. When the gas is delivered to a processing plant, the processor is responsible for compressing the gas to transmission line pressure. For compressor sizing purposes we use disjunction (2.19).

$$\bigvee_{c\in\mathcal{C}_0}\begin{bmatrix} Z_{c,j,q,t}^{COMPR} \\ k^{C}\cdot F_{j,q,t}^{JQ}\le \lambda_{j,q}^{0}+\lambda_{c}\end{bmatrix} \qquad \forall (j,q)\in\mathcal{DSR}, t\in\mathcal{T} \qquad (2.19)$$

$$\bigvee_{\tau=1}^{t-\tau^{C}} Y_{c,j,q,\tau}^{COMPR} \Leftrightarrow Z_{c,j,q,t}^{COMPR} \qquad \forall c\in\mathcal{C},(j,q)\in\mathcal{DSR}, t\in\mathcal{T} \qquad (2.20)$$

This disjunction states that at any point in time a particular compressor size (in terms of compression power) must be selected along every candidate direct sales route, i.e., exactly one Boolean variable $Z_{c,j,q,t}^{COMPR}$ has to be true in every time period $t\in\mathcal{T}$ along every arc $(j,q)\in\mathcal{DSR}$. Since inlet and outlet pressures of the compressor are fixed and given, the compressor power selection will determine precisely how much compression capacity is necessary along every candidate delivery sales route $(j,q) \in \mathcal{DSR}$, i.e., how much gas $F^{JQ}_{j,q,t}$ can be compressed along the respective arc. It is important to note here that the set of commercially available compressor sizes $c \in \mathcal{C}_0$ explicitly includes the *zero-size* c_0. Hence, it is possible to select no compression power along an arc which corresponds to the design decision of excluding that candidate compressor station from the final gathering system. Details regarding the compressor sizing procedure are provided in Appendix C: Compressor Sizing Guidelines.

We note that the disjunction (2.19) does account for pre-installed compression power $\lambda^0_{j,q}$. If a certain amount of compression power has already been installed along a direct sales arc $(j,q) \in \mathcal{DSR}$, then the corresponding compression capacity is already available. Hence, the proposed formulation allows for an increase in compression power, which is the common in industry. Compression increase in practice is typically modular, i.e., additional compressors are installed in parallel. As such, the pressure potential between the suction and the discharge sides of the compressors is identical.

As before, disjunction (2.19) is transformed into a set of mixed-integer linear constraints using the Hull Reformulation. We refer to Appendix D: Compressor Sizing Formulation for the full reformulation.

Water management constraints

Hydraulic fracturing of horizontal wells requires large amounts of fracturing fluid, oftentimes several million liters of water per well. Hence, it must be ensured that the demand for water can be met by the available set of water supply sources. In this work it is assumed that the water demand for fracturing is given in terms of the location-specific parameter fwd_p.

$$fwd_p \cdot \sum_{n \in \mathcal{N}} n \cdot y^{DEV}_{n,p,t} \le \sum_{f \in \mathcal{F}} FWS_{f,p,t} \qquad \forall p \in \mathcal{CP}, t \in \mathcal{T} \tag{2.21}$$

Constraint (2.21) ensures that the water supply $FWS_{f,p,t}$ from the available set of water sources $f \in \mathcal{F}$ satisfies the water demand at every well pad, depending on how many wells are being developed in parallel. In turn, constraint (2.22) balances the water supplied to all well pads with the water availability at all water sources, given by the parameter $fwa_{f,t}$.

$$\sum_{p \in \mathcal{CP}} FWS_{f,p,t} \le fwa_{f,t} \qquad \forall f \in \mathcal{F}, t \in \mathcal{T} \tag{2.22}$$

Rig and crew allocation constraints

In practice upstream operators generally only have a limited set of drilling rigs and completion crews at their disposal in a particular development area. The allocation of these resources is a challenging and complicating factor in the planning process. Hence, we introduce a binary decision variable $y^{RIG}_{r,p,t}$ that is active if a drilling rig and completion crew $r \in \mathcal{R}$ are present at a candidate pad location $p \in \mathcal{CP}$ in time period $t \in \mathcal{T}$. Constraint (2.23) ensures that a drilling rig and completion crew are on site for as long as any number of wells are being developed at a candidate pad location. A drilling rig and completion crew may not be assigned to more than one well pad at any time as expressed by Eq. (2.24).

$$\sum_{n \in \mathcal{N}} \sum_{\tau = t - \tau^{DR}_n + 1}^{t} y^{DRILL}_{n,p,\tau} \le \sum_{r \in \mathcal{R}} y^{RIG}_{r,p,t} \qquad \forall p \in \mathcal{CP}, t \in \mathcal{T} \tag{2.23}$$

$$\sum_{p \in \mathcal{CP}} y_{r,p,t}^{RIG} \leq 1 \qquad \forall r \in \mathcal{R}, t \in \mathcal{T} \tag{2.24}$$

Strategic development constraints

In practice, upstream operators oftentimes have the flexibility to choose from a set of candidate delivery nodes that are within the vicinity of their gathering system. These take-away options range from direct taps into nearby interstate transmission pipelines to processing plants that purify the raw gas prior to its injection into a transmission system. In addition to selecting the preferred delivery node, the operators also need to determine what kind of delivery agreements to arrange and how much delivery capacity to procure. The arrangement of these agreements is a quality-sensitive and nontrivial aspect of the overall long-term shale gas development problem.

In this section we define the constraints that govern the strategic selection of: a) a preferred delivery node, b) delivery agreements, and c) necessary delivery or “take-away” capacity. Fig. 2.3 illustrates these three levels of strategic decisions and the particular categories of constraints that they involve. The proposed formulation for the incorporation of strategic development constraints is motivated by Park et al. (2006) who include the selection of different types of contracts into existing supply chain optimization models using disjunctive programming. However, whereas Park et al. (2006) focus on generic purchasing and sales contracts between suppliers and customers, our models are tailored to the unique structure of the natural gas industry.

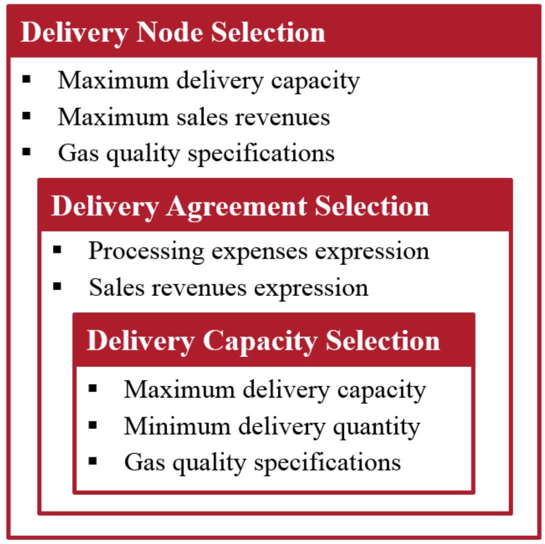

Fig. 2.3: Illustration of the three levels of strategic development constraints

In this work we capture the corresponding strategic development constraints using disjunction (2.25). This disjunction itself is characterized by a set of embedded disjunctions, and thus exploits the inherent structure of the strategic decision-making process.

$$
\bigvee_{(j,q)\in\mathcal{JQA}} \left[\begin{gathered} Y^{DEL}_{j,q} \\ F^{JQ}_{j,q,t} \le f^{\max}_{j,q,t} \qquad \forall t \in \mathcal{T} \\ \sum_{p\in\mathcal{P}} F^{0}_{p,t} \le f^{\max}_{j,q,t} \quad \forall t \in \mathcal{T} \\ REV_{j,q,t} \le rev^{\max}_{j,q,t} \quad \forall t \in \mathcal{T} \\ F^{JQ}_{j,q,t} \cdot h^{\min}_{j,q} \le \sum_{k\in\mathcal{K}} F^{KJQ}_{k,j,q,t} \cdot h_k \le F^{JQ}_{j,q,t} \cdot h^{\max}_{j,q} \quad \forall t \in \mathcal{T} \\ \bigvee_{da\in\mathcal{DA}} \left[\begin{gathered} Y^{AGR}_{da,j,q} \\ PRE_{j,q,t} = f^{PR}_{da}\left(F^{KJQ}_{k,j,q,t}\right) \quad \forall t \in \mathcal{T} \\ REV_{j,q,t} = f^{REV}_{da}\left(F^{KJQ}_{k,j,q,t}\right) \qquad \forall t \in \mathcal{T} \\ \bigvee_{dc\in\mathcal{DC}} \left[\begin{gathered} Z^{CPTY}_{dc,da,j,q,t} \\ F^{JQ}_{j,q,t} \le \sigma_{dc,da,j,q} \quad \forall t \in \mathcal{T} \\ \varphi_{dc,da,j,q} \le F^{JQ}_{j,q,t} + F^{S}_{j,q,t} \quad \forall t \in \mathcal{T} \\ F^{JQ}_{j,q,t} \cdot h^{\min}_{dc,da,j,q} \le \sum_{k\in\mathcal{K}} F^{KJQ}_{k,j,q,t} \cdot h_k \le F^{JQ}_{j,q,t} \cdot h^{\max}_{dc,da,j,q} \quad \forall t \in \mathcal{T} \end{gathered} \right] \end{gathered} \right] \end{gathered} \right] \tag{2.25}
$$

At the highest level, upstream operators have to select their preferred delivery node for a particular gathering system. This selection is of significant importance as it can vary between two conceptually disparate delivery options: *processing sales routes* and *transmission sales routes*. Whereas processing plants along processing sales routes $(j,q) \in \mathcal{PSR}$ are designed to purify off-spec raw gas deliveries, transmission lines along direct sales routes $(j,q) \in \mathcal{DSR}$ generally only accept pipeline-quality gas deliveries. This diversity in terms of delivery options can be interpreted as a strategic degree of freedom to the upstream operator providing the decision-makers with a certain degree of flexibility. On the other hand, the conditions and terms of each delivery option also complicate long-term strategic commitments and add to the challenge of the development problem.

The Boolean variable $Y_{j,q}^{DEL}$ controls the outermost disjunction (2.25) and allows for the selection of a particular delivery arc $(j,q) \in \mathcal{JQA}$. This selection bounds the maximum take-away capacity $f_{j,q,t}^{\max}$, the maximum attainable revenues $rev_{j,q,t}^{max}$ and it imposes gas quality specification constraints in terms of the heating value of the gas delivery $h_{j,q}^{min}$ and $h_{j,q}^{max}$. In this section we assume that the delivery node selection may only be made once throughout the planning horizon, hence disjunction (2.25) is truly exclusive. The relaxation of this restriction is discussed in section 2.5.3 Model Formulation: Multiple Delivery Node Problem.

Besides the selection of a preferred take-away node, upstream operators must also choose from a limited set of delivery agreement options they are offered. In terms of processing plants, for example, these contracts range from *fee-based* to *percent-of-proceeds* and *keep-whole* processing agreements (Pan, 2013). These agreements are conceptually different with regards to how the upstream operator compensates the processor for the processing service, and how revenues are generated for either party. Under *fee-based* contracts the operator simply pays a volume-based fee for the processing service, under *percent-of-proceeds* contracts the operator and the processor split revenues from marketing the gas and extracted NGLs, and under *keep-whole* contracts the processor retains title to all extracted NGLs as a method of payment. In addition, every possible delivery agreement may involve further specific terms and conditions regarding contract durations, delivery capacities or gas quality specifications. Delivery agreement options along direct sales routes are generally limited but may vary as well.

In this work, we embed the selection of the optimal delivery agreement within disjunction (2.25). For this purpose we introduce the Boolean variable $Y_{da,j,q}^{AGR}$ which is true if a particular delivery agreement $da \in DA$ is arranged along a take-away arc $(j,q) \in \mathcal{JQA}$. This selection will determine the form of the processing cost function $f_{da}^{PR}(F_{k,j,q,t}^{KJQ})$ and the revenue function $f_{da}^{REV}(F_{k,j,q,t}^{KJQ})$. Constraint (2.26) ensures that if the Boolean variable $Y_{j,q}^{DEL}$ is true, i.e., a particular take-away node has been selected, then one of the available delivery agreements needs to be arranged, i.e., a corresponding Boolean variable $Y_{da,j,q}^{AGR}$ has to be true, too. The reverse statement holds true as well.

$$Y_{j,q}^{DEL} \quad \Leftrightarrow \quad \bigvee_{da \in \mathcal{DA}} \quad Y_{da,j,q}^{AGR} \qquad \forall (j,q) \in \mathcal{JQA} \tag{2.26}$$

In addition, the logic constraints (2.27) and (2.28) are imposed to explicitly distinguish between *processing agreements* and *transmission agreements* that operators may enter into depending on which type of delivery node is selected. The set of processing agreements $pa \in \mathcal{PA}$ and transmission agreements $ta \in \mathcal{TA}$ complement the set of delivery agreements $da \in DA$. Constraint (2.27) expresses that if a delivery node among the set of processing sales routes $(j,q) \in \mathcal{PSR}$ is selected, then one of the available processing agreements $pa \in \mathcal{PA}$ has to be arranged. Vice versa, constraint (2.28) states that deliveries along transmission sales routes $(j,q) \in \mathcal{TSR}$ must be governed by one of the available transmission agreements $ta \in \mathcal{TA}$.

$$Y_{j,q}^{DEL} \quad \Leftrightarrow \quad \bigvee_{pa \in \mathcal{PA}} \quad Y_{pa,j,q}^{AGR} \qquad \forall (j,q) \in \mathcal{PSR} \tag{2.27}$$

$$Y_{j,q}^{DEL} \quad \Leftrightarrow \quad \bigvee_{ta \in \mathcal{TA}} \quad Y_{ta,j,q}^{AGR} \qquad \forall (j,q) \in \mathcal{DSR} \tag{2.28}$$

Due to the complexity of the bilateral negotiation process between upstream operators and downstream entities, we assume that the arrangement of any delivery agreement may only be made once throughout the planning horizon. For this reason the center disjunction contained in disjunction (2.25) is exclusive.

Finally, upstream operators have to determine how much delivery capacity to request at a particular delivery node. Generally, only discrete increments of take-away capacity can be procured, typically classified as *limited*, *average*, or *extended* delivery capacity. The more delivery capacity an upstream operator wishes to secure, the longer the duration of an agreement tends to be. Downstream entities, including processing plants and transmission lines, will specify minimum delivery quantities for the duration of a delivery agreement to ensure that they can recover their expenses for providing take-away capacity. Commonly, these minimum delivery clauses involve so-called *take-or-pay provisions* that obligate the upstream operator to either deliver the specified quantity, i.e., "take" the capacity, or to compensate the delivery entity, i.e., "pay" for unutilized capacity. Depending on how much take-away capacity is requested, additional and more restrictive gas quality specifications may be imposed as well. A midstream processor, for example, may offer limited processing capacity over a short period of time provided the delivered gas meets strict quality specifications.

Within the embedded, innermost delivery capacity selection disjunction (2.25) we introduce the Boolean variable $Z_{dc,da,j,q,t}^{CPTY}$ which is true if delivery capacity $dc \in \mathcal{DC}$ is *available* as part of delivery agreement $da \in \mathcal{DA}$ along delivery arc $(j,q) \in \mathcal{JQA}$ in time period $t \in \mathcal{T}$. If this Boolean variable is true, then the gas flowrate $F_{j,q,t}^{JQ}$ along the corresponding delivery arc is bounded by the maximum delivery quantity parameter

$\sigma_{dc,da,j,q}$. In addition, a minimum delivery quantity restriction $\varphi_{dc,da,j,q}$ may apply. Given the characteristic shale well decline curves these minimum delivery restrictions can be especially challenging to meet. In order to ensure a steady supply of natural gas, operators will generally try to turn new wells in line continuously. In this context we account for common take-or-pay provisions by introducing the slack variable $F^{S}_{j,q,t}$. This variable closes the gap between the actually delivered gas flow $F^{JQ}_{j,q,t}$ and the arranged minimum delivery quantity $\varphi_{dc,da,j,q}$. As such, the slack variable $F^{S}_{j,q,t}$ represents procured but unutilized capacity. Finally, the embedded delivery capacity selection disjunction involves the aforementioned gas quality specifications $h^{min}_{dc,da,j,q}$ and $h^{max}_{dc,da,j,q}$ that may or may not apply.

The logic constraint (2.29) guarantees that delivery capacity is available whenever a particular delivery agreement is selected and vice versa. This constraint links the agreement selection disjunction with the embedded capacity selection disjunction.

$$Y^{AGR}_{da,j,q} \quad \Leftrightarrow \quad \bigvee_{dc \in \mathcal{DC}} Z^{CPTY}_{dc,da,j,q,t} \qquad \forall da \in \mathcal{DA}, (j,q) \in \mathcal{JQA}, t \in \mathcal{T} \tag{2.29}$$

Similar to the case of delivery agreements, we distinguish between delivery capacity in terms of *processing capacity* and *transmission capacity*. Increments of processing capacity $pc \in \mathcal{PC}$ are only available along processing sales routes $(j,q) \in \mathcal{PSR}$ as part of processing agreements $pa \in \mathcal{PA}$, whereas transmission capacity increments $tc \in \mathcal{TC}$ are restricted to transmission agreements $ta \in \mathcal{TA}$ along transmission sales routes $(j,q) \in \mathcal{DSR}$. The logic constraints (2.30) and (2.31) establish these links among the embedded delivery agreement and delivery capacity selection disjunctions.

$$Y_{pa,j,q}^{AGR} \quad \Leftrightarrow \quad \bigvee_{pc \in \mathcal{PC}} \quad Z_{pc,pa,j,q,t}^{CPTY} \qquad \forall pa \in \mathcal{PA}, (j,q) \in \mathcal{PSR}, t \in \mathcal{T} \tag{2.30}$$

$$Y_{ta,j,q}^{AGR} \quad \Leftrightarrow \quad \bigvee_{tc \in \mathcal{TC}} \quad Z_{tc,ta,j,q,t}^{CPTY} \qquad \forall ta \in \mathcal{TA}, (j,q) \in \mathcal{DSR}, t \in \mathcal{T} \tag{2.31}$$

We define the parameter $\tau_{dc,da}^{A}$ that specifies the agreement length for delivery capacity $dc \in \mathcal{DC}$ under delivery agreement $da \in \mathcal{DA}$. We also introduce the Boolean variable $Y_{dc,da,j,q,t}^{CPTY}$ that represents the *selection* of delivery capacity $dc \in \mathcal{DC}$ as part of delivery agreement $da \in \mathcal{DA}$ along delivery arc $(j,q) \in \mathcal{JQA}$ in time period $t \in \mathcal{T}$, i.e., this Boolean variable marks the *beginning* of the capacity availability. Based on this variable declaration, constraint (2.32) states that delivery capacity, denoted by the Boolean variable $Z_{dc,da,j,q,t}^{CPTY}$, is only available as long as the beginning of the arrangement occurred within the previous $\tau_{dc,da}^{A}$ time periods. During this time, all corresponding restrictions including minimum delivery quantities and gas quality specifications apply.

$$\bigvee_{\tau = t-\tau_{dc,da}^{A}}^{t} \quad Y_{dc,da,j,q,\tau}^{CPTY} \quad \Leftrightarrow \quad Z_{dc,da,j,q,t}^{CPTY} \qquad \forall dc \in \mathcal{DC}, da \in \mathcal{DA}, (j,q) \in \mathcal{JQA}, t \in \mathcal{T} \tag{2.32}$$

Since the innermost disjunction contained in disjunction (2.25) is exclusive, some increment of delivery capacity is available along every delivery arc $(j,q) \in \mathcal{JQA}$ at any point in time. Technically, however, the set of available delivery capacities $dc \in \mathcal{DC}$ will always involve a *zero-capacity* element dc_0.

In this work the disjunctions are reformulated as mixed-integer linear constraints using both the big-M and the Hull Reformulation. For this purpose we introduce the binary variables $y_{j,q}^{DEL}$, $y_{da,j,q}^{AGR}$, $y_{dc,da,j,q,t}^{CPTY}$ and $z_{dc,da,j,q,t}^{CPTY}$ that correspond directly to the respective Boolean variables defined previously.

The outer disjunction (2.25) capturing the delivery node selection is transformed into a set of mixed-integer linear constraints using the Hull Reformulation. This disjunction involves the continuous decision variables $F^{JQ}_{j,q,t}$, $F^{KJQ}_{k,j,q,t}$, $REV_{j,q,t}$ and $F^{0}_{p,t}$. In this case only the latter variable needs to be disaggregated as $F^{0}_{p,j,q,t}$ for each disjunctive term $(j,q) \in \mathcal{JQA}$ as expressed in constraint (2.33).

$$F^{0}_{p,t} = \sum_{(j,q) \in \mathcal{JQA}} F^{0}_{p,j,q,t} \qquad \forall p \in \mathcal{P}, t \in \mathcal{T} \tag{2.33}$$

For the special case of the single delivery node problem, we can take advantage of the disaggregated variable $F^{0}_{p,j,q,t}$ when imposing the component flow balance Eq. (2.34).

$$F^{KJQ}_{k,j,q,t} = \sum_{p \in \mathcal{P}} F^{0}_{p,j,q,t} \cdot x^{0}_{p,k} \qquad \forall k \in \mathcal{K}, (j,q) \in \mathcal{JQA}, t \in \mathcal{T} \tag{2.34}$$

The reasoning for this constraint is as follows: by "design" the single delivery node problem forces all flows to converge to one delivery node eventually, i.e., regardless of the final design of the gathering system all of the gas that is extracted within the development area will be delivered to one and the same take-away hub. Since the composition of the extracted gas $x^{0}_{p,k}$ is known at every well pad, we can enforce constraint (2.34), which balances how much of each component $k \in \mathcal{K}$ is produced at all well pads in every time period with the component flow to all available delivery nodes. This explains why the single delivery node problem can indeed be solved as a mixed-integer *linear* program.

In addition, we impose the upper and lower bound constraints (2.35)-(2.38) for all decision variables involved in the outer disjunction.

$$0 \le F^{0}_{p,j,q,t} \le f^{\max}_{j,q,t} \cdot y^{DEL}_{j,q} \qquad \forall (j,q) \in \mathcal{JQA}, t \in \mathcal{T} \tag{2.35}$$

$$0 \le F^{JQ}_{j,q,t} \le f^{\max}_{j,q,t} \cdot y^{DEL}_{j,q} \qquad \forall (j,q) \in \mathcal{JQA}, t \in \mathcal{T} \tag{2.36}$$

$$0 \le F^{KJQ}_{k,j,q,t} \le f^{\max}_{k,j,q,t} \cdot y^{DEL}_{j,q} \qquad \forall (j,q) \in \mathcal{JQA}, t \in \mathcal{T} \tag{2.37}$$

$$0 \le REV_{j,q,t} \le rev^{\max}_{j,q,t} \cdot y^{DEL}_{j,q} \qquad \forall (j,q) \in \mathcal{JQA}, t \in \mathcal{T} \tag{2.38}$$

We note here that constraints (2.33) and (2.35) are not absolutely necessary, but are rather imposed to tighten the formulation. The gas quality specification constraint is adopted directly as it holds regardless of which disjunctive term is active.

$$F^{JQ}_{j,q,t} \cdot h^{\min}_{j,q} \le \sum_{k \in \mathcal{K}} F^{KJQ}_{k,j,q,t} \cdot h_k \le F^{JQ}_{j,q,t} \cdot h^{\max}_{j,q} \quad \forall t \in \mathcal{T} \tag{2.39}$$

Constraint (2.40) ensures that only one node may be selected for delivery, i.e., only one term can be active in the outer disjunction (2.25).

$$\sum_{(j,q) \in \mathcal{JQA}} y^{DEL}_{j,q} = 1 \tag{2.40}$$

The logic link (2.26) between the outer delivery node selection disjunction and the embedded center disjunction concerning agreement arrangements is reformulated into the algebraic constraint (2.41). The same transformation holds for the specialized logic propositions (2.27) and (2.28) affecting deliveries along processing and transmission sales routes.

$$y^{DEL}_{j,q} = \sum_{da \in \mathcal{DA}} y^{AGR}_{da,j,q} \qquad \forall (j,q) \in \mathcal{JQA} \tag{2.41}$$

$$y^{DEL}_{j,q} = \sum_{pa \in \mathcal{PA}} y^{AGR}_{pa,j,q} \qquad \forall (j,q) \in \mathcal{PSR} \tag{2.42}$$

$$y^{DEL}_{j,q} = \sum_{ta \in \mathcal{TA}} y^{AGR}_{ta,j,q} \qquad \forall (j,q) \in \mathcal{DSR} \tag{2.43}$$

The constraints within the embedded center disjunction itself are converted into mixed-integer linear constraints using a big-M reformulation. For this purpose we define the big-M parameters $m^{PRE}_{da,j,q}$ and $m^{REV}_{da,j,q}$. Depending on which agreement type $da \in \mathcal{DA}$ is selected, i.e., which binary variable $y^{AGR}_{da,j,q}$ is active, determines which processing expenses accrue and how revenues are generated. Eq. (2.44) states the general expression for processing expenses where the processing cost coefficient α^{A}_{da} changes depending on which type of agreement is selected.

$$\alpha^{A}_{da} \cdot \left(F^{JQ}_{j,q,t} + F^{S}_{j,q,t}\right) - PRE_{j,q,t} \leq m^{PRE}_{\mathrm{da},j,q} \cdot \left(1 - y^{AGR}_{da,j,q}\right) \quad \forall da \in \mathcal{DA}, (j,q) \in \mathcal{JQA}, t \in \mathcal{T} \tag{2.44}$$

The functional form of the revenue expression, on the other hand, changes fundamentally depending on the type of agreement between an upstream operator and a processing plant. In Appendix E: Delivery Agreements, we review the most common types of delivery agreements in more detail, i.e., *fee-based, percent-of-proceeds, keep-whole,* and *direct delivery* contracts and we present the individual processing and revenue functions.

Constraint (2.45) ensures that only one particular delivery agreement can be selected along every delivery arc $(j,q) \in \mathcal{JQA}$.

$$\sum_{da \in \mathcal{DA}} y^{AGR}_{da,j,q} = 1 \qquad \forall (j,q) \in \mathcal{JQA} \tag{2.45}$$

We link the embedded center and innermost disjunctions through constraint (2.46) that corresponds to the logical proposition (2.29). As before, this transformation also holds for the specialized logic propositions (2.30) and (2.31) addressing processing and transmission agreements.

$$y^{AGR}_{da,j,q} = \sum_{dc \in \mathcal{DC}} z^{CPTY}_{dc,da,j,q,t} \qquad \forall da \in \mathcal{DA}, (j,q) \in \mathcal{JQA}, t \in \mathcal{T} \tag{2.46}$$

$$y_{pa,j,q}^{AGR} = \sum_{pc \in \mathcal{PC}} z_{pc,pa,j,q,t}^{CPTY} \qquad \forall pa \in \mathcal{PA}, (j,q) \in \mathcal{PSR}, t \in \mathcal{T} \qquad (2.47)$$

$$y_{ta,j,q}^{AGR} = \sum_{tc \in \mathcal{TC}} z_{tc,ta,j,q,t}^{CPTY} \qquad \forall ta \in \mathcal{TA}, (j,q) \in \mathcal{DSR}, t \in \mathcal{T} \qquad (2.48)$$

The embedded innermost disjunction in (2.25) capturing the delivery capacity selection is converted into algebraic constraints by using a big-M reformulation. The constraints involved in this disjunction address minimum delivery restrictions, capacity constraints, and gas quality specifications. By introducing sufficiently large parameters $m_{dc,da,j,q}^{\varphi}$, $m_{dc,da,j,q}^{\sigma}$, $m_{dc,da,j,q}^{h^{min}}$ and $m_{dc,da,j,q}^{h^{max}}$ we can derive the big-M constraints (2.50)-(2.52), respectively.

$$F_{j,q,t}^{JQ} - \sigma_{dc,da,j,q} \le m_{dc,da,j,q}^{\sigma} \cdot \left(1 - z_{dc,da,j,q,t}^{CPTY}\right) \qquad \forall dc \in \mathcal{DC}, da \in \mathcal{DA}, (j,q) \in \mathcal{JQA}, t \in \mathcal{T} \qquad (2.49)$$

$$\varphi_{dc,da,j,q} - \left(F_{j,q,t}^{JQ} + F_{j,q,t}^{S}\right) \le m_{dc,da,j,q}^{\varphi} \cdot \left(1 - z_{dc,da,j,q,t}^{CPTY}\right) \qquad \forall dc \in \mathcal{DC}, da \in \mathcal{DA}, (j,q) \in \mathcal{JQA}, t \in \mathcal{T} \qquad (2.50)$$

$$F_{j,q,t}^{JQ} \cdot h_{dc,da,\mathrm{j},q}^{\min} - \sum_{k \in \mathcal{K}} F_{k,j,q,t}^{KJQ} \cdot h_k \le m_{dc,da,j,q}^{h^{min}} \cdot \left(1 - z_{dc,da,j,q,t}^{CPTY}\right) \qquad \forall dc \in \mathcal{DC}, da \in \mathcal{DA}, (j,q) \in \mathcal{JQA}, t \in \mathcal{T} \qquad (2.51)$$

$$\sum_{k \in \mathcal{K}} F_{k,j,q,t}^{KJQ} \cdot h_k - F_{j,q,t}^{JQ} \cdot h_{dc,da,\mathrm{j},q}^{\max} \le m_{dc,da,j,q}^{h^{max}} \cdot \left(1 - z_{dc,da,j,q,t}^{CPTY}\right) \qquad \forall dc \in \mathcal{DC}, da \in \mathcal{DA}, (j,q) \in \mathcal{JQA}, t \in \mathcal{T} \qquad (2.52)$$

Finally, the logic proposition (2.32) governing the length of delivery capacity agreements is reformulated as constraint (2.53).

$$\sum_{\tau = t - \tau_{da,da}^{A}}^{t} y_{dc,da,j,q,\tau}^{CPTY} = z_{dc,da,j,q,t}^{CPTY} \qquad \forall dc \in \mathcal{DC}, da \in \mathcal{DA}, (j,q) \in \mathcal{JQA}, t \in \mathcal{T} \qquad (2.53)$$

2.5.2 Model Formulation: Objective Function

The objective for shale gas development from the operator's perspective is to maximize the net present value (NPV) over an extended planning horizon. The proposed objective function (2.54) accounts for revenues from natural gas and natural gas liquids sales REV_t, development expenses DVE_t, installation expenses for flow pipelines FPE_t, gathering pipelines GPE_t, delivery pipelines DPE_t, compressor installation expenses CIE_t, compressor operating expenses COE_t, production and maintenance expenses PME_t, water acquisition expenses FWE_t, royalty payments RRE_t, rig transition expenses RTE_t, rig downtime expenses RDE_t, site construction expenses SCE_t and processing expenses PRE_t.

$$
\begin{aligned}
\max \quad & NPV = \sum_{t \in \mathcal{T}} (1+dr)^{-t} \cdot \\
& \{REV_t - DVE_t - FPE_t - GPE_t - DPE_t - CIE_t - \\
& COE_t - PME_t - FWE_t - RRE_t - RTE_t - RDE_t - SCE_t - PRE_t\} \\
& + \sum_{t \in T} \sum_{p \in P} \sum_{k \in K} NWP_{p,t} \cdot \zeta_{p,\mathrm{T}-\mathrm{t}} \cdot x_{p,k}^0 \cdot \tilde{p}_k
\end{aligned} \tag{2.54}
$$

The last term in the objective function (2.54) captures the terminal value of the development project. Since the wells are expected to produce many years beyond the explicit planning horizon these revenues need to be factored into the net present value. For this purpose we consider the number of wells that are turned in-line at every pad in every time period $NWP_{p,t}$, the expected, discounted, cumulative production of a well beyond the explicit planning horizon $\zeta_{p,T-t}$, the gas composition $x_{p,k}^0$, and an expected price forecast beyond the explicit planning horizon for every gas component $\tilde{p}_k$. Assuming that the implicit planning horizon extends to time period $t = \tilde{T}$ we determine the expected, discounted cumulative production of a well beyond the explicit planning horizon as follows:

$$\zeta_{p,T-t} = \sum_{\tau=T-t}^{\tilde{T}-t} \gamma_{p,\tau} \cdot (1+dr)^{-\tau+t+1} \tag{2.55}$$

The overall revenues REV_t are driven by natural gas and NGLs sales along the delivery sales routes $(j,q) \in \mathcal{JQA}$ as outlined in constraint (2.56). The explicit expressions for individual revenue streams along particular sales routes $REV_{j,q,t}$ depend on the arrangement of particular processing agreements.

$$REV_t = \sum_{(j,q)\in \mathcal{JQA}} REV_{j,q,t} \qquad \forall t \in \mathcal{T} \tag{2.56}$$

Economies of scale play a crucial role in shale gas development since the major capital investment expenses for drilling wells, laying out pipelines and installing compressor stations are well-known to obey these scaling principles (Moore, 1959; Haldi & Whitcomb, 1967; Tribe & Alpine, 1986). Dawson et al. (2012) go as far as to argue that the success or failure of unconventional gas development hinges upon the principles of economies of scale.

Commonly, economies of scale are captured by concave investment cost functions of the form,

$$f(x) = \alpha \cdot x^{\beta} \qquad 0 < \beta < 1$$

where $f(x)$ are the equipment cost, x represents the equipment size, and finally α and β are cost parameters. The design variable x, i.e., the equipment size such as the pipeline diameter or compression power is commonly treated as a continuous variable. However, due to the concave nature of the cost function above, these expressions can give rise to multiple local optima and unbounded gradients at zero values for equipment sizes ($x = 0$), leading to failures in NLP algorithms. Moreover, a posteriori rounding of equipment sizes can lead to suboptimal or even infeasible solutions.

We overcome these difficulties by taking advantage of the discrete nature of the design variables involved in the shale gas development problem. Since pipeline diameters and compressor sizes are standardized in practice, we restrict the respective design variables to a finite set of discrete values $x_i \in \{x_1, x_2, \ldots, x_N\}$ (as shown in Fig. 2.4) and introduce binary variables $y_i \in \{0,1\}$ to select the optimal equipment sizes. This allows us to derive the following mixed-integer linear constraints for investment costs that are subject to economies of scale.

$$f(y_i) = \sum_{i=1}^{N} \alpha \cdot x_i^{\beta} \cdot y_i$$

$$\sum_{i=1}^{N} y_i \leq 1$$

The important feature of the proposed reformulation is that it readily allows the consideration of discrete sizes and that it avoids nonlinear cost terms in the objective function due to economies of scale. However, depending on the number of discrete sizes, a large number of binary variables may be introduced that could render the mixed-integer programs expensive to solve.

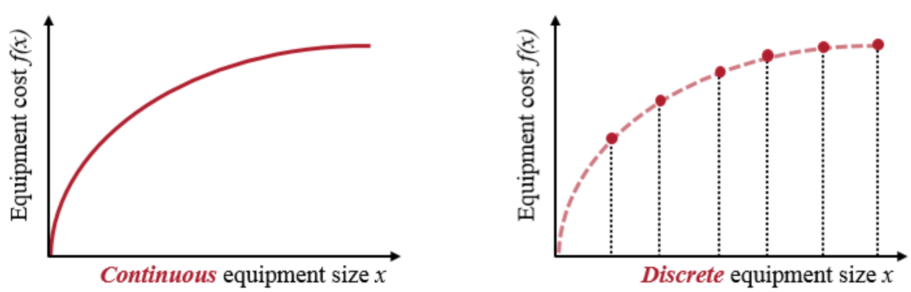

Fig. 2.4: Illustration of equipment costs subject to economies of scale

In terms of the proposed model, we assume that expenses related to well developments as well as pipeline and compressor installations are subject to economies of scale. Hence, the respective cost expressions correspond to the modified cost function. Regarding well development expenses, for instance, the number of wells that can be drilled at any candidate pad location is an element of the discrete set $n \in \mathcal{N}$. By defining the cost parameters α^D and β^D we can take advantage of the previously introduced binary variable $y_{n,p,t}^{DEV}$ and express the development expenses using constraint (2.57). This expression is linear even though it captures the nonlinear nature of economies of scale.

$$DVE_t = \sum_{p \in \mathcal{P}} \sum_{n \in \mathcal{N}} \alpha^D \cdot n^{\beta^D} \cdot y_{n,p,t}^{DRILL} \qquad \forall t \in \mathcal{T} \tag{2.57}$$

The same procedure can be applied to investment costs arising from the installation of delivery, gathering, flow and well pipelines. In all four cases we rely on the corresponding binary variables $y_{d,j,q,t}^{PIPE}$, $y_{d,j,\hat{j},t}^{PIPE}$, $y_{d,p,j,t}^{PIPE}$ and $y_{d,p,\hat{p},t}^{PIPE}$ to derive the cost expressions (2.58)-(2.60).

$$DPE_t = \sum_{(j,q) \in \mathcal{JQA}} \sum_{d \in \mathcal{D}} l_{j,q} \cdot \alpha^P \cdot \delta_d^{\beta^P} \cdot y_{d,j,q,t}^{PIPE} \qquad \forall t \in \mathcal{T} \tag{2.58}$$

$$GPE_t = \sum_{(j,\hat{j}) \in \mathcal{JJA}} \sum_{d \in \mathcal{D}} l_{j,\hat{j}} \cdot \alpha^P \cdot \delta_d^{\beta^P} \cdot y_{d,j,\hat{j},t}^{PIPE} \qquad \forall t \in \mathcal{T} \tag{2.59}$$

$$FPE_t = \sum_{d \in \mathcal{D}} \alpha^P \cdot \delta_d^{\beta^P} \cdot \left(\sum_{(p,j) \in \mathcal{PJA}} l_{p,j} \cdot y_{d,p,j,t}^{PIPE} + \sum_{(p,\hat{p}) \in \mathcal{PPA}} l_{p,\hat{p}} \cdot y_{d,p,\hat{p},t}^{PIPE} \right) \qquad \forall t \in \mathcal{T} \tag{2.60}$$

The constraints involve the cost parameters α^P and β^P as well as the lengths of candidate pipeline segments $l_{j,q}$, $l_{j,\hat{j}}$, $l_{p,j}$ and $l_{p,\hat{p}}$. The parameter δ_d stands for commercially available pipeline diameters and is linked to elements of the set $d \in \mathcal{D}$.

Expenses related to the installation of compression power are captured in a similar fashion. We assume that compressors only need to be installed along direct sales routes $(j,q) \in \mathcal{DSR}$ leading to interstate transmission pipelines. We define the parameter δ_c to represent commercially available compressor sizes $c \in \mathcal{C}$ and use the cost parameters α^C and β^C to describe the characteristic economies of scale. Consequently, the selection of a particular compressor size, denoted by the binary variable $y_{c,j,q,t}^{COMPR}$, determines the compressor installation expenses as given by expression (2.61).

$$CIE_t = \sum_{(j,q)\in \mathcal{DSR}} \sum_{c \in \mathcal{C}} \alpha^C \cdot \lambda_c^{\beta^C} \cdot y_{c,j,q,t}^{COMPR} \qquad \forall t \in \mathcal{T} \tag{2.61}$$

Expenses for the operation of compressors as well as other production and maintenance costs, are captured by Eqs. (2.62) and (2.63). For simplicity we assume that compression expenses are directly proportional to the gas flow through the respective compressors. Similarly, production and maintenance expenses depend primarily on how much gas is extracted at all well pads within the development area.

$$COE_t = \sum_{(j,q)\in \mathcal{DSR}} \alpha^O \cdot F_{j,q,t}^{JQ} \qquad \forall t \in \mathcal{T} \tag{2.62}$$

$$PME_t = \sum_{p \in \mathcal{P}} \alpha^I \cdot F_{p,t}^0 \qquad \forall t \in \mathcal{T} \tag{2.63}$$

In many U.S. states minimum royalty rates are prescribed by law and set to approximately 13% of the value of the extracted oil or gas. In this work we introduce a parameter to represent the royalty rate rr_p and impose the expression (2.64).

$$RRE_t = \sum_{p \in \mathcal{P}} nd \cdot F^0_{p,t} \cdot \sum_{k \in \mathcal{K}} x^0_{p,k} \cdot p^0_{k,t} \cdot rr_p \qquad \forall t \in \mathcal{T} \tag{2.64}$$

Freshwater acquisition expenses for fracturing operations are described by Eq. (2.65). We define the cost parameter α^W and assume that the cost of water acquisition is proportional to the amount of water that is required, $WS_{f,p,t}$, and the distance between a water source and the well pad $l_{f,p}$.

$$FWE_t = \sum_{f \in \mathcal{F}} \sum_{p \in \mathcal{P}} \alpha^W \cdot l_{f,p} \cdot WS_{f,p,t} \qquad \forall t \in \mathcal{T} \tag{2.65}$$

In practice, significant expenses accrue whenever a drilling rig is moved from one well pad to another. These are mainly due to the costly assembly and disassembly of the rigs. We define the rig transition cost parameter α^R and assume that transition expenses accumulate whenever a drilling rig is either assembled or disassembled at a well pad. Since the binary variable $y^{RIG}_{r,p,t}$ identifies whether a drilling rig is located at a particular well pad or not, we use constraint (2.66) to anticipate rig transition expenses. The proposed constraints (2.66) - (2.68) are derived from the reformulation of the absolute value $\left| RTE_{r,p,t} \right|$.

$$RTE^+_{r,p,t} - RTE^-_{r,p,t} \geq \alpha^R \cdot (y^{RIG}_{r,p,t} - y^{RIG}_{r,p,t-1}) \qquad \forall r \in \mathcal{R}, p \in \mathcal{P}, t \in \mathcal{T} \tag{2.66}$$

$$RTE^+_{r,p,t}, RTE^-_{r,p,t} \geq 0 \qquad \forall r \in \mathcal{R}, p \in \mathcal{P}, t \in \mathcal{T} \tag{2.67}$$

$$RTE_t = \sum_{r \in \mathcal{R}} \sum_{p \in \mathcal{P}} RTE^+_{r,p,t} + RTE^-_{r,p,t} \qquad \forall t \in \mathcal{T} \tag{2.68}$$

Usually, upstream operators will enter servicing agreements with rig companies and lease drilling rigs over several years. Under these agreements, the upstream operators are typically required to compensate the rig companies even when their services are not needed. These so-called *rig downtime expenses* are on the order of \$50,000 per day, and hence contribute significantly to the overall development expenses. We account for rig downtime expenses RDE_t in Eq. (2.69).

$$RDE_t = \left(\sum_{p \in \mathcal{P}} \sum_{r \in \mathcal{R}} y^{RIG}_{r,p,t} - \sum_{p \in \mathcal{P}} \sum_{n \in \mathcal{N}} \sum_{\tau = t - \tau_n^{DR}}^{t} y^{DRILL}_{n,p,\tau} \right) \cdot \alpha^{RD} \qquad \forall t \in \mathcal{T} \qquad (2.69)$$

For as long as the employed number of rigs are drilling on a well pad – captured by an active binary variable $y^{DRILL}_{n,p,t}$ and the drilling lead time parameter τ_n^{DR} – no expenses accrue. For any rig that is not involved in drilling operations in time period $t \in \mathcal{T}$ the rig downtime expense α^{RD} applies.

The construction of a well site may take place several months prior to the beginning of drilling operations. Based on the site construction cost coefficient α^S and the binary variable $y^{CON}_{p,t}$ – which marks the begin of construction operations – we calculate the site construction expenses SCE_t using constraint (2.70).

$$SCE_t = \sum_{n \in \mathcal{N}} \sum_{p \in \mathcal{P}} \alpha_n^S \cdot y^{CON}_{n,p,t} \qquad \forall t \in \mathcal{T} \qquad (2.70)$$

Processing expenses accrue only along processing sales routes $(j,q) \in \mathcal{PSR}$ and depend on what type of processing agreement is arranged. Constraint (2.71) accounts for processing expenses along all candidate processing arcs.

$$PRE_t = \sum_{(j,q) \in \mathcal{PSR}} PRE_{j,q,t} \qquad \forall t \in \mathcal{T} \qquad (2.71)$$

In conclusion, the proposed model for the single delivery node development problem is composed of constraints (2.1)-(2.11), (2.14)-(2.18), (2.21)-(2.24), (2.33)-(2.71). Since these constraints consist solely of mixed-integer linear constraints, the suggested formulation corresponds to an MILP that can be solved to global optimality.

2.5.3 Model Formulation: Multiple Delivery Nodes Problem

The previously proposed formulation for the single delivery node development problem can easily be extended to account for multiple delivery nodes. In fact, production constraints (2.1)-(2.8), flow balances (2.9)-(2.11), equipment sizing constraints (2.14)-(2.18), water management constraints (2.21)-(2.22), rig and crew allocation constraints (2.23)-(2.24), as well as the objective function (2.54) and the matching expressions used to capture revenues and expenses (2.56)-(2.71) can be adapted directly.

The major differences in terms of the model formulation arise with the strategic development constraints, previously defined by the disjunction (2.25) and the corresponding constraints (2.26)-(2.53). Before, we introduced this set of constraints to capture the selection of a) a preferred delivery node, b) delivery agreements and c) necessary delivery or "take-away" capacity. Since the multiple delivery node problem explicitly allows for simultaneous gas deliveries to several take-away nodes, these constraints reduce to two levels of strategic decision-making: delivery agreements and "take-away" capacity. At the same time the exact distribution of gas deliveries to the given set of candidate delivery nodes, i.e. the ideal *split factor*, becomes a key degree of freedom.

Now, the modified strategic disjunction (2.72) replaces disjunction (2.25) involved in the single delivery node model. Unlike before, the outer disjunction now governs the selection of a particular delivery agreement, whereas the inner disjunction is concerned with the procurement of delivery capacity.

$$\bigvee_{da\in\mathcal{DA}}\left[\begin{array}{c} Y^{AGR}_{da,j,q} \\ PRE_{j,q,t} = f^{PR}_{da}\left(F^{KJQ}_{k,j,q,t}\right) \quad \forall t\in\mathcal{T} \\ REV_{j,q,t} = f^{REV}_{da}\left(F^{KJQ}_{k,j,q,t}\right) \quad \forall t\in\mathcal{T} \\ \bigvee_{dc\in\mathcal{DC}}\left[\begin{array}{c} Z^{CPTY}_{dc,da,j,q,t} \\ F^{JQ}_{j,q,t} \le \sigma_{dc,da,j,q} \quad \forall t\in\mathcal{T} \\ \varphi_{dc,da,j,q} \le F^{JQ}_{j,q,t} + F^{S}_{j,q,t} \quad \forall t\in\mathcal{T} \\ F^{JQ}_{j,q,t}\cdot h^{\min}_{dc,da,j,q} \le \sum_{k\in\mathcal{K}} F^{KJQ}_{k,j,q,t}\cdot h_k \le F^{JQ}_{j,q,t}\cdot h^{\max}_{dc,da,j,q} \quad \forall t\in\mathcal{T} \end{array}\right] \end{array}\right] \quad \forall\left(j,q\right)\in\mathcal{JQA}$$

(2.72)

Since disjunction (2.72) is exclusive, it already ensures that no more than one delivery agreement is selected along every arc $\left(j,q\right)\in\mathcal{JQA}$. In addition, we impose the logic constraints (2.73)-(2.74) to distinguish between processing agreements and transmission agreements.

$$\underline{\bigvee}_{pa\in\mathcal{PA}} \quad Y^{AGR}_{pa,j,q} \qquad \forall(j,q)\in\mathcal{PSR} \tag{2.73}$$

$$\underline{\bigvee}_{ta\in\mathcal{TA}} \quad Y^{AGR}_{ta,j,q} \qquad \forall(j,q)\in\mathcal{DSR} \tag{2.74}$$

As with the single delivery node problem, we include the following logic constraints (2.75)-(2.78) for the delivery capacity selection.

$$Y^{AGR}_{da,j,q} \quad \Leftrightarrow \quad \bigvee_{dc\in\mathcal{DC}} \quad Z^{CPTY}_{dc,da,j,q,t} \qquad \forall da\in\mathcal{DA},(j,q)\in\mathcal{JQA},t\in\mathcal{T} \tag{2.75}$$

$$Y^{AGR}_{pa,j,q} \quad \Leftrightarrow \quad \bigvee_{pc\in\mathcal{PC}} \quad Z^{CPTY}_{pc,pa,j,q,t} \qquad \forall pa\in\mathcal{PA},(j,q)\in\mathcal{PSR},t\in\mathcal{T} \tag{2.76}$$

$$Y^{AGR}_{ta,j,q} \quad \Leftrightarrow \quad \bigvee_{tc \in \mathcal{TC}} \quad Z^{CPTY}_{tc,ta,j,q,t} \qquad \forall ta \in \mathcal{TA}, (j,q) \in \mathcal{DSR}, t \in \mathcal{T} \quad (2.77)$$

$$\bigvee_{\tau = t - \tau^{A}_{dc,da}}^{t} \quad Y^{CPTY}_{dc,da,j,q,\tau} \quad \Leftrightarrow \quad Z^{CPTY}_{dc,da,j,q,t} \qquad \forall dc \in \mathcal{DC}, da \in \mathcal{DA}, (j,q) \in \mathcal{JQA}, t \in \mathcal{T} \quad (2.78)$$

The disjunction (2.72) is reformulated using big-M constraints. However, since these constraints compare directly to those introduced previously in section 2.5.1 Model Formulation: Single Delivery Node Problem, we do not list them here but refer to Appendix F: Reformulation Multiple Delivery Node Disjunction.

In addition, we explicitly account for the fact that the composition of the extracted gas will generally vary throughout a shale gas development area. Fig. 2.5 below depicts a multiple delivery node gathering system where the shades of grey within the development area indicate qualitatively how the composition of the extracted gas can vary spatially (each shade of grey indicates a different gas quality). These composition variations are important to consider for several reasons. For one, the quality of the gas that can potentially be extracted at every candidate well pad will determine how profitable individual pads may be. Depending on the given forecasts for natural gas and natural gas liquids prices, upstream operators may want to target particular gas qualities at certain times and refrain from extracting these at other times. Secondly, while it is assumed that the composition of the gas is known at every candidate pad, the composition of the gas blend at the splitting node is an unknown since it depends on development decisions that determine which pads produce how much gas over time.

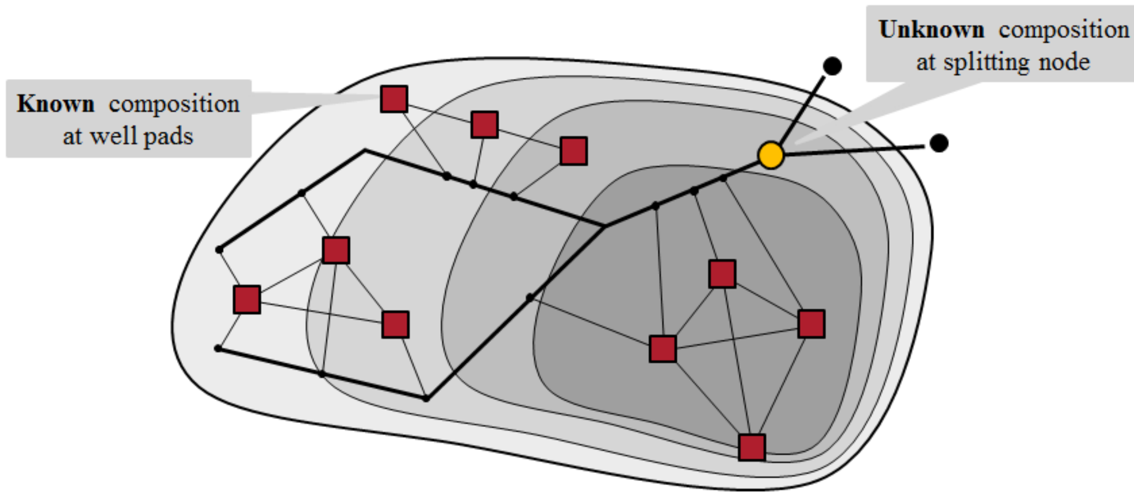

Fig. 2.5: Multiple delivery node development problem indicating gas composition variations (grey shades)

In fact, the composition of the gas blend at a splitting node will generally change over time since individual wells feed different gas qualities into the gathering system at varying production rates throughout the planning horizon. This variation in gas composition adds to the challenge of the overall shale gas development problem since the operators have to satisfy gas quality specifications at the delivery nodes. Interstate transmission pipelines, for instance, will only allow pipeline-quality gas into their pipeline systems. Hence, if operators do not manage to blend the extracted gas such that the gas quality specifications at the delivery nodes are satisfied, then the pipeline companies have the right to refuse the deliveries and can therefore shut-in an entire gathering system. Hence, we reemphasize that the shale gas development problem is *quality-sensitive*.

We note that the spatial composition variations are just as important to consider in the single delivery node problem as in the multiple delivery node problem. However, whereas the single delivery node problem can be modeled as an MILP, we show that in the multiple delivery node problem these gas composition variations lead to nonlinear and nonconvex expressions, which complicate the solution of this problem. For this reason, we examine the component flow balances at the splitting node in greater detail. First, we establish the fact that all gas that is extracted within the development area eventually flows to an intermediate splitting node from where it is distributed along delivery arcs $(j,q) \in \mathcal{JQA}$ to the given set of take-away hubs as seen in Fig. 2.6. This configuration is characteristic for most shale gas gathering systems.

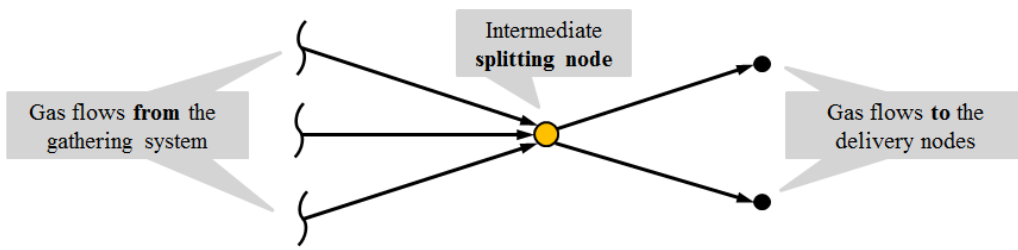

Fig. 2.6: Illustration of gas flows at the intermediate splitting node.

Rather than explicitly balancing all incoming and outgoing component flows at the intermediate splitting node, we propose Eq. (2.79) to ensure that the material balance holds. The left-hand side of Eq. (2.79) sums up the products of all the produced gas flows $F^0_{p,t}$ at the given set of well pads $p \in \mathcal{P}$ and the (known) gas composition at the respective pads – captured by the molar fraction parameter $x^0_{k,p}$. The left-hand side expression has to balance exactly with the component gas flows $F^{KJQ}_{k,j,q,t}$ that are directed to the given set of delivery nodes. The advantage of this formulation is that this expression is entirely linear.

$$\sum_{p \in \mathcal{P}} F^0_{p,t} \cdot x^0_{k,p} = \sum_{(j,q) \in \mathcal{JQA}} F^{KJQ}_{k,j,q,t} \qquad \forall k \in \mathcal{K}, t \in \mathcal{T} \qquad (2.79)$$

However, the component gas flow rates $F_{k,j,q,t}^{KJQ}$ in Eq. (2.79) need to be linked to the total gas flows $F_{j,q,t}^{JQ}$ along the delivery arcs $(j,q) \in \mathcal{JQA}$ through an additional flow balance, Eq. (2.80).

$$F_{k,j,q,t}^{KJQ} = F_{j,q,t}^{JQ} \cdot XF_{k,j,t}^{J} \qquad \forall k \in \mathcal{K}, (\mathrm{j},\mathrm{q}) \in \mathcal{JQA}, t \in \mathcal{T} \tag{2.80}$$

Since both the gas flow rate $F_{j,q,t}^{JQ}$ and the molar fraction $XF_{k,j,t}^{J}$ characterizing the gas composition at the splitting node are continuous decision variables, their product is bilinear, and hence nonlinear and nonconvex. While Eq. (2.80) may seem deceptively simple, it turns the multiple delivery node development problem into a nonconvex MINLP problem and as such complicates the solution of the corresponding optimization problem significantly.

It should be noted here that several alternative formulations for the flow balances at the splitting node can be explored. In particular, we mention the *split flow formulation* (Quesada & Grossmann, 1995) here. However, since it is challenging to specify tight bounds on split variables that lie between zero and one, we prefer to choose the above *composition flow formulation*. This proposed formulation allows us to efficiently impose tight bounds on the molar fraction variables $XF_{k,j,t}^{J}$ as we outline in detail in the next section.

2.6 Solution Strategy

Whereas the single delivery node development problem can be solved to global optimality directly with a mixed-integer linear solver, the more general MINLP multiple delivery node problem calls for a tailored solution strategy. As outlined previously, the non-convexities in the shale gas development problem are due to bilinear terms in the flow balances that arise in the general case of spatial gas composition variations in the development area and multiple downstream delivery nodes. We propose a solution strategy, see Fig. 2.7, which yields near-global and optimal solutions given the presence of the bilinear terms.

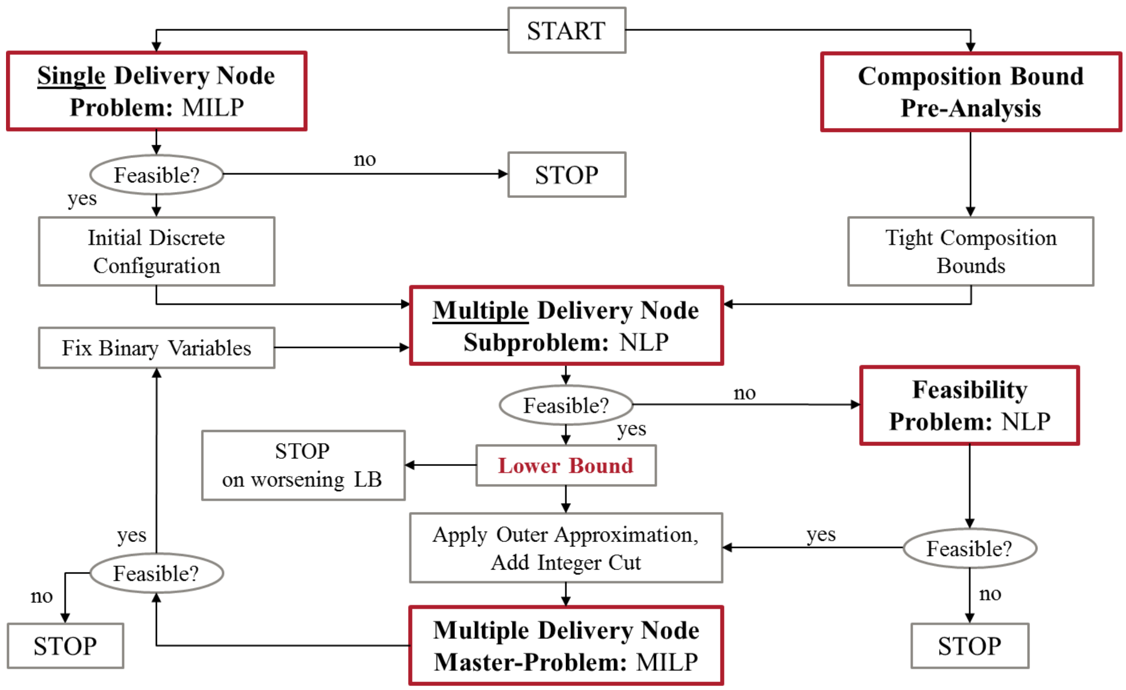

Fig. 2.7: Proposed solution algorithm when using the outer approximation method to decompose the multiple delivery node MINLP

The first step in the proposed strategy involves the solution of the shale gas development problem restricted to a single delivery node, which is a special case of the general multiple delivery node shale gas development problem. As demonstrated previously, this restricted problem can be solved as an MILP even when considering spatial variations in the shale gas composition. The solution of the single delivery node problem provides an initial, feasible solution to the general MINLP, i.e. it represents a *lower bound* to the full-scale MINLP maximization problem. It is important to note here that the solution of the single delivery node problem considers gas quality specifications that may be imposed along all candidate delivery nodes. Hence, the solution of this initialization problem ensures that these constraints are satisfied. Moreover, if the initial single delivery node problem turns out to be infeasible, then we can conclude that the full-scale multiple delivery node problem is infeasible as well. This reasoning holds because additional delivery nodes merely offer opportunities to: a) sell more gas in total, or b) exploit different sales options by, for instance, targeting predominantly dry gas wells for some time and then producing wet gas at other times. We note that when only a few candidate delivery nodes are considered, it can be computationally beneficial to explore these options individually, i.e., selecting the delivery nodes "manually" one by one and determining the most profitable option may take less time than solving for the optimal delivery node explicitly.

In addition, we perform a composition pre-analysis step to identify tight bounds for the molar fractional variables involved in the splitting node flow balance. The reasoning for this pre-analysis is as follows: The composition of the gas at the splitting node is unknown throughout the planning horizon since it depends on which development strategy is selected, i.e., when wells are turned in line, which quality gas the pads produce and how the gas flows are distributed within the gathering system. The composition of the gas at the well pads, on the other hand, is assumed to be known. Hence, this information can be used to specify tight bounds on the composition at the splitting nodes. For example, if the highest methane concentration at any well pad throughout the development area is 94%, then this bound may be imposed on the molar fraction of methane at the splitting node. Regardless of which development strategy is ultimately selected, the composition of the gas at the splitting node may never exceed 94%. The specification of these bounds has a positive impact on the performance of the nonlinear programming (NLP) solver, and is therefore an important step in solving the multiple delivery node development problem.

Provided a feasible solution to the single delivery node problem exists and tight composition bounds are identified, the proposed solution strategy aims to solve the full-scale multiple delivery node problem (an MINLP) next. Technically, we can rely on any MINLP solver capable of solving large-scale problems for this task. The key idea is to initialize the MINLP solver with the solution obtained from solving the single delivery node problem and impose the composition bounds identified in the pre-analysis step. We choose to decompose the MINLP into an NLP subproblem and an MILP master problem in the spirit of the outer approximation method (Duran & Grossmann, 1986) using DICOPT 24.4.1 (Viswanathan & Grossmann, 1990). By default, DICOPT will solve the NLP relaxation of the MINLP program to obtain an initial solution. Instead, we fix all binary decision variables involved in the multiple delivery node problem to the solution of the single delivery node problem. This turns the MINLP into an NLP subproblem. During the first iteration the solution of the subproblem will match the solution of the single delivery node initialization problem, since no additional degrees of freedom are available. The next step in the proposed solution strategy consists of deriving outer-approximations, i.e. linearizations, of all nonlinear constraints at the optimal solution of the preceding NLP subproblem. These linearizations turn the original MINLP into an MILP master problem. This master problem is then solved to identify an alternative solution to the shale gas development problem that has the potential of being optimal, i.e. a set of planning, design and strategic development decisions. Provided the MILP master problem is feasible, the proposed algorithm progresses by fixing all binary variables of the full-scale MINLP to the solution of the master problem, and once again, solving the resulting NLP subproblem. If this subproblem is feasible and yields an improved objective function value, i.e. an increased net present value, the algorithm continues in an iterative fashion to solve a sequence of MILP master problems and NLP subproblems. If during the course of iterations a subproblem is found to be infeasible, a feasibility problem is solved instead, which aims to minimize the violation of the nonlinear constraints. The solution strategy terminates on a worsening lower bound.

It is important to note that the proposed solution method does not guarantee convergence to a global optimum although DICOPT 24.4.1 has provisions to handle non-convexities. The NLP subproblems can get trapped in local solutions, and the linearizations of the master problem can potentially cut into the feasible region of the full-space MINLP yielding suboptimal solutions. Yet, the proposed solution strategy does increase the likelihood of obtaining near-global and optimal solutions, or at least identifying good feasible solutions to realistic problem instances, which are intractable for existing commercial global MINLP solvers such as BARON, SCIP or ANTIGONE.

2.7 Case Studies

The proposed model is applied to two case studies that demonstrate the value of tactical, computational decision-making support tools for long-term shale gas development.

Case Study 1

Our first example is concerned with the expansion of an existing shale gas gathering system. The problem we present is based on a real-world development project that a major upstream operator undertook in the Appalachian Basin. As part of a "lookback" our analysis goes back in time, and assumes the operator had access to the proposed modeling and optimization framework several years ago. Our objective is to use our computational model to identify the most profitable development strategy at the time, and compare it to the actual historic development. This direct comparison allows us to quantify the economic potential of the proposed models. For confidentiality reasons we cannot disclose the exact location of the gathering system nor the particular time period the analysis covers.

Fig. 2.8 shows the gathering system as it exists at the beginning of the planning horizon (Note: this schematic is not drawn to scale). The solid orange ovals indicate existing well pads that are already producing gas, whereas the dashed green ovals represent candidate well pads that are considered for development. Long-term production and gas quality forecasts are available for all candidate and producing pads. Based on the given acreage position within the development area, only a certain number of wells can be developed at every candidate pad. The solid lines in Fig. 2.8 specify existing pipelines that have already been laid out in the development area; the numerical figures along the individual segments indicate the size of those pipelines in inches. Evidently, the size of the installed pipelines constrains the flow capacity along every pipeline segment. In addition, the illustration depicts candidate pipeline routes as dashed lines. New pipelines may be laid out along these routes or besides existing pipelines. All of the gas that is extracted within the considered development area is delivered to a single compressor station. In Fig. 2.8 this compressor station is represented by a solid grey triangle. At the beginning of the planning horizon this station provides 3,535 kW of compression power.

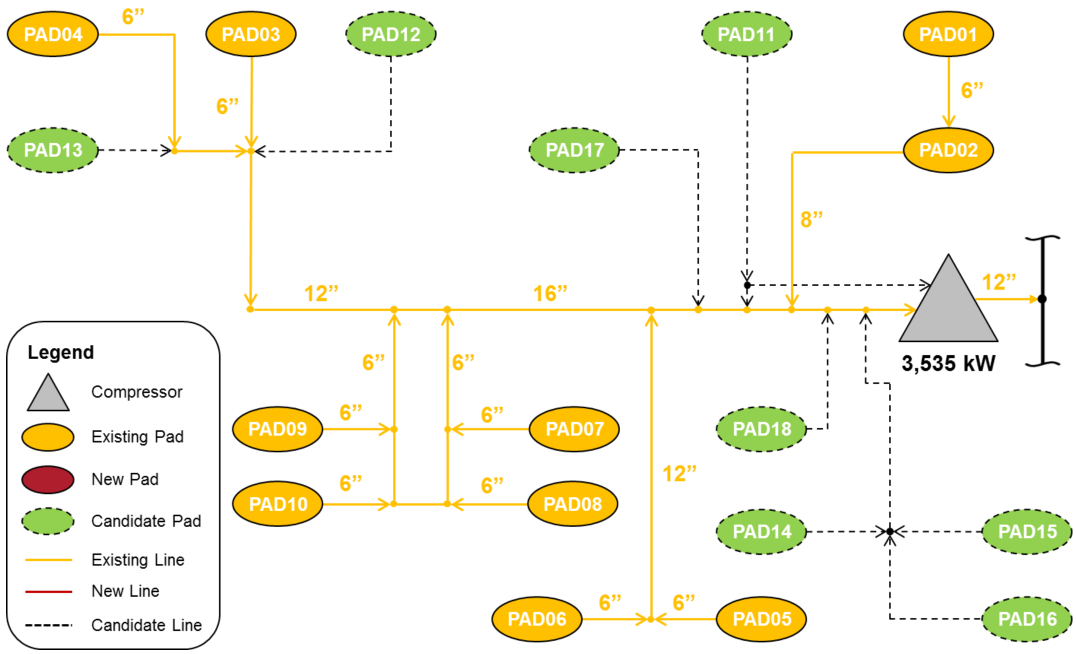

Fig. 2.8: Given gathering system superstructure for Case Study 1

It is assumed that the well pads feed into the gathering system at approximately 1.7 MPa, the compressor suction pressure is set to 1.3 MPa (due to the pressure drop along the gathering lines) and the compressor discharges gas into the delivery line at roughly 8.3 MPa. The development area produces predominantly wet gas with a methane concentration between 77% and 83%, i.e., the extracted raw gas needs to be purified and fractionated at a processing facility outside of the development area (not depicted in Fig. 2.8). Hence, gas quality specifications are not imposed at the delivery node. We consider a two year planning horizon, and assume that the gathering system is not capacity-constrained downstream during this time. All candidate wells are clear-to-build within the given time frame. Due to the limited planning horizon, we do not consider the arrangement of delivery agreements as part of this case study.

After discretizing the two year planning horizon into months, the problem involves a total of 30,336 binary variables, 4,686 continuous variables and 12,817 constraints. Given that this development project corresponds to a single delivery node problem we can formulate it as an MILP while still considering variable gas composition at the given set of well pads. Using IBM CPLEX 12.6.0.0 in GAMS 24.2.2 the problem, which has an LP relaxation gap of 16%, can be solved to a 3.5% optimality gap within 2.5 hours on an Intel i7, 2.93 Ghz machine with 12 GB RAM exploring a total of 125,000 nodes in the branch and bound tree. The predicted NPV is 214 million USD. Fig. 2.9 shows the optimal gathering system at the end of the planning horizon.

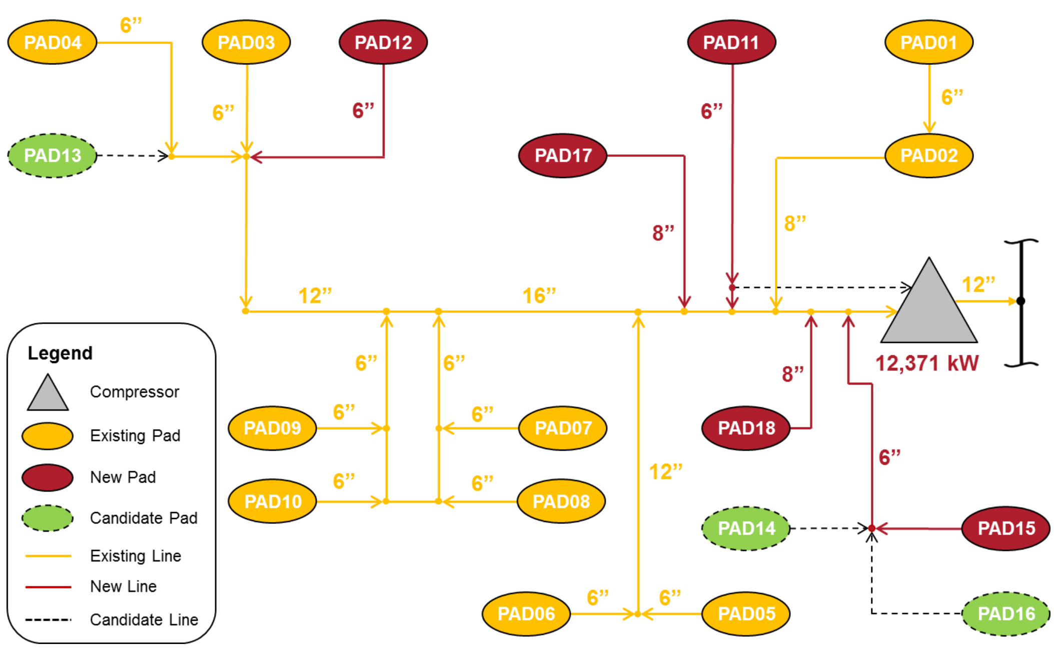

Fig. 2.9: Optimal gathering system at the end of the planning horizon for Case Study 1

In Fig. 2.9 the solid red ovals represent candidate well pads that are meant to be developed within the planning horizon, the solid red lines show newly installed pipelines, and the numbers next to these segments specify the selected pipeline sizes in inches. Finally, Fig. 2.9 indicates a proposed expansion of the available compression power to 12,371 kW. It is interesting to note here that the optimizer chooses not to develop a total of three candidate pads, namely PAD13, PAD14 and PAD16 – our a posteriori analysis suggests that this is most likely due to their unfavorable production forecasts. Along with the gathering system, the solution reveals the optimal development strategy as seen in the left chart in Fig. 2.10.

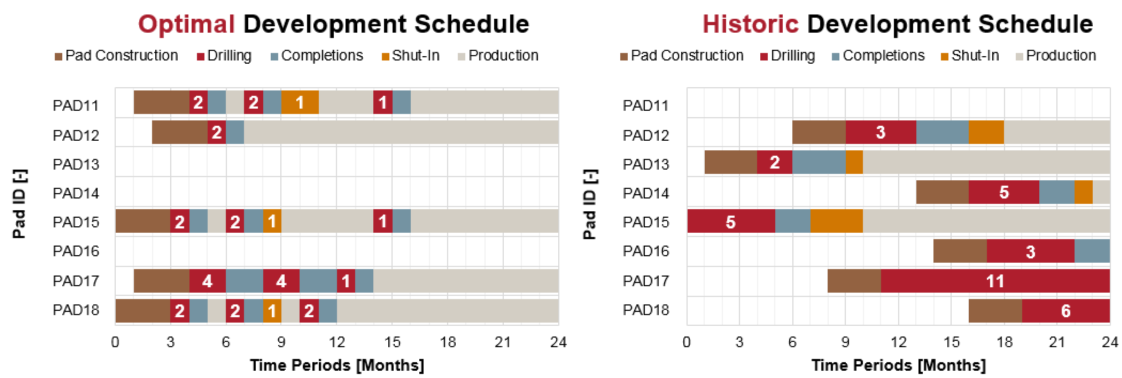

Fig. 2.10: Optimal development schedule (left) and historic development schedule (right) for Case Study 1

This Gantt chart displays the candidate pads on the left axis and the two year planning horizon discretized by 24 time periods (months) on the bottom axis. The chart shows when pads are built (brown bars), how many wells are drilled over which period of time (white numbers in red bars), how long it takes to complete the wells (blue bars), if wells are shut-in temporarily and for how long (white numbers in orange bars), and when the respective pads start to produce gas (gray bars). It is apparent from Fig. 2.10 that the optimal development strategy is characterized by a large number of so-called *return-to-pad operations*, i.e., the optimizer chooses to drill, complete and turn in-line a relatively small number of wells, but then returns to the same pad eventually to repeat the process. For instance, rather than developing 9 wells all at once at candidate pad PAD17, the optimizer "splits the pad". It proposes to build a pad, move a rig onto location, drill 4 wells, move the rig off location, complete the 4 wells, turn them in-line, move a rig back onto location again, drill another 4 wells, move the rig off location again, complete these 4 wells, turn them in-line, etc. These return-to-pad operations are rarely seen in practice as can be seen from the right chart in Fig. 2.10, which depicts the historic development strategy for this system.

The historic development schedule does not involve any return-to-pad operations. In fact, the schedule gives reason to believe that the development strategy at the time was driven by trying to drill as many wells as possible at every given candidate location. At PAD17, for instance, the operator decided to drill and complete 11 wells in one sequence, and eventually turned all of them in-line at once. The chart reveals that the drilling operation itself lasted over a year. During this time, the pad was not producing any gas. The optimal development strategy, on the other hand, proposes to drill and complete only 4 wells upfront – which lasts merely 4 months. Upon completion these 4 wells already start to produce gas and the operator sees an early return on investment. This observation holds for several other pads as well. In all of these cases the return-to-pad operations allow the operator to feed gas into the system much sooner than the historic development strategy.

Furthermore, return-to-pad operations also allow the operators to use smaller size pipelines for their gathering systems. Usually, when a large number of wells on a pad are turned in-line all at once, the respective pipelines need to be designed to handle large quantities of gas in a short period of time. However, considering the characteristic shale gas decline curves, these pipelines are oftentimes oversized and underutilized in a matter of months. With return-to-pad operations, on the other hand, the flow pipelines can be sized smaller because only a few wells are turned in-line at one time. Moreover, since new wells are continuously brought online, the pipelines are also kept “full” over a longer period of time which improves the overall equipment utilization. In this context return-to-pad operations appear especially suitable for shale gas development projects.

Fig. 2.11 shows the production profiles based on the optimal and the historic development strategies. In the left chart, displaying the optimal production profile, it can be seen that at first, the system produces roughly 1.7 x 10^6 m^3/day until time period 7 when the production is increased to nearly 4.5 x 10^6 m^3/day. Thereafter, the production profile remains at a relatively steady level, which indicates a fairly high equipment utilization that should generally benefit the arrangement of downstream delivery agreements. Historically, however, the gathering system was producing merely 2.5 x 10^6 m^3/day within the given time frame as can be seen in the right chart in Fig. 2.11.

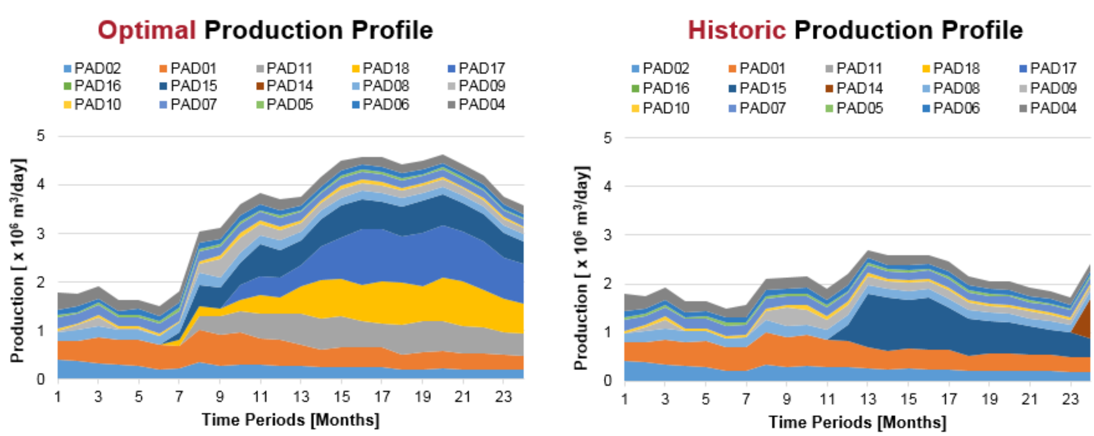

Fig. 2.11: Optimal production profile (left) and historic production profile (right) for Case Study 1

As indicated earlier, the proposed development strategy yields a positive NPV of 214 million USD. Total development expenses amount to 360 million USD. Well development expenses, i.e., for drilling, fracturing and completing the wells, account for 43% of the total expenses, royalties take up 21% and the compressor expansion requires another 10%. In comparison, the historic development strategy yields an NPV of merely 81 million USD. Given the overall increase in gas production the proposed development strategy appears much more favorable economically. Our results suggest that a shift in shale gas production philosophy could have a major impact on the profitability of shale gas development projects. Considering the time value of money and the characteristic shale gas decline curves return-to-pad operations appear very promising and may be much more suitable than previous development strategies aimed at simply drilling as many wells as possible at any given pad.

Case Study 2

In our second example, we study a greenfield development project over a 6 year planning horizon. In this case study we explicitly consider the arrangement of processing agreements. Fig. 2.12 shows the given gas gathering superstructure including candidate pads, pipeline routes and delivery nodes.

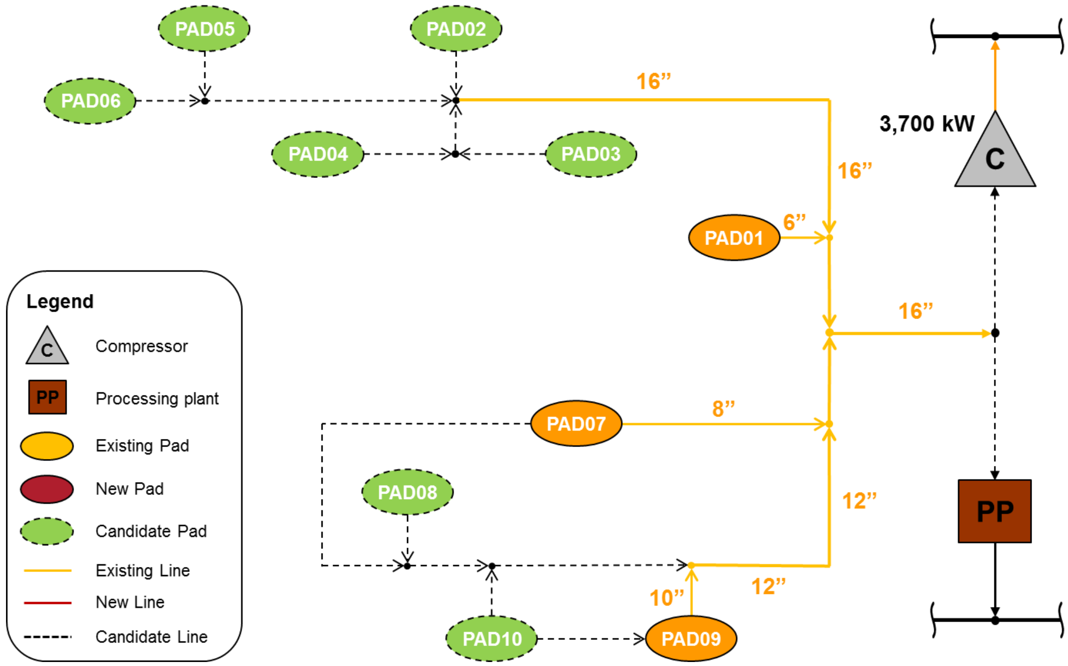

Fig. 2.12: Given gathering system superstructure for Case Study 2

We assume that the operator has already laid out two gathering lines: one 16” line extending to the North and one 12” line extending to the South. However, it has not been decided yet whether the extracted gas will: a) be fed directly into a transmission line using an existing compressor station at which 3,700 kW of compression power are available, or b) delivered to a natural gas processing plant that is operated by an independent midstream company. Gas deliveries to the compressor station must meet gas quality specifications, i.e., the heating value of the gas must be at least 34 MJ/m^3 (900 Btu/scf) and may not exceed 45 MJ/m^3 (1,200 Btu/scf). Gas deliveries to the processing plant on the other hand require the arrangement of strategic processing agreements. The operator can choose between one of three different contract types, either: a) a fee-based, b) a percent-of-proceeds, or c) a keep-whole processing agreement. For either one the operator may procure a) limited, b) average or c) extensive processing capacity at any point in time throughout the planning horizon. Table 2.1

summarizes the conditions of all available processing agreements in terms of minimum delivery quantities, maximum delivery capacities and durations of contracts.

Agreement type	Keep-Whole			Percent-of-Proceeds			Fee-Based		
Processing capacity	Limited	Average	Extensive	Limited	Average	Extensive	Limited	Average	Extensive
Minimum delivery [x 10^6 m^3/day]	0	0.85	1.7	0	0.85	1.7	0	0.85	1.7
Maximum delivery [x 10^6 m^3/day]	0.85	1.1	2.3	0.85	1.1	2.3	0.85	1.1	2.3
Duration of contract [months]	4	12	24	4	12	24	4	12	24

Table 2.1: Available processing agreements and their conditions for Case Study 2

For simplicity, we assume that direct gas deliveries via the compressor station are not governed by any particular transmission agreements. Out of the given ten pads exactly three pads have already been pre-selected for development, namely PAD01, PAD07 and PAD09 – all other pads are true candidates for development. We assume that the gas composition varies significantly within the considered development area: the methane concentration, for instance, varies gradually between 79% in the Northwest (PAD05 and PAD06) and 97% in the South (PAD09, PAD10), i.e., the gas becomes “wetter” in the northwestern direction. Based on the projected acreage position all pads are subject to *clear-to-build constraints*, i.e., they may not be developed prior to a given start date.

Since this development project considers both variable gas composition and a total of two candidate delivery nodes (the compressor and the processing plant) our formulation yields a nonconvex MINLP. Based on a monthly discretization of the planning horizon the problem involves 59,680 binary variables, 21,707 continuous variables, 56,859 constraints and 1,008 bilinear terms. We use the proposed solution algorithm as described in section 2.6 Solution Strategy to identify the most profitable development strategy. For this purpose we solve the single delivery node (SDN) problem first. Using IBM CPLEX 12.6.0.0 in GAMS 24.2.2 this problem can be solved to a 5% relative optimality gap in slightly under 2 hours on an Intel i7, 2.93 Ghz machine with 12 GB RAM. This solution yields a positive NPV of 187.2 million USD. Fig. 2.13 depicts the optimal gathering system when the optimizer is restricted to select only one delivery node.

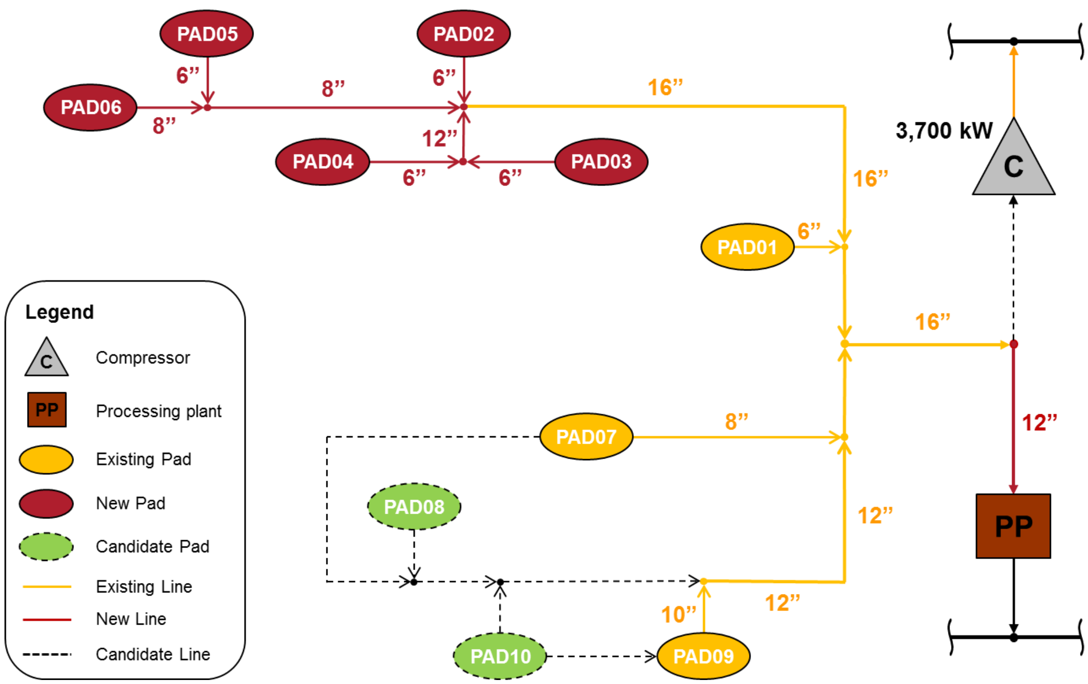

Fig. 2.13: Optimal gathering system for the SDN problem of Case Study 2

The illustration in Fig. 2.13 reveals that two candidate well pads (PAD08 and PAD10) remain undeveloped – most likely due to their unfavorably “dry” gas quality. All other candidate pads are developed by the end of the planning horizon. The processing plant is selected as the exclusive delivery node, i.e., all the produced gas is purified and fractionated, which allows the upstream operator to market the extracted

NGLs at favorable prices. In this case the optimizer chooses to select a *fee-based* processing agreement to have the raw gas processed. The illustration in Fig. 16 shows which processing agreements need to be arranged as part of the proposed development strategy: three limited capacity contracts providing no more than 0.85 x 10^6 m^3/day of processing capacity over 4 months each, and three extensive capacity contracts spanning 2 years each. The latter extensive agreements require the upstream operator to deliver at least 1.7 x 10^6 m^3/day, but no more than 2.3 x 10^6 m^3/day of raw gas. It is important to note that these are take-or-pay contracts, meaning that the operator does not necessarily have to meet the minimum delivery requirements ("take the capacity") but will have to pay for unutilized processing capacity ("pay for capacity"). Fig. 2.14 shows that at the end of the planning horizon the proposed development strategy does not succeed at delivering enough gas to take full advantage of the procured processing capacity.

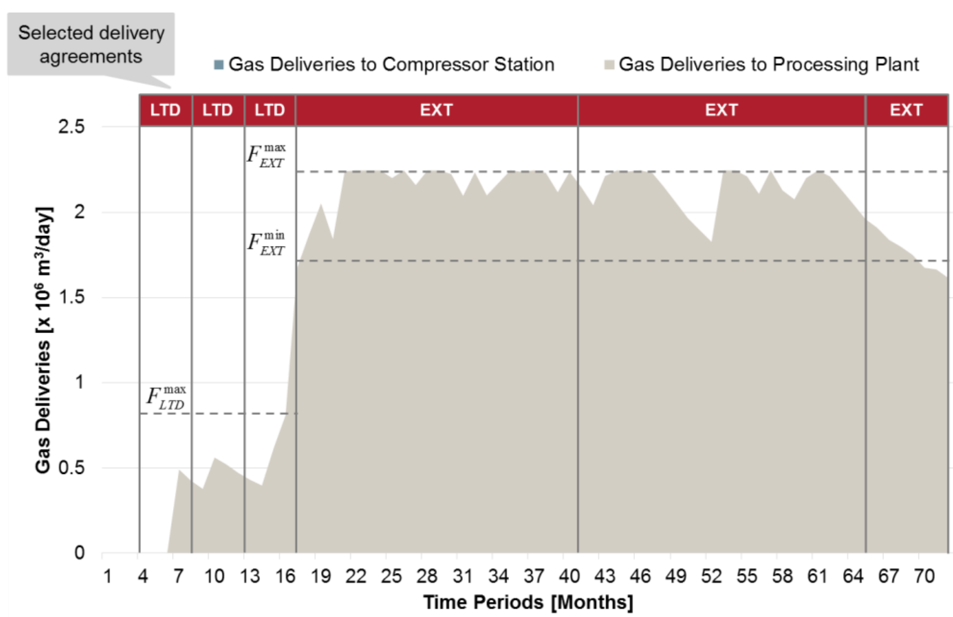

Fig. 2.14: Gas deliveries and selected processing agreements for the SDN problem of Case Study 2

As outlined in section 2.6 Solution Strategy, we use the solution obtained from solving the SDN problem to initialize the multiple delivery node (MDN) problem. By design, the SDN solution is a feasible solution to the MDN problem. Using DICOPT 24.2.1, IBM CPLEX 12.6.0.0 and CONOPT 3 24.4.1 in GAMS 24.2.2 on the same computing machine as before, the algorithm terminates after a little less than an hour and reports a positive NPV of 197.4 million USD – a 5% increase compared to the solution of the SDN problem. DICOPT requires a total of two iterations to identify this solution. The major computational effort lies in solving the MILP master problems, whereas the NLP subproblems are solved within less than 15 seconds each. Provided the same initial solution as DICOPT 24.2.1, the best upper bound BARON 15.6.5 reports – after 16 hours on the computing machine above – is 252.9 million USD.

The illustration on the left in Fig. 2.15 shows the proposed development strategy for the proposed gathering system. As seen in the previous case study, the development is characterized by a large number of return-to-pad operations. The schedule also reveals increased development activity early on in the planning horizon, which makes economic sense considering the time value of money. The illustration on the right in Fig. 2.15 shows the matching gas production profile over time, and highlights which pads contribute how much gas to the overall production. Fig. 2.16 shows the proposed gathering system for the multiple delivery node problem.

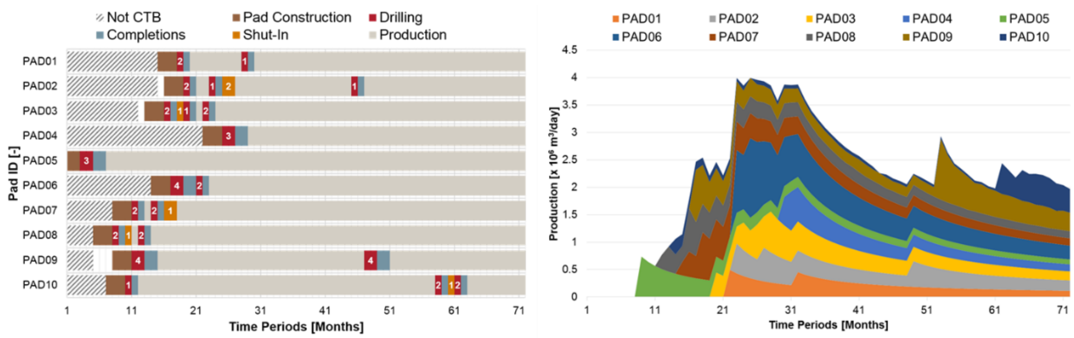

Fig. 2.15: Proposed development strategy (left) and gas production profile (right) for the MDN problem of Case Study 2

The proposed gathering system in Fig. 2.16 reveals that now all candidate well pads are developed within the planning horizon - contrary to the solution of the single delivery node problem. Moreover, delivery pipelines are laid out to both the processing plant and the compressor station, indicating that an additional delivery node does improve the profitability of the development project.

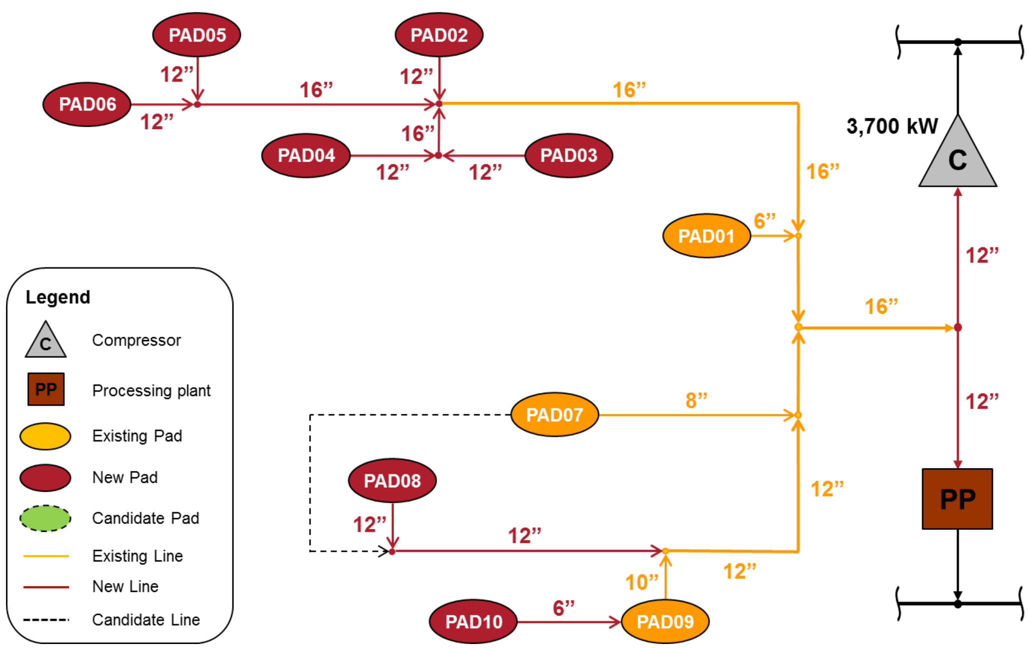

Fig. 2.16: Proposed gathering system for the MDN problem of Case Study 2

Fig. 2.17 shows how much gas is delivered to the processing plant and how much gas is sent to the compressor station over time. In addition, the illustration also indicates how much processing capacity needs to be procured to fit the proposed development strategy: one limited capacity arrangement and three extensive processing capacity contracts. In this case too, the optimizer proposes to arrange a *fee-based* processing agreement with the midstream company. We find that the selection of the processing agreement has a significant impact on the profitability of the development project. Given a *keep-whole* processing agreement the NPV for the exact same development problem reduces to 126.8 million USD – a 36% reduction compared to the solution we obtain with a *fee-based* agreement. Moreover, for a *percent-of-proceeds* processing agreement the NPV diminishes to a mere 102.1 million USD – 95.3 million USD less than the solution we report.

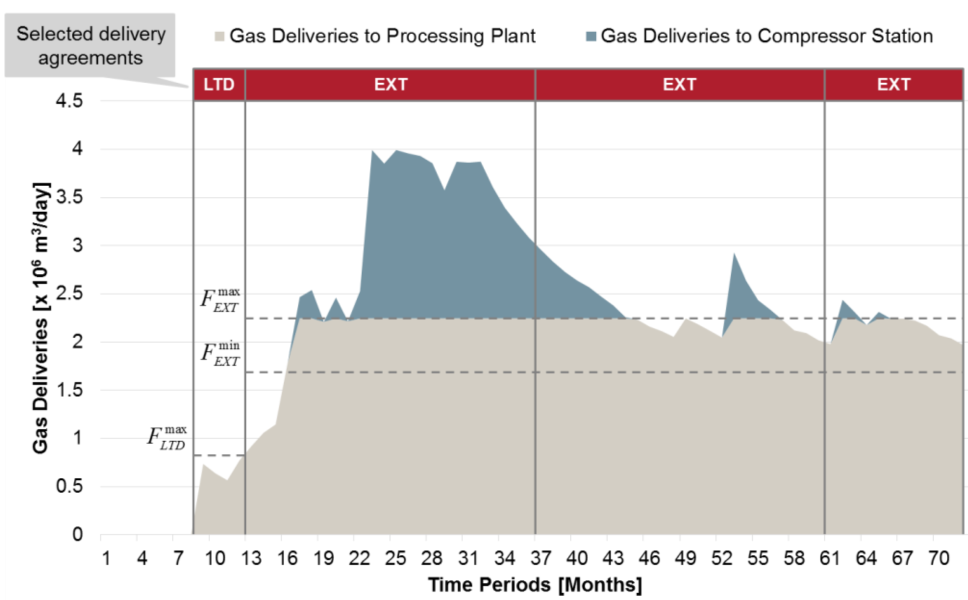

Fig. 2.17: Gas deliveries and selected processing agreements for the MDN problem of Case Study 2

Upon closer examination it becomes apparent that the direct delivery arc via the compressor station is used to market "excess" gas that cannot be processed by the processing plant due to capacity constraints. Since we assume that these gas deliveries are not governed by any particular transmission agreements they are much easier to arrange – provided the gas quality specifications are satisfied. However, it is important to note that the NGLs that are marketed along the direct delivery route are sold at the price of methane – which is far less favorable than typical liquids prices. In this particular case, it is not necessary to install additional compression power at the compressor station since the available 3,700 kW are sufficient. Finally, we present a breakdown of the overall development expenses in the left illustration of Fig. 2.18.

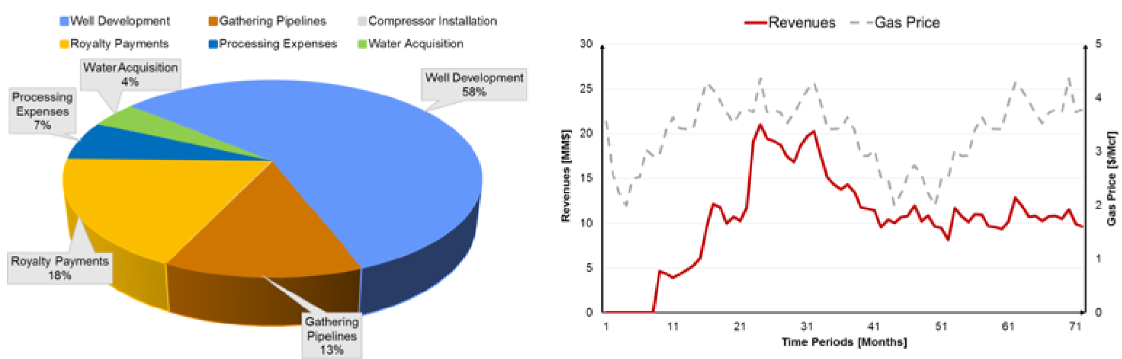

Fig. 2.18: Breakdown of development expenses (left) and projected revenues (right) for the MDN problem of Case Study 2

The chart on the left in Fig. 2.18 reveals that well development expenses account for more than half of all expenses, followed by royalty payments at nearly 20% and pipeline installation expenses at 13%. In total, the development expenses amount to 441.5 million USD. The chart on the right in Fig. 20 shows the projected revenues that yield an NPV of 197.4 million USD based on the given gas price forecast. It can be seen that the revenues are very sensitive to gas price fluctuations and that the solution exploits the projected peak in price forecasts between time periods 19-37.

Altogether, this second case study demonstrates the value of having additional take-away options for shale gas gathering systems. Chances of being capacity-constrained at some point in time throughout the development operation diminish significantly when multiple delivery nodes can be selected. In addition, these configurations allow the operators to exploit fluctuations in natural gas and NGL prices: when NGL prices are high it makes economic sense to purify and fractionate raw gas, whereas low NGL prices favor direct deliveries into transmission pipelines such that processing expenses can be avoided.

2.8 Conclusions

In this chapter, we have presented a large-scale, deterministic, multi-period, MINLP model to address the long-term shale gas development problem given a superstructure that reflects real world gathering systems. We exploited the discrete nature of the design variables involved in this problem, i.e., standardized pipeline diameters and compressor sizes, to systematically derive disjunctive models using Generalized Disjunctive Programming (GDP). By enforcing discrete equipment sizes we were able to use mixed-integer linear constraints to capture economies of scale that are typically expressed by concave investment cost functions. Furthermore, we extended the scope of the shale gas development problem to account for the arrangement of processing and transmission agreements, which impose additional restrictions on shale gas development strategies. Here, too, we relied on disjunctive models which are characterized by a set of embedded disjunctions that allowed us to exploit the inherent structure of the strategic decision-making process.

Finally, we emphasized that the shale gas development problem is quality sensitive, i.e., spatial variations in the composition of the extracted gas need to be taken into consideration. We proposed a nonconvex MINLP formulation to capture these composition variations, and we developed a solution strategy that yields the global optimum for the case of a single delivery node, while it yields near-global solutions for the case of multiple delivery nodes. The two case studies we presented clearly demonstrate that return-to-pad operations, improved equipment utilization and the arrangement of strategic delivery agreements can increase the profitability of shale gas development projects by several million U.S. dollars. With regards to the arrangement of delivery agreements we note that, in practice, upstream operators evidently cannot arrange delivery agreements of their own accords. Instead, these agreements are the result of complex, iterative, and bilateral negotiation processes – between operators and processors or operators and transmission lines. We did not capture these negotiations in this work. Rather, the objective of this work was to develop a framework that allows upstream operators to identify the optimal delivery agreements for their particular gathering systems. In that sense, the proposed extension of the shale gas development model to account for strategic decisions is intended to be used as a negotiation support tool for upstream operators.

We conclude that the proposed computational decision-making framework can support upstream operators significantly in identifying cost-effective development strategies, and that it can help them remain profitable even in low-price environments.

Future work will exploit pressure optimization opportunities within the gathering system, and address uncertainties and disruptions realizing throughout the planning horizon.

2.9 Nomenclature

Sets

$c \in \mathcal{C}$	Compressor sizes
$d \in \mathcal{D}$	Pipeline diameters
$f \in \mathcal{F}$	Fresh water sources
$p \in \mathcal{P}$	Well pads
$p \in \mathcal{CP}$	Candidate well pads; subset of well pads
$p \in \mathcal{PP}$	Producing well pads; subset of well pads
$j \in \mathcal{J}$	Gathering junctions
$k \in \mathcal{K}$	Natural gas components
$k \in \mathcal{NGL}$	Natural gas liquids; subset of natural gas components
$n \in \mathcal{N}$	Number of wells
$q \in \mathcal{Q}$	Delivery nodes
$r \in \mathcal{R}$	Drilling rigs
$t \in \mathcal{T}$	Time periods
$da \in \mathcal{DA}$	Delivery agreements
$pa \in \mathcal{PA}$	Processing agreements; subset of delivery agreements
$ta \in \mathcal{TA}$	Transmission agreements; subset of delivery agreements
$dc \in \mathcal{DC}$	Delivery capacities
$tc \in \mathcal{TC}$	Transmission capacities; subset of delivery capacities
$pc \in \mathcal{PC}$	Processing capacities; subset of delivery capacities
$(p, \hat{p}) \in \mathcal{PPA}$	Well pipeline arcs
$(p, j) \in \mathcal{PJA}$	Flow pipeline arcs
$(j, \hat{j}) \in \mathcal{JJA}$	Gathering pipeline arcs
$(j, q) \in \mathcal{JQA}$	Delivery pipeline arcs
$(j, q) \in \mathcal{DSR}$	Direct sales routes; subset of delivery pipeline arcs
$(j, q) \in \mathcal{PSR}$	Processing sales routes; subset of delivery pipeline arcs
$(p, j, \hat{j}) \in \mathcal{NDA}$	Non-decreasing pipeline capacity arcs

Binary Variables

$y_{n,p,t}^{DRILL}$	Active if n wells drilled at well pad p in time period t
$y_{n,p,t}^{CON}$	Active if well pad p fitting $n \in \mathcal{N}$ wells under construction in time period t
$y_{r,p,t}^{RIG}$	Active if drilling rig r on location at well pad p in time period t
$y_{d,j,q,t}^{PIPE}$	Active if pipeline diameter d installed between junction j and delivery node q in time period t
$y_{c,j,q,t}^{COMPR}$	Active if compressor size c installed between junction j and delivery node q in time period t
$z_{d,j,q,t}^{PIPE}$	Active if pipeline diameter d available between junction j and delivery node q in time period t
$z_{c,j,q,t}^{COMPR}$	Active if compressor size c available along delivery arc j,q in time period t
$y_{j,q}^{DEL}$	Active if delivery arc j,q selected for raw gas delivery
$y_{da,j,q}^{AGR}$	Active if delivery agreement da arranged along delivery arc j,q
$y_{dc,da,j,q,t}^{CPTY}$	Active if delivery capacity dc selected within delivery agreement da along delivery arc j,q in time period t
$z_{dc,da,j,q,t}^{CPTY}$	Active if delivery capacity dc available within delivery agreement da along delivery arc j,q in time period t

Boolean Variables

$Y_{d,j,q,t}^{PIPE}$	True if pipeline diameter d installed between junction j and delivery node q in time period t
$Y_{c,j,q,t}^{COMPR}$	True if compressor size c installed between junction j and delivery node q in time period t
$Z_{d,j,q,t}^{PIPE}$	True if pipeline diameter d available between junction j and delivery node q in time period t
$Z_{c,j,q,t}^{COMPR}$	True if compressor size c available junction j and delivery node q in time period t

$Y_{j,q}^{DEL}$	True if arc j,q selected for raw gas delivery
$Y_{da,j,q}^{AGR}$	True if delivery agreement da arranged along delivery arc j,q
$Y_{dc,da,j,q,t}^{CPTY}$	True if delivery capacity dc selected within delivery agreement da along delivery arc j,q in time period t
$Z_{dc,da,j,q,t}^{CPTY}$	True if delivery capacity dc available within delivery agreement da along delivery arc j,q in time period t

Continuous Variables

$F_{p,t}^{0}$	Flow rate produced gas at well pad p in time period t
$F_{p,\mathrm{j},\mathrm{q},t}^{0}$	Flow rate produced gas at well pad p intended for delivery arc j,q in time period t (disaggregated variable)
$F_{p,j,t}^{PJ}$	Gas flow rate from well pad p to junction j in time period t
$F_{p,\hat{p},t}^{PP}$	Gas flow rate from well pad p to well pad $\hat{p}$ in time period t
$F_{j,\hat{j},t}^{JJ}$	Gas flow rate from junction j to junction $\hat{j}$ in time period t
$F_{j,q,t}^{JQ}$	Gas flow rate along delivery arc j,q in time period t
$F_{k,j,q,t}^{KJQ}$	Gas flow rate component k along delivery arc j,q in time period t
$F_{j,q,t}^{S}$	Slack gas flow rate along delivery arc j,q in time period t
$XF_{k,j,t}^{J}$	Molar fraction gas component k at junction j in time period t
DVE_t	Development expenses (drilling, fracturing, completion) in time period t
FPE_t	Flow pipeline construction expenses in time period t
GPE_t	Gathering pipeline construction expenses in time period t
DPE_t	Delivery pipeline construction expenses in time period t
CIE_t	Compressor installation expenses in time period t
COE_t	Compressor operating expenses in time period t
PME_t	Production and maintenance expenses in time period t
RRE_t	Royalty expenses in time period t
RDE_t	Drilling rig downtime expenses in time period t

RTE_t	Drilling rig transition expenses in time period t
$RTE^{+}_{r,p,t}$	Drilling rig transition expenses in time period t
$RTE^{-}_{r,p,t}$	Drilling rig transition expenses in time period
SCE_t	Well site construction expenses in time period t
PRE_t	Processing expenses in time period t
$PRE_{j,q,t}$	Processing expenses along delivery arc j,q in time period t
REV_t	Revenues from natural gas sales in time period t
$REV_{j,q,t}$	Revenues from natural gas sales along arc j,q in time period t
$NWD_{p,t}$	Number of wells that completed at well pad p in time period t
$NWP_{p,t}$	Number of wells producing shale gas at well pad p in time period t
$FWS_{f,p,t}$	Freshwater supply from source f to well pad p in time period t
NPV	Net present value of the shale gas development project

Parameters

dr	Discount rate
nd	Number of days per time period
$x^{0}_{p,k}$	Molar fraction shale gas component k produced gas at well pad p
$p_{k,q,t}$	Price of natural gas component k at delivery node q in time period t
α^{D}	Well development cost coefficient
α^{A}_{da}	Processing cost coefficient for delivery agreement da
α^{P}	Pipeline construction cost coefficient
α^{C}	Compressor installation cost coefficient
α^{I}	Production cost coefficient
α^{O}	Compressor operating cost coefficient
α^{W}	Fresh water acquisition cost coefficient
α^{R}	Rig transition cost coefficient
α^{RD}	Rig downtime cost coefficient

α^S	Site construction cost coefficient
β^D	Well development cost exponent
β^P	Pipeline construction cost exponent
β^C	Compressor installation cost exponent
δ_d	Commercially available pipeline diameters
$\delta^0_{j,q}$	Pre-installed pipeline capacity (diameter) along arc j,q
$\delta^0_{j,\tilde{j}}$	Pre-installed pipeline capacity (diameter) along arc $j,\tilde{j}$
$\delta^0_{\mathrm{i,j}}$	Pre-installed pipeline capacity (diameter) along arc i, j
$\delta^0_{\mathrm{i},\tilde{i}}$	Pre-installed pipeline capacity (diameter) along arc i, j
$l_{j,q}$	Pipeline segment length from junction j to delivery node q
$l_{j,\hat{j}}$	Pipeline segment length from junction j to junction $\hat{j}$
$l_{p,j}$	Pipeline segment length from well pad p to junction j
$l_{p,\hat{p}}$	Pipeline segment length from well pad p to well pad $\hat{p}$
$l_{f,p}$	Pipeline segment length from fresh water source f to well pad p
λ_c	Commercially available compressor sizes
$\lambda^0_{j,q}$	Pre-installed compression power along arc j,q
rr_p	Royalty rate at well pad p
τ^S_p	Site construction lead time well pad p
τ^{WD}_n	Well development lead time for a total of n wells
τ^{DR}_n	Drilling lead time for a total of n wells being drilled
τ^{HF}_n	Fracturing lead time for a total of n wells being completed
τ^P	Pipeline construction lead time
τ^C	Compressor installation lead time
$\tau^A_{dc,da}$	Agreement length for delivery capacity dc under delivery agreement
$n^{max}_{p,t}$	Maximum number of wells permitted at well pad p in time period t

$\gamma_{p,\mathrm{t}-\tau}$	Well productivity at well pad p for a well of age $a = t - \tau$ time periods
$\sigma_{dc,da,j,q}$	Maximum delivery quantity under delivery capacity dc within delivery agreement da along delivery arc j,q
$\varphi_{dc,da,j,q}$	Minimum delivery quantity under delivery capacity dc within delivery agreement da along delivery arc j,q
k^P	Pipeline capacity coefficient
k^C	Compressor capacity coefficient
fwd_p	Specific fresh water demand per well pad p
$fwa_{f,t}$	Fresh water availability at fresh water source f in time period t
$f_{j,q,t}^{max}$	Maximum molar gas flowrate along delivery arc j,q in time period t
$rev_{j,q,t}^{max}$	Maximum revenues along delivery arc j,q in time period t
$capex_t^{max}$	Capital expenditures limit
h_k	Heating value gas component k
$h_{dc,da,j,q}^{\min}$	Minimum heating value imposed for delivery capacity dc within delivery agreement da along delivery arc j,q
$h_{dc,da,j,q}^{\max}$	Maximum heating value imposed for delivery capacity dc within delivery agreement da along delivery arc j,q
$m_{da,j,q}^{PRE}$	Big-M parameter for processing expenses under delivery agreement da along delivery arc j,q
$m_{da,j,q}^{REV}$	Big-M parameter for revenues under delivery agreement da along delivery arc j,q
$m_{dc,da,j,q}^{\varphi}$	Big-M parameter for minimum delivery quantity under delivery capacity dc within delivery agreement da along delivery arc j,q
$m_{dc,da,j,q}^{\sigma}$	Big-M parameter for maximum delivery quantity under delivery capacity dc within delivery agreement da along delivery arc j,q

$m^{h^{min}}_{dc,da,j,q}$ Big-M parameter for minimum heating value specification under delivery capacity dc within delivery agreement da along delivery arc j,q

$m^{h^{max}}_{dc,da,j,q}$ Big-M parameter for maximum heating value specification under delivery capacity dc within delivery agreement da along delivery arc j,q

CHAPTER 3

Mixed-Integer Programming Models for Impaired Water Management in Active Shale Gas Development Areas

3.1 Introduction

Fig. 3.1 highlights the scope of this work and demonstrates selected degrees of freedom within water management operations in active shale gas development areas. At the center of the illustration lies a candidate well pad. A candidate well pad is a location where an upstream operator intends to drill, fracture and complete a set of shale gas wells in the foreseeable future. Since this work focuses on development activity in low-price environments, we assume that the timing of individual fracturing jobs is flexible and has not been determined yet. Hence, the fracturing schedule is a significant degree of freedom. In order to fracture any of the selected wells on a particular candidate pad, the producer needs to acquire significant volumes of water.

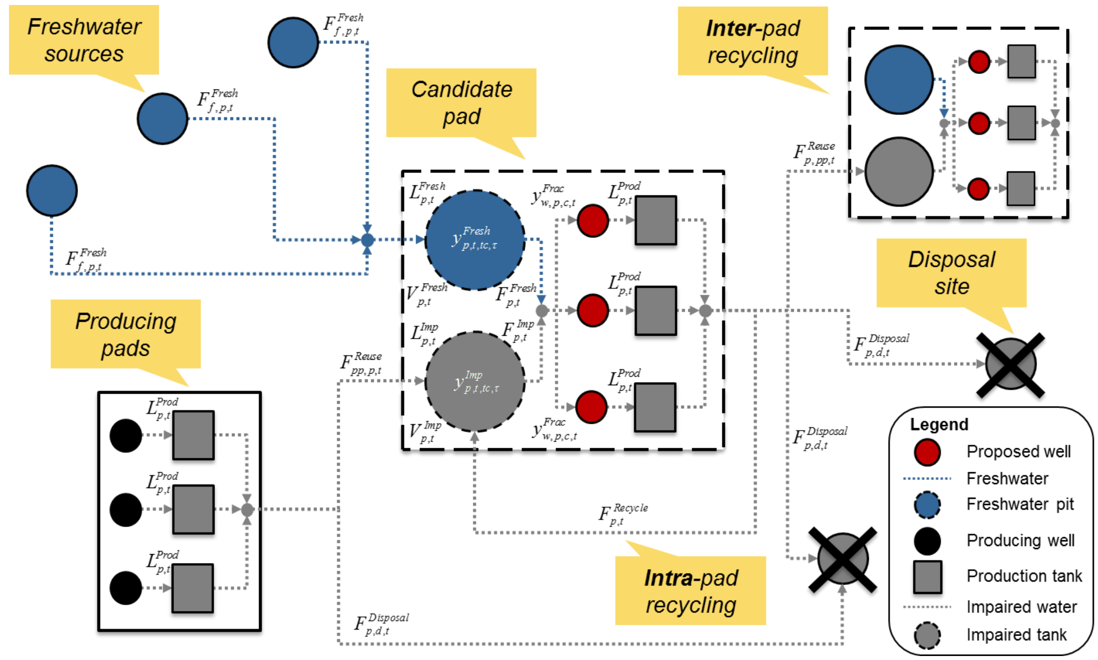

Fig. 3.1: Illustration of water management operations in active development areas

Clearly, one possible option is to use freshwater for fracturing purposes. For this reason producers will typically scout out active development areas and locate as many freshwater sources within the vicinity of a candidate pad as possible. Water availability forecasts, maximum withdrawal rates and acquisition expenses are all pre-determined for these freshwater sources. Hence, the producer only needs to decide how much water to transport from each of these available sources to a given candidate pad at any given point in time. Companies may choose to either truck freshwater on-site (typically from rivers or lakes), or use temporary water lines to pipe water to the pad (typically from nearby creeks). Generally, it is preferable to pipe water since it is much more cost-effective than trucking as shown by Yang et al. (2014). If freshwater is used to stimulate selected wells, then sufficient on-site freshwater storage capacity needs to be provided. This storage capacity is typically realized by either constructing a freshwater pit or installing temporary above-ground storage tanks (so-called *ASTs* for short). Generally, the operator can decide which storage option to select and how much storage capacity to provide for development operations.

As an alternative to freshwater, the producer may choose to use impaired water to fracture wells on a candidate pad. Impaired water can be obtained from so-called *producing pads* surrounding the active development area. A producing pad is a location where completed shale wells are actively producing natural gas, and impaired water. The impaired water is typically fed into limited capacity production tanks. The water stored in these tanks can either be sent to disposal or hauled to a candidate-pad for reuse. How much water is sent to disposal, and, how much is recycled at any point in time, is an additional degree of freedom. If a company decides to haul impaired water onto a candidate pad, then sufficient impaired water storage capacity needs to be provided. Impaired water may not be stored in freshwater pits or freshwater ASTs, but only in dedicated, temporarily installed impaired water ASTs. Assuming that both freshwater and impaired water are available at a candidate pad, the operator needs to determine how much of each to use for every individual fracturing job. This so-called *blending ratio* is one of the key degrees of freedom in impaired water management.

Once the prospective wells on a candidate well pad have been fractured, completed and turned in-line, they too will produce flowback water, and eventually, produced water. As on producing pads, these wells will feed their impaired water into production tanks, which – due to their limited capacity – need to be emptied regularly. Any producer has three alternative options for processing these volumes: (a) the water can be reused for an upcoming fracturing job on a neighboring candidate pad (*inter-pad recycling*), (b) the water can be sent to attainable disposal sites, or (c) the recovered water can be recycled on-site by feeding it back into an available impaired water storage tank (*intra-pad recycling*). Since all three options are generally feasible and not exclusive to each other, the operator needs to evaluate carefully how to schedule impaired water deliveries over time. Hence, given the operational setup described above, the goal is to identify the most cost-effective fracturing schedule and water management strategy simultaneously.

3.2 General Problem Statement

The problem addressed in this chapter can be stated as follows. Within an active shale gas development area as shown in Fig. 3.1, an upstream operator wishes to fracture and complete a set of previously drilled shale gas wells. Such assets are also referred to as drilled but uncompleted wells or “DUCs” (EIA, 2016). Type curve production forecasts, individual well lateral lengths, the water demand for fracturing, estimated completions durations and costs are pre-determined for every well. In addition, a set of attainable water sources can be used to service all considered candidate pads. For every water source the water availability as well as water transfer costs – accounting for trucking and piping options if available – are known.

Given the information described above, the problem is to determine: (a) the optimal fracturing schedule, (b) the optimal water supply sourcing and distribution strategy, and (c) optimal on-site water storage solutions including their capacities. The fracturing schedule specifies when each targeted well is fractured. The water management strategy determines the optimal water blending ratio for each well, i.e., how much freshwater is used to fracture a well compared to how much impaired water is used for the fracturing job. Moreover, the water management strategy specifies how much of the recovered impaired water is reused on-site, off-site or sent to disposal, and when. A crucial component of the selected water management strategy involves the selection of necessary freshwater and impaired water storage equipment. This selection includes the determination of preferred freshwater pit impoundment capacities as well as freshwater and impaired water AST capacities and rental durations. The objective is to determine the optimal fracturing schedule and water management strategy such that the net present value of the development project is maximized.

3.3 Literature Review

A number of rigorous optimization models for shale gas water management have been proposed in recent years. In this section we highlight some of these works and we distinguish our contribution from previous publications.

Yang et al. (2014) propose a two-stage stochastic mixed-integer linear programming model to determine the optimal fracturing schedule, water transport, treatment and reuse strategies. The authors explicitly consider uncertainty in terms of water availability. The main opportunity for optimization is recognized as the trade-off between trucking and piping opportunities for water transport. The work assumes that all wells on a pad are completed before a fracturing crew moves on to another pad; return-to-pad operations are not considered. Moreover, the authors assume that the ratio of freshwater to impaired water for every fracturing job is predetermined. Yang et al. (2015) extend their previously proposed optimization model by specifically focusing on impaired water treatment technologies. The technologies considered include reverse osmosis, forward osmosis, membrane distillation and mechanical vapor recompression. As before, however, the authors assume that the water blending ratio is fixed a priori.

Gao & You (2014) develop a mixed-integer linear fractional programming model to design and operate water supply chain networks for shale gas production. The authors only consider on-site impaired water reuse, but no inter-pad recycling. In terms of water storage solutions, Gao & You (2014) do not distinguish between freshwater and impaired water, although it is strictly prohibited to store contaminated water in freshwater tanks or pits. Similar to previous works, the authors assume that the water blending ratio is set.

Guerra et al. (2016) present an optimization framework for the integration of shale gas supply chain design and related water management challenges. For planning purposes the proposed model selects from a given set of well pad “designs” for every prospective well-site. The well pad designs are essentially predetermined development configurations that differ in terms of total number of wells, the lateral lengths of individual wells and the completions design. In this sense, the presented framework is not intended to propose a particular fracturing schedule, neither is it designed to consider return-to-pad operations explicitly as a means to reducing impaired water disposal volumes. Moreover, the authors assume that water demand for fracturing purposes can only be met by using freshwater or impaired water that has undergone processing at a dedicated treatment facility. The possibility of reusing impaired water directly, i.e., without treatment, is not considered. The proposed optimization model is capable of sizing wastewater treatment plants and tracking impaired water quality (e.g. in terms of total dissolved solids concentration) over time. The sizing of on-site water storage solutions for freshwater and impaired water, on the other hand, is not within the scope of the proposed framework.

Lira-Barragán et al. (2016a) develop a mathematical programming formulation for synthesizing water networks associated with shale gas fracturing operations while accounting for uncertainty in terms of completions water demand and the accuracy of flowback water forecasts. The work assumes that all flowback water has to be treated prior to being reused, or even disposed of. For simplicity, the authors also fix the fracturing schedule in advance, thereby eliminating opportunities to reduce disposal volumes by re-organizing the sequence of fracturing jobs. Lira-Barragán et al. (2016b) also propose a mixed-integer nonlinear programming model to minimize cost for the optimal management of flowback water in shale gas development operations. The nonlinearities in the model formulation are due to the consideration of economies of scale applying to the capital costs for water storage units. In their work the authors assume that the fracturing schedule has already been fixed and, hence, they do not consider return-to-pad operations.

Bartholomew and Mauter (2016) present a multi-objective mixed-integer linear programming model for assessing tradeoffs between water management costs in shale gas development operations and the associated human health and environmental (HHE) impacts. Their goal is to identify water management strategies that minimize financial cost, HHE costs, and combined costs. The authors propose a two-step strategy to address the integrated problem. First, a fracturing schedule is determined such that the profit of the development project is maximized. Thereafter, based on the fixed fracturing schedule, a multi-objective model is used to determine water management strategies that minimize financial, HHE, and combined costs. The authors require all wells on a pad to be fractured and completed before a fracturing crew can move on to another well-site.

As a result, return-to-pad operations are not considered. It is also assumed that impaired water use for fracturing purposes is limited by TDS. In other words, impaired water can only make up a limited percentage of the fracturing fluid. Hence, the water blending ratio of freshwater to impaired water is explicitly restricted. Through a case study that is representative of shale gas development in the Marcellus Play, the authors observe significant variations in financial and HHE costs when considering different objective functions and regulatory scenarios.

In this work, we place considerable emphasis on exploiting any flexibility in terms of the fracturing schedule to optimize water management operations. In essence, the question we raise is whether the fracturing schedule should largely be driven by water operations – as opposed to the other way around, which is common practice. In particular, we explore whether, and to which extent, return-to-pad operations can allow the shale gas industry to minimize impaired water disposal volumes. Unlike previous works, we also assume that the water blending ratio for fracturing jobs is completely unrestricted. In other words, up to 100% impaired water can be used for fracturing purposes. In addition, our work emphasizes the selection and sizing of on-site water storage solutions for freshwater and impaired water. In practice, producers frequently argue that impaired water storage bottlenecks prevent them from increasing recycle rates. In terms of ASTs in particular, we explicitly consider the discrete sizes of these water storage solutions, and we recognize that shale companies need to decide for how long they wish to lease them.

Finally, we present a real-world case study based on data from one of the largest upstream operators in the Appalachian Basin to demonstrate the proposed optimization framework.

3.4 Model Assumptions

The key modeling assumptions in this work are highlighted below:

- The planning horizon is discretized into a set of time periods, which typically represent weekly increments. A natural gas price forecast is given for the entire planning horizon.
- The fracturing schedule is assumed to be unconstrained. In particular, this implies that all gas gathering systems within the considered development area are not capacity-constrained downstream.
- Type curve production forecasts are provided for all prospective wells.
- The water blending ratio for fracturing jobs is unrestricted. Operators can use arbitrarily contaminated water for fracturing purposes, due to technological advances in the performance of friction reducing additives. This assumption is supported by an expert elicitation of trends in Marcellus oil and gas wastewater management that was recently conducted by Mauter & Palmer (2014). The results of this elicitation clearly suggest that impaired water reuse is <u>not</u> inhibited by high concentrations of total dissolved solids (TDS). More specifically, the survey also reveals that shale gas producers do not factor salinity into decisions about whether to save impaired water for reuse. Expert responses from operators indicate that water quality is <u>not</u> a barrier to reusing water in the Marcellus. It is reported that high-salinity tolerant friction-reducers that remain hydrant at concentrations up to

150,000 ppm TDS were cited by respondents as a major innovation in recent years. In fact, many producers speculated that fracturing water salinity had little bearing on the productivity of their wells. As a result, companies also reported blend rates between 20 and 90% in this survey.

- Consequently, we only distinguish between two water qualities in this work, namely freshwater and impaired water.

3.5 Model Description

In this section we describe the proposed mixed-integer linear programming model to address the impaired water management problem.

Allocation Constraints

As expressed in the general problem statement, we assume that an "inventory" of targeted wells $w \in W$ on a set of candidate pads $p \in CWP$ is to be completed within an active development area. Hence, we enforce Eq. (3.1) to ensure that by the end of the planning horizon $t \in T$ all wells are completed by one of the available fracturing crews $c \in C$.

$$\sum_{t \in \mathcal{T}} \sum_{c \in \mathcal{C}} y^{Frac}_{w,p,c,t} = 1 \qquad \forall w \in \mathcal{W}, p \in \mathcal{CWP} \tag{3.1}$$

In low-price environments, the number of active fracturing crews is often limited to lower operational expenses and to accommodate the reduced development activity. We add Eq. (3.2) to our model, which states that at any point in time every fracturing crew may only be assigned to one particular candidate well pad $p \in CWP$. In this case, the assignment corresponds to the completion of the well, which is assumed to last a total of $\tau^{Frac}_{w,p,c}$ time periods.

$$\sum_{p \in \mathcal{CWP}} \sum_{w \in \mathcal{W}} \sum_{tt=t-\tau_{w,p,c}^{Frac}+1}^{t} y_{w,p,c,tt}^{Frac} \leq 1 \qquad \forall c \in \mathcal{C}, t \in \mathcal{T} \tag{3.2}$$

General Water Mass Balances

The fracturing of every well requires a certain volume of water that is determined by two main factors: (a) the well's lateral length $l_{w,p}^{Lateral}$ and (b) the preferred completions design, which translates into a specific water demand $wd_{w,p}^{Well}$ per unit length of treated interval. Eq. (3.3) captures the water demand at a particular pad once a fracturing crew has been assigned to complete a well. We note that the total water demand is divided by the number of weeks it requires to complete the well $\tau_{w,p,c}^{Frac}$. If, for instance, a well with an extended lateral length requires several weeks to be completed, then the total water demand is evenly distributed across the duration of the fracturing job.

$$WD_{p,t}^{Pad} = \sum_{w \in \mathcal{W}} \sum_{c \in \mathcal{C}} \sum_{tt=t-\tau_{w,p,c}^{Frac}+1}^{t} l_{w,p}^{Lateral} \cdot wd_{w,p}^{Well} \cdot \frac{1}{\tau_{w,p,c}^{Frac}} \cdot y_{w,p,c,tt}^{Frac} \qquad \forall p \in \mathcal{CWP}, t \in \mathcal{T} \tag{3.3}$$

The water demand $WD_{p,t}^{Pad}$ can be met by using freshwater $F_{p,t}^{Fresh}$ and/or impaired water $F_{p,t}^{Imp}$. The exact ratio of freshwater to impaired water determines the water blending ratio of a particular job.

$$WD_{p,t}^{Pad} = F_{p,t}^{Imp} + F_{p,t}^{Fresh} \qquad \forall p \in \mathcal{CWP}, t \in \mathcal{T} \tag{3.4}$$

In this work we distinguish between two distinct water qualities: freshwater and impaired water. Hence, we enforce mass balances for both. The following paragraphs describe the key constraints and bounds that we consider.

Impaired Water Mass Balances

In order to determine how much impaired water is stored at a given well pad at every point in time, we track four metrics, as seen in Eq. (3.5): the impaired water volume in the previous time period $L_{p,t-1}^{Imp}$, how much impaired water is delivered from surrounding pads $F_{pp,p,t}^{Reuse}$, how much impaired water is recycled on-site $F_{p,t}^{Recycle}$, and how much impaired water is consumed for fracturing $F_{p,t}^{Imp}$.

$$L_{p,t}^{Imp} = L_{p,t-1}^{Imp} + \sum_{p \in \mathcal{P}} F_{pp,p,t}^{Reuse} + F_{p,t}^{Recycle} - F_{p,t}^{Imp} \qquad \forall p \in \mathcal{CWP}, t \in \mathcal{T} \tag{3.5}$$

We also assume that in order to use impaired water for any fracturing job, it needs to be available on-site in the previous time period. Vice-versa, the available impaired water storage capacity $V_{p,t-1}^{Imp}$ limits how much impaired water can be stored on-site. Both constraints are captured in Eq. (3.6).

$$F_{p,t}^{Imp} \le L_{p,t-1}^{Imp} \le V_{p,t-1}^{Imp} \qquad \forall p \in \mathcal{CWP}, t \in \mathcal{T} \tag{3.6}$$

Fresh Water Mass Balances

The mass balances that are imposed for freshwater are similar to the previous constraints. In terms of available freshwater volume on-site, however, Eq. (3.7) only involves three terms: (a) the freshwater volume in the previous time period $L_{p,t-1}^{Fresh}$, (b) freshwater deliveries to the candidate pad from surrounding water sources $F_{f,p,t}^{Source}$, and (c) freshwater used for fracturing $F_{p,t}^{Fresh}$.

$$L_{p,t}^{Fresh} = L_{p,t-1}^{Fresh} + \sum_{f \in \mathcal{F}} F_{f,p,t}^{Source} - F_{p,t}^{Fresh} \qquad \forall p \in \mathcal{CWP}, t \in \mathcal{T} \tag{3.7}$$

In Eq. (3.8) we consider the fact that the freshwater availability may be limited at times.

$$\sum_{p \in \mathcal{P}} F_{f,p,t}^{Source} \le \psi_{f,t}^{Source} \qquad \forall f \in \mathcal{F}, t \in \mathcal{T} \tag{3.8}$$

As before, we assume that freshwater may only be used to perform a fracturing job if it is stored on-site in the previous time period. Also, the total freshwater volume on-site is constrained by the available freshwater storage capacity $V_{p,t-1}^{Fresh}$, which consists of constructed freshwater pits and installed ASTs.

$$F_{p,t}^{Fresh} \leq L_{p,t-1}^{Fresh} \leq V_{p,t-1}^{Fresh} \qquad \forall p \in \mathcal{CWP}, t \in \mathcal{T} \tag{3.9}$$

Production Water Mass Balances

Wells that have been turned in-line, typically feed into so-called production tanks, which recover flowback and produced water – depending on how long a well has been actively producing. We classify both water categories as impaired water in this work. The impaired water volume in the production tanks depends on a number of factors captured in Eq. (3.10): (a) the impaired water volume stored in the production tank in the previous time period $L_{p,t-1}^{Prod}$, (b) the produced water recovered from active wells $WP_{p,t}^{Pad}$, (c) impaired water sent to disposal $F_{p,ds,t}^{Disposal}$, (d) impaired water sent to a neighboring well pad for reuse $F_{p,pp,t}^{Reuse}$, and (d) impaired water recycled on-site $F_{p,t}^{Recycle}$.

$$L_{p,t}^{Prod} = L_{p,t-1}^{Prod} + WP_{p,t}^{Pad} - \sum_{ds \in \mathcal{DS}} F_{p,d,t}^{Disposal} - \sum_{pp \in \mathcal{CWP}} F_{p,pp,t}^{Reuse} - F_{p,t}^{Recycle} \qquad \forall p \in \mathcal{P}, t \in \mathcal{T} \tag{3.10}$$

The amount of produced water $WP_{p,t}^{Pad}$ that is recovered from active wells has two contributions: the produced water forecast of wells previously turned in-line (existing wells), and forecasted produced water volumes from wells that need to be completed within the planning horizon.

$$WP_{p,t}^{Pad} = wp_{p,t}^{Pad} + \sum_{w \in \mathcal{W}} \sum_{c \in \mathcal{C}} \sum_{tt=1}^{t-\tau_{w,p,c}^{Frac}} wp_{w,t-tt}^{Well} \cdot y_{w,p,c,tt}^{Frac} \qquad \forall p \in \mathcal{P}, t \in \mathcal{T} \tag{3.11}$$

As shown in Eq. (3.12) the total volume of impaired water stored in these production tanks is limited due to their fairly modest capacity $\psi_{p,t}^{Prod}$.

$$L_{p,t}^{Prod} \leq \psi_{p,t}^{Prod} \qquad \forall p \in \mathcal{P}, t \in \mathcal{T} \tag{3.12}$$

Impaired Water Storage

In order to provide for sufficient impaired water storage capacity at a well pad, dedicated ASTs need to be installed on-site. These ASTs are only available in certain sizes and are typically rented from third-party providers for as long as they are required. We model the selection of impaired water storage capacity using logic propositions and disjunctions (Raman and Grossmann, 1991, Grossmann and Trespalacios, 2013). For this purpose we introduce two Boolean variables: first, a Boolean variable $Y_{p,tc,t,d}^{ImpAST}$ which is true if an impaired water AST with storage capacity $tc \in \mathcal{TC}_0$ is rented on a candidate well pad $p \in \mathcal{CWP}$ for a duration of $d \in \mathcal{D}$ time periods in the current time period $t \in \mathcal{T}$. Next, we introduce a matching Boolean variable $Z_{p,tc,t}^{ImpAST}$ which is only true if an impaired water AST with storage capacity $tc \in \mathcal{TC}_0$ is available on candidate well pad $p \in \mathcal{CWP}$ in the current time period $t \in \mathcal{T}$. Based on these declarations, we express the logic constraint (3.13) which governs the relation between these two Boolean variables. This constraint states that an impaired water AST of a certain size is only *available* on-site for the duration it was *rented* for.

$$Z_{p,tc,t}^{ImpAST} \quad \Leftrightarrow \quad \bigvee_{d \in \mathcal{D}} \bigvee_{tt=t-\tau_d^{Rental}}^{t} \quad Y_{p,tc,tt,d}^{ImpAST} \qquad \forall p \in \mathcal{P}, tc \in \mathcal{TC}_0, t \in \mathcal{T} \tag{3.13}$$

We note that the set of available AST sizes $\mathcal{TC}_0$ explicitly includes the zero-element, which allows the optimizer not to install an AST. Also, we consider the fact that AST rental terms τ_d^{Rental} are oftentimes discretized in weekly increments.

Next, we introduce disjunction (3.14) which states that if the Boolean variable $Z_{p,tc,t}^{ImpAST}$ is true, i.e., an impaired water AST with storage capacity $tc \in \mathcal{TC}_0$ is available on a candidate pad $p \in \mathcal{CWP}$ in time period $t \in \mathcal{T}$, then the pre-existing, on-site impaired water storage capacity v_p^0 is increased by the corresponding increment δ_{tc}, setting the total storage capacity to $V_{p,t}^{Imp}$.

$$\bigvee_{tc \in \mathcal{TC}_0} \begin{bmatrix} Z_{p,tc,t}^{ImpAST} \\ V_{p,t}^{Imp} = v_p^0 + \delta_{tc} \end{bmatrix} \qquad \forall p \in \mathcal{CWP}, t \in \mathcal{T} \tag{3.14}$$

Finally, we add Eq. (3.15) to express that disjunction (3.14) is exclusive.

$$\underline{\bigvee}_{tc \in \mathcal{TC}_0} \quad Z_{p,tc,t}^{ImpAST} \qquad \forall p \in \mathcal{CWP}, t \in \mathcal{T} \tag{3.15}$$

In this case we choose to transform the logic proposition (3.13) and the disjunction (3.14) intro a set of mixed-integer constraints using the Compact Hull Reformulation (Castro and Grossmann, 2012; Cafaro et al., 2016). For this purpose the Boolean variables $Y_{p,tc,t,d}^{ImpAST}$ and $Z_{p,tc,t}^{ImpAST}$ are converted into the corresponding binary variables $y_{p,tc,t,d}^{ImpAST}$ and $z_{p,tc,t}^{ImpAST}$. Based on this conversion, the logic proposition (3.13) can be expressed as the mixed-integer constraint Eq. (3.16).

$$z_{p,tc,t}^{ImpAST} = \sum_{d \in \mathcal{D}} \sum_{tt=t-\tau_d^{Rental}}^{t} y_{p,tc,tt,d}^{ImpAST} \qquad \forall p \in \mathcal{CWP}, tc \in \mathcal{TC}_0, t \in \mathcal{T} \tag{3.16}$$

Similarly, the disjunction (3.14) itself is transformed into Eq. (3.17) to govern impaired water AST capacity extension at every candidate pad in every time period.

$$V_{p,t}^{Imp} = v_p^{ImpairedAST,0} + \sum_{tc \in \mathcal{TC}} \delta_{tc} \cdot z_{p,tc,t}^{ImpAST} \qquad \forall p \in \mathcal{CWP}, t \in \mathcal{T} \qquad (3.17)$$

Lastly, Eq. (3.15) is expressed through the multiple choice constraint (3.18).

$$\sum_{tc \in \mathcal{TC}_0} z_{p,tc,t}^{ImpAST} = 1 \qquad \forall p \in \mathcal{CWP}, t \in \mathcal{T} \qquad (3.18)$$

We point out that the binary variable $y_{p,tc,tt,d}^{ImpAST}$ can be treated as a continuous variable due to constraints (3.16) and (3.18), which enforce integrality for 0-1 values of the binary variable $z_{p,tc,t}^{ImpAST}$.

Freshwater Storage

We proceed in a similar fashion to model the selection of freshwater storage capacity. However, in addition to installing freshwater ASTs, producers have the ability to construct freshwater pits. Hence, the total freshwater storage capacity $V_{p,t}^{Fresh}$ on every candidate pad consists of the available AST storage capacity $V_{p,t}^{FreshAST}$ and the available pit storage capacity $V_{p,t}^{FreshPit}$, as shown in Eq. (3.19).

$$V_{p,t}^{Fresh} \leq V_{p,t}^{FreshAST} + V_{p,t}^{FreshPit} \qquad \forall p \in \mathcal{CWP}, t \in \mathcal{T} \qquad (3.19)$$

As before, we model the selection of freshwater AST capacity using two Boolean variables: one to capture the installment-decision $Y_{p,tc,t,d}^{FreshAST}$, and one to capture the availability of the AST $Z_{p,tc,t}^{FreshAST}$. Eq. (3.20) links these Boolean variables for every candidate pad.

$$Z_{p,tc,t}^{FreshAST} \quad \Leftrightarrow \quad \bigvee_{d \in \mathcal{D}} \bigvee_{tt=t-\tau_d^{Rental}}^{t} \quad Y_{p,tc,tt,d}^{FreshAST} \qquad \forall p \in \mathcal{P}, tc \in \mathcal{TC}_0, t \in \mathcal{T} \quad (3.20)$$

The corresponding disjunction (3.21) governs the temporary extension of AST capacity for freshwater.

$$\bigvee_{tc\in\mathcal{TC}_0}\begin{bmatrix} Z_{p,tc,t}^{FreshAST} \\ V_{p,t}^{FreshAST}=v_p^{FreshAST,0}+\delta_{tc}\end{bmatrix} \qquad \forall p\in\mathcal{CWP},t\in\mathcal{T} \tag{3.21}$$

In this case, too, we add Eq. (3.22) to express that disjunction (3.22) is exclusive.

$$\underline{\vee}_{tc\in\mathcal{TC}_0} \quad Z_{p,tc,t}^{FreshAST} \qquad \forall p\in\mathcal{CWP},t\in\mathcal{T} \tag{3.22}$$

The conversion of Eqs. (3.20)-(3.22) is analogous to the previous transformation and leads to the mixed-integer constraints (3.23)-(3.25).

$$z_{p,tc,t}^{FreshAST}=\sum_{d\in\mathcal{D}}\sum_{tt=t-\tau_d^{Rental}}^{t} y_{p,tc,tt,d}^{FreshAST} \qquad \forall p\in\mathcal{CWP},tc\in\mathcal{TC}_0,t\in\mathcal{T} \tag{3.23}$$

$$V_{p,t}^{FreshAST}=v_p^{FreshAST,0}+\sum_{tc\in\mathcal{TC}}\delta_{tc}\cdot z_{p,tc,t}^{FreshAST} \qquad \forall p\in\mathcal{CWP},t\in\mathcal{T} \tag{3.24}$$

$$\sum_{tc\in\mathcal{TC}_0} z_{p,tc,t}^{FreshAST}=1 \qquad \forall p\in\mathcal{CWP},t\in\mathcal{T} \tag{3.25}$$

Once again, the binary variables $y_{p,tc,tt,d}^{FreshAST}$ can be treated as continuous variables to reduce the complexity of the optimization problem. In addition to installing temporary AST storage capacity, operators can construct freshwater pits on candidate well pads. These pits can store significantly more water than ASTs, and they are oftentimes less costly on a per-barrel basis than renting ASTs over extended periods of time. We introduce Eq. (3.26) in our model to track the available freshwater pit storage capacity at very point in time. The parameter $v_p^{FreshPit,0}$ specifies pre-existing storage capacity, whereas the continuous variable $V_{p,t}^{FreshPitInstall}$ allows the optimizer to construct or expand a freshwater pit.

$$V_{p,t}^{FreshPit}=v_p^{FreshPit,0}+\sum_{tt=1}^{t}V_{p,tt}^{FreshPitInstall} \qquad \forall p\in\mathcal{CWP},t\in\mathcal{T} \tag{3.26}$$

We introduce the binary variable $y_{p,t}^{FreshPitInstall}$ which becomes active if a freshwater pit is installed on a candidate pad in a certain period of time. Eq. (3.27) ensures that the installed pit capacity does not exceed a pre-determined upper bound based on spatial well pad constraints.

$$V_{p,t}^{FreshPitInstall} \leq V_{p}^{FreshPitInstall,UP} \cdot y_{p,t}^{FreshPitInstall} \qquad \forall p \in \mathcal{CWP}, t \in \mathcal{T} \tag{3.27}$$

Finally, the multiple choice constraint (3.28) guarantees that a pit construction or extension does not occur more than once over the planning horizon.

$$\sum_{t \in T} y_{p,t}^{FreshPitInstall} \leq 1 \qquad \forall p \in \mathcal{CWP} \tag{3.28}$$

Objective Function

The objective for shale gas development is typically to maximize the net present value of a field development project. The proposed objective function (3.29) considers revenues from natural gas sales at every well pad $REV_{p,t}$, development expenses for fracturing wells $DVE_{p,t}$, freshwater acquisition expenses $FAE_{p,t}$, impaired water hauling expenses $IHE_{p,t}$, impaired water AST rental expenses $IARE_{p,t}$, freshwater AST rental expenses $FARE_{p,t}$, freshwater pit installation expenses $FPIE_{p,t}$, impaired water disposal expenses $IDE_{p,t}$, and friction reducer expenses $FRE_{p,t}$ – all discounted back to their present value.

$$\begin{aligned}\Phi = \sum_{t \in \mathcal{T}} (1+r)^{-t/52} \cdot \sum_{p \in \mathcal{P}} \Big(& REV_{p,t} - DVE_{p,t} - FAE_{p,t} - IHE_{p,t} - IARE_{p,t} \\ & - FARE_{p,t} - FPIE_{p,t} - IDE_{p,t} - FRE_{p,t} \Big)\end{aligned} \tag{3.29}$$

The revenues from gas sales at every well pad in every time period are linked to the timing of the fracturing operation $y^{Frac}_{w,p,c,t}$, every well's individual type curve forecast $\gamma_{w,p,t}$ and the gas price forecast θ_t.

$$REV_{p,t} = \sum_{tt=1}^{t} \sum_{w \in \mathcal{W}} \sum_{c \in \mathcal{C}} y^{Frac}_{w,p,c,tt} \cdot \gamma_{w,p,t-tt} \cdot \theta_t \qquad \forall p \in \mathcal{P}, t \in \mathcal{T} \qquad (3.30)$$

Development expenses for fracturing wells consider the prospective wells' lateral lengths $l^{Lateral}_{w,p}$ and well-specific stimulation and completions costs α^{Dev}_{w}.

$$DVE_{p,t} = \sum_{c \in \mathcal{C}} \sum_{w \in \mathcal{W}} y^{Frac}_{w,p,c,t} \cdot l^{Lateral}_{w,p} \cdot \alpha^{Dev}_{w} \qquad \forall p \in \mathcal{CWP}, t \in \mathcal{T} \qquad (3.31)$$

Freshwater acquisition expenses depend on a number of factors: the amount of water that is hauled from a freshwater source f to a well pad p, the respective source travel time $\tau^{Source}_{f,p}$, the source-dependent freshwater acquisition cost coefficient $\rho^{Source}_{f,p}$ and the standard water hauling truck capacity stc.

$$FAE_{p,t} = \sum_{f \in \mathcal{F}} F^{Source}_{f,p,t} \cdot \tau^{Source}_{f,p} \cdot \rho^{Source}_{f,p} \cdot {}^{1}\!/_{stc} \qquad \forall p \in \mathcal{CWP}, t \in \mathcal{T} \quad (3.32)$$

Impaired water hauling expenses are determined similar to freshwater acquisition expenses. The costs depend on the amount of water hauled from one pad to another $F^{Reuse}_{p,pp,t}$, the inter-pad travel time $\tau^{Travel}_{p,pp}$, the individual water transfer cost coefficient $\alpha^{Reuse}_{p,pp}$, and the standard water hauling truck capacity stc.

$$IHE_{p,t} = \sum_{pp \in \mathcal{P}} F^{Reuse}_{p,pp,t} \cdot \tau^{Travel}_{p,pp} \cdot \alpha^{Reuse}_{p,pp} \cdot {}^{1}\!/_{stc} \qquad \forall p \in \mathcal{CWP}, t \in \mathcal{T} \quad (3.33)$$

Expenses for renting impaired water and freshwater ASTs are directly linked to the binary variables $y_{p,tc,t,d}^{ImpAST}$ and $y_{p,tc,t,d}^{FreshAST}$, as well as the respective cost coefficients $\alpha_{tc,d}^{ImpAST}$ and $\alpha_{tc,d}^{FreshAST}$, which consider water storage capacity tc and rental duration d.

$$IARE_{p,t} = \sum_{tc \in \mathcal{TC}} \sum_{d \in \mathcal{D}} \alpha_{tc,d}^{ImpAST} \cdot y_{p,tc,t,d}^{ImpAST} \qquad \forall p \in \mathcal{CWP}, t \in \mathcal{T} \qquad (3.34)$$

$$FARE_{p,t} = \sum_{tc \in \mathcal{TC}} \sum_{d \in \mathcal{D}} \alpha_{tc,d}^{FreshAST} \cdot y_{p,tc,t,d}^{FreshAST} \qquad \forall p \in \mathcal{CWP}, t \in \mathcal{T} \qquad (3.35)$$

Freshwater pit installation expenses, on the other hand, depend on the increase in water storage capacity $V_{p,t}^{FreshPitInstall}$ and the expansion cost coefficient $\alpha^{PitInstall}$.

$$FPIE_{p,t} = V_{p,t}^{FreshPitInstall} \cdot \alpha^{PitInstall} \qquad \forall p \in \mathcal{CWP}, t \in \mathcal{T} \qquad (3.36)$$

Expenses for impaired water disposal are linked to the amount of impaired water delivered to a disposal site $F_{p,d,t}^{Disposal}$, the distance between a well pad p and a disposal site ds, and the disposal cost coefficient $\alpha_{p,ds}^{Disposal}$.

$$IDE_{p,t} = \sum_{ds \in \mathcal{DS}} F_{p,ds,t}^{Disposal} \cdot l_{p,ds} \cdot \alpha_{p,ds}^{Disposal} \qquad \forall p \in \mathcal{P}, t \in \mathcal{T} \qquad (3.37)$$

Friction reducers need to be added during well completions to ensure that the fracturing water is “slick” and to reduce pressure losses. Pressure increases during fracturing lead to reduced frac pump rates, which increase the risk of premature screen-outs (Schilling, 2016). Hence, friction reducer expenses are determined by how much impaired water $F_{p,t}^{Imp}$ is used for fracturing and the cost of purchasing the additive α_p^{FR}. Since, technically, these expenses may also depend on how contaminated the impaired water is (e.g. TDS concentration), we intentionally overestimate them in this work.

$$FRE_{p,t} = F_{p,t}^{Imp} \cdot \alpha_p^{FR} \qquad \forall p \in \mathcal{CWP}, t \in \mathcal{T} \qquad (3.38)$$

3.6 Case Study

The proposed model is applied to a real-world case study to demonstrate the value of rigorous, mathematical optimization for impaired water management in shale gas development. The data for this case study is provided by one of the largest upstream operators in the Appalachian Basin. For confidentiality reasons we cannot disclose the company's identity, nor the focus area of the case study. However, we provide a detailed discussion of the impaired water management strategy proposed for this particular problem to illustrate and convey the potential impact of rigorous optimization in this domain.

3.6.1 Setup of the Impaired Water Management Problem

For the purpose of the case study we wish to determine the optimal fracturing schedule and water coordination strategy for a given, active development area. This development area contains a total of nine well pads: four "candidate" pads (henceforth referred to as PAD_A, PAD_B, PAD_C and PAD_D) and five "producing" pads (labeled as PAD_E, PAD_F, PAD_G, PAD_H and PAD_I). The producing pads are characterized by the fact that the wells on these sites have already been turned in-line previously, whereas a total of 29 wells still need to be drilled and completed on the candidate pads within the next year. Lateral lengths, completions times, completions designs, type curve forecasts, and expected development costs are given for all 29 prospective wells. For the existing wells, on the other hand, an impaired water production forecast can be provided. This forecast, as shown in Fig. 3.2, indicates how much impaired water each and every existent pad in the development area is expected to produce over the given one year planning horizon. We note that according to this forecast more than 2.75 million barrels of impaired water will be produced over a twelve month period – and they need to be either disposed of and/or recycled.

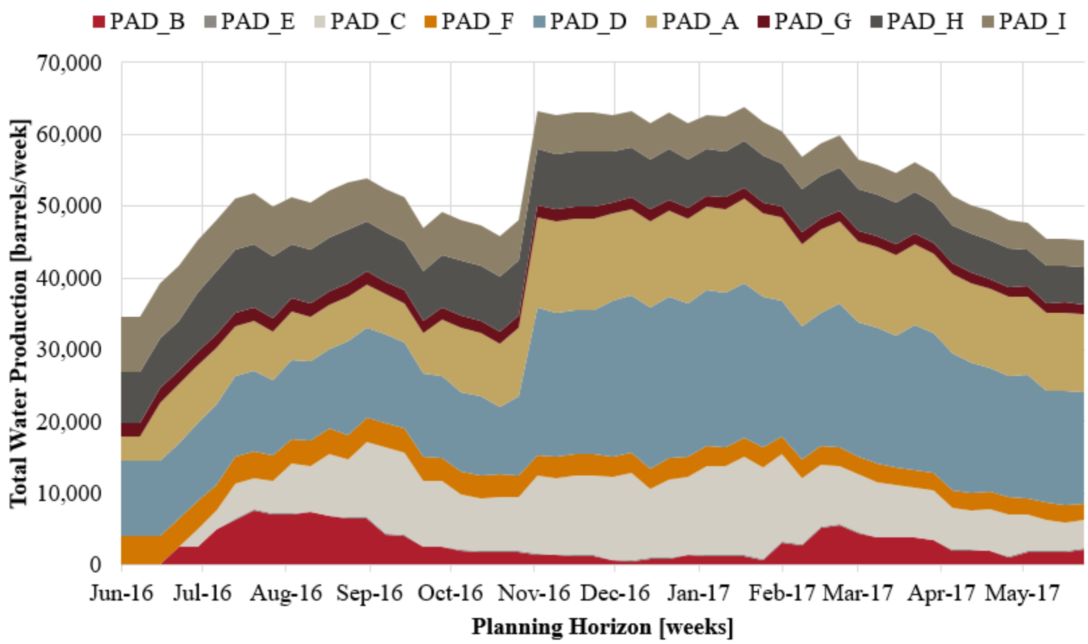

Fig. 3.2: Impaired water production forecast over the planning horizon

We assume that no more than two fracturing crews are available to complete the jobs. However, due to a depressed price-environment at the time, we assume that there is complete flexibility in terms of the fracturing schedule. Finally, a natural gas price forecast is given for the one year planning horizon, which is split into 52 weekly increments. In addition, we make the following three assumptions: (a) the gathering system in the given development area is not capacity-constrained downstream, (b) due to regulatory changes no new impaired water pits may be installed in this area, and (c) for simplicity, we neglect fracture communication between individual wells. The objective is to use the proposed optimization model to determine the most economic fracturing schedule and corresponding water management strategy for this particular development area.

3.6.2 Proposed Impaired Water Management Strategy

The presented optimization model given by Eqs. (3.1)-(3.12), (3.16)-(3.19), (3.23)-(3.38) yields a mixed-integer linear programming problem with 5,304 binary decision variables, 31,253 continuous variables and 10,278 constraints. Using IBM CPLEX 12.6.0.0 in AIMMS 4.30.5 on an Intel i7, 2.93 Ghz machine with 12 GB RAM the problem can be solved to a 6% optimality gap in less than 1.5 hours. The reported NPV is 64.5 MM$. In the following paragraphs we highlight selected aspects of the proposed solution, and we analyze why and how it makes economic and practical sense.

First and foremost, the optimization yields the optimal fracturing schedule as seen in Fig. 3.3. This Gantt chart shows when exactly to complete each and every prospective well over the given one year planning horizon. The proposed schedule is color-coded to reflect which wells are on which pads. One of the most striking observations that can be made right away is that the optimization clearly suggests to "split pads" as can be seen for PAD_B and PAD_D. In both cases the solution suggests to fracture a few wells at first and then return to the pad eventually to stimulate the remaining wells, rather than completing all jobs at once. Also, the schedule is clearly characterized by "widespread" development activity. Given the two available fracturing crews, the optimizer could have proposed to complete all 29 jobs as quickly as possible, to turn wells in-line and generate revenues early on. Considering the time value of money, such a development strategy may intuitively appear economically promising. However, as our analysis will demonstrate, there is reason to believe that the proposed fracturing schedule is highly cost-effective and that it may improve the economics of the overall development project significantly.

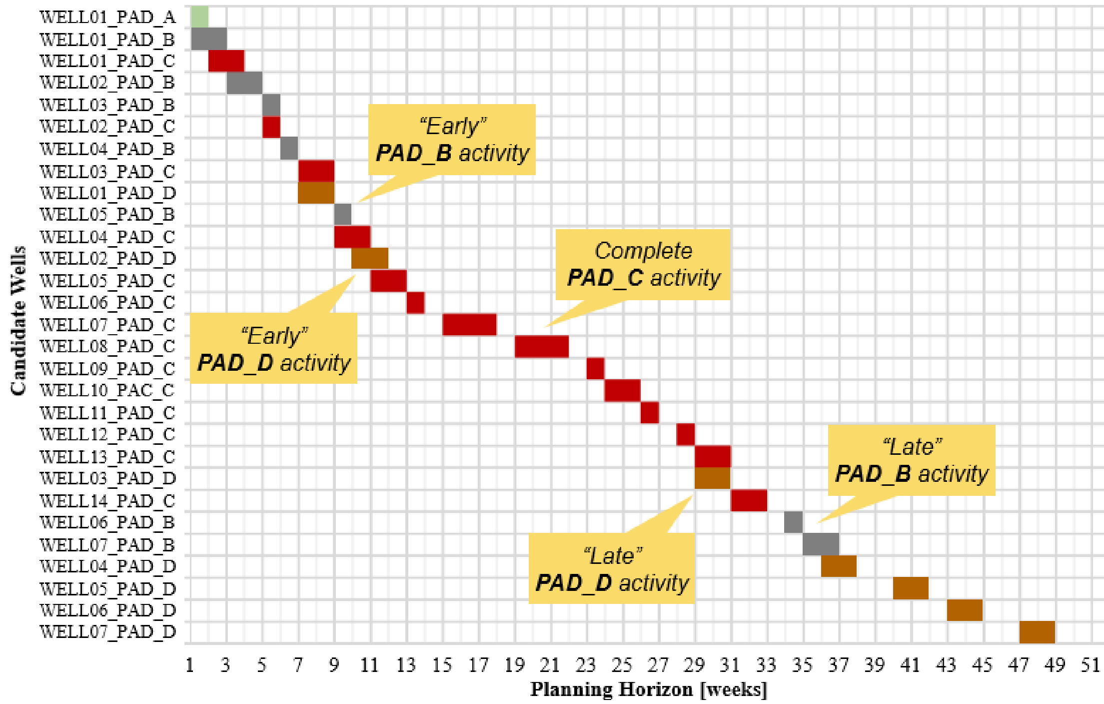

Fig. 3.3: Proposed fracturing schedule for the given development area

We begin our analysis by focusing on the "early" development activity on PAD_B. As Fig. 3.3 shows, a total of five wells are scheduled to be fractured on this pad early on in the planning horizon. The obvious question here is: why does the optimization model prefer to complete these five wells at this particular point in time? To answer this question we turn to Fig. 3.4, which shows the impaired water production forecast for the given development area (in grey) on the left axis, and proposed water deliveries from neighboring well pads to PAD_B (in red) on the right axis. If we focus on the highlighted time window – between June 2016 and July 2016 – we recognize that nearly all of the available impaired water from surrounding well pads is delivered to said PAD_B during this particular period in time: up to 40,000 barrels of impaired water per week.

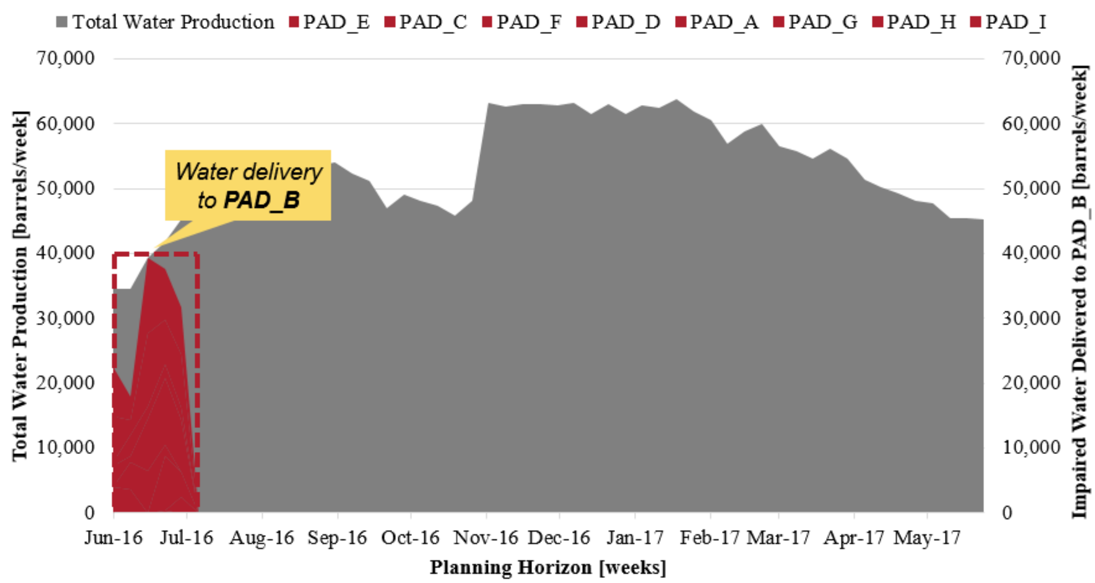

Fig. 3.4: Impaired water production forecast and impaired water deliveries to PAD_B over time

Consequently, the optimization proposes to install an impaired water AST on PAD_B that can hold up to 40,000 barrels of water for a total of five weeks to store and process the delivered water. Fig. 3.5 shows the complete AST rental schedule for all four candidate pads. The AST on PAD_B is filled with impaired water from neighboring pads, and then the water is used to fracture the five wells on PAD_B as indicated by the fracturing schedule in Fig. 3.3.

Altogether, 154,640 barrels of impaired water are delivered to PAD_B during this time window, at an estimated cost of $103,148. However, the data reveals that in order to fracture all five wells based on their individual completions designs, approximately 820,361 barrels of water are required. Therefore, the impaired water deliveries are not sufficient to complete all five wells on PAD_B. And indeed, the solution reveals that 665,721 barrels of freshwater need to be hauled to the pad from surrounding freshwater sources, at an approximate expense of $1,224,927.

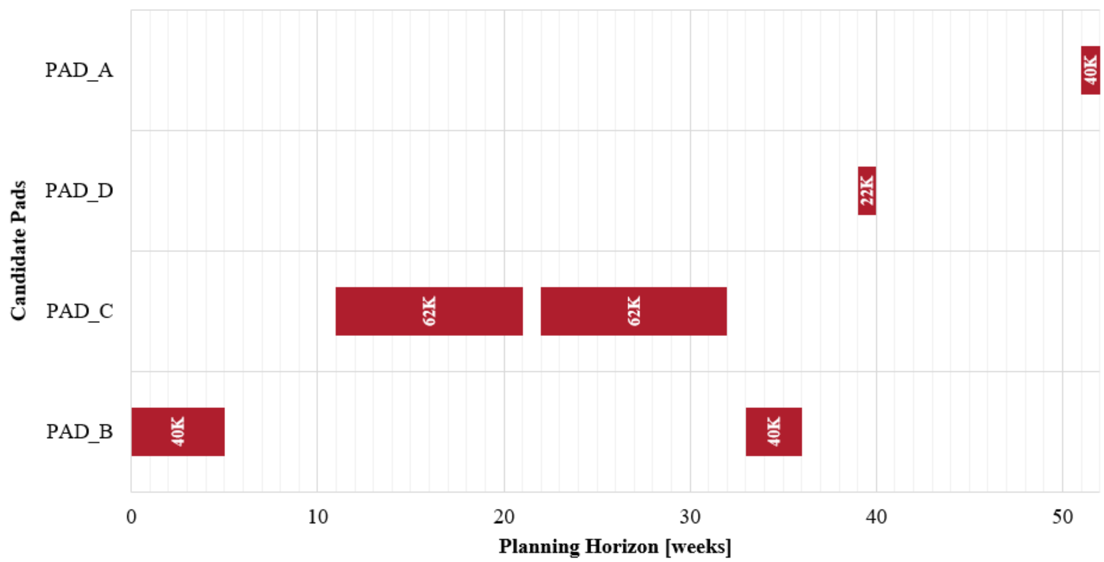

Fig. 3.5: Proposed impaired water AST rental schedule for candidate pads over time

At this point we rely on the so-called blending ratio to support the analysis and interpretation of the results. The blending ratio is defined as the amount of impaired water that is used to perform a fracturing job, compared to the total amount of water required (freshwater and impaired water combined).

Fig. 3.6 shows the blending ratio over time for all four candidate pads. Upon closer inspection, the chart reveals that during this time window of "early" activity on PAD_B, the blending ratio reaches, at times, up to 30%. This implies that only a relatively small portion of the total water demand can be met by relying on impaired water. At the same time, the impaired water forecast in Fig. 3.4 shows that during this particular period of time, the amount of impaired water that is available is rather limited. In other words, we claim that the optimization proposes to fracture the five wells on PAD_B for two reasons: a) completing and turning in-line these five wells results in a considerable stream of revenues from gas sales, and b) by fracturing these particular wells, nearly all available impaired water is reused, rather than sent to a disposal site.

This observation is in line with the following analysis and it supports the working theory that the proposed fracturing schedule is primarily driven by trying to minimize impaired water disposal as much as possible.

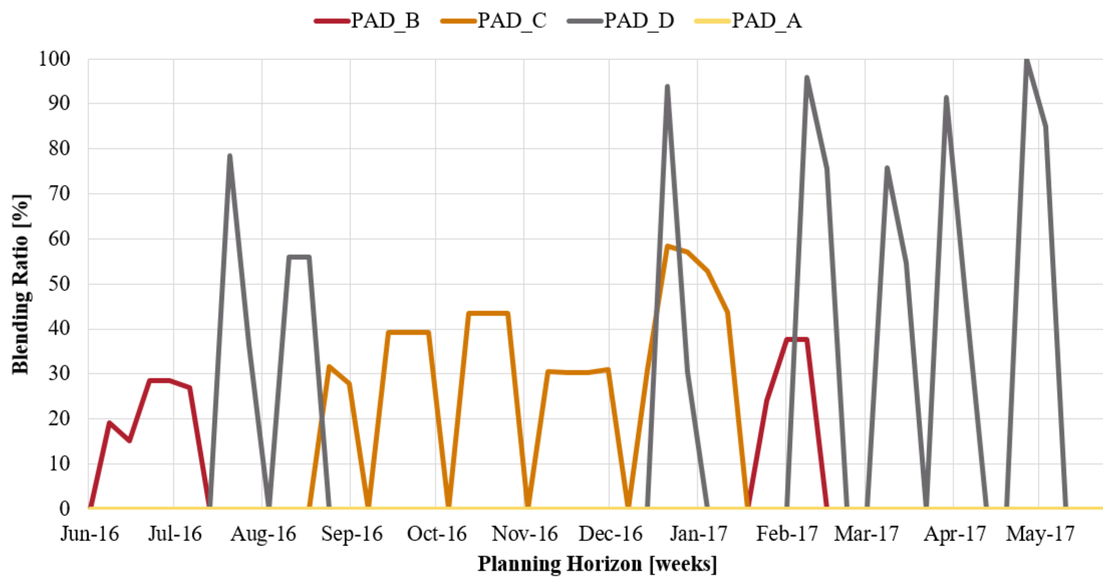

Fig. 3.6: Water blending ratio (defined as impaired water used for fracturing compared to total amount of water required) over time for all candidate pads

Next, we analyze the "early" development activity on PAD_D in more detail. As the fracturing schedule in Fig. 3.3 shows, the optimization suggests to fracture merely two wells on this pad at this time. As before, we find that during this time window a significant portion of the impaired water available at neighboring well pads should be delivered to PAD_D. Fig. 3.7 shows that up to 50,000 barrels of impaired water are hauled onto this pad per week. Interestingly, it turns out that on PAD_D the operator can rely on a legacy impaired water pit for water storage purposes. This pit can store over 100,000 barrels of water, which can then be used for fracturing.

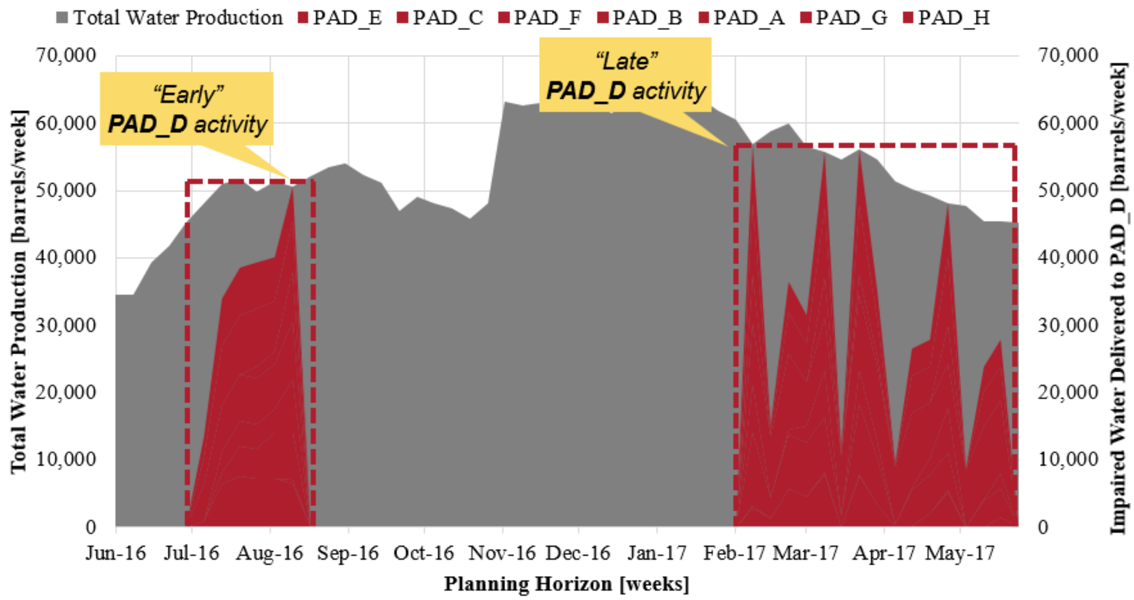

Fig. 3.7: Impaired water production forecast and impaired water deliveries to PAD_D over time

In fact, Fig. 3.8 shows that this impaired pit steadily receives water deliveries from surrounding well pads until its maximum storage capacity is reached. Once the water level in this pit has reached (near-) maximum storage capacity, the optimization immediately schedules a fracturing job. As a result, the blending ratio for these two well completions is very high, ranging between 55-80% (see Fig. 3.6 for details). This implies that more than half of the total water demand for these fracturing jobs is met by recycling available impaired water. Specifically, the water demand for fracturing is met by using a total of 343,266 barrels of impaired water (which therefore do not need to be sent to disposal) as opposed to 263,191 barrels of freshwater. Based on the results, impaired water deliveries to PAD_D are estimated to cost roughly $162,594, whereas freshwater acquisition expenses amount to approximately $426,369. The significance of the proposed solution for PAD_D is that, once again, it is clear that the optimization intentionally schedules fracturing jobs such that they use up as much of the available impaired water as possible.

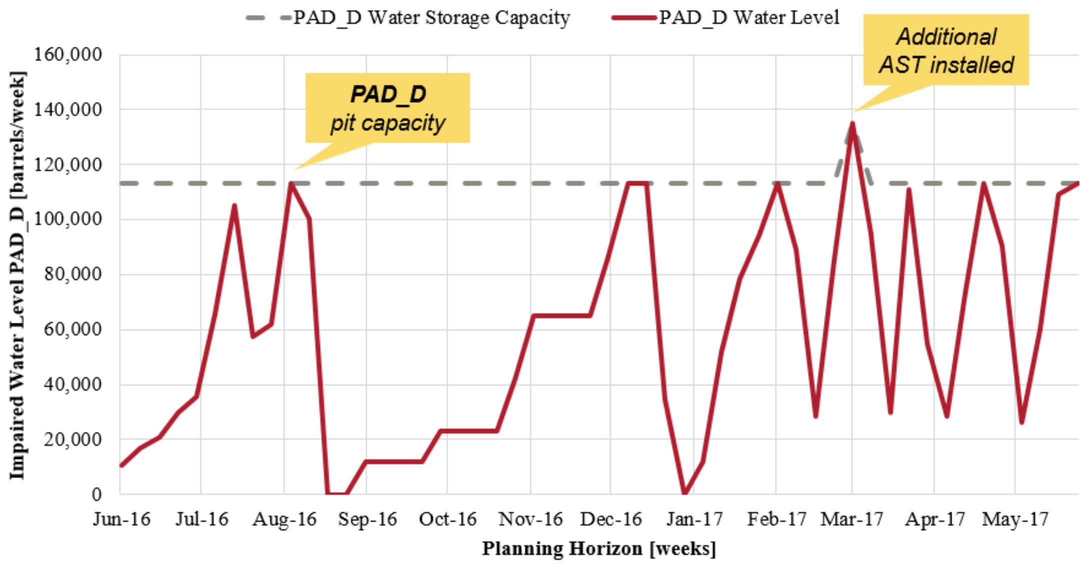

Fig. 3.8: Impaired water storage capacity utilization over time for PAD_D

At this point we also analyze the "late" development activity on PAD_D to demonstrate why it can make economic sense to "split" fracturing jobs on the same pad (rather than completing all in one trip). As the fracturing schedule in Fig. 3.3 indicates, the optimization proposes to complete the remaining five prospective wells on PAD_D towards the end of the planning horizon. Once again Fig. 3.7 shows that during this time window significant volumes of impaired water are delivered to PAD_D. As can be seen in Fig. 3.8, the optimization fully utilizes the available storage capacity in the existing impaired water pit. At one point in time, it even proposes to temporarily install a 22,000 barrels AST at the well pad for a single week to store even more impaired water on-site. Not surprisingly, the available impaired water is used to meet the total water demand for fracturing. Altogether, a remarkable 931,372 barrels of impaired water are recycled for the scheduled completion of the five wells (hauling costs amount to $362,055). In comparison, 333,708 barrels of freshwater need to be acquired (at an estimated \$540,607). In fact, in order to perform the last scheduled fracturing job within the planning horizon (WELL07_PAD_D) the optimization uses impaired water exclusively; no freshwater is necessary to meet the total completions water demand. As a result, the blending ratio for this job is 100%.

3.6.3 Benefits of the Proposed Impaired Water Management Strategy

Finally, we summarize some of the qualitative and quantitative benefits of the proposed water management strategy. Qualitatively, we find that the optimization is carefully coordinating when to perform individual fracturing jobs, it evaluates where to source water from, which water quality to use (impaired water vs. freshwater) and how to take advantage of the available water storage capacity. Moreover, though, we can actually quantify some of the potential gains. As outlined earlier, the impaired water forecast, as shown in Fig. 3.2, suggests that within the respective development area over 2.75 million barrels of impaired water need to be dealt with, i.e. either disposed of or recycled. The optimization results show that if the producer were able to implement the proposed fracturing schedule and coordinate water deliveries as suggested, then out of the 2.75 million barrels of water merely 7,500 barrels would have to be disposed of. Estimated expenses for impaired water disposal amount to less than \$60,000 for the entire year.

Fig. 3.9 shows the total, forecasted impaired water volume with respect to the anticipated disposal volumes. Practically speaking, the proposed water management strategy promises to translate to an effective water disposal rate of less than 0.3%, which is remarkable and exceptionally low. In practice, despite the industry's efforts to maximize impaired water recycle volumes, disposal rates currently range between 10-30%. If we assume that only 10% of the expected impaired water volumes in this case study could not have been recycled, then water disposal costs would have amounted to roughly $2,200,000. In some sense, the results appear to suggest that impaired water should be a considered a (valuable) resource, rather than the "burden" that it oftentimes presents to upstream operators. Clearly, the results demonstrate that the optimization is driven by trying to minimize water disposal as much as possible, while simultaneously maximizing the amount of impaired water that is reused.

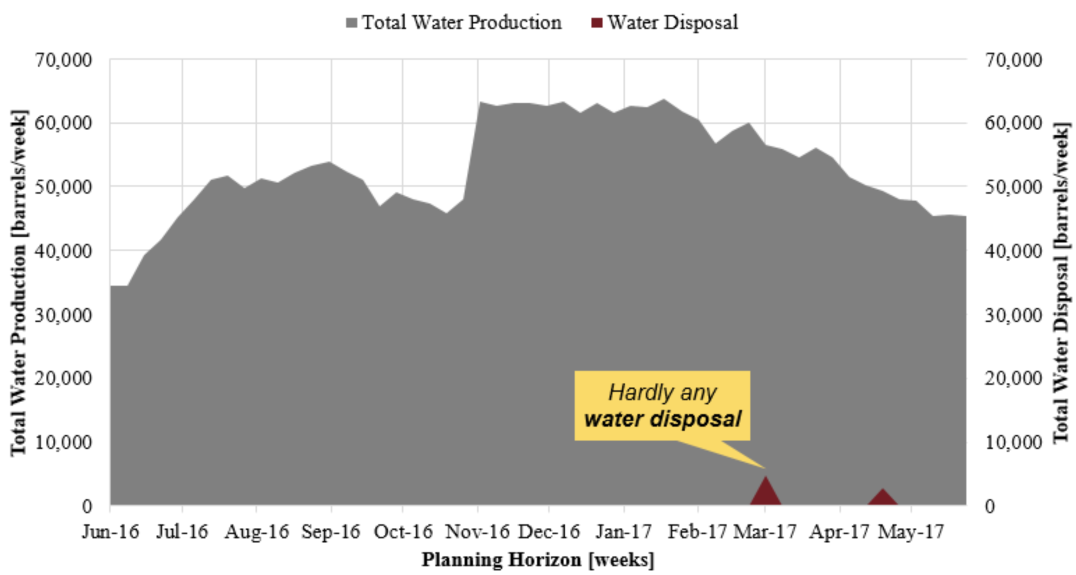

Fig. 3.9: Impaired water production forecast and impaired water disposal volumes over time

Obviously, the increased impaired water recycle rate comes at an expense. Most importantly, costs for providing impaired water storage capacity and costs for hauling impaired water from one well-site to another can be expected to increase. It should also be noted that in order to handle increasing blending ratios for fracturing jobs based on up to 100% of impaired water, operators need to use special, advanced friction reducers and other additives to ensure that the well performance is not negatively affected. For the purpose of this case study, these expenses were intentionally over-estimated. Based on the proposed water management strategy the producer would spend up to $1,283,200 on high-salinity tolerant additives. Nevertheless, we find that there is a clear, cost-driven incentive for drastically increasing impaired water recycle rates. Specifically, in this case study we find that rearranging the fracturing schedule and coordinating water deliveries based on rigorous optimization reduces potential freshwater consumption by nearly 2.75 million barrels. At the same time impaired water disposal volumes are lessened by the same amount. Therefore, we believe that the shale gas industry has a lot to gain from relying on rigorous optimization models for improving impaired water management strategies.

3.7 Conclusions

In this chapter, we presented a mixed-integer linear programming model for impaired water management in active shale gas development areas. This model determines the optimal fracturing schedule along with a water management strategy that maximizes the net present value. The water management strategy includes water sourcing and distribution decisions, as well as the selection of water storage solutions including above-ground storage tanks. In this work we explicitly considered return-to-pad operations and we allowed for unrestricted water blending ratios, i.e., fracturing jobs can be completed with impaired water exclusively.

The proposed optimization model was applied to a real-world case study based on data provided from one of the largest upstream operators in the Appalachian Basin. The results of the case study clearly suggest that the optimization is driven to minimize impaired water disposal as much as possible. We found that splitting the development of a well pad into several trips can make sense in order to increase impaired water recycling. In other words, fracturing jobs on the same pad should not necessarily be scheduled in quick succession, but such that their timing aligns with the availability of impaired water volumes. Overall, we concluded that the fracturing schedule should be driven more by the optimal water management strategy and not vice versa. The solution also suggested that impaired water storage solutions – and sufficient storage capacity in particular – are essential to effective water management strategies. Ultimately, we found that water management strategies based on rigorous, mathematical optimization can allow the shale industry to reduce impaired disposal rates significantly and thereby support companies in striving towards more cost-effective shale gas development.

3.8 Nomenclature

Sets

$c \in \mathcal{C}$	Fracturing crews
$d \in \mathcal{D}$	AST rental durations
$ds \in \mathcal{DS}$	Disposal sites
$f \in \mathcal{F}$	Freshwater sources
$fr \in \mathcal{FR}$	Friction reducers
$i \in \mathcal{I}$	Impaired water sources
$p \in \mathcal{P}$	Well pads
$p \in \mathcal{EWP}$	Existing well pads
$p \in \mathcal{CWP}$	Candidate well pads

$r \in \mathcal{R}$ Treatment facilities

$s \in \mathcal{S}$ Water sources

$t \in \mathcal{T}$ Time periods

$tc \in \mathcal{TC}$ Available AST sizes

$w \in \mathcal{W}$ Candidate wells

Binary Decision Variables

$y_{w,p,c,t}^{Frac}$ Active if well w on pad p stimulated using fracturing crew c in time period t

$y_{p,tc,t,d}^{ImpAST}$ Active if on well pad p impaired tank capacity tc installed in time period t for the duration of d time periods

$z_{p,tc,t}^{ImpAST}$ Active if on well pad p impaired tank capacity tc available on well pad in time period t

$y_{p,tc,t,d}^{FreshAST}$ Active if on well pad p fresh tank capacity tc installed in time period t for the duration of d time periods

$z_{p,tc,t}^{FreshAST}$ Active if on well pad p fresh tank capacity tc available on well pad in time period t

$y_{p,t}^{FreshPitInstall}$ Active if a freshwater pit is installed on well pad p in time period t

$y_{fr,p,t}^{FR}$ Active if friction reducer type fr selected on pad p in time period t

Continuous Decision Variables

$F_{p,pp,t}^{Reuse}$ Flow rate impaired water from well pad pp to well pad p in time period t (*inter-pad-recycling*)

$F_{p,t}^{Recycle}$ Flow rate impaired water recycled from well pad p in time period t (*intra-pad-recycling*)

$F_{p,t}^{Imp}$ Flow rate impaired water used for fracturing on well pad p in time period t

$F_{p,t}^{Fresh}$ Flow rate freshwater used for fracturing on well pad p in time period t

$F_{f,p,t}^{Source}$ Flow rate freshwater from freshwater source f to well pad p in time period t

$F_{p,d,t}^{Disposal}$ Flow rate disposal water from well pad p to disposal site d in time period t

$F_{p,r,t}^{Treatment}$ Flow rate to treatment from well pad p to treatment facility r in time period t

$L_{p,t}^{Imp}$ Impaired water impound level on well pad p in time period t

$L_{p,t}^{Fresh}$ Freshwater impound level on well pad p in time period t

$L_{p,t}^{Prod}$ Production water tank level on well pad p in time period t

$V_{p,t}^{Imp}$ Impaired water impound capacity on well pad p in time period t

$V_{p,t}^{Fresh}$ Freshwater impound level on well pad p in time period t

$V_{p,t}^{FreshAST}$ Total freshwater AST capacity on well pad p in time period t

$V_{p,t}^{FreshPit}$ Total freshwater pit capacity on well pad p in time period t

$V_{p,t}^{FreshPitInstall}$ Freshwater pit expansion on well pad p in time period t

$WD_{p,t}^{Pad}$ Water demand on well pad p in time period t

$WP_{p,t}^{Pad}$ Water produced on well pad p in time period t

$REV_{p,t}$ Revenues generated from well pad p in time period t

$FAE_{p,t}$ Freshwater acquisition expenses for well pad p in time period t

$IAE_{p,t}$ Impaired water acquisition expenses for well pad p in time period t

$IDE_{p,t}$ Impaired water disposal expenses for well pad p in time period t

$ITE_{p,t}$ Impaired water treatment expenses for well pad p in time period t

$ICE_{p,t}$ Impaired water trade expenses for well pad p in time period t

$IIE_{p,t}$ Impaired water impoundment installation expenses for pad p in time period t

$FIE_{p,t}$ Freshwater impoundment installation expenses for pad p in time period t

Parameters

$\tau_{c,p,pp}^{Trans}$ Time required to move crew c from well pad p to well pad pp

$\tau_{w,p,c}^{Frac}$ Time to fracture well w on well pad p using fracturing crew c

$wd_{w,p}^{Well}$ Specific water demand for fracturing well w at every well pad p

$l_{w,p}^{Lateral}$ Lateral length of well w on well pad p

$wp_{w,p,t}^{Well}$ Produced water forecast for well w on well pad p in time period t

$wp_{p,t}^{Pad}$ Produced water forecast for well pad p in time period t

δ_{tc} Tank capacity for commercially available impaired tank capacity tc

$l_{f,p}$ Distance from freshwater source f to well pad p

$l_{i,p}$ Distance from impaired water source i to well pad p

$l_{p,d}$ Distance from well pad p to disposal site d

$l_{p,r}$	Distance from well pad p to treatment facility r
$l_{p,k}$	Distance from well pad p to competitor k
$\tau_{p,pp}^{Travel}$	Travel time from well pad p to well pad pp
$\tau_{f,p}^{Source}$	Travel time from freshwater source f to well pad p
τ_{d}^{Rental}	Equipment rental duration $d \in \mathcal{D}$
$\rho_{f,p}^{Source}$	Freshwater acquisition cost coefficient from source f to pad p
$\rho_{i,p}$	Impaired water acquisition cost coefficient from source i to pad p
α_{w}^{Dev}	Well development expenses for well w
$\alpha_{tc,d}^{ImpAST}$	Impaired water AST rental cost coefficient for capacity tc for d time periods
$\alpha_{tc,d}^{FreshAST}$	Freshwater AST rental cost coefficient for capacity tc for d time periods
$\alpha^{PitInstall}$	Freshwater pit installation expense cost coefficient
$\alpha_{p,d}^{Disposal}$	Disposal cost coefficient from well pad p to disposal site d
α_{p}^{FR}	Friction reducer expense on well pad p
$\alpha_{p,pp}^{Reuse}$	Impaired water transportation cost coefficient from pad p to pad pp
$\gamma_{w,p,t}$	Type curve forecast for well w on well pad p in time period t
θ_{t}	Natural gas price forecast in time period t
$v_{p}^{ImpairedAST,0}$	Initial impaired water AST impoundment capacity on well pad p
$v_{p}^{ImpairedPit,0}$	Initial impaired water pit impoundment capacity on well pad p
$v_{p}^{FreshAST,0}$	Initial freshwater AST impoundment capacity on well pad p
$v_{p}^{FreshPit,0}$	Initial freshwater pit impoundment capacity on well pad p
v_{p}^{Prod}	Production water tank level restriction on well pad p
adr	Annual discount rate
$\psi_{f,t}^{Source}$	Freshwater availability at freshwater source f in time period t

$\psi_{i,t}^{Impaired}$ Impaired water availability at impaired water source i in time period t

$\psi_{d,t}^{Disposal}$ Maximum capacity at disposal site d in time period t

$\psi_{r,t}^{Treatment}$ Maximum capacity at treatment site r in time period t

$\psi_{k,t}^{Competitor}$ Maximum capacity at competitor k in time period t

$\psi_{p,t}^{Prod}$ Maximum production tank capacity at well pad p in time period t

$\psi_{p,t}^{Impaired}$ Maximum impaired water impoundment capacity at well pad p in time period t

$\psi_{p,t}^{Fresh}$ Maximum freshwater impoundment capacity at well pad p in time period t

r_{fr} Frac ratio threshold for friction reducer type fr

ϑ_{fr} Cost coefficient for friction reducer type fr

stc Standard water hauling truck capacity

CHAPTER 4

Mixed-Integer Nonlinear Programming Models for Line Pressure Optimization in Shale Gas Gathering Systems

4.1 Introduction

Shale gas producing companies generally struggle with the so-called *backoff effect*. Fig. 4.1 shows the historic gas production rate of a shale well in the Appalachian Basin over time, along with its wellhead pressure. The data shows that sudden line pressure variations have a direct and pronounced impact on the shale well's production. For instance, in mid-February 2014 the respective gathering system experienced an abrupt pressure increase (possibly due to an unscheduled compressor shut-down). The well's response is almost instantaneous, and it is characterized by a striking production backoff. The other way around, when the wellhead pressure dropped in mid-June 2014, this particular well saw a clear and immediate increase in production. The pressure spike is almost mirrored by the production rate.

It should also be pointed out that the pressure and production data in Fig. 4.1 shows dynamic effects and measurement variances. The purpose of this work is not to capture these dynamic effects that occur on a daily basis, or to account for measurement errors. Instead, we focus on the dominant backoff effects which are directly tied to strategic development decisions, such as deliberate line pressure variations or bringing new wells online. The problems we wish to address are characterized by extended planning horizons (3 to 12 months) and they assume that a weekly discretization of time is sufficient. Hence, we believe that the use of steady-state models with semi-dynamic extensions is applicable and justified.

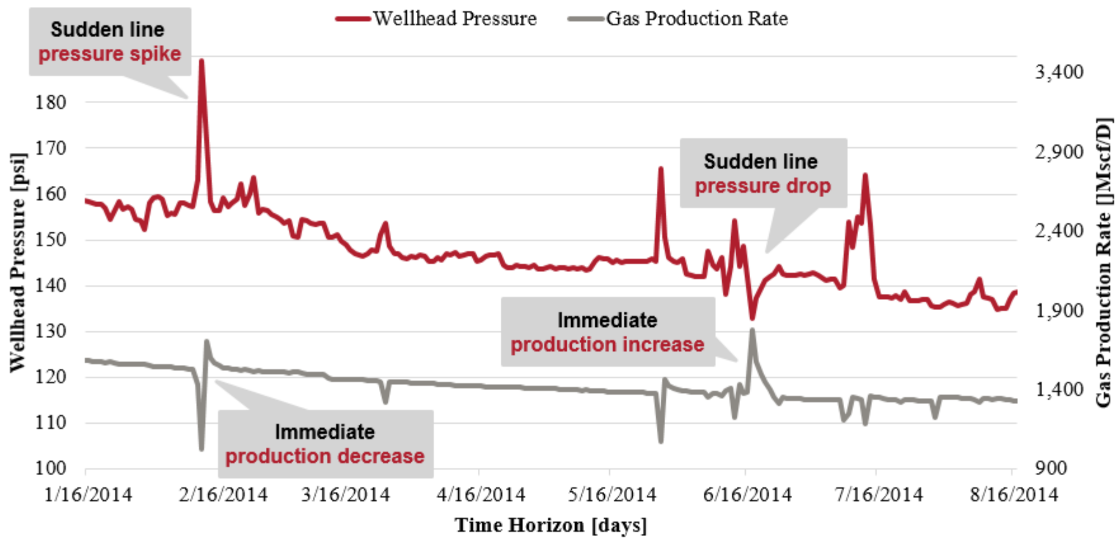

Fig. 4.1: Historic wellhead pressure and gas production rate of a single shale well over time

The backoff-effect itself is particularly prominent when new shale wells are turned in-line. Due to the characteristically high initial production rates of shale gas wells, gathering systems will experience pronounced line pressure increases. These sudden pressure spikes result in immediate production cutbacks by all wells, but especially existing wells experience serious recovery declines. To demonstrate this effect, we turn to Fig. 4.2. This figure shows the overall gas production rate and average line pressure for a gas gathering system over time. The red dotted line shows the forecasted production of all existent wells – assuming that no new wells are opened up. Clearly, these wells are expected to experience a gradual decline with age.

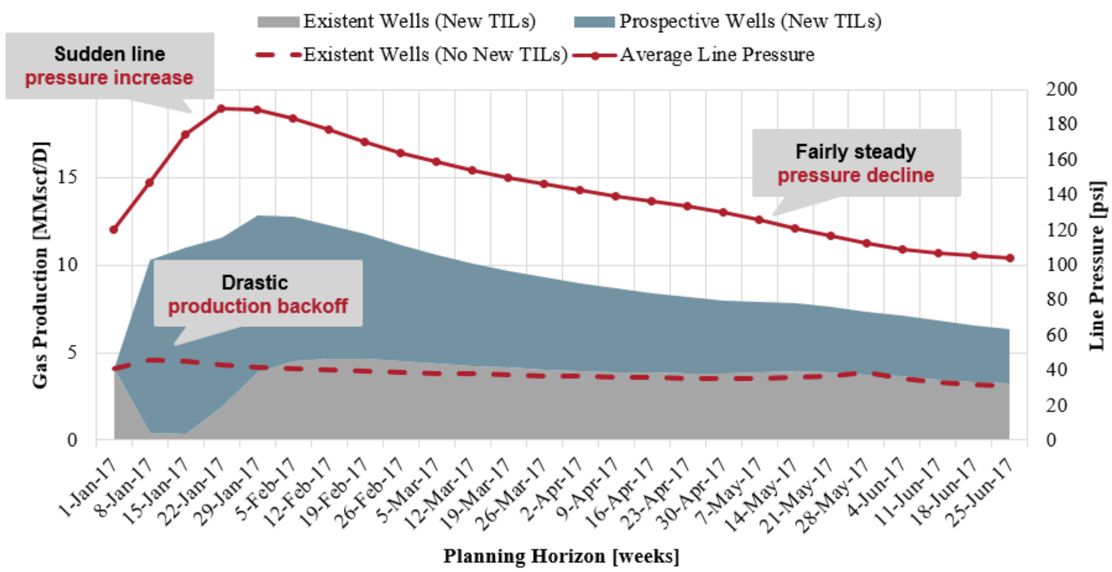

Fig. 4.2: Demonstration of the "backoff effect" in a shale gas gathering system when too many prospective wells are turned in-line at the same time

For demonstration purposes let us assume that an upstream operator decides to turn seven prospective shale wells in-line on January 1, 2017. For this scenario the stacked charts in grey and blue show the expected production of the existent and prospective wells respectively. In addition, the solid red line indicates how this development decision would affect the average line pressure in the gathering system. As expected, the line pressure increases by nearly 70 psi once the new wells are brought online. However, this sudden pressure spike results in an almost immediate, drastic production backoff by the existing wells collectively. These wells nearly cease to produce at all. What this implies is that a majority of the incremental production volumes added by turning new wells in-line is "lost" to making up for the reduced production of the existent wells. In other words, the system does not exhibit the desired production increase that one would expect from bringing seven additional wells online. Shale gas producers regularly struggle with this phenomenon since it seriously complicates development decisions regarding the right timing for turning wells in-line. For this precise reason the "backoff effect" lies at the heart of the line pressure optimization problem in shale gas gathering systems.

4.2 General Problem Statement

In this work we present a multiperiod mixed-integer nonlinear programming model to address the line pressure optimization problem in shale gas gathering systems. The problem at hand can be stated as follows. Within an active development area, an upstream operator is actively producing natural gas from a set of existing shale wells into an existing gas gathering system. This pipeline system delivers the produced gas to a compressor station which feeds into a long-distance, wide-diameter, high-pressure transmission line. Within the foreseeable future the producer wishes to open up additional prospective wells to maximize the utilization of the available gas gathering capacity.

Our work is concerned with: a) determining the optimal schedule to turn prospective wells in-line, also referred to as the "turn-in-line (TIL) schedule", b) identifying the optimal pressure profile within the gas gathering network, and c) calculating the required compression power to deliver the gas into the interstate transmission network. The problem is complicated by the fact that as new wells are brought online, the production of previously producing wells is negatively affected. In other words, the increase in line pressure due to additional gas production curtails gas recovery from mature wells. This effect is particularly prominent due to the characteristically steep decline curves of new shale gas wells. Hence, the objective of this work is to determine the optimal "TIL" schedule, line pressure profile and compressor operation such that the net present value of the field development project is maximized.

4.3 Literature Review

Over the years many researchers have proposed mathematical programming models for pressure optimization in natural gas transmission systems. Recently, Ríos-Mercado and Borraz-Sánchez (2015) published a comprehensive review of previous efforts in this domain to-date. The authors distinguish between three different topics in this general research area: a) line-packing problems focused on short-term natural gas storage in pipelines (Carter & Rachford, 2003; Krishnaswami et al., 2004; Zavala, 2014), b) pressure drop models capturing pressure losses due to frictional resistance along pipeline segments (Duran & Grossmann, 1986; De Wolf & Smeers, 2000; Martin et al., 2006), and c) fuel cost minimization problems that focus on compressor station modeling (Wu et al., 2000; Ríos-Mercado et al., 2006; Misra et al., 2015). All three topics have been addressed extensively – both individually and collectively. We only highlight selected papers focused on the use of mathematical programming techniques. For a comprehensive summary of related publications we refer to the work by Ríos-Mercado and Borraz-Sánchez (2015).

To the best of our knowledge, we are the first to address the rigorous line pressure optimization problem in the context of shale gas development. Previous optimization frameworks addressing the shale gas development problem do not rigorously capture pressure variations within gas gathering networks (Cafaro & Grossmann, 2014; Guerra et al., 2016; Drouven & Grossmann, 2016). In this work we explicitly consider three important aspects of the development problem: a) the incorporation of reduced-order, nonlinear shale well reservoir models, b) the rigorous consideration of pressure drops along gas gathering pipelines based on nonlinear and nonconvex gas flow equations, and c) the inclusion of nonlinear and nonconvex compressor models to determine necessary compression power. Specifically, in this work we rely on a pressure normalized decline model proposed by Anderson et al. (2012) to capture and quantify how line pressure variations affect individual well production rates. Anderson et al. (2012) observe that shale wells display a harmonic decline of pressure normalized production rate over time. In fact, the authors demonstrate that a linear relationship between pressure normalized production rate and cumulative gas production can be established in a semi-log plot. Fig 4.3 shows this linear relationship for selected wells from the Haynesville play. For more details regarding the proposed reservoir function we refer to section 4.5 Model Description.

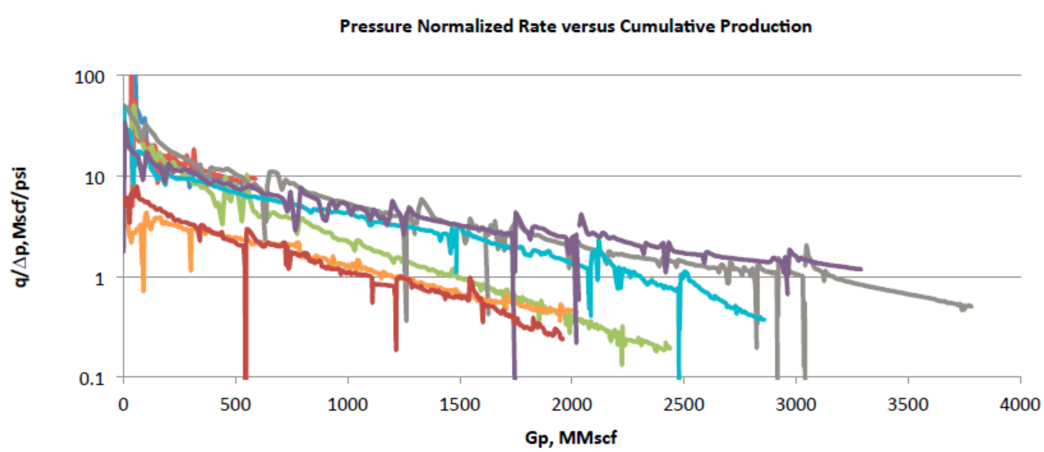

Fig. 4.3: Pressure normalized production rate over cumulative gas production for selected shale wells (Source: Anderson et al. 2012)

We also note that to date several alternative shale well reservoir models have been proposed. In particular, we highlight those proposed by Knudsen & Foss (2013),

(2015) who derive reduced-order shale well and reservoir proxy models using first-principles physics of the subsurface storage and transport mechanisms. These models are particularly suitable for capturing rapid reservoir dynamics, such as those occurring during shut-in operations. Empirically derived reservoir models, on the other hand, generally assume steady-state operations and therefore these models are not suitable for the explicit consideration of short-term line pressure manipulations.

4.4 Model Assumptions

- The planning horizon is discretized by weeks. This discretization is motivated by the fact that it typically takes one week to turn a prospective well in-line. Moreover, by splitting the planning horizon into weekly time intervals we can track the dynamics of the gas gathering system (in terms of pressure variations and compression requirements) with sufficient accuracy.
- The reservoir model proposed by Anderson et al. (2012) captures the production of shale gas wells based on their cumulative production and the respective wellhead pressure.
- The focus of this work is on turning prospective wells in-line. Therefore, we assume that either, a) all prospective wells have already been drilled and completed, or b) any outstanding drilling and completions operations can be scheduled according to the preferred TIL schedule.

4.5 Model Description

In this section we describe the proposed mixed-integer nonlinear programming model to address the line pressure optimization problem in shale gas gathering systems.

Reservoir Model Constraints

The reservoir model proposed by Anderson et al. (2012) is one of the fundamental building blocks of the line pressure optimization model we present. Its purpose is to tie the default gas production rate of any shale well $F_{w,t}^{W,S}$ to its wellhead pressure $P_{p,t}^{W}$ and cumulative production $Q_{w,t}^{S}$. As outlined by Anderson et al. (2012) this can be accomplished by considering four parameters: a) the initial bottomhole pressure of the well $p_{w,t}^{0}$, b) the cumulative production of the well at the beginning of the planning horizon $q_{w}^{0,S}$, c) a slope parameter $m_{w,p}$, and d) an intercept parameter $a_{w,p}$. The latter two parameters need to be fit to historic production data for existent wells and estimated for prospective wells based on forecasted type curves. By including this reservoir model in our framework we can quantify how pressure variations will affect gas production rates.

Eq. (4.1) represents the default reservoir model for existing wells. It turns out that this model is nonlinear and nonconvex within the domain of interest. It is also important to note that the default reservoir model inherently assumes that any line pressure variations occur gradually, over extended periods of time. As we established earlier, shale gas gatherings systems oftentimes experience abrupt and pronounced line pressure changes. These are not captured adequately by the default reservoir model.

$$\log\left(\frac{F_{w,t}^{W,S}}{p_{w,t}^{0}-P_{p,t}^{W}}+\epsilon\right)\le m_{w,p}\cdot\left(q_{w}^{0,S}+Q_{w,t}^{S}\right)+a_{w,p}\quad \forall w\in\mathcal{EW},(w,p)\in\mathcal{WPA},t\in\mathcal{T} \quad (4.1)$$

Therefore, we propose a "backoff extension" to the default reservoir model. The extension in Eq. (4.2) considers wellhead pressures at pads in consecutive time periods along with a well-specific backoff parameter Δ_{w}^{B} in order to predict the backoff $F_{w,t}^{B,S}$.

If the wellhead pressure increases from one time period to another, then this backoff extension in Eq. (4.2) will result in a production backoff "penalty", i.e., the well's production is less than forecasted by the default reservoir model. The extension also holds in the reverse direction, i.e., when the wellhead pressure drops, then the production will increase accordingly. This backoff parameter itself can be fit to historic data for existing wells but for prospective wells it has to be estimated.

$$F_{w,t}^{B,S} = -\left(P_{p,t-1}^{W} - P_{p,t}^{W}\right) \cdot \Delta_{w}^{B} \qquad \forall w \in \mathcal{EW}, \left(w, p\right) \in \mathcal{WPA}, t \geq 1 \tag{4.2}$$

Ultimately, the default reservoir model and the backoff extension are combined for all wells (existent and prospective) in Eq. (4.3) to capture the shale well's final production $F_{w,t}^{F,S}$. We note that typical gas production units (GPUs) are rate-restricted. Hence, we impose Eq. (4.4) using the maximum production rate parameter γ_w to ensure that the well cannot produce at infinitely high rates early in its lifespan.

$$F_{w,t}^{F,S} = F_{w,t}^{W,S} - F_{w,t}^{B,S} \qquad \forall w \in \mathcal{W}, t \in \mathcal{T} \tag{4.3}$$

$$F_{w,t}^{F,S} \leq \gamma_w \qquad \forall w \in \mathcal{W}, t \in \mathcal{T} \tag{4.4}$$

Although the modified reservoir model transfers over directly from existing to prospective wells, we examine the model formulation of the latter in more detail. We rely on a disjunctive programming formulation for prospective wells to link the corresponding reservoir model to the turn in-line decision. For this reason we introduce the Boolean variable $Y_{w,t}^{PROD}$ which is true if the prospective well $w \in \mathcal{PW}$ on pad $p \in \mathcal{P}$ is actively producing in time period $t \in \mathcal{T}$. This Boolean variable is involved in the disjunction in Eq. (4.5) to model the fact that as long as the well is not actively producing, its default production $F_{w,t}^{W,S}$ is less or equal than zero and the production backoff $F_{w,t}^{B,S}$ is greater or equal than zero. Due to the formulation of Eq. (4.3) the optimization will generally aim for "negative" backoff (resulting in a production increase), hence this inequality ensures that the inactivity of a prospective well does not lead to any actual production.

$$\begin{bmatrix} Y_{w,t}^{PROD} \\ \log\left(\dfrac{F_{w,t}^{W,S}}{p_{w,t}^{0}-P_{p,t}^{W}}+\epsilon\right) \le m_{w,p}\cdot\left(q_{w}^{0,S}+Q_{w,t}^{S}\right)+a_{w,p} \\ F_{w,t}^{B,S} = -\left(P_{p,t-1}^{W}-P_{p,t}^{W}\right)\cdot\Delta_{w}^{B} \end{bmatrix} \vee \begin{bmatrix} \neg Y_{w,t}^{PROD} \\ F_{w,t}^{W,S} \le 0 \\ F_{w,t}^{B,S} \ge 0 \end{bmatrix} \tag{4.5}$$

$$\forall w \in \mathcal{PW}, (w,p) \in \mathcal{WPA}, t \in \mathcal{T}$$

On the other hand, if the Boolean variable $Y_{w,t}^{PROD}$ is true, the well is active, and its production will be governed by the default reservoir model and the backoff extension as outlined previously. We should also note that the initial cumulative production of prospective wells $q_{w}^{0,S}$ in Eq. (4.5) is typically zero.

The disjunction in Eq. (4.5) is transformed into the mixed-integer constraints Eq. (4.6)-(4.10) using the big-M reformulation (Grossmann & Trespalacios 2013). For this purpose we introduce a corresponding binary variable $y_{w,t}^{Prod}$ for the Boolean variable $Y_{w,t}^{PROD}$. We note that the big-M parameters $M_1, \ldots, M_5$ need to be defined independently.

$$\log\left(\frac{F_{w,t}^{W,S}}{p_{w,t}^{0}-P_{p,t}^{W}}+\epsilon\right) \le m_{w,p}\cdot\left(q_{w}^{0,S}+Q_{w,t}^{S}\right)+a_{w,p}+M_1\cdot\left(1-y_{w,t}^{PROD}\right) \tag{4.6}$$

$$\forall w \in \mathcal{PW}, (w,p) \in \mathcal{WPA}, t \in \mathcal{T}$$

$$F_{w,t}^{B,S} \le -\left(P_{p,t-1}^{W}-P_{p,t}^{W}\right)\cdot\Delta_{w}^{B}+M_2\cdot\left(1-y_{w,t}^{PROD}\right) \qquad \forall w \in \mathcal{PW}, (w,p) \in \mathcal{WPA}, t \ge 1 \tag{4.7}$$

$$F_{w,t}^{B,S} \ge -\left(P_{p,t-1}^{W}-P_{p,t}^{W}\right)\cdot\Delta_{w}^{B}-M_3\cdot\left(1-y_{w,t}^{PROD}\right) \qquad \forall w \in \mathcal{PW}, (w,p) \in \mathcal{WPA}, t \ge 1 \tag{4.8}$$

$$F_{w,t}^{W,S} \le M_4\cdot y_{w,t}^{PROD} \qquad \forall w \in \mathcal{PW}, (w,p) \in \mathcal{WPA}, t \in \mathcal{T} \tag{4.9}$$

$$F_{w,t}^{B,S} \geq -M_5 \cdot y_{w,t}^{PROD} \qquad \forall w \in \mathcal{PW}, (w,p) \in \mathcal{WPA}, t \geq 1 \tag{4.10}$$

At this point we establish a direct link between the decision to bring a well online and its "active production status". In order to accomplish this we introduce an additional binary variable $y_{w,t}^{TIL}$ which marks the time period in which the well is turned in-line ("TIL" for short). Using this binary variable we first impose Eq. (4.11) which ensures that any prospective well may be opened at most once over the planning horizon. We note that the formulation explicitly allows for rejecting the development of a candidate well.

$$\sum_{t \in \mathcal{T}} y_{w,t}^{TIL} \leq 1 \qquad \forall w \in \mathcal{PW} \tag{4.11}$$

Next, we add Eqs. (4.12) and (4.13) to the model formulation. These inequalities impose additional constraints on the timing of TIL operations. Eq. (4.12) limits the number of wells that can be brought online simultaneously to $n^{TIL,max}$. Eq. (4.13) on the other hand restricts in which time periods prospective wells may be turned in-line through the so-called land-cleared parameter $lc_{w,t}$.

$$\sum_{w \in \mathcal{PW}} y_{w,t}^{TIL} \leq n^{TIL,max} \qquad \forall t \in \mathcal{T} \tag{4.12}$$

$$\sum_{t \in \mathcal{T}} y_{w,t}^{TIL} \leq lc_{w,t} \qquad \forall w \in \mathcal{PW}, t \in \mathcal{T} \tag{4.13}$$

Finally, the logic constraint Eq. (4.14) states that any prospective well that has been turned in-line in one of the previous time periods has to be actively producing. In other words, unless the TIL operation has already occurred, a prospective well cannot be producing.

$$\sum_{\tilde{t}=1}^{t} y_{w,\tilde{t}}^{TIL} = y_{w,t}^{PROD} \qquad \forall w \in \mathcal{PW}, t \in \mathcal{T} \tag{4.14}$$

Pressure Drop Constraints

Next, we focus on how to capture pressure drops along gathering pipeline segments due to frictional resistance. In this work we rely on the Weymouth Equation to link gas flowrates with up- and downstream pressures (Weymouth, 1912). This equation is commonly used to estimate pressure drops in small-diameter, short-distance gathering pipelines. The Weymouth Equation considers the diameter of the pipeline segment d, its length l, the specific gravity of the gas S^g, its compressibility Z and the inlet temperature T^L. We apply the Weymouth equation to all network arcs within the gathering system, which includes: a) Eq. (4.15) for pipelines connecting well pads and network nodes $(p,n) \in \mathcal{PNA}$, b) Eq. (4.16) for segments connecting network nodes leading up to the compressor station $(n,\tilde{n}) \in \mathcal{NNA}$, and c) Eq. (4.17) for delivery pipelines connecting the compressor station and the transmission line $(n,\tilde{n}) \in \mathcal{DNA}$. In terms of pressures we explicitly distinguish between wellhead pressures $P^L_{p,t}$ at the pads and line pressures $P^L_{n,t}$ at the network nodes. It should be noted that all inequality constraints below are nonlinear and nonconvex.

$$F^{PN,S}_{p,n,t} \leq 1.1 \cdot \left(d_{p,n}\right)^{2.67} \cdot \left[\frac{\left(P^P_{p,t}\right)^2 - \left(P^P_{n,t}\right)^2}{l_{p,n} \cdot S^g \cdot Z \cdot T^L}\right]^{1/2} \qquad \forall (p,n) \in \mathcal{PNA}, t \in \mathcal{T} \qquad (4.15)$$

$$F^{NN,S}_{n,\tilde{n},t} \leq 1.1 \cdot \left(d_{n,\tilde{n}}\right)^{2.67} \cdot \left[\frac{\left(P^L_{n,t}\right)^2 - \left(P^L_{\tilde{n},t}\right)^2}{l_{n,\tilde{n}} \cdot S^g \cdot Z \cdot T^L}\right]^{1/2} \qquad \forall (n,\tilde{n}) \in \mathcal{NNA}, t \in \mathcal{T} \qquad (4.16)$$

$$F^{NN,S}_{n,\tilde{n},t} \leq 1.1 \cdot \left(d_{n,\tilde{n}}\right)^{2.67} \cdot \left[\frac{\left(P^L_{n,t}\right)^2 - \left(P^L_{\tilde{n},t}\right)^2}{l_{n,\tilde{n}} \cdot S^g \cdot Z \cdot T^L}\right]^{1/2} \qquad \forall (n,\tilde{n}) \in \mathcal{DNA}, t \in \mathcal{T} \qquad (4.17)$$

Along with Eqs. (4.15)-(4.17) we impose the inequalities (4.18)-(4.20) to ensure that – due to the pressure drops – upstream and downstream pressures of pipeline segments are not identical. In this case ϵ is a sufficiently small parameter.

$$P_{p,t}^{P} \geq P_{n,t}^{L} + \epsilon \qquad \forall (p,n) \in \mathcal{PNA}, t \in \mathcal{T} \tag{4.18}$$

$$P_{n,t}^{L} \geq P_{\tilde{n},t}^{L} + \epsilon \qquad \forall (n,\tilde{n}) \in \mathcal{NNA}, t \in \mathcal{T} \tag{4.19}$$

$$P_{n,t}^{L} \geq P_{\tilde{n},t}^{L} + \epsilon \qquad \forall (n,\tilde{n}) \in \mathcal{DNA}, t \in \mathcal{T} \tag{4.20}$$

Flow Balances

We include flow balances in the proposed line pressure optimization model to ensure the conservation of mass. In particular, Eq. (4.21) has to hold for every network node $n \in \mathcal{N}$ within the gathering system in every time period $t \in \mathcal{T}$. We distinguish between the following flows: a) gas flows $F_{p,n,t}^{PN,S}$ from well pads to network nodes $(p,n) \in \mathcal{PNA}$, b) gas flows $F_{n,\tilde{n},t}^{NN,S}$ between regular network nodes $(n,\tilde{n}) \in \mathcal{NNA}$, c) gas flows $F_{n,\tilde{n},t}^{NN,S}$ through the compressor station $(n,\tilde{n}) \in \mathcal{CNA}$, and d) gas flows $F_{n,\tilde{n},t}^{NN,S}$ along the delivery arc $(n,\tilde{n}) \in \mathcal{DNA}$. All flows are measured in volume units at standard conditions (15° C and 101.325 kPa).

$$\begin{aligned} &\sum_{(p,n)\in\mathcal{PNA}} F_{p,n,t}^{PN,S} + \sum_{(\bar{n},n)\in\mathcal{NNA}} F_{\bar{n},n,t}^{NN,S} + \sum_{(\bar{n},n)\in\mathcal{CNA}} F_{\bar{n},n,t}^{NN,S} = \\ &\sum_{(n,\tilde{n})\in\mathcal{NNA}} F_{n,\tilde{n},t}^{NN,S} + \sum_{(n,\tilde{n})\in\mathcal{CNA}} F_{n,\tilde{n},t}^{NN,S} + \sum_{(n,\tilde{n})\in\mathcal{DNA}} F_{n,\tilde{n},t}^{NN,S} \qquad \forall n \in \mathcal{N}, t \in \mathcal{T} \end{aligned} \tag{4.21}$$

In addition, Eq. (4.22) allows the gas produced at a well pad to be delivered to multiple network nodes (only applies if the respective pad is actually connected to multiple network nodes).

$$\sum_{(p,n)\in\mathcal{PNA}} F^{PN,S}_{p,n,t} = F^{P,S}_{p,t} \qquad \forall (p,n)\in\mathcal{PNA}, t\in\mathcal{T} \tag{4.22}$$

Eq. (4.23) determines how much gas every pad produces based on the final production rates of individual wells located at the respective pad.

$$F^{P,S}_{p,t} = \sum_{w\in\mathcal{W}} F^{F,S}_{w,t} \qquad \forall (w,p)\in\mathcal{WPA}, t\in\mathcal{T} \tag{4.23}$$

Finally, Eq. (4.24) calculates the cumulative gas production $Q^{S}_{w,t}$ of every well in every time period based on its weekly production rates $F^{F,S}_{w,t}$.

$$Q^{S}_{w,t} = \sum_{\tilde{t}=1}^{t} F^{F,S}_{w,\tilde{t}} \qquad \forall w\in\mathcal{W}, t\in\mathcal{T} \tag{4.24}$$

Compression Power

The compression model is included in the line pressure optimization model to capture the tradeoff between low line pressures and high operating costs. This model explicitly accounts for the pressure differential that needs to be overcome between the low-pressure gathering system and the high-pressure transmission line. In this case we rely on a straightforward compression model reported in Biegler et al. (1997), which is nonlinear and nonconvex. It calculates the necessary compression power W_t to process the gas flowrate $F^{NN,S}_{n,\tilde{n}}$ from suction pressure $P^{L}_{n,t}$ to discharge pressure $P^{L}_{\tilde{n},t}$. The parameters that need to be specified include: a) the heat capacity ratio k, b) the compressibility Z and c) the compressor efficiency η^{CE}. It should be noted that we consider multi-stage compressors in this work.

$$W_t \geq F^{NN,S}_{n,\tilde{n}} \cdot 43.6 \cdot \left(\frac{k}{k-1}\right) \cdot \left[\left(\frac{P^{L}_{\tilde{n},t}}{P^{L}_{n,t}}\right)^{\frac{k-1}{k}} - 1\right] \cdot Z \cdot {}^{1}\!/_{\eta^{CE}} \qquad \forall (n,\tilde{n})\in\mathcal{CNA}, t\in\mathcal{T} \tag{4.25}$$

For practical purposes we impose lower and upper bounds on the compression power since many compressors should not or cannot be operated below certain engine speeds.

$$W^{MIN} \leq W_t \leq W^{MAX} \qquad \forall t \in \mathcal{T} \tag{4.26}$$

Objective Function

The objective function for the line pressure optimization problem considers three line items to maximize the net present value of the field development project: a) revenues from natural gas sales, b) expenses for turning wells in-line, and c) expenses for compressor operation. In this work we assume that the compressor is powered by natural gas. Hence, the compression expenses translate to lost revenues from reduced gas sales. All revenues and expenses are discounted back to the present time. The parameters included in the objective function in Eq. (4.27) are: a) the natural gas price forecast π_t, b) the cost of turning any prospective well in-line $\delta^{TIL}_{w,p}$, and c) the compressor fuel consumption coefficient φ^C.

$$\begin{aligned} \max NPV = \sum_{t\in\mathcal{T}} (1+dr)^{-t/52} \Bigg[& \sum_{(n,\tilde{n})\in\mathcal{DNA}} F^{NN,S}_{n,\tilde{n},t} \cdot \pi_t \\ & - \sum_{w\in\mathcal{PW}} \sum_{(w,p)\in\mathcal{WPA}} y^{TIL}_{w,p,t} \cdot \delta^{TIL}_{w,p} - \sum_{(n,\tilde{n})\in\mathcal{CNA}} W_t \cdot \varphi^C \cdot \pi_t \Bigg] \end{aligned} \tag{4.27}$$

Altogether, the proposed line pressure optimization MINLP model. In the following section we describe a tailored solution strategy for addressing this problem.

4.6 Solution Strategy

As outlined in the previous section, the line pressure optimization problem in shale gas gathering systems gives rise to large-scale, nonconvex MINLPs. Solving these problems to optimality with commercial solvers can be very challenging, and even finding good feasible solutions is not trivial. Due to the nonconvexities involved in the pressure drop constraints and the compression model, the proposed optimization model can exhibit multiple local optima. Hence, we present a tailored solution strategy for this particular problem type. Fig. 4.4 shows an overview of the proposed solution strategy.

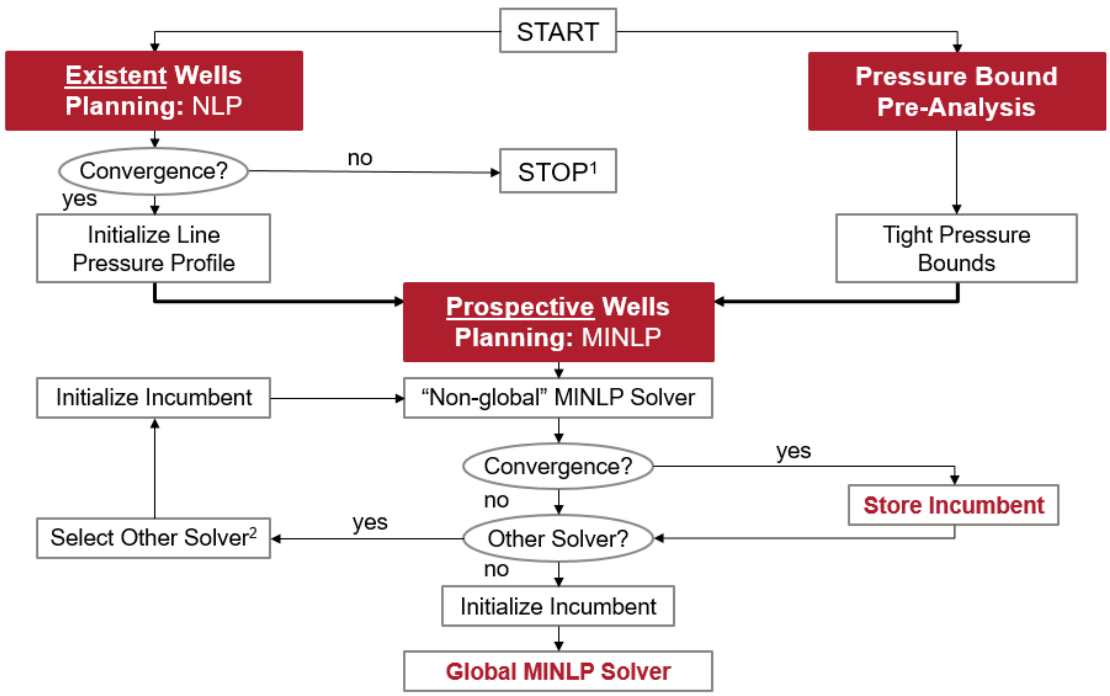

Fig. 4.4: Proposed solution strategy for addressing the line pressure optimization problem in shale gas gathering systems

The solution strategy illustrated in Fig. 4.4 begins by addressing a simplified version of the line pressure optimization problem, namely the *existent wells planning problem*. Initially, we only consider existing wells and do not account for any prospective wells that may be turned in-line. In particular, this version of the problem does not include Eqs. (4.6)-(4.14), and the objective function does not account for costs associated with TIL operations. Since the remaining model constraints do not include any binary variables, the existent wells planning problem reduces to a nonlinear programming problem. In general, the simplified NLP should be much easier to solve than the full-scale MINLP. Yet, the solution to the NLP yields a valid feasible solution to the actual MINLP problem. After all, one possible solution to the scheduling problem at hand is not to open up any new wells. More importantly though, any solution to the existent wells planning problem provides an initial line pressure profile within the respective shale gas gathering network. In other words, the solution specifies wellhead pressures, line pressures and gas flowrates throughout the network. This information can be used to effectively initialize the line pressure problem including any available prospective wells. We should note that the existent wells planning problem yields a nonconvex NLP. Hence, it may be necessary to use global NLP solvers such as BARON (Tawarmalani & Sahinidis, 2005) or SCIP (Achterberg, 2009) to obtain the global optimum.

Parallel to addressing the existent wells planning problem, we propose to perform a rigorous pressure bound pre-analysis throughout the gathering network. Oftentimes tight bounds can be specified on pressure variables by considering maximum allowable operating pressures (individually by pipeline segments) or low/high suction/discharge pressures at compressor inlets/outlets, respectively. These bounds are essential for strengthening the upper bounds of any (mixed-integer) nonlinear programming solver to increase the likelihood of convergence.

Finally, we address the full-scale line pressure optimization problem including any prospective wells. Despite all initialization and bound tightening attempts, this nonconvex MINLP can still be quite challenging to solve. In our experience, even minor problem data variations can change which MINLP solver performs best. In the spirit of multi-start approaches, we propose a strategy of alternating between different (non-global) MINLP solvers while initializing any solver run with the incumbent solution. For instance, the MINLP could first be solved using alpha-ECP (Westerlund & Pettersson, 1995). If alpha-ECP provides a feasible solution that yields a better objective function value than the solution of the existent wells planning problem, then this solution is stored as the incumbent. Next, the initialized problem could be solved with DICOPT (Viswanathan & Grossmann, 1990) by using CPLEX as the MIP solver and CONOPT as the NLP solver. Assuming that this solver combination does not yield a better solution, DICOPT could be run again – with the same incumbent as a starting solution – but now with IPOPT as the NLP solver. Our experimental analysis does not reveal a universally preferable sequence of MINLP solvers. However, considering the relatively short time it takes for most non-global MINLP solvers to converge, it can make sense to evaluate different possibilities depending on the problem data at hand. It should also be noted that this procedure does not guarantee convergence to the global optimum. In fact, all non-global solvers might fail at identifying the global optimum. Yet, in our experience, the proposed strategy increases the likelihood of converging to near-global solutions in a reasonable amount of time. Once all non-global solvers (or solver combinations) have been explored, the incumbent can be passed on to a global MINLP solver such as BARON or SCIP.

4.7 Case Study

For our case study we consider the mid-size shale gas gathering system shown in Fig. 4.5. This system itself consists of four existing well pads, a fully established pipeline network with segments of varying sizes, a single multi-stage compressor station providing up to 5,000 HP of compression power, and an interconnect to a long-distance transmission pipeline. Altogether, 21 wells are actively producing natural gas within the respective development area. In addition, there is the possibility to turn 14 additional wells in-line on the existent pads (five wells on PAD1, three wells on PAD2 and six wells on PAD4). We assume that all prospective wells have already been drilled, and that completions operations for these wells can be coordinated according to any feasible TIL schedule. Regardless of which schedule is ultimately selected, all produced gas must be delivered to the transmission line at 940 psi. Furthermore, the following pressure constraints need to be considered: the maximum allowable operating pressure throughout the gathering system is 1,440 psi, the suction pressure at the compressor inlet is constrained from above and below (70 psi and 250 psi respectively), and the discharge pressure at the compressor outlet may not exceed 1,400 psi. All of this information is used to impose tight bounds on line and wellhead pressures within the gathering network. Lastly, we assume that no more than two TIL operations can be performed per week. For a planning horizon of 26 weeks, we wish to determine the optimal TIL schedule and pressure profile within the gathering network that maximizes the net present value of the development project. We note that the data for this case study is provided by one of the largest upstream operators in the Appalachian Basin. For confidentiality reasons we cannot disclose the company’s identity, nor the focus area of the case study.

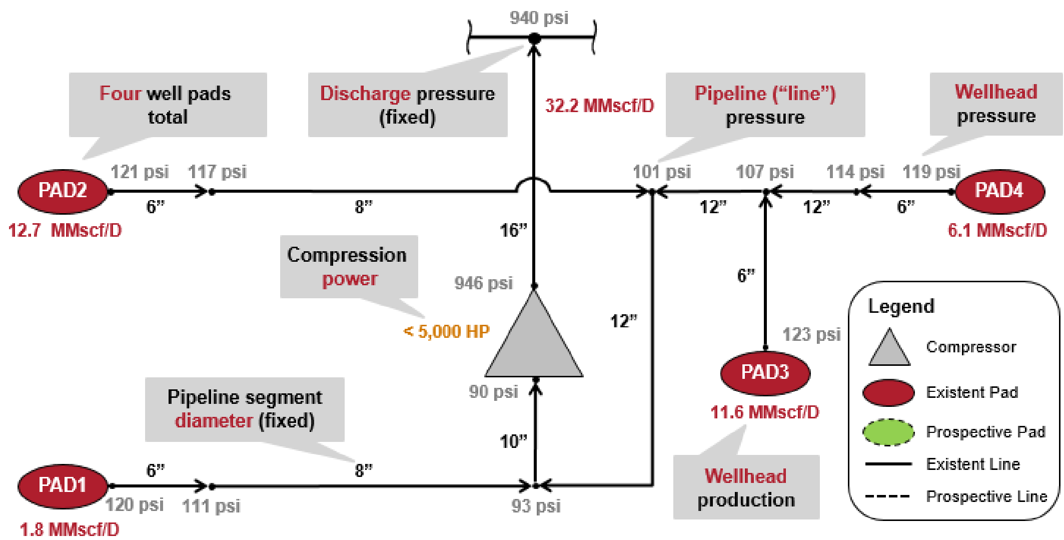

Fig. 4.5: Schematic of the mid-size gathering system considered for the case study

This particular line pressure optimization problem yields a nonconvex MINLP with 728 binary variables, 4,499 continuous variables and 6,530 constraints. We apply the solution strategy proposed in the previous section to this problem and terminate it after 10,000 s. All sub-problems and solvers are run on an Intel i7 with 2.93 Ghz and 12 GB RAM using GAMS 24.7.3. The reported NPV is 13.3 MM$.

Fig. 4.6 shows the improvement of the objective function value over time based on the proposed solution strategy. Initially, the simplified version of the problem is solved by only considering existing wells in the gathering system. This problem yields a nonconvex NLP which is initially solved using CONOPT 3.17. After approximately 20 seconds CONOPT converges to a solution with an NPV of 11.8 MM$. Due to the nonconvex nature of the existent wells planning problem, we initialize the global solver SCIP 3.2 with this solution and terminate its run after reaching an optimality gap of less than 10%.

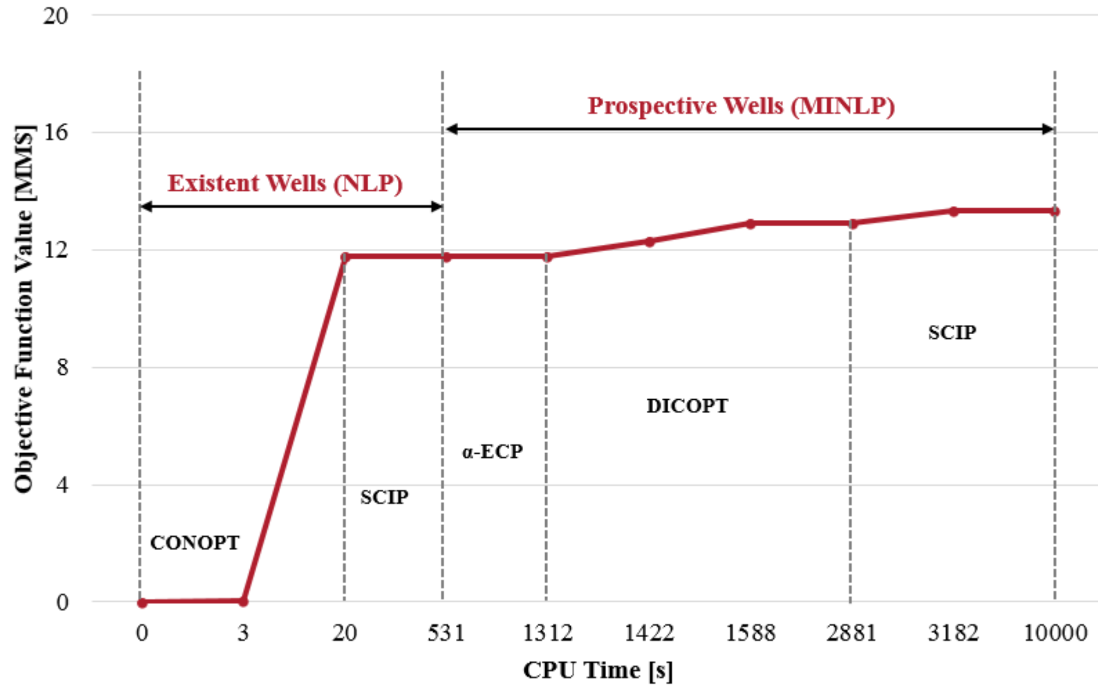

Fig. 4.6: Objective function value improvement over time based on the proposed solution strategy applied to the case study

The solution obtained from solving the existent wells planning problem provides an excellent starting point for addressing the full-scale line pressure optimization problem including all available prospective wells. The corresponding MINLP is first optimized using the non-global MINLP solver AlphaECP 2.20.06. This solver terminates after 780 s but does not manage to improve the objective function value beyond the solution of the existent wells planning problem. Next, we initialize the non-global MINLP solver DICOPT 24.7.3 using CPLEX 12.6.3.0 and CONOPT 3.17 with the incumbent. Fortunately, DICOPT converges to a solution with an improved objective function value. After 1,569s including 6 major iterations the reported NPV is 12.9 MM$ (up from 11.8 MM$) – and the solution suggests to turn selected prospective wells in-line. Finally, we pass this solution on to the global MINLP solver SCIP 3.2.

Interestingly, SCIP identifies a solution with a slightly better objective function value of 13.3 MM$ within 300 s. Thereafter, SCIP spends 6,800 s attempting to close the optimality gap. Yet, the final gap after more than 7,100 s remains high, since the upper bound SCIP reports is 19.5 MM$. Nevertheless, it is important to note that SCIP provides a valid and rigorous upper bound to the problem that non-global MINLP solvers do not. Instead of SCIP, we also tested the global MINLP solver BARON 16.5.16. It turns out that BARON provides a slightly tighter upper bound (19.0 MM$). However, BARON converges to a marginally lower objective function value than SCIP within the time limit of 10,000 s.

First and foremost, the optimization yields the proposed TIL schedule as shown in Fig. 4.7. Altogether, a total of 9 out of 14 prospective wells are brought online: four on PAD1, three on PAD2 and two on PAD4. In the following paragraphs we analyze the implications of this schedule in more detail – and we attempt to outline why the timing and coordination of these particular TIL operations makes economic and practical sense.

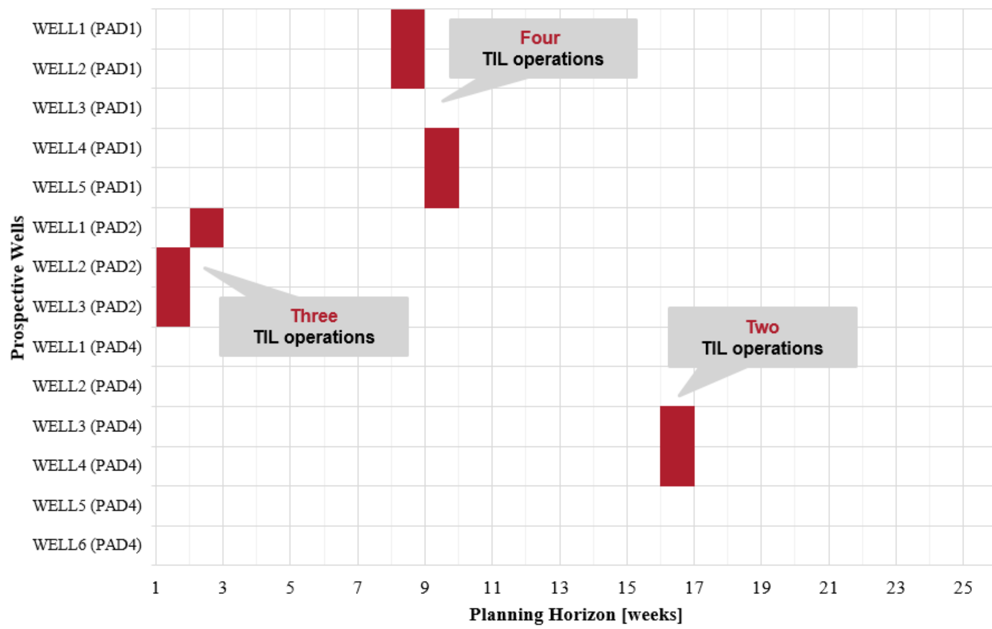

Fig. 4.7: Proposed TIL schedule for the shale gas gathering system considered in the case study

Fig. 4.8 shows production volumes by pads over time based on the proposed TIL schedule. Clearly, the entire system experiences volume growth over the full planning horizon, driven by new wells being brought online. At the same time, Fig. 4.8 reveals that the scheduled TIL operations are having a pronounced effect on the pressure profile within the gathering system. Every time a set of prospective wells are turned in-line, the line pressure increases noticeably, but then decreases again eventually. Unexpectedly though, the suction pressure does not appear to be abating between weeks 2 and 7 – after the TIL operations on PAD2 and before prospective wells are being brought online on PAD1.

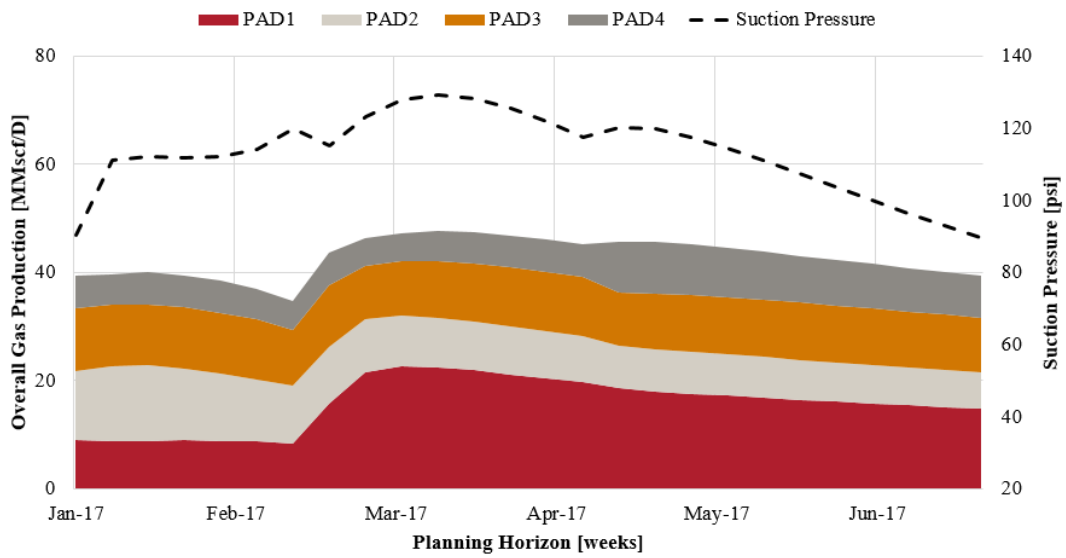

Fig. 4.8: Production volumes by pads over time compared to suction pressure at the compressor inlet

In fact, a detailed analysis of the solution in week 7 (towards the end of February 2017) allows for a number of interesting observations. As seen in Fig. 4.9, line pressure throughout the gathering system is fairly elevated even though the system is far from reaching its maximum capacity. This is unusual, since upstream operators typically try to lower line pressure as quickly as possible to increase output of their shale wells. Moreover, the elevated line pressure implies that the pressure differential that needs to be overcome by the compressor is reduced. This explains why the compressor is running far below its maximum power of 5,000 HP.

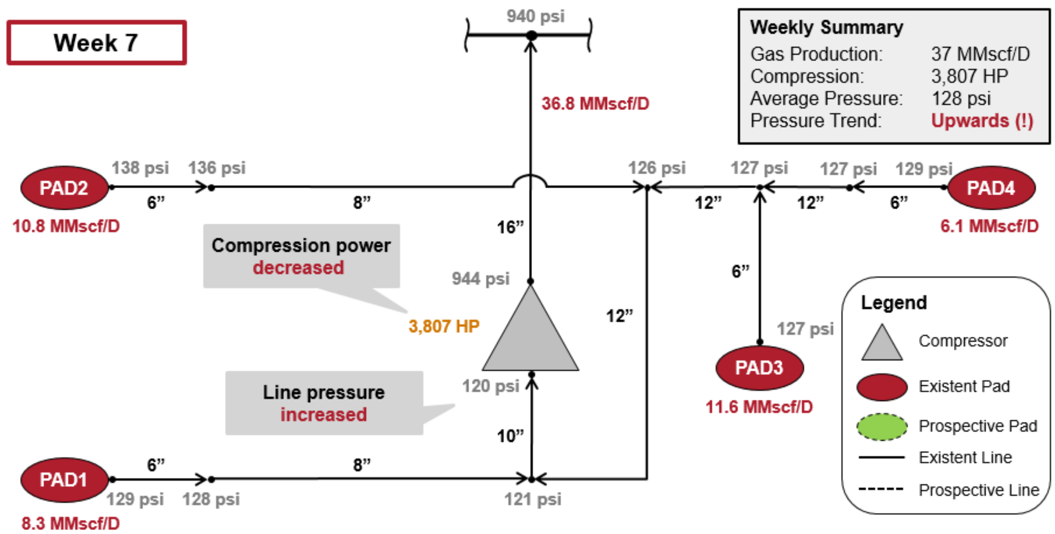

Fig. 4.9: Specific analysis of the proposed solution for week 7 of the case study

We turn to Fig. 4.10 to provide an explanation for the counter-intuitive solution suggested by the optimization. This figure shows overall gas production over time for two different cases. The lower dotted, red line marks the expected production of all existing wells assuming that no new wells are brought online. The grey and blue stacked charts, on the other hand, show how much gas existent and prospective wells, respectively, contribute towards overall production based on the proposed TIL schedule. The direct comparison of these two cases reveals that the backoff effect is having a prominent impact on gas production. Every time new wells are turned in-line, the existing wells produce significantly less than they would have by default. Yet, Fig. 4.10 allows for an intriguing observation. Although the pressure profile within the gathering system tracks the volume decline towards the end of the planning horizon, it does not do so early on. In fact, the clearly visible pressure increase between weeks 2 and 7 appears to be directly linked to the four TIL operations scheduled on PAD1. In other words, we have reason to believe that the optimization proactively raises line pressure throughout the system prior to bringing these four new wells online. In doing so, the optimization is actively mitigating the backoff effects associated with the upcoming TIL operations. Otherwise, if the pressure had subsided along with the production profile after week 2, the system would have experienced a pronounced pressure spike in week 8 (when the new wells are scheduled to come online). This pressure spike likely would have resulted in a substantial production loss – to the point where the existent wells might not have produced at all temporarily. Instead, the optimization proposes to "ready" and prepare the system for the upcoming pressure increase by maintaining the elevated pressure profile, and thereby effectively minimizing production backoff.

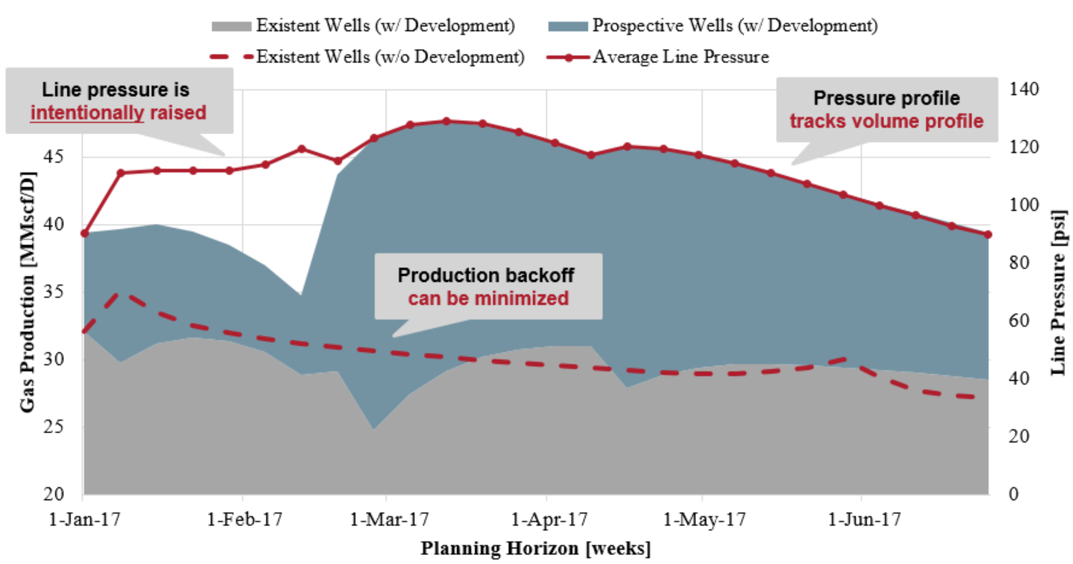

Fig. 4.10: Production volumes and pressure over time distinguished by a) existent wells without development and b) existent and prospective wells with development

The findings described above are significant because they suggest that upstream operators can take a much more active role in terms of line pressure management when timing TIL operations. Rather than "wasting" the production potential of existing wells, the results suggest that producers need to evaluate carefully when new shale wells are turned in-line, and how their gathering systems should be operated prior to these events.

4.8 Conclusions

In this chapter we have proposed a nonconvex mixed-integer nonlinear programming model for line pressure optimization in shale gas gathering systems. This model is designed to support shale gas producers in deciding when and how many prospective wells should be turned in-line, as well as how to manage line pressures and compressor stations throughout the gathering network. The model itself is based on three fundamental building blocks: a) a nonlinear and nonconvex reduced-order shale reservoir model, b) a nonlinear and nonconvex pressure drop model, and c) a nonlinear and nonconvex compression model. We modified the reservoir model specifically to account for production backoff effects that are prominent in shale gas gathering systems whenever new wells are brought online. Due to the nonconvex nature of the proposed model, we developed a tailored solution strategy that aims to provide valid and good initial solutions. Lastly, we applied the proposed optimization framework to a real-world case study using data from one of the largest upstream operators in the Appalachian Basin. Our results demonstrate that shale gas producers can proactively manage line pressures in their gathering systems to reduce undesirable production backoff as new wells are brought online.

4.9 Nomenclature

Sets

$t \in \mathcal{T}$	Time periods
$n \in \mathcal{N}$	Network nodes
$w \in \mathcal{W}$	Wells
$p \in \mathcal{P}$	Pads
$w \in \mathcal{EW}$	Existent wells
$p \in \mathcal{PW}$	Prospective wells
$(w, p) \in \mathcal{WPA}$	Well-to-pad assignments
$(p, n) \in \mathcal{PNA}$	Pad-to-node arcs
$(n, \tilde{n}) \in \mathcal{NNA}$	Node-to-node arcs
$(n, \tilde{n}) \in \mathcal{CNA}$	Compression node arcs
$(n, \tilde{n}) \in \mathcal{DNA}$	Delivery node arc

Binary Decision Variables

$y_{w,p,t}^{TIL}$	Active if well w on pad p turned in-line in time period t
$y_{w,p,t}^{PROD}$	Active if well w on pad p actively producing in time period t

Continuous Decision Variables

$P_{n,t}^{L}$	Line pressure at network node n in time period t [psi]
$P_{p,t}^{P}$	Wellhead pressure at pad p in time period t [psi]
$F_{w,t}^{W,S}$	Default gas flow at well w in time period t (at standard conditions)
$F_{w,t}^{B,S}$	Backoff gas flow at well w in time period t (at standard conditions)
$F_{w,t}^{F,S}$	Final gas flow at well w in time period t (at standard conditions)
$F_{p,t}^{P,S}$	Gas flow at pad p in time period t (at standard conditions)

$F_{p,n,t}^{PN,S}$ Gas flow from pad p to network node n in time period t (at standard conditions)

$F_{n,\tilde{n},t}^{NN,S}$ Gas flow from network node n to network node $\tilde{n}$ in time period t (at standard conditions)

$F_{n,\tilde{n},t}^{NN,\mathrm{A}}$ Gas flow from network node n to network node $\tilde{n}$ in time period t (at actual conditions)

W_t Compressor power in time period t

$Q_{w,t}^{S}$ Cumulative gas production well w in time period t (at standard conditions)

$U_{n,t}^{L}$ Substitute line pressure at network node n in time period t

$U_{p,t}^{P}$ Substitute wellhead pressure at pad p in time period t

Parameters

$d_{p,n}$ Pipeline diameter for segment from pad p to network node n

$d_{\tilde{n},n}$ Pipeline diameter for segment from network node $\tilde{n}$ to network node n

$l_{p,n}$ Pipeline length for segment from pad p to network node n

$l_{\tilde{n},n}$ Pipeline length for segment from network node $\tilde{n}$ to network node n

$a_{w,p}$ Slope parameter pressure normalized decline curve for well w on pad p

$m_{w,p}$ Intercept parameter pressure normalized decline curve for well w on pad p

$lc_{w,t}$ Land-cleared date for well w in time period t

M Big-M parameter

$p_{p}^{L,MIN}$ Minimum wellhead pressure at pad p

$p_{w,p}^{0}$ Initial bottomhole pressure well w on pad p [psi]

$p_p^{L,MIN}$	Minimum wellhead pressure at pad p
$p_n^{L,MIN}$	Minimum line pressure at network node n
$p_p^{L,MAX}$	Maximum wellhead pressure at pad p
$p_n^{L,MAX}$	Maximum line pressure at network node n
q_w^0	Cumulative gas production existent wells at begin of planning horizon
S^g	Specific gravity of gas
W^{MAX}	Maximum compression power
Z	Compressibility factor for gas
T^L	Gas temperature along pipelines
$\delta_{w,p}^{TIL}$	Well development cost at well w on pad p
π_t	Gas price in time period t
φ^C	Compressor fuel coefficient
γ_w	Rate restriction well w
N	Number of compressor stages
k	Heat capacity ratio
η^{CE}	Compression efficiency
R	Gas constant
dr	Annual discount rate
Δ_w^B	Backoff parameter well w

CHAPTER 5

Deterministic Programming Models for Planning Shale Gas Well Refracture Treatments

5.1 Introduction

Refracturing presents a promising strategy for addressing the characteristically steep decline rates of shale gas wells (Jacobs, 2014). The core idea behind refracturing is to restimulate the reservoir such that it yields previously untapped hydrocarbons and improves the overall production profile of a well. Whether or not a refracture treatment will reinvigorate a shale gas well depends on a number of factors, including the characteristics of the reservoir and the initial completions design. Historically, refracture treatments have been applied predominantly to shale gas wells suffering from low production rates due to known suboptimal initial stimulations and completions.

However, over the past years, the use of real-time microseismic hydraulic fracture mapping and other analytical tools has allowed operators to improve completions and stimulation designs, leading to a larger number of treated stages per well, meticulous stage selection, and increased fluid and proppant volumes (Baihly et al., 2011). Clearly, refracture treatments designed and performed under these revised insights can be expected to improve hydrocarbon recovery from unconventional reservoirs.

Moreover, Dozier et al. (2003) argue that even wells with effective initial treatments have shown significant production improvements when restimulated after an initial period of production and partial reservoir depletion. On the one hand, the success of these workovers can be attributed to the fact that fracture conductivity is known to decrease over time as proppant packs become damaged or deteriorate with scale buildup during reservoir-pressure drawdown. Additional fracturing measures can address this issue, reestablish flow into the wellbore and reinvigorate a well's production profile. On the other hand, Dozier et al. (2003) also point out that stress changes are known to occur around effective initial fractures as a result of reservoir depletion during production. These stress changes in turn lead to a fracture reorientation, which initiates new fractures along different azimuthal planes. Therefore, refracturing treatments performed at the right time can provide access to under- or unstimulated zones of the reservoir through these reoriented, newly created fractures. As such, well restimulations appear promising even for wells with effective initial treatments – especially in low permeability formations such as shale gas reservoirs.

The left image in Fig. 5.1 shows a horizontal wellbore and a typical fracture network induced by a wide-spaced hydraulic well stimulation. In contrast, the image on the right in Fig. 5.1 shows the same lateral wellbore and the surrounding reservoir after a refracture treatment. A comparison of the two images reveals that refracturing can add entirely new perforations to the existing fracture network and also extend previous fractures in new directions. Clearly, the enhanced fracture network has an increased surface area and reaches into previously unattainable areas of the reservoir.

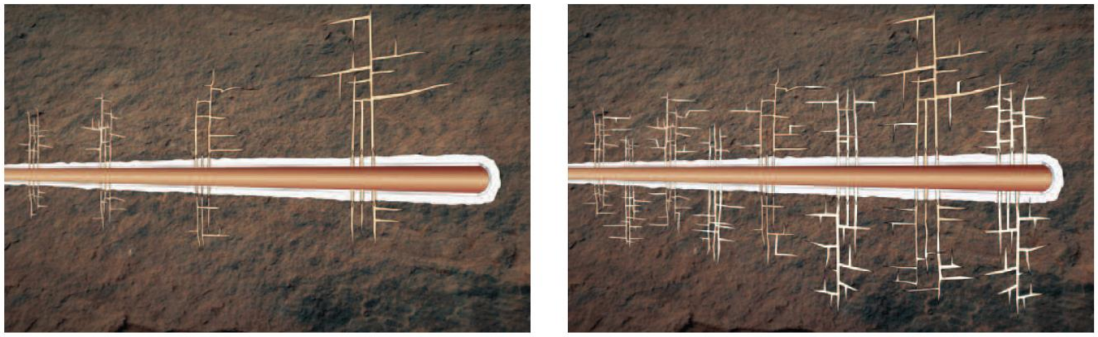

Fig. 5.1: A shale well and the surrounding fracture network after initial well stimulation (left) and after refracturing (right), Source: Allison and Parker (2014)

Refracturing is known to cause a peak in the production rate that often matches up to 60% of the initial production peak, as seen in Fig. 5.2. In addition to restoring well productivity, refracture treatments present an opportunity to improve the completions design and can therefore alter long-term decline curves favorably by, for instance, enhancing fracture conductivity. Based on recent results, operators are increasingly confident that refracturing can enhance estimated ultimate recoveries (EUR) in excess of 30%, and thereby extend the expected lifespan of their shale wells beyond 20-30 years, especially when considering the possibility of multiple refracture treatments. This strategy seems particularly appealing given that refracturing an existing well generally costs less than half as much as completing a new well (Jacobs, 2014); operators do not have to secure additional acreage, drill a well, or install pipelines for access to gathering systems. By reusing the existing infrastructure, refracturing also reduces surface disruption significantly, and therefore benefits the overall environmental impact of any field development project.

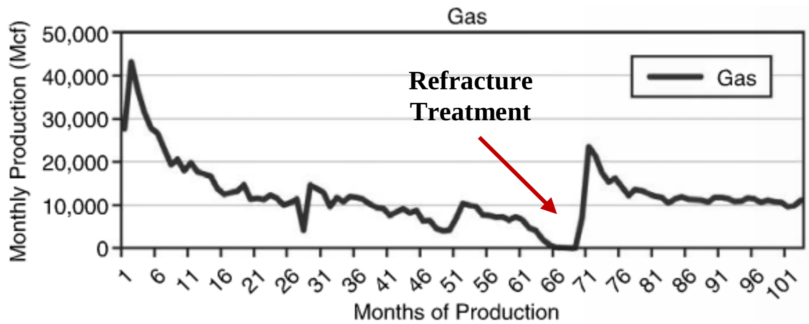

Fig. 5.2: Production profile of a refractured horizontal well in the Barnett Shale, Source: Allison and Parker (2014)

5.2 Literature Review

To this day, refracturing planning has received fairly little attention in the literature. One of the few contributions in this domain is a comprehensive report by Sharma (2013), who addresses improved reservoir access through refracture treatments in greater detail. The author argues that refracturing has long been recognized as a successful way to restore production rates – particularly in low-permeability gas wells – by improving the productivity of previously unstimulated or understimulated reservoir zones. However, Sharma (2013) also recognizes that the selection of candidate wells for refracturing is often very difficult based on the limited information available to decision-makers. The author claims that the timing of secondary reservoir stimulations, in particular, is critical for optimizing well performance. In the report, Sharma (2013) proposes a number of dimensionless criteria to: (a) identify candidate wells for refracturing, and (b) determine the optimal refracture time in a well's lifespan. Among these criteria are a *well completions number* (indicating the quality of the initial completions), a *reservoir depletion number* (quantifying the extent of depletion around a particular well), a *production decline number* (reflecting the extent and quality of a reservoir) and a *stress reorientation number* (revealing the potential for additional fractures to propagate into underdepleted regions of the reservoir). In addition, the author proposes the use of dimensionless type curves to estimate the optimal time-window for refracture treatments.

Eshkalak et al. (2014) focus on the economic feasibility of refracture treatments for horizontal shale wells. For an unconventional gas field consisting of 50 horizontal wells – all of which are considered candidates for refracturing – the authors calculate the net present value (NPV) and internal rate of return (IRR) for various refracturing scenarios that differ in terms of: (a) how many wells are refractured, (b) when wells are refractured, and (c) the given gas price forecast. The timing of the refracture treatments is specified in advance and the authors assume that the production increase due to restimulation is given by a fixed long-term refracturing efficiency factor. Based on the results of their analysis, Eshkalak et al. (2014) conclude that refracturing shale gas wells makes economic sense over a wide range of price forecasts.

Tavassoli et al. (2013) also address the refracturing planning problem. Motivated by the fact that – although refracturing strategies seem promising conceptually – merely 15-20% of all wells that have been refractured thus far achieved the desired performance targets, the authors develop a numerical, dual-permeability (matrix-fracture), two-phase (gas-water) simulation model. This model allows them to study the effect of different reservoir parameters (permeability, porosity) and operational decisions (initial fracture spacing, refracture timing) on refracturing performance. Their findings, too, suggest that the timing of a refracture job is absolutely crucial for success. In an attempt to provide some guidance for the optimal timing of refracturing treatments, the authors study typical shale gas well production decline curves in detail. They highlight the fact that typical shale well productivity curves evolve from steep, pronounced declines to more steady rates. Based on this analysis, the authors suggest that refracture treatments should be performed when the production decline rate falls below 10-15%, which – based on their numerical simulation studies – marks the point when gas production decline rates generally level off.

From the above we conclude that it is generally accepted that refracture timing is critical for optimizing the performance of any shale well. Yet, Lantz et al. (2008) report that in practice, the time between the original completions stimulation and refracture treatments varies greatly. The authors describe a shale oil well refracturing program in the Bakken formation where some wells were refractured after 2 years while other wells produced for 3.5 years until they were restimulated. Previous work provides some guidelines or general heuristics as to when refracture treatments should be performed, but these indicators appear vague and often do not account for important economic factors, such as price forecasts or fracturing expenses. Therefore, the objective of this work is to develop a modeling framework for planning optimal shale gas well refracture treatments.

5.3 General Problem Statement

The problem addressed in this chapter can be stated as follows. We assume that a candidate shale gas well has been identified for refracturing. For this well, a long-term production forecast as well as the production profile after additional refracture treatments at any point in time over the planning horizon is given. A gas price forecast along with expenses for drilling, fracturing, completions and refracturing operations are also given.

Our goal is to determine: (a) whether or not the well should be refractured, (b) how often the well should be refractured over its entire lifespan, and (c) when exactly the refracture treatments should be scheduled. The objective is to maximize either: (a) the estimated ultimate recovery (EUR) of the well, or (b) the net present value (NPV) of the well development project.

This chapter is organized as follows. First, we present a continuous-time nonlinear programming (NLP) model to determine whether or not a shale gas well should be refractured, and when to schedule the refracture treatment. The NLP model relies on the assumption that the well productivity profile – prior to and after a refracture treatment – can be predicted by a decreasing power function of time. For this purpose we propose an effective forecast function that mimics real-life curves. In the following section we extend the proposed framework to allow for multiple refracture treatments and present a discrete-time mixed-integer linear programming (MILP). In this context, we review three alternative model formulations and explore their trade-offs in terms of model sizes and computational performance. Finally, we apply the discrete-time MILP model to two case studies to demonstrate the value of optimization for refracturing planning applications.

5.4 Continuous-Time Refracturing Planning Model

Typically, the productivity curve of an ordinary shale gas well can be captured using a decreasing power function of time as stated in Eq. (5.1). Fig. 5.3 shows the fitness of such a function to forecasted production data provided by the EQT Corporation – a major shale gas producer in the Appalachian Basin (United States).

$$p(t) = k \cdot t^{-a} \qquad t \geq 1 \tag{5.1}$$

In Eq. (5.1) the productivity $p(t)$ is commonly specified in terms of MMscf/month, k is a parameter representing the initial production peak observed during the first month after turning a well in line, and $a > 0$ is the exponent representing the steepness of the production decline. We note that the productivity function $p(t)$ is only defined for $t \geq 1$. By our convention, we assume that time $t = 0$ corresponds to the beginning of drilling and completions operations, and that the well is ready to produce gas exactly one month later (i.e., at $t = 1$).

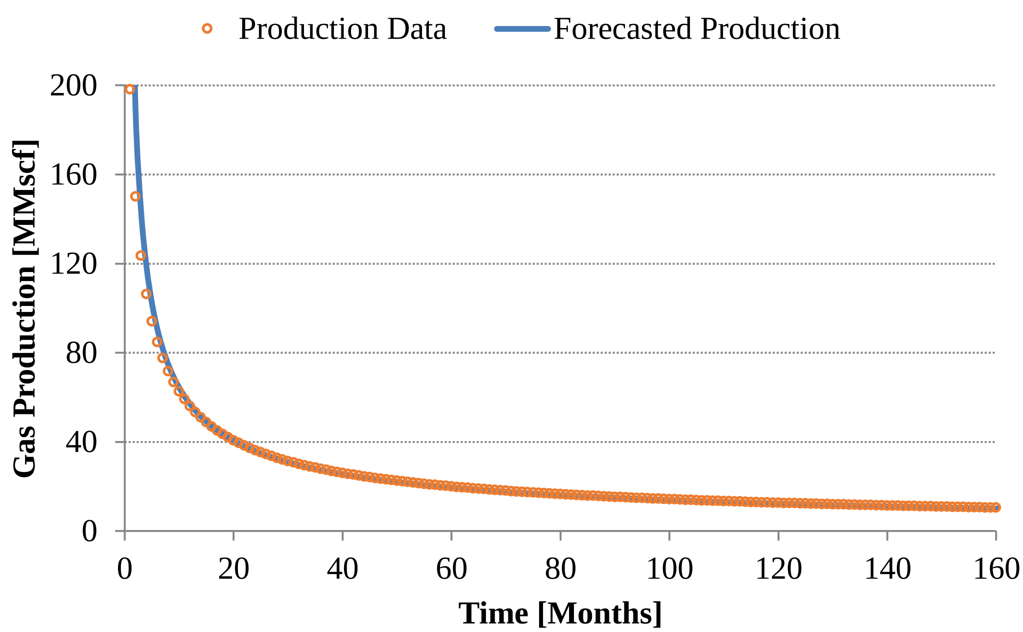

Fig. 5.3. Comparison of real production forecast data and a fitted power function for a shale gas well

While a shale gas well is being refractured, it does not produce any gas. We refer to this as the refracuring period *rt*. Once the refracture treatment has been completed and the well is turned in line again, a new peak in gas production is observed. Generally, this secondary production peak represents a fraction of the original peak and depends strongly on the characteristics of the reservoir, the refracturing technique and the original completions design. In this work we assume that the secondary peak can be expressed as $r = \beta \cdot k$, with typically $0.50 \le \beta \le 0.80$. Moreover, the production decline after refracturing follows a new decline curve, which is often steeper than the original decline following the original completions (Tavassoli et al., 2013). Motivated by real world data, we assume that the steepness of the productivity decline after refracturing (i.e., the magnitude of the exponent in the power function) increases linearly with the time between the original completions and the refracturing operation (namely, *trf*). On the other hand, given that the refracture operation can affect original fractures either favorably or unfavorably, the productivity of the original fractures is multiplied with the factor γ. In practice, the parameter γ needs to be specified in close coordination with completions design engineers, geologists and reservoir engineers, who are most familiar with the initial completions design as well as the particular reservoir characteristics. As a result, the productivity curve after refracturing can be represented by the function given in Eq. (5.2).

$$p(t) = \gamma \cdot k \cdot t^{-a} + r \cdot \left(t - trf - rt\right)^{-a-b \cdot trf} \qquad t \ge trf + rt + 1 \quad (5.2)$$

The variable *trf* is the time when refracturing starts (in months, after the original completions operation), γ is the factor that accounts for the increase or decrease in productivity of the original fractures, and *b* is the coefficient capturing the increase of the decline steepness after refracturing. Finally, we can express the productivity of a shale gas well before, during and after having been refractured using the function in Eq. (5.3).

$$p(t)=\begin{cases} k\cdot t^{-a} & 1\le t\le trf \\ 0 & trf\le t\le trf+rt+1 \\ \gamma\cdot k\cdot t^{-a}+r\cdot\left(t-trf-rt\right)^{-a-b\cdot trf} & trf+rt+1\le t\le T \end{cases} \quad (5.3)$$

In Fig. 5.4 we plot the function in Eq. (5.3) for different refracture start dates. We assume that a refracturing operation takes one month and that the resulting secondary peak (parameter r) is independent of the timing of the well restimulation. The latter assumption is supported by the work of Tavassoli et al (2013).

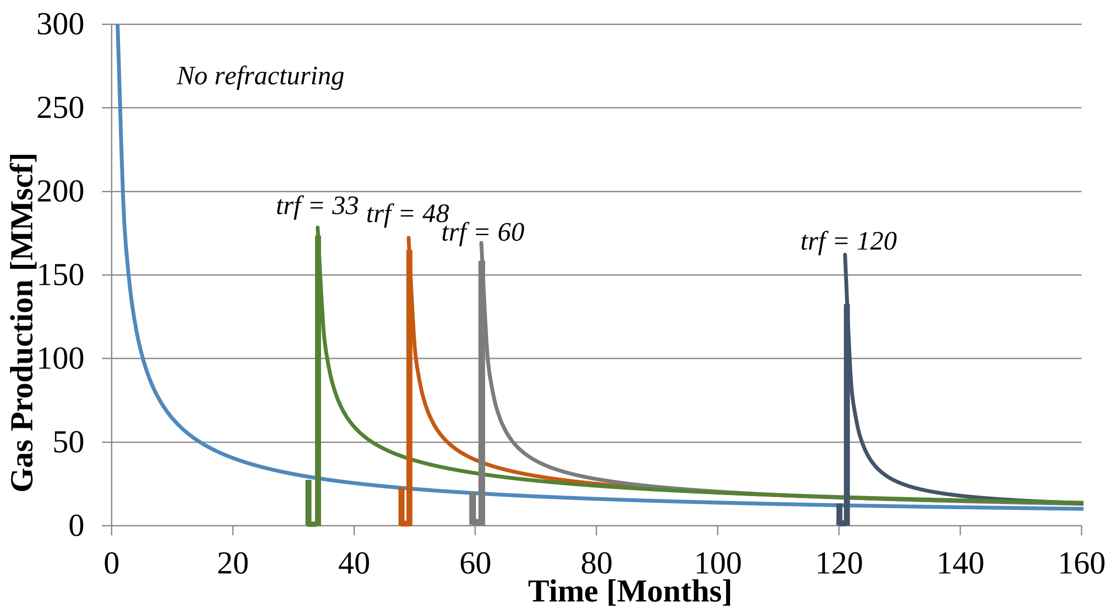

Fig. 5.4 Productivity curves of a shale gas well for different refracture start dates (trf)

To determine the total amount of gas that can be recovered from a shale gas well that has been refractured, we can integrate function (5.3) from t = 1 to t =T, where T represents the expected productive lifespan of the well. This key indicator of any shale gas well is usually referred to as the estimated ultimate recovery (EUR).

$$EUR(trf) = \frac{k}{1-a} \cdot \left[trf^{1-a} - 1 \right] + \frac{\gamma \cdot k}{1-a} \cdot \left[T^{1-a} - \left(trf + rt + 1 \right)^{1-a} \right] + \frac{r}{1-a-b \cdot trf} \cdot \left[\left(T - trf - rt \right)^{1-a-b \cdot trf} - 1 \right] \tag{5.4}$$

The EUR function in Eq. (5.4) assumes that: (1) $a \neq 1$, and (2) $a + b\ trf \neq 1$. To identify the optimal time to refracture a well such that the EUR is maximized, we propose a continuous-time nonlinear optimization model as in Eq. (5.5).

$$\begin{aligned} \max \quad & EUR(trf) = \frac{k}{1-a} \cdot \left[trf^{1-a} - 1 \right] + \frac{\gamma \cdot k}{1-a} \cdot \left[T^{1-a} - \left(trf + rt + 1 \right)^{1-a} \right] + \\ & \frac{r}{1-a-b \cdot trf} \cdot \left[\left(T - trf - rt \right)^{1-a-b \cdot trf} - 1 \right] \\ \text{s.t.} \quad & 1 \leq trf \leq T - rt - 1 \end{aligned} \tag{5.5}$$

This optimization model presents a singularity when $trf = (1 - a) / b$ for $1 \leq (1 - a) / b \leq T - rt - 1$. When this is the case, the denominator in the third term in Eq. (5.5) equals zero, leading to a division by zero. This explains why local and global solvers such as MINOS, CONOPT, BARON, COUENNE or LINDOGLOBAL (McCarl, 2011) will oftentimes fail to converge to the optimal solution. For this reason, we propose to solve the problem in Eq. (5.5) as two separate optimization problems by dividing the planning horizon into two domains. First, we solve for $1 \leq trf \leq (1-a)/b - \varepsilon$, where ε is a small tolerance:

$$\begin{aligned} \max \quad & EUR(trf) = \frac{k}{1-a} \cdot \left[trf^{1-a} - 1 \right] + \frac{\gamma \cdot k}{1-a} \cdot \left[T^{1-a} - \left(trf + rt + 1 \right)^{1-a} \right] + \\ & \frac{r}{1-a-b \cdot trf} \cdot \left[\left(T - trf - rt \right)^{1-a-b \cdot trf} - 1 \right] \\ \text{s.t.} \quad & 1 \leq trf \leq (1-a)/b - \varepsilon \end{aligned} \tag{5.6}$$

Next, we solve for $(1-a)/b + \varepsilon \leq trf \leq T - rt - 1$:

$$\max \quad EUR(trf) = \frac{k}{1-a}\cdot\left[trf^{1-a} - 1\right] + \frac{\gamma \cdot k}{1-a}\cdot\left[T^{1-a} - \left(trf + rt + 1\right)^{1-a}\right] + \frac{r}{1-a-b\cdot trf}\cdot\left[\left(T - trf - rt\right)^{1-a-b\cdot trf} - 1\right] \tag{5.7}$$

$$\text{s.t.} \quad (1-a)/b + \varepsilon \le trf \le T - rt - 1$$

It should be noted that it is very unlikely that the optimal value for *trf*, i.e., the optimal time to refracture a well, matches the singular value $(1 - a) / b$ at the optimum. Generally, $(1 - a) / b > T$, which implies that the singular value for *trf* lies outside the feasible region and far beyond the expected lifespan of an ordinary shale gas well.

Fig. 5.5 shows the relationship between the timing of the refracture treatment *trf* and the EUR for different steepness values *a* based on the function in Eq. (5.4). All other parameters remain the same. It can be observed that refracturing can raise the *EUR* up to 22.5%, depending on the productivity curve. We also note that the wells featuring higher values of *a* (i.e., steeper declines) should be refractured later in their lifespan, achieving lower increases in the well reserves.

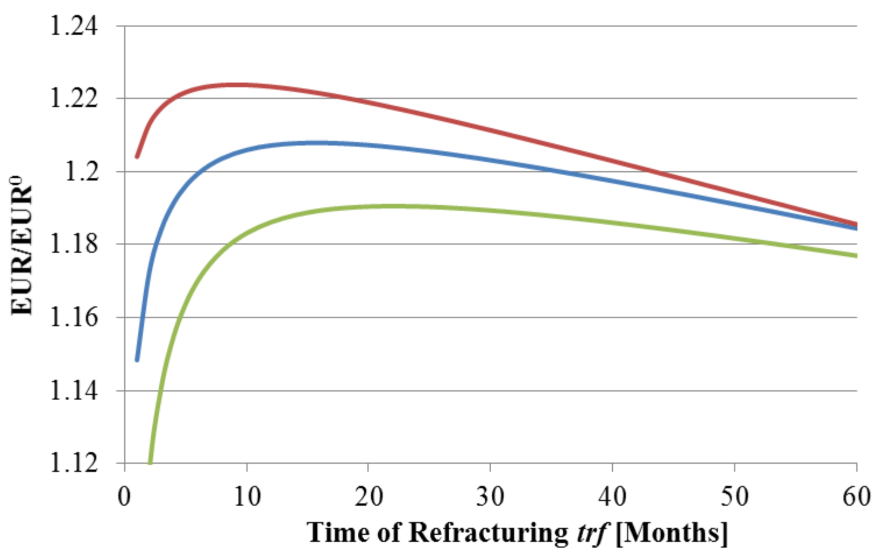

Fig. 5.5. EUR ratios with and without refracturing with regards to the time of refracturing

5.5 Multiperiod Refracturing Planning Model

The continuous-time NLP model presented in the previous section is particularly useful for identifying the optimal time for refracturing a typical shale gas well so as to maximize its expected ultimate recovery (EUR). In practice, however, the NLP model has the following shortcomings: (a) it is not suitable for planning multiple refracture treatments over the expected lifespan of the well, (b) it does not allow for the evaluation of economic objective functions, such as the net present value (NPV), and (c) it only admits forecasted production decline curves strictly following the fundamental power function given by Eq. (5.1). To overcome these limitations, we also present a discrete-time, multiperiod mixed-integer linear programming (MILP) model that – unlike the continuous model – is capable of planning multiple refracturing operations while accounting for an economic evaluation of the well development project.

We assume that the planning horizon has been discretized into a set of time periods $t \in T$, usually months. The decision-maker is considering a candidate number of refracture treatments $i \in I_0$ that are ordered chronologically. We note that the set I_0 explicitly contains the zero-element, i.e. $I_0 = \{i_0\} \cup I = \{i_0; i_1; i_2;...\}$. The practical interpretation of this element is that the well may not be refractured at all. Generally, we recommend to set $|I| = 2$ to 3 for a planning horizon of 10 years, even though some researchers[11] argue that up to five refracture treatments may be performed over the expected lifetime of a shale gas well. Moreover, we advise to set $|T| = 120$ to 360 – corresponding to 10 to 30 years. Next, we introduce the binary variable $x_{i,t}$ which is active if the well is refractured for the i-th time in time period t. Then, the following equations hold.

$$\sum_{t \in T} x_{i,t} \leq 1 \qquad \forall i \in I \tag{5.8}$$

$$x_{i,t} \leq \sum_{\tau < t - rt} x_{i-1,\tau} \qquad \forall i \in I, t \in T, i > 1 \tag{5.9}$$

Eq. (5.8) states that a well cannot be refractured for the *i*-th time more than once. In fact, the formulation allows the well not to be refractured at all since this is a true degree of freedom in practice. Moreover, Eq. (5.9) ensures that if a well is refractured for the *i*-th time in time period *t*, then it has to have been refractured for the (*i*-1)-th time in one of the previous time periods $\tau < t - rt$, where *rt* is the number of time periods it takes to restimulate the well.

5.5.1 Production Profile

From the analysis of shale gas productivity curves before, during, and after a refracture treatment, we can state that prior to any refracturing operation, the production curve obeys a decreasing power function as given in Eq. (5.1). Hence, the gas production in time period *t* can be bounded from above as follows.

$$P_t \leq k \cdot t^{-a} + \hat{k} \cdot \sum_{\tau \leq t} x_{i1,\tau} \qquad \forall t \in T \tag{5.10}$$

We note that constraint (5.10) is relaxed if the well has been refractured once or more often by time period *t*. $\hat{k}$ is an overestimator of the new production peak we expect after a refracture treatment. Usually, we set $\hat{k} = k$. During the refracturing procedure itself, the well will not produce any gas. Therefore, during the *rt* time periods it takes to restimulate the well, the production is set to zero by constraint (5.11).

$$P_t \leq \max(k, \hat{k}) \cdot \left(1 - \sum_{\tau = t - rt + 1}^{t} \sum_{i \in I} x_{i,\tau}\right) \qquad \forall t \in T \tag{5.11}$$

In fact, Eq. (5.11) states that if the well was refractured in any of the previous $rt - 1$ time periods, then the production rate in time period *t* must be zero. Once a well has been refractured, it becomes more challenging to model its production rate, since the well's productivity depends on precisely how often and also when a restimulation was last performed. For this purpose, we introduce the binary decision variable $y_{i,t} \in [0,1]$ (can be treated as a continuous variable) that is meant to become active (i.e., equal to one) if by the end of time period *t* the well has been refractured *i* times. This distinction is important because in any time period *t* the well may have been refractured *i* times even though the last refracturing operation occurred in a previous time period $\hat{t} < t$. We derive the following mixed-integer constraints through propositional logic (Raman & Grossmann, 1991) to capture the relation between the decision variables $x_{i,t}$ and $y_{i,t}$ by using their equivalent Boolean variables.

$$x_{i,t} \quad \Rightarrow \quad y_{i,t} \qquad \forall i \in I_0, t \in T \tag{5.12}$$

Eq. (5.12) states that if the well is refractured for the *i*-th time in time period *t*, then the well has been refractured *i* times by the end of that period. This logic statement can be expressed through Eq. (5.13).

$$x_{i,t} \leq y_{i,t} \qquad \forall i \in I_0, t \in T \tag{5.13}$$

Next, we argue that if the *i*-th refracturing is the last that occurred as of the end of time period *t*, i.e., the decision variable $y_{i,t}$ is active, then in one of the previous time periods the well had to have been refractured for the *i*-th time.

$$y_{i,t} \quad \Rightarrow \quad x_{i,t1} \vee x_{i,t2} \vee x_{i,t3} \vee \ldots \vee x_{i,t} \qquad \forall i \in I_0, t \in T \tag{5.14}$$

The corresponding mixed-integer constraint is given by Eq. (5.15).

$$y_{i,t} \le \sum_{\tau \le t} x_{i,\tau} \qquad \forall i \in I_0, t \in T \tag{5.15}$$

Indeed, if by the end of time period t-1 the well has been refractured a total of i times, i.e., the decision variable $y_{i,t-1}$ is active, but in the subsequent time period t the decision variable $y_{i,t}$ is no longer active, then the well must have been refractured for the (i+1)-th time in this time period t, i.e., the decision variable $x_{i+1,t}$ has to be active.

$$y_{i,t-1} \quad \wedge \quad \neg y_{i,t} \quad \Rightarrow \quad x_{i+1,t} \qquad \forall i < |I_0|, t > 1 \tag{5.16}$$

Eq. (5.16) matches exactly with Eq. (5.17) in mixed-integer form.

$$y_{i,t} \ge y_{i,t-1} - x_{i+1,t} \qquad \forall i < |I_0|, t > 1 \tag{5.17}$$

Finally, we ensure that in any time period only a single number of refracture operations i may have occurred previously.

$$\sum_{i \in I_0} y_{i,t} = 1 \qquad \forall t \in T \tag{5.18}$$

Next, we propose three alternative formulations for capturing the productivity profile of a shale gas well after it has been refractured once or more often.

5.5.2 Big-M Formulation

Given the decision variables $x_{i,\hat{t}}$ and $y_{i,t}$ we can impose an upper bound on the production of the shale gas well after refracturing, as stated by constraint (5.19).

$$P_t \le \gamma^i \cdot k \cdot t^{-a} + \beta_{i,\hat{t}} \cdot r \cdot \left(t - \hat{t} - rt + 1\right)^{-a-b\cdot\hat{t}} + \hat{k} \cdot \left(2 - y_{i,t} - x_{i,\hat{t}}\right) \qquad \forall i \in I, t \in T, \hat{t} \le t - rt \tag{5.19}$$

Constraint (5.19) is a key part of the model and deserves to be analyzed in detail. It is an upper bound only imposed on the gas production in time period t when – at the end of time period t – the well has been refractured i times ($y_{i,t}$ = 1) and this i-th refracturing operation occurred in time period $\hat{t} < t - rt$ ($x_{i,\hat{t}} = 1$). The production of the well during time period t is composed of two parts: (a) the contribution of the original fractures, which is increased or decreased by the factor γ (normally $\gamma < 1$) every time a new refracture treatment is performed, and (b) the contribution of newly induced fractures. In the latter case, it is assumed that the first refracturing operation yields a peak of magnitude r, and every further refracture treatment yields a smaller peak derived from multiplying the previous peak with the factor $\beta_{i,\hat{t}} < 1$. Hence, the parameter $\beta_{i,\hat{t}}$ depends on two factors: (a) how often the well has been refractured (index i), and (b) when the last refracture treatment occurred (index $\hat{t}$). For simplicity, one may assume that $\beta_{i,\hat{t}}$ = β_i, which implies that every additional refracture treatment yields the same reduction in the post-refracture production peak, regardless of when it is performed. Similar to the continuous model, the corresponding production curves' declines are steeper the later the refracturing is performed, which is driven by the exponent $(-a - b\,\hat{t})$. We refer to Eq. (5.19) as the *big-M formulation* (BMF).

5.5.3 Disjunctive Formulation: Standard Hull-Reformulation

Given the decision variables $x_{i,\hat{t}}$ and $y_{i,t}$ we can also introduce an additional binary variable $z_{i,t,\hat{t}}$. This variable is active if and only if at the end of time period t the well has been refractured a total of i times ($y_{i,t}$ =1) and the last refracturing occurred in time period $\hat{t}$ ($x_{i,\hat{t}}$ =1). This binary variable is defined by the following logic.

$$y_{i,t} \wedge x_{i,\hat{t}} \Rightarrow z_{i,t,\hat{t}} \qquad \forall i \in I_0, t \in T, \hat{t} \le t - rt \tag{5.20}$$

We can easily transform Eq. (5.20) into the following mixed-integer constraint using propositional logic (Raman & Grossmann, 1991).

$$y_{i,t} + x_{i,\hat{t}} \leq z_{i,t,\hat{t}} + 1 \qquad \forall i \in I_0, t \in T, \hat{t} \leq t - rt \tag{5.21}$$

In addition, we include the reverse logic statement as well.

$$z_{i,t,\hat{t}} \Rightarrow y_{i,t} \wedge x_{i,\hat{t}} \qquad \forall i \in I_0, t \in T, \hat{t} \leq t - rt \tag{5.22}$$

This, too, can easily be transformed into the following two constraints:

$$z_{i,t,\hat{t}} \leq y_{i,t} \qquad \forall i \in I_0, t \in T, \hat{t} \leq t - rt \tag{5.23}$$

$$z_{i,t,\hat{t}} \leq x_{i,\hat{t}} \qquad \forall i \in I_0, t \in T, \hat{t} \leq t - rt \tag{5.24}$$

The advantage of having introduced the binary variable $z_{i,t,\hat{t}}$ is that we can derive a disjunctive model for the key production constraint.

$$\vee_{i \in I_0, \hat{t} \in 1 \ldots t-rt} \left[\begin{array}{c} z_{i,t,\hat{t}} \\ P_t \leq \tilde{\gamma}_i \cdot k \cdot t^{-a} + \tilde{\beta}_{i,\hat{t}} \cdot r \cdot \left(t - \hat{t} - rt + 1 \right)^{-a-b\cdot\hat{t}} \end{array} \right] \qquad \forall t \in T \tag{5.25}$$

$$\underline{\vee}_{i \in I_0, \hat{t} \in 1 \ldots t-rt} \quad z_{i,t,\hat{t}} \qquad \forall t \in T \tag{5.26}$$

It is important to note that in the formulation above, $\tilde{\gamma}_i$ and $\tilde{\beta}_{i,\hat{t}}$ are *parameters*. In particular, we clarify that $\tilde{\gamma}_{io} = 1$ and $\tilde{\beta}_{i0,\hat{t}} = 0$. Moreover, we highlight the fact that the binary variable $z_{i,t,\hat{t}}$ can be declared as a *continuous variable* due to constraints (5.21) ,(5.23),(5.24), which enforce integrality for 0-1 values of $x_{i,t}$ and $y_{i,t}$. As outlined by Grossmann and Trespalacios (2013) we use the Hull-Reformulation (HR) to transform disjunctions (5.25)-(5.26) into the set of mixed-integer constraints (5.27)-(5.29).

$$P_{i,t,\hat{t}} \leq \left(\tilde{\gamma}_i \cdot k \cdot t^{-a} + \tilde{\beta}_{i,\hat{t}} \cdot r \cdot \left(t - \hat{t} - rt + 1 \right)^{-a-b\cdot\hat{t}} \right) \cdot z_{i,t,\hat{t}} \qquad \forall i \in I, \hat{t} \in 1 \ldots t - rt, t \in T \tag{5.27}$$

$$P_t = \sum_{i \in I_0} \sum_{\hat{t}=1}^{t-rt} P_{i,t,\hat{t}} \qquad \forall t \in T \tag{5.28}$$

$$\sum_{i\in I_0}\sum_{\hat{t}=1}^{t-rt} z_{i,t,\hat{t}} = 1 \qquad \forall t \in T \tag{5.29}$$

We refer to constraints (5.27)-(5.29) as the *Standard Hull-Reformulation* (SHR).

5.5.4 Disjunctive Formulation: Compact Hull-Reformulation

In this particular case it is possible to derive a more compact reformulation of the disjunctive model. For this purpose we sum up constraint (5.27) over all $\hat{t} \in 1 \ldots t - rt$ for every time period $t \in T$ and every number of candidate refracture operations $i \in I_0$. Also, we introduce the partially disaggregated variable $P_{i,t} = \sum_{\hat{t}=1}^{t-rt} P_{i,t,\hat{t}}$. The result is shown in Eqs. (5.30)-(5.31).

$$P_{i,t} \le \sum_{\hat{t}=1}^{t-rt}\left(\tilde{\gamma}_i \cdot k \cdot t^{-a} + \tilde{\beta}_{i,\hat{t}} \cdot r \cdot \left(t - \hat{t} - rt + 1\right)^{-a-b\cdot\hat{t}}\right)\cdot z_{i,t,\hat{t}} \qquad \forall i \in I_0, t \in T \tag{5.30}$$

$$P_t = \sum_{i\in I_0} P_{i,t} \qquad \forall t \in T \tag{5.31}$$

$$\sum_{i\in I_0}\sum_{\hat{t}=1}^{t-rt} z_{i,t,\hat{t}} = 1 \qquad \forall t \in T \tag{5.32}$$

The key advantage is that the triple-indexed disaggregated variables $P_{i,t,\hat{t}}$ can be replaced by the double-indexed variables $P_{i,t}$, hence reducing the total number of decision variables. Also, the formulation in Eqs. (5.30)-(5.32) involves fewer constraints. In fact, the proposed formulation can be improved even further by summing up constraint (5.30) over all $i \in I_0$ in every time period $t \in T$.

$$P_t \le \sum_{i\in I_o}\sum_{\hat{t}=1}^{t-rt}\left(\tilde{\gamma}_i \cdot k \cdot t^{-a} + \tilde{\beta}_{i,\hat{t}} \cdot r \cdot \left(t - \hat{t} - rt + 1\right)^{-a-b\cdot\hat{t}}\right)\cdot z_{i,t,\hat{t}} \qquad \forall t \in T \tag{5.33}$$

$$\sum_{i\in I_0}\sum_{\hat{t}=1}^{t-rt} z_{i,t,\hat{t}} = 1 \qquad \forall t \in T \tag{5.34}$$

Now the formulation does not involve any disaggregated variables or the corresponding constraints, and hence we refer to the aggregated Eqs. (5.33)-(5.34) as the *Compact Hull-Reformulation* (CHR). For more details regarding the CHR we refer to the Appendix G: Compact Hull-Reformulation (Tradeoffs).

Finally, we note that in certain cases, when rigorous reservoir simulation tools are available, the forecasted production profile after any number of refracture treatments can be directly specified as a parameter, namely $Q_{i,t,\hat{t}}$. This parameter captures the predicted production of the well in time period t when the well has been refractured i times, and the last refracture treatment started in time period $\hat{t} < t - rt$. If so, Eqs. (5.19), (5.25), (5.27) and (5.30) turn into Eqs. (5.35)-(5.38), respectively, which represents a much more compact formulation.

$$P_t \leq Q_{i,t,\hat{t}} + \hat{k} \cdot \left(2 - y_{i,t} - x_{i,\hat{t}}\right) \qquad \forall i \in I, t \in T, \hat{t} \leq t - rt \quad (5.35)$$

$$\vee_{i \in I_0, \hat{t} \in 1 \ldots t-rt} \begin{bmatrix} z_{i,t,\hat{t}} \\ P_t \leq Q_{i,t,\hat{t}} \end{bmatrix} \qquad \forall t \in T \quad (5.36)$$

$$P_{i,t,\hat{t}} \leq Q_{i,t,\hat{t}} \cdot z_{i,t,\hat{t}} \qquad \forall i \in I_o, \hat{t} \in 1 \ldots t - rt, t \in T \quad (5.37)$$

$$P_{i,t} \leq \sum_{\hat{t}=1}^{t-rt} Q_{i,t,\hat{t}} \cdot z_{i,t,\hat{t}} \qquad \forall i \in I_0, t \in T \quad (5.38)$$

5.5.5 Objective Function

The intended goal of the multiperiod model is to maximize the net present value (NPV) of a shale gas well development project. Therefore, the objective function involves positive terms accounting for natural gas sales, as well as negative terms related to drilling, fracturing and refracturing expenses. All these terms are discounted back to the present time with a monthly discount rate *d*. Drilling costs (*DC*) and completions costs (CC) are considered to be expenditures at the present time. The unit shale gas profit (gp_t) is the difference between the unit gas price and the production costs, while RC is the total cost of a single refracture treatment. Hence, the objective function of the MILP is given by Eq.(39).

$$\max \quad NPV = \sum_{t \in T} \left(1+d\right)^{-t} \cdot \left[P_t \cdot gp_t - RC \cdot \sum_{i \in I} x_{i,t} \right] - DC - CC \quad (5.39)$$

5.6 Computational Results

We apply the proposed discrete-time MILP model to two case studies. Our first example is a typical shale gas well development planning problem with hypothetical data, whereas the second example is based on simulation results presented by Tavassoli et al. (2013) who rely on real-world data from a Barnett shale well.

5.6.1 Example 1

Given a 10 year planning horizon, we assume that the decision-maker is considering a total of two possible refracture treatments for a particular well development project. Production forecasts with and without refracture treatments are given and factored into the analysis. It is assumed that every additional well stimulation takes about one month during which the well cannot produce any gas. It is also assumed that original drilling, fracturing and completions expenses amount to 3 million USD, whereas every additional refracturing operation costs 800,000 USD. It is important to note that the optimal refracturing strategy is very sensitive to the assumed restimulations costs, which can vary greatly depending on the completions design. In a recent publication, several operators reveal that they expect to spend between 12.5 % and 20.0 % of the initial well development cost for every refracture treatment (WorldOil, 2015).

We decide to take a more conservative approach here and assume that the refracturing procedure costs nearly 30 % of the initial completions expenses. The monthly discount rate d to evaluate the project is 1 %. Lastly, we assume a fixed specific profit of \$ 1.5 per produced Mscf (\$ 0.05 per produced m^3) over the entire planning horizon. All other model parameters are specified in Tab. 5.1. The decision-maker's objective is to maximize the net present value of the well development project.

Model Parameters	Parameter Notation	Values	Units
Initial well production rate	k	299.4	[MMscf/month]
Production decline exponent	a	0.6674	[-]
Post-refracturing production rate	r	120	[MMscf/month]
Post-refracturing decline change	b	0.0005	[1/month]
Time required for refracturing	rt	1	[months]
Initial fractures contribution	γ	1	[-]

Tab 5.1 Model parameter specifications for Example 1.

We solve the MILP model for this problem to zero optimality gap, and identify a refracturing strategy that yields a positive NPV of 765,434 USD. The solution reveals a single refracturing operation, scheduled exactly 26 months after the original well stimulation. Our results suggest that this single refracture treatment allows the operator to increase the EUR from 3,696 MMscf (104.4×10^6 m^3) to 4,609 MMscf (130.2×10^6 m^3); a remarkable 25% increase over the given planning horizon. Without the well-restimulation, the projected NPV reduces to 625,664 USD.

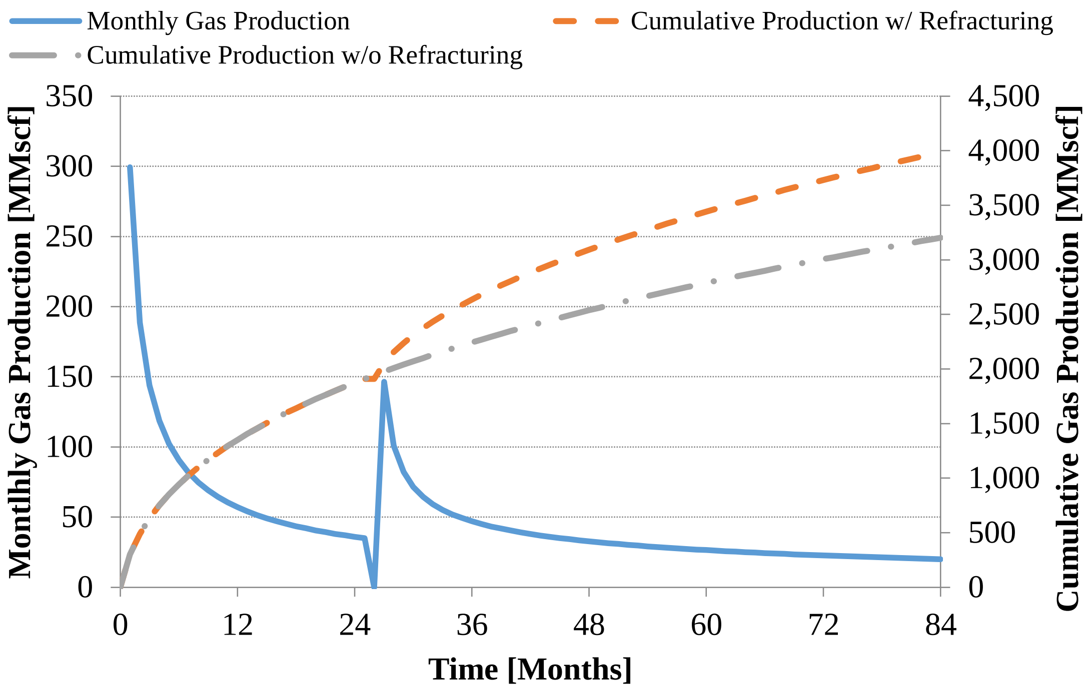

Fig. 5.6. Optimal production curve of a shale gas well studied in Example 1

The NLP model presented in section 5.4 can also be applied to this example – as long as only one single refracture treatment is allowed over the given planning horizon. In this case the objective function needs to be replaced by the maximization of the expected ultimate recovery (EUR) since, as outlined previously, the NLP model is not designed for economic objective functions. Here, the NLP model reveals that the best time for a single refracture treatment is *trf* = 29.72 months. This solution is obtained in less than one second using BARON 16.3 in GAMS 24.2.2. (McCarl, 2011). We find that using the MILP model yields a similar solution (*trf* = 28) when the EUR is maximized – rather than the NPV. The slight difference between both solutions can be attributed to the conversion of the continuous to the discrete time scale. We also note that the singular value for the variable *trf* in the NLP is (1 – a) / b = (1-0.6674)/0.0005 = 665.2 months, much larger than the extent of the planning horizon.

5.6.2 Comparison of Different Formulations

In this section we compare the three alternative MILP formulations, namely the *Big-M Formulation (BMF)*, the *Standard Hull-Reformulation (SHR),* and the *Compact Hull-Reformulation (CHR)* in terms of model size and computational performance. We note that all three formulations yield the exact same solution, as reported in the previous section. Table 5.2 summarizes selected computational statistics for all three formulations when solving Example 1 using Gurobi 5.6.2 in GAMS 24.2.2 on an Intel i7, 2.93 Ghz machine with 8 GB RAM.

	BMF	**SHR**	**CHR**
Binary variables	240	360	360
Continuous variables	481	44,161	22,381
Constraints	15,603	89,163	67,383
Nodes	7,786	0	0
Solution time [seconds]	**255**	**22**	**9**

Table 5.2. Computational statistics for the Big-M Formulation (BMF), the Standard Hull-Reformulation (SHR), and the Compact Hull-Reformulation (CHR) using Gurobi

Table 5.2 clearly shows that the BMF yields the smallest model size in terms of variables and constraints. However, out of the three proposed formulations it also requires the largest solution time (255 s). Despite the fact that the SHR leads to a significantly larger model, it takes less time to solve the same problem: merely 22 s. What is even more impressive is that Gurobi succeeds at solving the MILP problem to optimality at the root node, i.e., prior to branching on any discrete variable. Compared to the SHR, the CHR yields a reduced model size in terms of the number of continuous variables and constraints. As with the SHR, the problem is solved at the root node, but now it takes merely 9 s to obtain the global optimum. Table 5.3 summarizes the computational statistics of all three formulations when solving Example 1 using CPLEX 24.4.6 in GAMS 24.2.2 on an Intel i7, 2.93 Ghz machine with 8 GB RAM.

	BMF	**SHR**	**CHR**
Binary variables	240	360	22,140
Continuous variables	481	44,161	22,381
Constraints	15,603	89,163	67,383
Nodes	10,612	0	0
Solution time [seconds]	**64**	**12**	**11**

Table 5.3. Computational statistics for the Big-M Formulation (BMF), the Standard Hull-Reformulation (SHR), and the Compact Hull-Reformulation (CHR) using CPLEX

Conceptually, the computational results for solving Example 1 using CPLEX 24.4.6 as depicted in Table 5.3 compare directly to those obtained by solving the problem using GUROBI 5.6.2. However, it is interesting to note that the problem solves much faster using CPLEX, particularly for the BMF and SHR models. We also observe that the continuous linear programming (LP) relaxations of all three formulations are nearly identical. The fact that CPLEX and Gurobi solve the problem at the root node can be attributed to the structure of the SHR and CHR formulations, which allow the solvers to take advantage of added cutting planes, efficient heuristics and constraint propagation.

5.6.3 Example 2

In our second case study we rely on a numerical reservoir simulation model developed by Tavassoli et al. (2013) to determine optimal refracturing strategies for a well development project. For this purpose we assume that an upstream operator has already decided to develop a particular shale gas well. The reservoir simulation model proposed by Tavassoli et al. (2013) allows us to predict the well's production profile over a 30 year planning horizon based on real data from a Barnett shale well. Moreover, the model is capable of determining the well's production profile after refracture treatments induced 24, 36, 48, 60, or 72 months after the original well completions. However, unlike Tavassoli et al. (2013), we assume that the well may potentially be restimulated *twice* over its lifespan. The production forecast after secondary refracture treatments is estimated based on the simulation results by Tavassoli et al. (2013). Through a number of case study variations, we show that our proposed refracturing planning model is capable of determining different optimal restimulation strategies, depending on what type of price forecast is given. As before, we assume that drilling, fracturing and completions expenses amount to 3 million USD, whereas every additional refracturing operation costs 800,000 USD and takes exactly one month. The monthly discount rate d is assumed to be 1 %.

Price Forecast with a Seasonal Pattern

Our initial example assumes a price forecast with an underlying seasonal trend pattern. For demonstration purposes we rely on historic Henry Hub spot price data to simulate such a price forecast. The resulting MILP model involves a total of 6,873 binary variables, 7,576 continuous variables, and 22,026 constraints. We note that the decision variables $y_{i,t}$ and $z_{i,t,\hat{t}}$ can be declared as continuous variables, which can result in an improved computational performance depending on the solver selection. The problem is solved to global optimality in less than 2 seconds using CPLEX 24.4.6 on an Intel i7, 2.93 Ghz machine with 8 GB RAM.

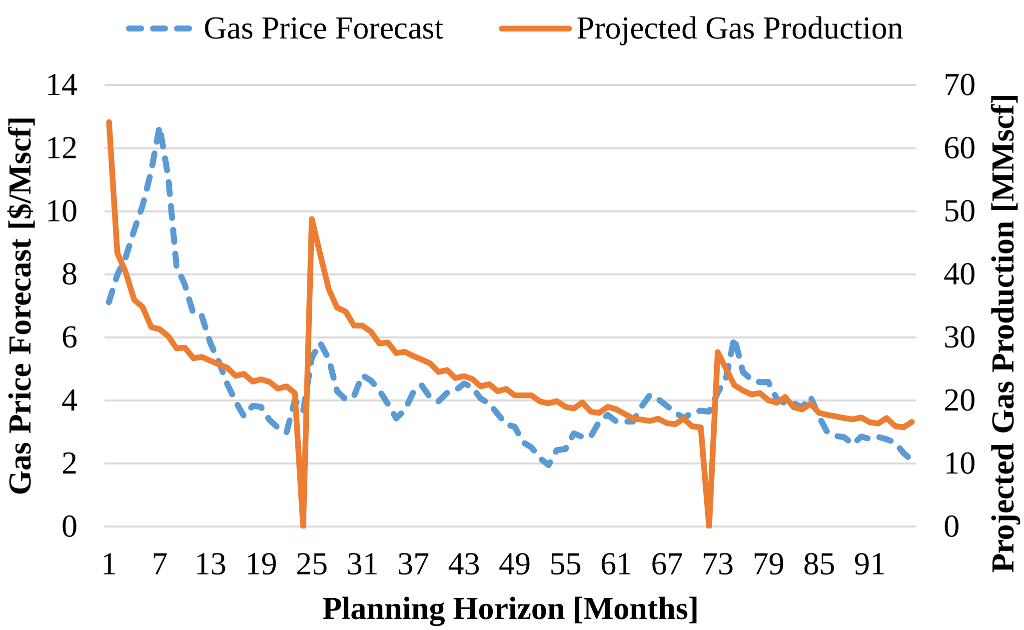

Fig. 5.7 Optimal production curve for a shale gas well given a price forecast (refracture treatments scheduled after 24 months and 72 months respectively)

The optimal solution we identify yields a positive NPV of 5.7 million USD. As shown in Fig. 5.7, the MILP optimizer proposes two refracturing treatments: one 24 months and the other 72 months after initial completions. A comparison of the given price forecast and the projected production profile in Fig. 5.7 suggests that both restimulations are scheduled such that they exploit price peaks in the forecast. Clearly, the given price forecast has a fundamental impact on the optimal well development strategy. Therefore, we also study two alternative future price forecasts assuming fewer stochastic price swings.

Upwards Trend Price Forecast with a Seasonal Pattern

We modify the underlying price forecast for the problem and assume an upwards trend price forecast with a seasonal pattern. This forecast is taken from the CME Group's Henry Hub natural gas futures quote in January 2016 (CME, 2016). The size of the optimization problem and the solution time are the same as in the previous variation of the example.

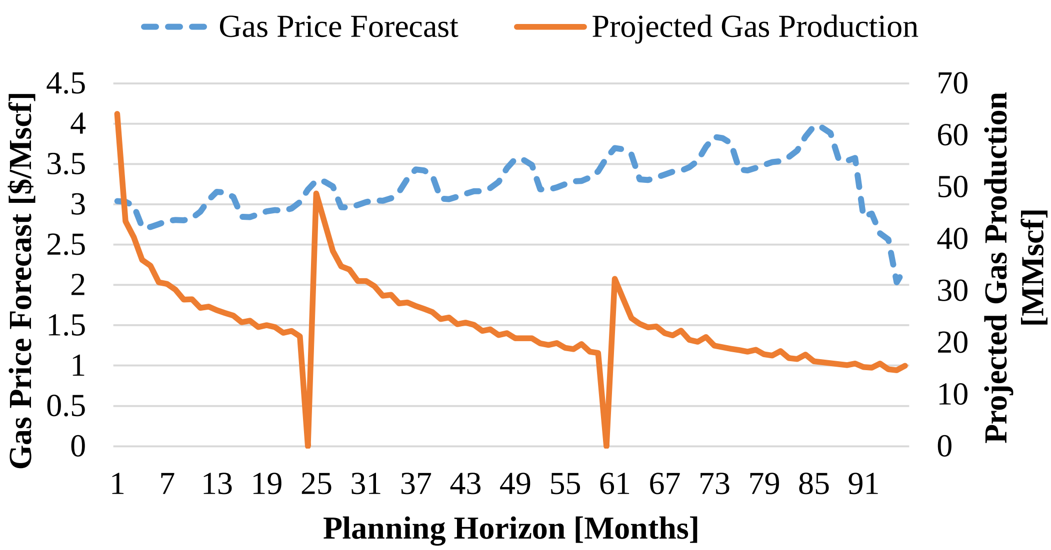

Fig. 5.8 Optimal production curve for a shale gas well given an upwards trend price forecast (refracture treatments scheduled after 24 months and 60 months respectively)

Given the price forecast seen in Fig. 5.8, the solution from the MILP model yields a positive NPV of 2.1 million USD. The decrease in well development profitability – compared to the previous variation of the example – is clearly due to a lower price forecast. However, in this case too, the solution suggests that a total of two refracturing treatments should be performed over the lifespan of the well: the first well restimulation should occur 24 months after well completions (as before) and the second one 3 years later (unlike 4 years before). Without additional refracturing treatments, the predicted NPV for this particular well development project diminishes to merely 1.6 million USD.

Downwards Trend Price Forecast with Seasonal Pattern

Finally, we modify the underlying price forecast for the problem once more and assume a downwards trend price forecast with a seasonal pattern. This forecast is entirely hypothetical but motivated by the CME Group's Henry Hub natural gas futures quotes (CME, 2016). As before, the size of the optimization problem and the solution time are the same as in the previous variation of the example.

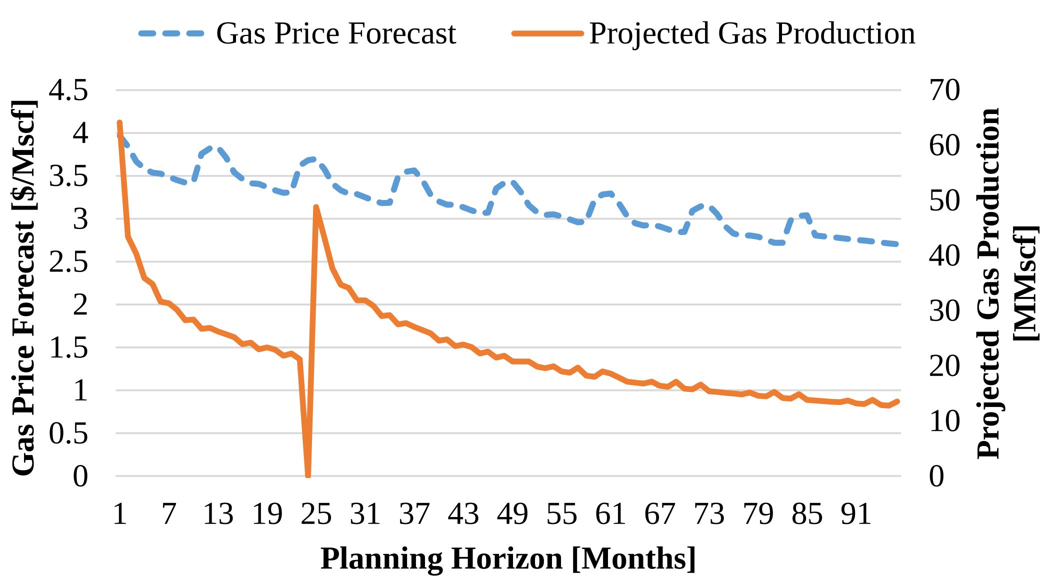

Fig. 5.9 Optimal production curve for a shale gas well given a downwards trend price forecast (single refracture treatment scheduled after 24 months)

Based on the revised price forecast shown in Fig. 5.9, the optimization yields a positive NPV for the well development project of 2.0 million USD. Despite the downward trend of the price forecast, the solution suggests that well development is economically favorable. However, in this particular case the solution shows that only a single refracture treatment should be performed, and it should occur two years into the planning horizon. Without this restimulation, the predicted NPV decreases to 1.5 million USD.

The above examples clearly demonstrate that price forecasts have a significant impact on optimal restimulation strategies – particularly on the frequency and timing of such measures. Hence, we argue that well development economics – and price forecasts in particular – need to be taken into account whenever refracture treatments are considered. Moreover, our results have shown that multiple refracture treatments can provide a viable means to improving the profitability of unconventional wells.

5.7 Conclusions

In this work, we have presented two optimization models for planning shale gas well refracture treatments. First, we proposed a novel forecast function for predicting pre- and post-refracturing productivity declines and a related continuous-time NLP model designed to determine whether or not a shale gas well should be refractured, and when exactly to perform the refracture treatment. We also presented a discrete-time, multiperiod MILP model that explicitly accounts for the possibility of multiple refracture treatments over the lifespan of a well. In the context of the latter, discrete-time model, we compared three alternative formulations: a big-M formulation as well as a disjunctive formulation transformed using Standard and Compact Hull-Reformulations. Applied to a representative well development project that considers the possibility of multiple refracture treatments, we found that the Compact Hull-Reformulation yields the best computational performance in terms of solution times.

The proposed modeling framework can be applied to planned, new well development projects, but also to existing, already producing wells to determine whether or not refracture treatments make economic sense. If, for instance, a price peak appears imminent in the near future, our modeling framework can help to decide whether the magnitude and extent of the projected price peak justifies a well restimulation. We applied the proposed MILP model to two case studies to demonstrate that refracturing can increase the expected ultimate recovery of a well over its lifespan by up to 25 %, and improve the profitability of a well development project by several hundred thousand USD. We find that the optimal number of refracture treatments and their timing are highly sensitive to the given natural gas price forecast. Therefore, our work is meant to lay the foundation for a more rigorous analysis of planning refracture treatments for field-wide development projects, considering price forecast uncertainty. At this time work is currently under progress to: (a) expand the proposed modeling framework in the context of stochastic programming to account for uncertain price forecasts and post-refracture well-performance, and (b) incorporate a reduced-order shale gas well and reservoir proxy model – such as those proposed by Knudsen and Foss (2013) and Knudsen et al. (2014) – directly into our model.

5.8 Nomenclature

Sets

$i \in I$	Refracture treatments
$t \in T$	Time periods

Binary variables

$x_{i,t}$	Active if well refractured for the *i*-th time in time period *t*
$y_{i,t}$	Active if in time period *t* the well has been refractured a total of *i* times
$z_{i,t,\hat{t}}$	Active if in time period *t* the well has been refractured a total of *i* times and the last refracturing occurred in time period $\hat{t}$

Continuous variables

P_t	Shale gas well production in time period *t*
trf	Timing of refracture treatment

Parameters

a	Production decline exponent
b	Post-refracturing decline change
d	Discount rate
k	Initial well production peak
r	Post-refracturing production peak
rt	Duration of refracture treatment
T	Expected lifespan of the shale gas well
$Q_{i,t,\hat{t}}$	Forecasted production of a well in time period *t* after a total of *i* refracture treatments when the last one occurred in time period $\hat{t}$
β	Post-refracturing peak reduction factor
γ	Initial fractures contribution

CHAPTER 6

Stochastic Programming Models for Optimal Shale Well Development and Refracturing Planning under Exogenous and Endogenous Uncertainties

6.1 Introduction

The oilfield service company Schlumberger estimates that roughly 10,000 horizontal shale oil and gas wells drilled in the past five years in North America are candidates for refracturing (Sider & Ailworth, 2013). The belief is that a well restimulation can restore production to near-initial levels at far less cost than drilling and completing a new well (Johnson, 2016). Fig. 6.1 shows the production history of a Marcellus shale well refractured by Consol Energy after approximately four years. In this particular case the production data clearly reveals that the restimulation was very effective; production rates are restored, and even the decline appears to be less drastic following the recompletion. Naturally, restimulation costs vary between operators or development areas and generally they depend on the selected refracturing technique. While Consol Energy estimates that a restimulation costs approximately two million USD, Encana is refracturing wells for less than one million USD (Miller, 2015). In comparison, the process of drilling, fracturing and completing a new shale well in the Marcellus Play ranges in cost between three and six million USD.

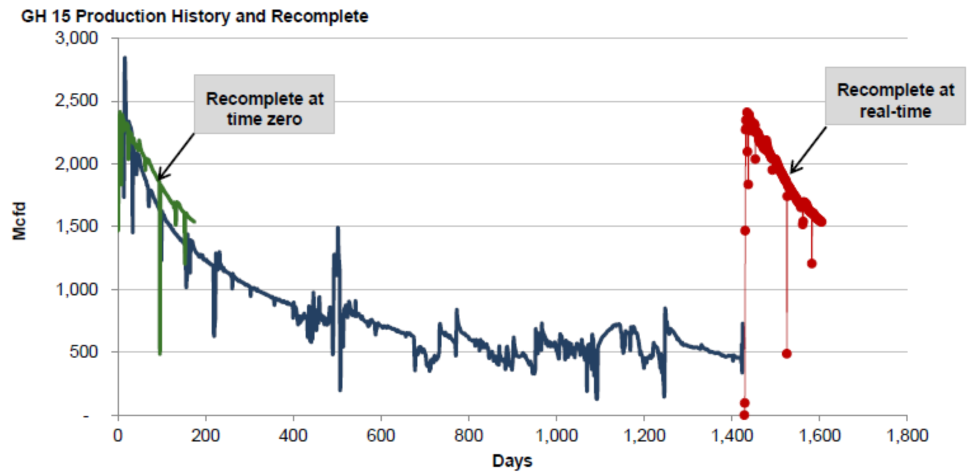

Fig. 6.1: Production history of a Marcellus shale well refractured after approximately four years. Source: Analyst presentation Consol Energy, June 2014

However, not only does the cost of restimulations vary between operators. King (2015) reports that both timing and frequency of recompletions oftentimes differ too. While some operators choose to refracture early into the lifespan of their wells, others wait several years to restimulate horizontal laterals. Moreover, there is increasing evidence suggesting that multiple restimulations of the same wellbore may make economic sense. In fact, Broderick et al. (2011) claim that shale gas wells could be refractured up to five times over their expected lifespan of 20-25 years.

6.2 Literature Review

Despite its practical potential, the refracturing planning problem is not a well-studied problem in the literature. To this day, notably few researchers have addressed the challenges that shale gas producers face when scheduling and performing well restimulations. Among the few works that have been published in this field, Sharma (2013) proposes guidelines and dimensionless type curves to accomplish two things: a) determine the ideal timing of a refracture treatment in the life of a well, and b) evaluate the potential increase in well production after the restimulation. Eshkalak et al. (2014) study the refracturing planning problem with an emphasis on the economics of well restimulations. Through a comprehensive case study involving a total of 50 shale wells, the authors find that refracturing is profitable even in low-price environments, although the actual timing of the well restimulations is pre-determined. Tavassoli et al. (2013) propose a comprehensive, numerical simulation model to evaluate the impact of well restimulations on the production performance of shale wells as a function of reservoir parameters, the recompletions design, and the timing of the refracture treatment. As a rule of thumb, the authors advise upstream operators to consider the restimulation of their shale wells whenever production decline rates are below 10-15%.

Lastly, Cafaro et al. (2016) present an optimization framework to plan shale gas well refracture treatments. In their work, the authors assume that the decision to drill, fracture and complete a prospective shale well has already been made. In order to determine if, when and how often the well should be restimulated over its lifespan, Cafaro et al. (2016) propose two optimization models: a continuous-time nonlinear programming (NLP) model and a discrete-time mixed-integer linear programming (MILP) model. Whereas the NLP model is primarily designed to identify the optimal time to refracture a well such that its expected ultimate recovery (EUR) is maximized, the MILP model can be used to schedule multiple refracture treatments over the life of a well. Both models, however, are purely deterministic in nature.

In this chapter we present an important extension of the work by Cafaro et al. (2016). Our primary objective is to explicitly account for two major sources of uncertainty: price developments over time, and production performance before/after restimulations. In addition, we present a generalized production estimate function, and a moving horizon framework that enables upstream operators to schedule refracture treatments as true recourse actions to uncertainty realizations and/or potential disruptions.

6.3 General Problem Statement

We assume that an upstream operator has identified a prospective location to drill, fracture and complete a single shale gas well. The estimated production of the prospective well over time is characterized by a given type curve. Once completed, it is assumed that this well can be refractured multiple times over its expected lifespan. Every restimulation leads to a reinvigoration of the well’s gas production rate.

However, in this work we recognize that a prospective well’s production rate over time cannot always be forecasted accurately a priori, i.e. before the well has actually been drilled and completed. Particularly, the post-refracture response performance can be difficult to anticipate. Hence, we assume that – in addition to the default type curve – a discrete set of well performance scenarios is provided. These scenarios account for the possibility that the gas production prior to and after any number of well restimulations exceeds or fails to meet expectations.

In addition to well performance scenarios, we assume that the operator chooses to consider a set of natural gas price forecast scenarios. These scenarios reflect the fact that it is generally challenging to predict natural gas price developments reliably over time, especially over multiple years. By considering a number of unique, potential price development scenarios, the intent is to “robustify” the proposed well development strategy over a wide range of possible outcomes.

In light of uncertain well production performance and uncertain gas price forecast, the goal of this work is to determine: (a) if a well should be drilled at the prospective location at the present time, (b) whether or not the well should be refractured eventually, (c) how often the well should be refractured over its expected lifespan, and (d) when exactly the refracture treatments should be performed. The objective is to maximize the expected net present value of the well development project.

The remainder of this chapter is organized as follows. Initially, we present a generalized production estimate function that explicitly considers the possibility of refracturing a shale well multiple times over its lifespan. Next, we briefly review general concepts of stochastic programming to address optimization problems under uncertainty and we discuss why two-stage stochastic programming is particularly suitable for addressing the well development and refracturing planning problem in light of exogenous price uncertainty and endogenous well performance uncertainty. The integrated planning problem is tackled with two distinct mixed-integer linear programming models: a) a two-stage stochastic programming model for well development planning, and b) a two-stage stochastic programming model for refracturing planning. Both models are embedded in a moving horizon strategy, which allows decision-makers to recognize refracturing as an opportunity to periodically respond to uncertainty realizations and/or potential disruptions. Moreover, we show that the moving horizon strategy can be used to effectively address the endogenous nature of the well performance uncertainty. Thereafter, we present a comprehensive case study to demonstrate how the proposed optimization framework can be used to solve the practical well development and refracturing planning problem under uncertainty. Lastly, we discuss qualitatively what role refracturing may have in field-wide shale development projects.

6.4 Generalized Production Estimate Function

In this section we propose a generalized production estimate function that predicts how much gas a well is expected to produce over time as a function of when and how often it has been restimulated. For this purpose we introduce the parameter $Q_{i,t,\hat{t},p}$. This parameter captures the amount of gas to be produced by a well in time period t given that it has been refractured i times total, and the last stimulation was performed in time period $\hat{t} < t$. Since we wish to account for the uncertainty in predicting gas production over time, this parameter also includes the well-performance scenario index p. This index highlights the fact that the estimated gas production is scenario-dependent, which will be outlined in more detail below.

As suggested by Cafaro et al. (2016), the gas production of an unconventional well can be represented adequately by a decreasing power function. This power function is defined by an expected initial production peak parameter k_p and an expected initial production decline parameter a_p, both of which are assumed to be scenario-dependent. Yet, these two parameters by themselves can only represent the production of a shale well that has not been refractured. In order to account for restimulation measures we propose Eq. (6.1).

$$Q_{i,t,\hat{t},p} \approx \tilde{\gamma}_{i,p} \cdot k_p \cdot t^{-a_p} + r_{i,\hat{t},p} \cdot \left(t - \hat{t} - rt + 1\right)^{-a_{i,p} - b_{i,p} \cdot \hat{t}} \tag{6.1}$$

The function in Eq. (6.1) contains the expected initial production peak parameter k_p and the expected initial production decline parameter a_p. However, this function also considers a number of additional factors that play an important role as soon as a well has been refractured once or more often. For instance, every time a shale well is refractured, the contribution of its initial fractures to the overall production changes. Some operators report an increase in production contribution, while others have experienced decreases. We introduce the parameter $\tilde{\gamma}_{i,p}$ to capture this aspect. Initially, after a well has been drilled and fractured for the first time, this parameter equals one. After every restimulation, however, the parameter may be set to a different expected value. This information can typically be provided by completions design engineers, geologists, or reservoir engineers. By default, we assume that $\tilde{\gamma}_{i,p} = \tilde{\gamma}_p{}^i$, meaning that every additional refracture treatment has the same impact on the original fractures.

More importantly, the second term of the gas production estimate function in Eq. (6.1) captures the characteristic peak in production following a well restimulation. We assume that every restimulation takes rt time periods (usually, one month). For this reason, we introduce the expected, supplemental production peak parameter $r_{i,\hat{t},p}$. The value of this parameter changes depending on how many times (i) the well has been refractured and when the last restimulation occurred, captured by the index $\hat{t}$. With every additional refracture treatment, this supplemental production peak becomes less pronounced. Also, field tests have revealed that the peak following a restimulation decreases the longer an upstream operator waits to refracture a well. We note that previous work by Cafaro et al. (2016) does not consider the timing of a well restimulation to anticipate the supplemental production peak following the refracture treatment. For simplicity, the authors assume that every time a well is refractured, the supplemental production peak lessens by a peak reduction factor $\beta_{i,p}$, which explicitly considers the number of total restimulations, but does not account for the timing of these measures. Conceptually, the approximation $r_{i,\hat{t},p} \approx \beta_{i,p} \cdot r_p$ is valid and may be used to simplify the problem at hand.

Finally, we address the exponent $(-a_{i,p} - b_{i,p} \cdot \hat{t})$ in Eq. (6.1). Essentially, this exponent is an estimate of the post-refracture production decline after *i* restimulations in scenario *p*. The term is made up of three critical factors that are believed to determine the production decline following a refracture treatment: a) the initially expected production decline of the well after *i* restimulations $a_{i,p}$ (which may vary depending on how many stages of the well are actually recompleted), b) the expected additional decline after *i* restimulations $b_{i,p}$, and c) the timing of the *i*-th refracture treatment $\hat{t}$. This composite decline exponent is motivated by the work of Tavassoli et al. (2013) who show that the post-refracture production decline increases the longer an upstream operator waits to refracture a shale well. As before, all production decline parameters are scenario-dependent and can therefore be defined to account for different well-performance scenarios *p*. Fig. 6.2 shows an illustration of the generalized production estimate function with added "noise" (created via Monte Carlo simulation). The type curves are representative for a well having been fractured once, twice or three times considering different production performance parameter settings.

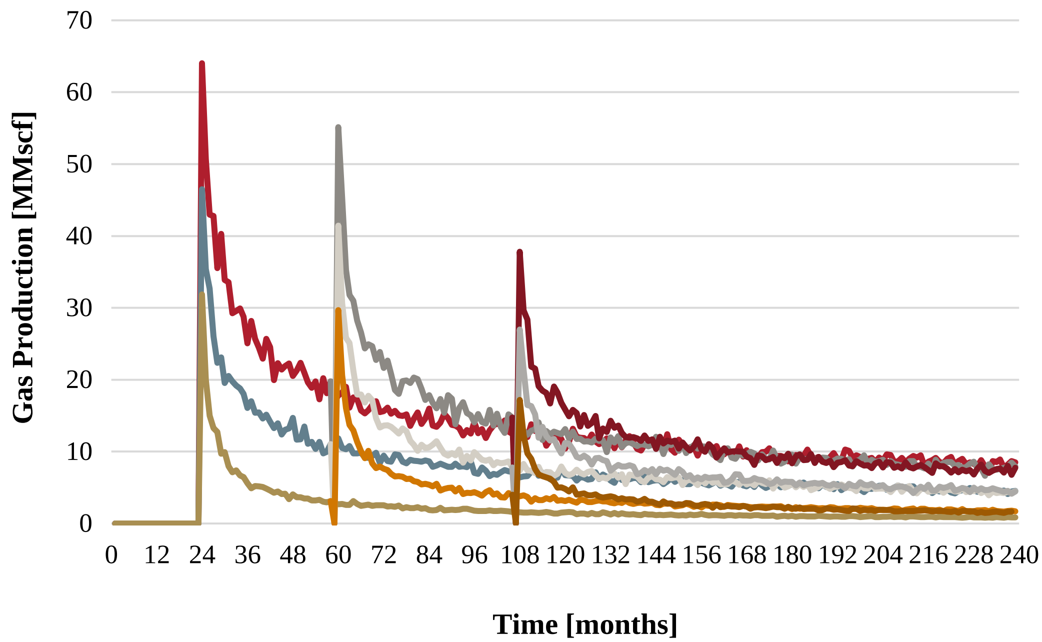

Fig. 6.2: Illustration of the generalized production estimate function for multiple refracturing treatments considering different production performance settings

Altogether, the generalized production estimate function in Eq. (6.1) is more rigorous and comprehensive than the previously proposed correlation by Cafaro et al. (2016), since it explicitly considers: a) how often a well has been refractured in total, b) when a well was last restimulated, and c) by how much production may deviate depending on the degree of uncertainty.

6.5 Concepts of Stochastic Programming

In this section, we briefly review concepts and premises of stochastic programming. The motivation for stochastic programming originates from the fact that decision-makers often face problems involving uncertain parameters. These parameters could include price forecasts, processing times, or cost assumptions. Stochastic programming allows decision-makers to solve problems involving uncertain parameters through rigorous mathematical optimization. The premise of stochastic programming is that a problem is essentially split into two broad categories of decisions: a) those that have to be made in light of the uncertainty, i.e., not knowing the actual realization of the uncertain parameters, and b) those decisions that can be taken as soon as the uncertainty has revealed itself. The former decisions are referred to as *here-and-now decisions*, whereas the latter can be classified as *wait-and-see, corrective* or *recourse actions*. The interpretation of this categorization is as follows: in light of uncertain parameters the goal is to identify a particular here-and-now solution strategy (e.g. a schedule, an assignment, or a particular design) that works best for a set of possible scenarios. This solution should be such that regardless of which of the scenarios is true, the selected strategy hedges against the risk of uncertainty and, in theory, it is prepared for any possible outcome. At the same time, the aforementioned recourse actions provide a decision-maker with the flexibility to respond to particular uncertainty realizations. The more flexibility a decision-maker has in terms of recourse actions, the less impactful the here-and-now decisions are. In stochastic programming the time horizon is generally discretized and all potential uncertainty realizations are obtained from discretized probability distributions. Therefore, a given set of discrete scenarios merely represents a finite set of different realizations for the uncertain parameters (Apap & Grossmann, 2016). Given the probability of each scenario, we use mathematical programming to maximize the expected value of the objective function, subject to the constraints from all scenarios. We refer to the formulations of these optimization problems as the *deterministic equivalent* of the stochastic problem.

In this work we primarily focus on two-stage stochastic programming (Birge and Louveax, 2011) where the entire set of decision variables is split into two subsets: here-and-now decision variables (stage one) and wait-and-see decision variables (stage two recourse actions). Alternatively, optimization problems under uncertainty can be addressed via multi-stage stochastic programming. In this case decision-makers have the opportunity to make here-and-now decisions at three or more stages throughout the time horizon. Clearly, multi-stage stochastic programming is a more rigorous and accurate representation of the decision-making process in practice. However, these formulations lead to significantly larger models that are oftentimes computationally intractable.

Within the realm of stochastic programming, we can distinguish between two types of uncertainty: exogenous and endogenous uncertainty. Exogenous uncertainty realizes regardless of what a decision-maker does. If we consider the future natural gas price as an uncertain parameter, for instance, we can presume that the uncertainty will realize eventually, i.e., the market will settle on a particular gas price – regardless of whether a shale gas producer drills or refractures a prospective well or not. The realization of endogenous uncertainty, on the other hand, depends on what a decision-maker ends up doing. For example, in this work we assume that the production performance of an unconventional well before and/or after a restimulation is uncertain prior to actually drilling the well. However, once an upstream operator has actually drilled the lateral section of the well, completions engineers gather reservoir data including permeability and porosity readings, which in turn can be used to predict the well's production performance much more accurately. Therefore, we consider well performance to be an endogenous uncertainty. It is worth mentioning that in the past, optimization problems under exogenous and endogenous uncertainty have been addressed almost exclusively with multi-stage stochastic programming. For a detailed examination of multi-stage stochastic programming under endogenous and exogenous uncertainties we refer to the comprehensive work by Apap & Grossmann (2016).

6.6 Stochastic Programming Model for Well Development Planning

In this work, we assume that the practical well development planning problem under exogenous price uncertainty and endogenous well performance uncertainty can be formulated as a two-stage stochastic programming approach. First, we consider the premise of the generic well development planning problem. Initially, an upstream operator has identified a prospective location to drill, fracture and complete a single shale gas well. For this well, a long-term forecast of its production over time can be estimated. However, since this production estimate is uncertain, the operator wants to consider alternative well performance scenarios. Moreover, even at this stage in the development process, the operator may want to consider the possibility of refracturing the well at some point over the course of its life, possibly even multiple times.

Although the post-refracture production performance can also be estimated, it is likely that the operator's confidence in this estimate is limited. To this day, operators have drilled thousands of unconventional wells, but only restimulated a small fraction of them. Therefore, the post-refracture well performance is also assumed to be uncertain. In order to hedge against the risk of uncertainty, we consider a set of well performance scenarios $p \in P$, each with probability φ_p, as part of the well development planning problem.

The planning problem is also challenging because commodity prices are known to fluctuate dramatically. Upstream operators need to know that their potential investment in a prospective shale well makes economic sense across a range of possible price developments. Hence, we explicitly factor price uncertainty into our analysis, and therefore consider a set of price forecast scenarios $f \in F$. Furthermore, our framework gives operators the opportunity to assign a likelihood π_f to the realization of each scenario.

The purpose of the well development planning problem is then to determine, first and foremost, if an upstream operator should drill the prospective shale well at the present time. In the proposed optimization framework this key decision is captured by introducing the binary decision variable w^{DRILL}. In the context of two-stage stochastic programming, as outlined earlier, this variable is classified as a stage one, here-and-now decision. Without knowing what the ultimate production performance will be or how natural gas prices will develop, the optimization model sets this variable either to one or to zero in light of the considered spectrum of uncertainty scenarios. Beyond the actual well development, there are a number of decisions that can be made individually for every considered scenario; these are denoted as scenario-dependent, wait-and-see decisions. Among these decisions are: a) whether or not the well should be refractured eventually, b) how often the well should be restimulated over its expected lifetime, and c) when exactly the refracture treatments should be performed. All of the aforementioned aspects of the well development planning problem are captured by the binary decision variable $x_{i,t,f,p}$. This variable is equal to one if the well is scheduled to be restimulated for the *i*-th time in time period t under price scenario f and well performance scenario p. The following constraints are designed around these two key decision variables, w^{DRILL} and $x_{i,t,f,p}$.

For instance, the inequality in Eq. (6.2) is added to the proposed model to ensure that unless the well has actually been drilled, it cannot be refractured.

$$w^{DRILL} \geq x_{i,t,f,p} \qquad \forall i \in I, t \in T, f \in F, p \in P \tag{6.2}$$

We note that Eq. (6.2) is expressed as an inequality constraint to allow for the possibility of drilling the well but never actually refracturing it over its lifespan. In turn, Eq. (6.3) ensures that the prospective well cannot be restimulated for the *i*-th time more than once.

$$\sum_{t \in T} x_{i,t,f,p} \leq 1 \qquad \forall i \in I, f \in F, p \in P \tag{6.3}$$

Eq. (6.4) is a sequencing constraint ensuring that if in time period t the well is restimulated for the i-th time, then it has to have been refractured for the $(i-1)$-th time previously. We note that the parameter rt is introduced to represent the number of time periods it actually takes to recomplete the well.

$$x_{i,t,f,p} \leq \sum_{\tau < t-rt} x_{i-1,\tau,f,p} \qquad \forall i \in I, t \in T, f \in F, p \in P, i > 1 \tag{6.4}$$

At this point we rely on a simple but effective step to strengthen the quality of the proposed model formulation. We introduce an auxiliary binary variable $y_{i,t,f,p}$ to determine whether as of time period t the well has been refractured i times in scenarios f and p. Although the variables $x_{i,t,f,p}$ and $y_{i,t,f,p}$ are closely related, they serve different purposes. The variable $x_{i,t,f,p}$ marks the exact timing of a restimulation, whereas the variable $y_{i,t,f,p}$ keeps track of the "state of restimulation". For instance, it is entirely possible that in time period $t = 36$ (typically months) the well has been refractured twice for a particular scenario combination, hence $y_{i2,t36,f,p} = 1$. Yet, this does not necessarily imply that the restimulation actually occurred in this particular time period. Instead, the well could have been refractured in time period $t = 24$ for the second time, in which case $x_{i2,t24,f,p} = 1$. To establish the relationship between these two variables, we include Eqs. (6.5), (6.6) and (6.7) in the model.

$$x_{i,t,f,p} \le y_{i,t,f,p} \qquad \forall i \in I, t \in T, f \in F, p \in P \tag{6.5}$$

$$y_{i,t,f,p} \le \sum_{\tau \le t} x_{i,\tau,f,p} \qquad \forall i \in I, t \in T, f \in F, p \in P \tag{6.6}$$

$$y_{i,t,f,p} \ge y_{i,t-1,f,p} - x_{i+1,t,f,p} \qquad \forall i < |I_0|, f \in F, p \in P, t > 1 \tag{6.7}$$

All three equations above can easily be derived using propositional logic (Raman & Grossmann, 1991) and we refer to the work by Cafaro et al. (2016) for the actual derivation. Similar to the previously introduced Eq. (6.3), we also add Eq. (6.8) to the model.

$$\sum_{i \in I_0} y_{i,t,f,p} = w^{DRILL} \qquad \forall t \in T, f \in F, p \in P \tag{6.8}$$

However, we note that unlike Eq. (6.3), the above constraint is actually expressed as an equality constraint. That is because at any point in time the well has to be in a particular “refracturing state” $i \in I_0$, if drilled. In fact, the set I_0 includes the element i_o which represents the state “drilled and fractured, but not refractured”. Next, we introduce an additional binary variable $z_{i,t,\hat{t},f,p}$. This variable can be derived from the previously defined decision variables $x_{i,t,f,p}$ and $y_{i,t,f,p}$ as follows:

$$y_{i,t,f,p} \wedge x_{i,\hat{t},f,p} \Leftrightarrow z_{i,t,\hat{t},f,p} \qquad \forall i \in I, t \in T, \hat{t} \le t, f \in F, p \in P \tag{6.9}$$

Practically speaking, the variable $z_{i,t,\hat{t},f,p}$ indicates whether in time period t the well has been refractured i times in the past, and the last restimulation occurred in time period $\hat{t}$ for the scenario combination f and p. By applying propositional logic to the statement in Eq. (6.9), we derive Eqs. (6.10)-(6.12).

$$y_{i,t,f,p} + x_{i,\hat{t},f,p} \le z_{i,t,\hat{t},f,p} + 1 \qquad \forall i \in I, t \in T, \hat{t} \le t, f \in F, p \in P \tag{6.10}$$

$$z_{i,t,\hat{t},f,p} \le y_{i,t,f,p} \qquad \forall i \in I, t \in T, \hat{t} \le t, f \in F, p \in P \tag{6.11}$$

$$z_{i,t,\hat{t},f,p} \le x_{i,\hat{t},f,p} \qquad \forall i \in I, t \in T, \hat{t} \le t, f \in F, p \in P \tag{6.12}$$

For the particular element $i_o \in I_0$, Eqs. (6.10)-(6.12) take the following form:

$$y_{i,t,f,p} + w^{DRILL} \le z_{i,t,\hat{t},f,p} + 1 \qquad \forall i = i_o, t \in T, \hat{t} = t_1, f \in F, p \in P \tag{6.13}$$

$$z_{i,t,\hat{t},f,p} \le y_{i,t,f,p} \qquad \forall i = i_o, t \in T, \hat{t} = t_1, f \in F, p \in P \tag{6.14}$$

$$z_{i,t,\hat{t},f,p} \le w^{DRILL} \qquad \forall i = i_o, t \in T, \hat{t} = t_1, f \in F, p \in P \tag{6.15}$$

The actual gas production of the prospective well $P_{t,f,p}$ is directly linked to the previously proposed production estimate function $Q_{i,t,\hat{t},p}$ in Eq. (6.16).

$$P_{t,f,p} = \sum_{i \in I_o} \sum_{\hat{t}=1}^{t} Q_{i,t,\hat{t},p} \cdot z_{i,t,\hat{t},f,p} \qquad \forall t \in T, f \in F, p \in P \tag{6.16}$$

Since the previously introduced decision variable $z_{i,t,\hat{t},f,p}$ captures the current time period (index t), how often the well has been refractured (index i), and when the last restimulation occurred (index $\hat{t}$) for every scenario combination (indices f and p), we link it directly to the production $Q_{i,t,\hat{t},p}$ predicted by Eq. (6.1). However, we note that the proposed optimization framework can be linked to any alternative production forecast function simply by replacing $Q_{i,t,\hat{t},p}$ by the preferred estimation.

Finally, Eq. (6.17) ensures that, if drilled, the well should be in one "refracturing state" at every point in time for every scenario combination.

$$\sum_{i \in I_0} \sum_{\hat{t}=1}^{t} z_{i,t,\hat{t},f,p} = w^{DRILL} \qquad \forall t \in T, f \in F, p \in P \tag{6.17}$$

The objective of the well development project is to maximize the expected net present value. This means that in light of the considered price forecast uncertainty and well performance uncertainty, revenues from gas sales have to be maximized, whereas expenses for well development and recompletions are to be minimized.

$$\max ENPV = \underbrace{-\left(DC + CC\right) \cdot w^{DRILL}}_{\substack{\text{Stage 1 decision (here-and-now):} \\ \text{Develop the well: yes or no?}}} + \underbrace{\sum_{f \in F} \pi_f \sum_{p \in P} \varphi_p \sum_{t \in T} \left(1+d\right)^{-t} \cdot \left\{ P_{t,f,p} \cdot gp_{t,f} - \sum_{i \in I} rc_i \cdot x_{i,t,f,p} \right\}}_{\substack{\text{Stage 2 decisions (wait-and-see):} \\ \text{Restimulate the well: yes or no? how often? when? (scenario-dependent)}}} \tag{6.18}$$

The objective function in Eq. (6.18) clearly exemplifies the two-stage nature of the proposed optimization model. The initial summation term captures the stage one, here-and-now decision concerned with whether or not the well should be developed at the present time. This is a yes-or-no design decision that involves a development expense for drilling and completions operations, as represented by the parameters DC and CC, respectively. The binary variable w^{DRILL} is clearly scenario-independent, accounting for the fact that this decision needs to be made in light of the uncertainty, i.e., not knowing which of the scenarios will turn out to be true.

The second summation term in Eq. (6.18) represents the stage two, wait-and-see decisions that reflect whether or not, how often and when the well needs to be refractured. These decisions represent scenario-dependent recourse actions that can be made individually and independently for every single scenario combination of price forecast and well performance. Since every unique scenario combination may result in a different production profile and/or restimulation strategy, revenues and expenses may vary scenario-by-scenario. In particular, this term of the objective function contains the scenario-dependent gas price parameter $gp_{t,f}$ as well as the refracture cost rc_i which may depend on the total number of recompletions. Moreover, every scenario combination is individually weighted based on specified scenario realization probabilities, π_f and φ_p, for price forecasts and well performance, respectively. These probability parameters allow decision-makers to specify their confidence in individual scenarios, which will then be reflected in the solution identified by the optimization. Altogether, Eqs. (6.2)-(6.8) and (6.10)-(6.18) define the formulation of the well development planning problem.

In the previous section we pointed out that the pre-and post-refracture well performance uncertainty is endogenous in nature, whereas the price forecast uncertainty can be categorized as exogenous. However, at this stage in the planning process both uncertainty sources are treated the same because the prospective well has not actually been drilled and completed yet. Once this has been done, completions and reservoir engineers can use collected subsurface data to refine their production estimates to the point where a stochastic analysis is no longer necessary. This leads us to the refracturing planning problem, which will be addressed in greater detail in the following section.

6.7 Stochastic Programming Model for Refracturing Planning

The setup of the refracturing planning problem is as follows. Unlike before, we assume that an upstream operator is dealing with an actively producing shale gas well. Similar to the premise of the well development planning problem, however, a long-term type-curve forecast for this well's gas production is available. Yet, at this point into the well's lifespan we assume that the gas production over time can be predicted fairly accurately. Right after turning the well in-line, operators record the initial production and get early readings on its decline rate. Also, subsurface data gathered during drilling and fracturing operations allows producers to anticipate a well's response behavior to one or many restimulations relatively precisely. Hence, it is no longer necessary to account for well performance uncertainty as part of the refracturing planning problem. Price uncertainty, on the other hand, continues to present a major challenge to the operator. Therefore, we still consider a set of natural gas price forecast scenarios $f \in F$ with probability π_f when scheduling refracture treatments for the given well.

The refracturing planning problem is meant to address a number of important decisions that an upstream operator needs to make in the situation described above. The primary purpose is to determine if the active shale well should be refractured at the present time. That is ultimately the question that motivates this section. Beyond this decision, however, we also wish to determine: a) whether or not the well should be refractured <u>again</u>, b) how often it should be restimulated over its expected lifespan, and c) when exactly subsequent refracture treatments should ideally be scheduled. As before, we propose a two-stage stochastic programming model to address the refracturing planning problem in light of uncertain price forecasts. In the spirit of two-stage stochastic programming, the here-and-now design decision is concerned with the possibility of restimulating the well at the present time, whereas all other decisions can be classified as scenario-dependent, wait-and-see recourse actions. Although the model formulation of the refracturing planning problem is clearly inspired by the well development planning problem, there are some distinct differences that are highlighted below.

Eqs. (6.19)-(6.34), introduced next, compare directly to Eqs. (6.3)-(6.8), (6.10)-(6.12) in the previous section. However, there are a few notable differences. First, and most importantly, we introduce a new binary decision variable x^{REFRAC} to capture whether or not the actively producing well should be refractured at the present time. In the context of two-stage stochastic programming, x^{REFRAC} represents the stage one, here-and-now decision variable. Unlike before, we now also-link the index i to the "current refracture state" cr which tracks how often a well has been restimulated thus far. The introduction of the current refracture state is necessary since the model proposed in this section is intended to be used repeatedly over the course of a well's lifespan, even after multiple refracture treatments may already have occurred. For more details regarding this scheme we refer to the next section (Moving Horizon Framework for Well Development and Refracturing Planning). Lastly, we point out that unlike the previous model, the constraints below are <u>not</u> set up over the set of well performance scenarios $p \in P$ since the production uncertainty is assumed to have resolved itself at this point in the planning process.

The inequalities in Eqs. (6.19) and (6.20) are included in the refracturing planning model to make sure that the shale well cannot be refractured for the *i*-th time more than once. Here and in several other constraints below, the introduction of the stage-one decision variable x^{REFRAC} makes it necessary to distinguish between the first opportunity to recomplete the well (here-and-now), represented by the refracture state $i = cr + 1$ in time period t_1, and additional opportunities for future well restimulations $i > cr + 1$.

$$\sum_{t \in T} x_{i,t,f} + x^{REFRAC} \leq 1 \qquad \forall i = cr + 1, f \in F \tag{6.19}$$

$$\sum_{t \in T} x_{i,t,f} \leq 1 \qquad \forall i > cr + 1, f \in F \tag{6.20}$$

Eqs. (6.21) and (6.22) represent sequencing constraints ensuring that the optimizer cannot schedule the *i*- th well restimulation, unless the (*i*-1)-th recompletion has been performed. As before, the practical constraint is expressed via two inequalities due to the stage-one decision variable x^{REFRAC}.

$$x_{i,t,f} \leq \sum_{\tau < t - rt} x_{i-1,\tau,f} + x^{REFRAC} \qquad \forall i \in I, t \in T, f \in F, i = cr + 2 \tag{6.21}$$

$$x_{i,t,f} \leq \sum_{\tau < t - rt} x_{i-1,\tau,f} \qquad \forall i \in I, t \in T, f \in F, i > cr + 2 \tag{6.22}$$

Eqs. (6.23)-(6.28) are directly adapted from Eqs. (6.5)-(6.7) in section 6.6 Stochastic Programming Model for Well Development Planning. They are added to the model to account for the auxiliary variable $y_{i,t,f}$, which captures the "state of restimulation". For more details we refer to the previous section.

$$x^{REFRAC} \leq y_{i,t,f} \qquad \forall i = cr + 1, t = t_1, f \in F \tag{6.23}$$

$$x_{i,t,f} \leq y_{i,t,f} \qquad \forall i > cr, t > 1, f \in F \tag{6.24}$$

$$y_{i,t,f} \leq \sum_{\tau \leq t} x_{i,\tau,f} + x^{REFRAC} \qquad \forall i = cr + 1, t \in T, f \in F \tag{6.25}$$

$$y_{i,t,f} \leq \sum_{\tau \leq t} x_{i,\tau,f} \qquad \forall i > cr + 1, t \in T, f \in F \tag{6.26}$$

$$y_{i,t,f} \geq 1 - x^{REFRAC} \qquad \forall i = cr, t = t_1, f \in F \tag{6.27}$$

$$y_{i,t,f} \geq y_{i,t-1,f} - x_{i+1,t,f} \qquad \forall i \geq cr, t > 1, f \in F \tag{6.28}$$

As before, we also include Eq. (6.29) in the proposed model to ensure that at any point in time the well can be categorized by its "refracturing state" $i \in I_0$.

$$\sum_{i \geq cr} y_{i,t,f} = 1 \qquad \forall t \in T, f \in F \tag{6.29}$$

Eqs. (6.30)-(6.34) can be traced back to constraints (6.10)-(6.12) in the previous section. These inequalities capture the relation between the decision variables $z_{i,t,\hat{t},f}$, $y_{i,t,f}$, $x_{i,\hat{t},f}$ and x^{REFRAC}.

$$y_{i,t,f} + x^{REFRAC} \leq z_{i,t,\hat{t},f} + 1 \qquad \forall i = cr+1, t \in T, \hat{t} = t_1, f \in F \tag{6.30}$$

$$y_{i,t,f} + x_{i,\hat{t},f} \leq z_{i,t,\hat{t},f} + 1 \qquad \forall i \geq cr+1, t \in T, 1 < \hat{t} \leq t, f \in F \tag{6.31}$$

$$z_{i,t,\hat{t},f} \leq y_{i,t,f} \qquad \forall i \geq cr+1, t \in T, \hat{t} \leq t, f \in F \tag{6.32}$$

$$z_{i,t,\hat{t},f} \leq x^{REFRAC} \qquad \forall i = cr+1, t \in T, \hat{t} = t_1, f \in F \tag{6.33}$$

$$z_{i,t,\hat{t},f} \leq x_{i,\hat{t},f} \qquad \forall i \geq cr+1, t \in T, 1 < \hat{t} \leq t, f \in F \tag{6.34}$$

If the optimization concludes that a well restimulation is not justified here-and-now, then $x^{REFRAC} = 0$ and by Eq. (6.27) $y_{cr,t1,f} = 1$. This means that the well's "current refracturing state" cr does not change in time period $t1$. In fact, the well will remain in the refracturing state cr until an additional refracture treatment $cr+1$ is proposed as a recourse action in a future time period. To account for this particular case, we introduce the binary variable $z_{t,f}^{N}$. For as long as no refracture treatment is scheduled, this variable will be set to one according to Eq. (6.35).

$$\sum_{i \geq cr+1} \sum_{\hat{t}=1}^{t} z_{i,t,\hat{t},f} + z_{t,f}^{N} = 1 \qquad \forall t \in T,\, f \in F \tag{6.35}$$

We note that Eq. (6.35) ensures that $z_{t,f}^{N} = 0$ whenever a recompletion $i = cr + 1$ is performed, since the corresponding variable $z_{i,t,\hat{t},f}$ will automatically take value one. Finally, we determine the well's production in time period t for price forecast scenario f by Eq. (6.36).

$$P_{t,f} = \sum_{i > cr} \sum_{\hat{t}=1}^{t} Q_{i,t,\hat{t}} \cdot z_{i,t,\hat{t},f} + Q_{t}^{N} \cdot z_{t,f}^{N} \qquad \forall t \in T,\, f \in F \tag{6.36}$$

Similar to the well development planning model, the gas production in time period t depends on the "refracturing state" of the well at that time, which in general is determined by the variable $z_{i,t,\hat{t},f}$. This decision variable is multiplied by the parameter $Q_{i,t,\hat{t}}$, capturing the anticipated production of the well in time period t considering that it was last refractured for the *i*- th time in time period $\hat{t}$. However, in this refracturing planning model we introduce an additional term into this key constraint. If no further refracture treatment is scheduled during the first t time periods of the current planning horizon, and therefore $z_{i,t,\hat{t},f} = 0$, then the production is given by the parameter Q_{t}^{N}. This parameter reflects the default production of the well without any restimulations. For the refracturing planning problem we also rely on a slightly modified objective function as seen in Eq. (6.37).

$$\max ENPV = \underbrace{-RC \cdot x^{REFRAC}}_{\substack{\text{Stage 1 decision (here-and-now):} \\ \text{Refracture the well now: yes or no?}}} + \underbrace{\sum_{f \in F} \pi_f \sum_{t \in T} (1+d)^{-t} \cdot \left\{ P_{t,f} \cdot gp_{t,f} - rc_i \cdot \sum_{i > cr} x_{i,t,f} \right\}}_{\substack{\text{Stage 2 decisions (wait-and-see):} \\ \text{Restimulate the well later: yes or no? when? how often? (scenario-dependent)}}} \tag{6.37}$$

6.8 Moving Horizon Framework

For clarification purposes, we contrast moving and rolling horizon strategies since these expressions are sometimes used interchangeably by different authors. By moving horizon we mean that a fixed-length planning horizon is periodically moved forward in time, and the corresponding optimization problem is re-solved based on updated input data. We refer to Fig. 6.3 for a graphic illustration of the moving horizon concept. A rolling horizon approach, on the other hand, is often presented as a decomposition technique for planning and scheduling problems (Zamarripa et al., 2016), in which the entire time horizon is divided into two blocks: a detailed time block and a subsequent aggregate time block.

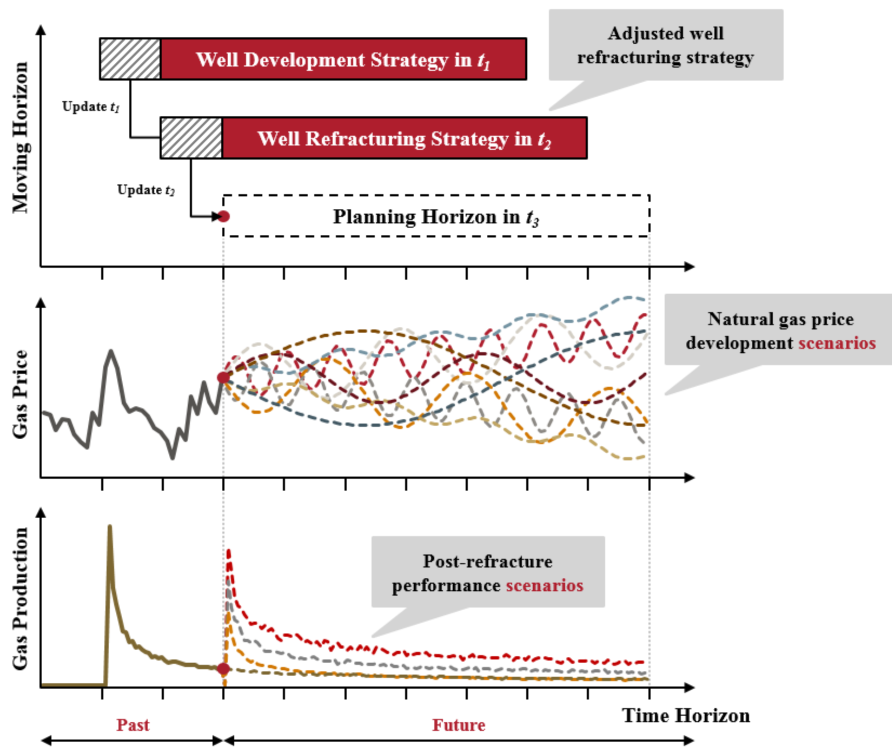

Fig. 6.3: Visualization of the two-stage stochastic programming models for well development and refracturing planning embedded in a moving horizon strategy

In this work, we propose a moving horizon strategy as shown in Fig. 6.3 to address the integrated well development and refracturing planning problem. At each step of this moving horizon strategy, we solve one of the two stochastic programming models presented in the previous sections. The overall algorithm is illustrated in Fig. 6.4. Which of the two models is used depends on the current stage of the well development plan. At the beginning of the planning horizon (current time $ct = t_1$), the well is considered to be in a "ready-for-drilling" state. At this point in time, the well development planning problem is solved considering endogenous and exogenous uncertainties. The key here-and-now model decision is whether or not to drill the shale well (represented by the binary variable w^{DRILL}). If w^{DRILL} is zero, stating that the well is <u>not</u> to be drilled at the present time, then the planning horizon moves forward *fwd* periods (typically one year) and the model is solved again at $t = ct + fwd$, at which point revised uncertainty scenarios can be incorporated. If instead the decision is to drill the well ($w^{DRILL} = 1$), then the planning horizon also moves forward *fwd* periods, but the problem at hand changes conceptually. Now, the well has actually been drilled, fractured and completed. The drilling time (*dt*) is recorded and its current state (*cr*) changes to i_o. Thereafter, the first gas production peak is observed. Moreover, after some time of continuous production, we are able to determine which of the well performance scenarios $p \in P$ has actually realized; we say that the "production estimate scenario" is revealed. In the next step, given that the actual performance of the shale gas well is now known, and after updating the gas price forecast scenarios, the refracturing planning problem is solved (only considering exogenous price uncertainty).

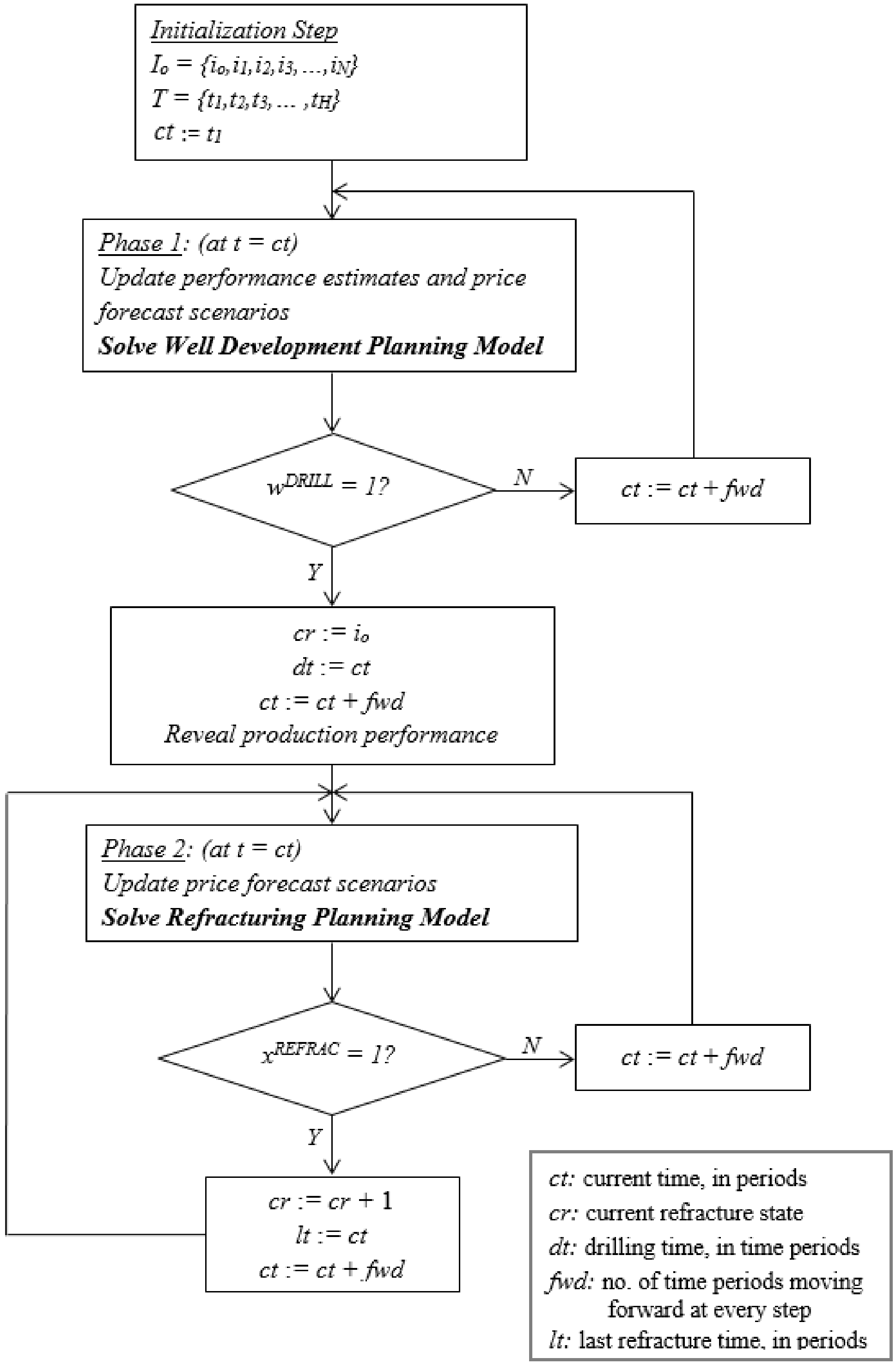

Fig. 6.4: Algorithm for embedding the proposed two-stage stochastic programming models for well development and refracturing planning in a moving horizon strategy

The problem now enters the second phase: deciding on recourse actions. The new key here-and-now decision is whether or not to refracture the well (denoted by the binary x^{REFRAC}). Note that the well is currently producing, and a restimulation will temporarily reduce production flow to zero. If the model proposes not to refracture the well at this time, then the well continues to produce, the planning horizon is moved forward *fwd* periods, and the potential recourse action (a restimulation) is evaluated once again at $t = ct + fwd$, under revised price scenarios. If, however, the decision is made to refracture ($x^{REFRAC} = 1$) then the refracturing time (lt) is registered, and a new production peak is induced. The magnitude of the peak and the production decline that follows depend on the age and the performance of the well. We assume that both of them are known data for the recourse model. The refracture state of the well changes to $cr = i_1$, the planning horizon moves forward once again, and the refracturing planning model is re-solved to determine if a further restimulation would be economically attractive, considering continuously revised price forecast scenarios.

We note that the proposed algorithm compares to the work by Cui & Engell (2010), who propose a moving horizon strategy based on a two-stage stochastic mixed-integer linear programming for multi-period, medium-term planning of a multiproduct batch plant considering uncertainty in terms of demand, plant capacity and product yields. However, in their work the authors do not consider endogenous uncertainty as part of the planning problem.

It is important to acknowledge some of the proposed framework's shortcomings, as well as some of its advantages. For instance, at every iterative step in the proposed algorithm in Fig. 6.4 the optimization assumes that upon the implementation of the here-and-now decisions, the considered price uncertainty realizes instantaneously over the entire remaining planning horizon. Practically speaking, this is obviously not the case. Hence, in the scheme in Fig. 6.4 we move the planning horizon up one time increment periodically and re-solve the problem in light of the uncertainty realization and under consideration of updated price forecasts (once again giving rise to a stochastic program). Yet, this sequential realization of uncertainty is not directly captured “a priori” at every step of the algorithm.

Other optimization frameworks, such as multi-stage stochastic programming, explicitly account for this sequence of here-and-now decisions, uncertainty realizations and recourse actions at specific, future points in time or “stages” (Apap & Grossmann, 2016). Hence, multi-stage stochastic programming is clearly a more rigorous and accurate representation of the decision-making process over extended periods of time. At the same time, it is well-known that multi-stage stochastic programming leads to significantly larger models that quickly become computationally intractable. Therefore, we advocate the proposed strategy of embedding two-stage stochastic programs in moving horizon approaches as a practical optimization framework for problems involving exogenous and endogenous uncertainty to bridge the existing gap between deterministic programming and multi-stage stochastic programming.

6.9 Case Study

In order to demonstrate how the proposed optimization framework can support upstream operators in deciding whether or not to drill and refracture shale wells, we present and discuss a comprehensive well development and refracturing planning case study. For this purpose, we assume that an operator has identified a prospective location to drill, fracture and complete a single shale gas well. The initial well development is assumed to cost \$3,000,000. Every potential restimulation of the well can be performed for \$700,000. The planning problem at hand is complicated by the fact that commodity prices are subject to significant fluctuations. For this reason, the operator wishes to consider a total of nine different, equally probable price development scenarios, all of which are defined by the operator's business development strategy. In considering all nine scenarios, the intention is to hedge against the risk of price uncertainty.

It is assumed that, once turned in-line, the prospective well could potentially be refractured up to five times over its expected lifespan of 20 years. However, we expect the operator's experience with shale well restimulations to be fairly limited – which is presently true for many oil & gas companies. As long as the prospective well has not actually been drilled yet, implying that access to subsurface geological data is very limited, it is difficult to anticipate the well's production. Hence, we explicitly consider well performance uncertainty in this case study to account for the possibility that the expected production performance of the well is under- or overestimated. In this case study a total of three different, equally probable production scenarios are considered ("low", "avg", "hgh"), determined by completions design engineers, geologists, or reservoir engineers based on production data of neighboring wells. However, it is assumed that once the well has been drilled and completed, the operator can refine the production forecast to the point where it becomes deterministic. Therefore, the case study at hand represents a well development and refracturing planning problem under exogenous price uncertainty and endogenous production uncertainty. Given a 10 year planning horizon, discretized by months, the operator wishes to maximize the expected net present value of the proposed project. In order to address the described problem, we rely on the proposed two-stage stochastic programming models and embed them in a moving horizon strategy based on annual re-evaluations.

Initially, in the first year of this case study, we assume that the market is operating in a low-to-moderate price environment as illustrated in Fig. 6.5. Natural gas is selling for $ 3.3 /Mscf. Future price uncertainty is captured by the aforementioned nine price scenarios defining a “cone of uncertainty” based on positive, null and negative price trends with underlying cyclic fluctuations. At this point in time, the key question that the operator faces is whether or not to drill the prospective shale well. The proposed MILP model for the well development planning problem involves 19,441 binary variables, 131,059 continuous variables and a total of 413,317 constraints. Using CPLEX 24.7.3 on an Intel i7, 2.93 Ghz machine with 8 GB RAM, the problem solves in 59 seconds. The optimization converges to the “zero-solution” (NPV= $0), indicating that it does not make economic sense to drill the prospective well at the present time despite the consideration of possible future refracture treatments. The assumed price environment does not allow for economic well development. As a result of this analysis, the operator would refrain from developing the prospective well at this time and pursue alternative, more promising investment opportunities.

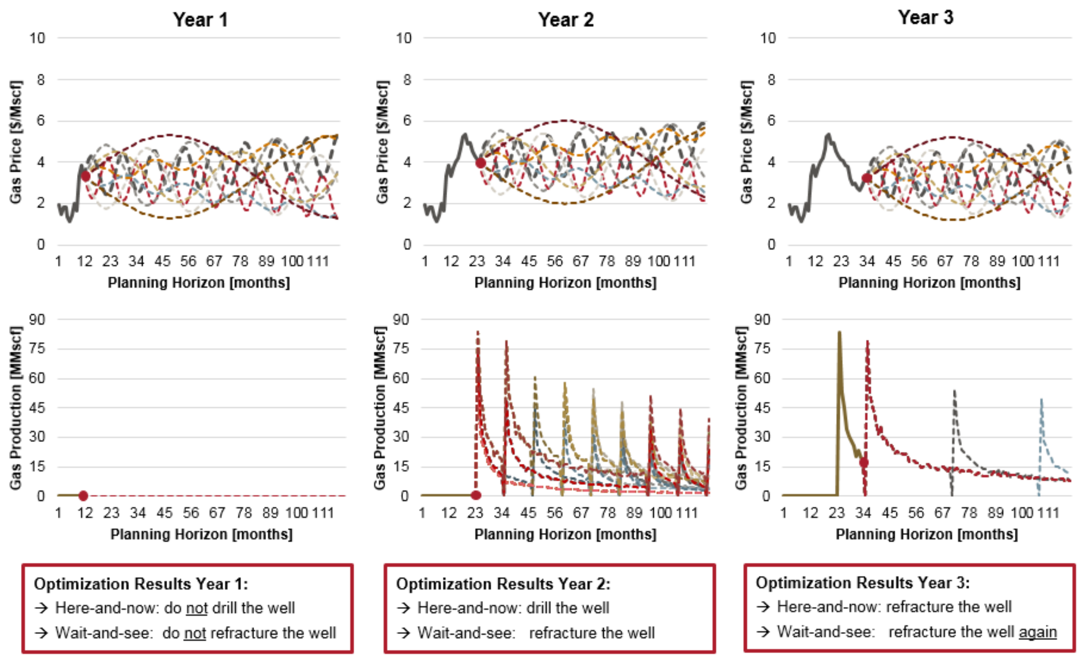

Fig. 6.5: Case study results for years 1-3 based on the assumption that by year 3 the well's production performance is revealed to be "high" according to the respective scenario

In the spirit of the moving horizon strategy, we fast-forward into year 2 of the case study (*fwd* = 12 months in Fig. 6.4). The prospective well is once again considered for development. We assume that in the meantime the natural gas price has climbed to $ 4.0 /Mscf as shown in Fig. 6.5. The well development planning model is re-applied to the problem at hand. Although the problem size is identical, it now takes 269 seconds to solve the problem to zero relative optimality gap on the same machine as before. In light of the elevated price environment, the optimization concludes that it does make sense to drill, fracture and complete the prospective well here-and-now. The expected NPV for the well development project is $195,482. At this point in the case study, the decision-maker and the optimization are still unaware of the well's true production performance over time. Either of the three performance scenarios ("low", "avg", "hgh") could potentially realize. However, the optimization rigorously evaluates all three well performance scenarios (and all nine price performance scenarios), and proposes a well development strategy for each possible realization. Upon closer inspection the results reveal that refracturing of the well is proposed in nearly all scenarios, although the timing of the restimulations varies significantly. If the performance of the well is found to be average or high, the model suggests to refracture early into the well's lifespan – almost regardless of which price scenario realizes. If, however, the well's performance turns out to be low, then the restimulations tend to be scheduled later in life, and oftentimes selectively for elevated price development scenarios. The results also show that multiple recompletions of the well (up to five times) are proposed for some scenario combinations. In the context of this case study, we assume that the decision-maker indeed agrees to drill and complete the prospective well.

Once more we fast-forward a year; now into year 3 of the case study. The well is assumed to have actively produced for the past twelve months. In addition to early production readings, the operator has also gathered sufficient reservoir data to refine the well's performance forecast. For the purpose of this case study we therefore assume that the production performance can now be classified as "high", according to the respective scenario. This marks the realization of the endogenous well performance uncertainty. The following, detailed analysis is based on this particular realization. However, Table 6.1 summarizes here-and-now decisions based on the moving horizon strategy for all possible well performance realizations.

Well performance realization	Year 3 (3.2 $/Mscf)	Year 4 (2.1 $/Mscf)	Year 5 (4.0 $/Mscf)	Year 6 (6.9 $/Mscf)
"LOW"	do not refracture	do not refracture	do not refracture	refracture (first time)
"AVG"	refracture (first time)	do not refracture	do not refracture	do not refracture
"HGH"	refracture (first time)	do not refracture	do not refracture	refracture (second time)

Table 6.1: Optimization results for here-and-now decisions for all three considered well performance scenario realizations in consecutive years of the case study

In year 3 of the case study, the natural gas price has decreased to $ 3.2 /Mscf. Since the well is actively producing at this point, we now rely on the proposed refracturing planning model for decision-support. As outlined earlier, this model no longer considers well performance uncertainty, but it does account for price forecast uncertainty. For the problem at hand, this model involves 541 binary variables, 44,767 continuous variables and 45,308 constraints. Using the same machine and solver as before, it takes 44 seconds to solve the problem to optimality. Under the current conditions, the optimization proposes to refracture the well here-and-now for the first time. Moreover, the results suggest that given the set of considered price development scenarios, additional well restimulations will be justified over time as shown in Fig. 6.5. The expected NPV for the proposed refracturing strategy is $ 2,927,232. It should be noted that the expected NPV is significantly higher in year 3 than in year 2 due to the realization of the well production uncertainty according to the "high" performance scenario. As before, we assume that the operator chooses to implement the proposed here-and-now decision, which results in the well being restimulated in year 3.

By year 4 of the case study the natural gas price has decreased further, down to $ 2.1 /Mscf as shown in Fig. 6.6. Re-applying the refracturing planning model reveals that the well should not be refractured at the present time under these circumstances. In light of the depressed price environment, the expected NPV diminishes to $ 1,756,846. Yet, the solution indicates that future restimulations can improve the economics of the well development project for selected price development scenarios. Year 5 is characterized by an increase in gas price to $ 4.0 /Mscf (Fig. 6.6). Interestingly however, the optimization does not propose to refracture the well at this time despite the higher price environment. It appears that the increase in expected revenues after the well reinvigoration does not outweigh the restimulation costs at this time. The improved expected NPV of $ 2,829,758 does show though, that the well development project clearly benefits from the recent price increase.

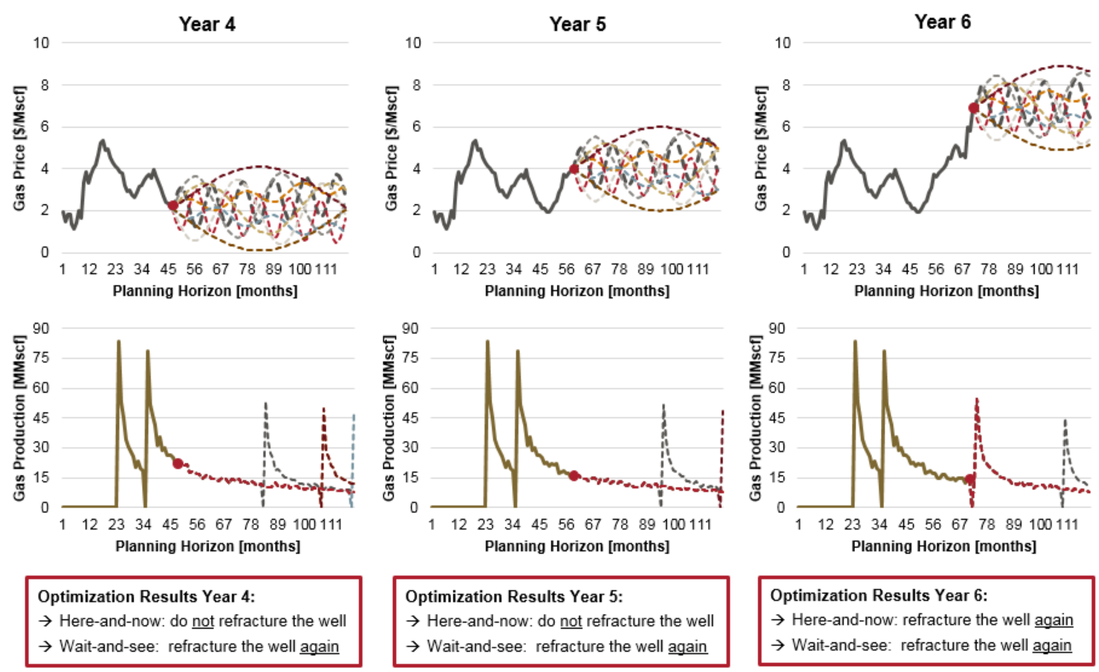

Fig. 6.6: Case study results for years 4-6

One last time, we fast-forward into year 6 of the case study and assume that the natural gas price has spiked to $ 6.9 /Mscf as illustrated in Fig. 6.6. Under these circumstances the optimization proposes to refracture the well <u>a second time</u> here-and-now, and it recognizes scenario-dependent opportunities for additional restimulations. If implemented, the suggested restimulation strategy leads to an expected NPV of $ 4,759,961. Although the analysis could be continued for several more years, we conclude our case study at this point. By year 6 of this case study we find that refracturing increases gas recovery from 805 MMscf (without refracturing) to 1,243 MMscf (with two refractures) and the profitability of the well development project is improved from -$ 173,311 (without refracturing) to $ 1,366,314 (with refracturing) over the first six years. This clearly indicates the potential of well restimulations for unconventional wells. More importantly, the analysis demonstrates that the proposed optimization framework can be used effectively to address the well development and refracturing planning problem under exogenous price uncertainty and endogenous well performance uncertainty.

6.10 General Recommendation for Refracturing Shale Wells

In this section we discuss general recommendations for refracturing shale wells motivated by the results of the case study presented in the previous section. First, if a recompletion is believed to be effective, then refracturing is promising early into the life of a shale well even when commodity prices are relatively low. The reasoning behind this is that early, effective well restimulations have a lasting impact on gas production over time. They alter the overall decline curve favorably, and thereby increase the expected ultimate recovery (EUR) significantly. Hence, economics greatly benefit from these early workovers even in low-price environments. In fact, King (2015) also argues that refracturing within the first two years of production may provide significant economic benefits, especially during periods of downturns in oil and gas prices when drilling budgets are oftentimes reduced.

Secondly, as wells mature, refracture treatments should only be performed: a) in elevated price environments, or b) in direct response to projected price peaks. The reasoning here is as follows: the longer a shale well has already been producing, the less effective and impactful a recompletion is typically expected to be. This practical observation is also reflected in the previously introduced generalized production estimate function. What this implies is that, assuming the cost of refracturing a well remains the same, the potential "return on investment" of a well restimulation generally diminishes over time.

In order to substantiate the above claims, we analyze a particular solution of the previously presented case study in more detail. In year 2 of the case study the situation is as follows: given is a prospective shale well. The decision has not yet been made whether, at the present time, this well should be drilled or not. The decision-maker faces price uncertainty and well performance uncertainty. The respective optimization problem is solved and reveals that, at the present time, well development does make economic sense. At the same time, the optimization specifies scenario-dependent refracturing strategies for every scenario combination of price and performance uncertainty. Here we examine the solution for one particular price forecast scenario in detail. As Fig. 6.7 shows, the optimization proposes to drill the well here-and-now, despite the fact that its true production performance is uncertain; it could turn out to be either "low", "average" or "high". For each of these possibilities the optimization proposes a refracturing strategy that would maximize economics, given the particular price forecast scenario.

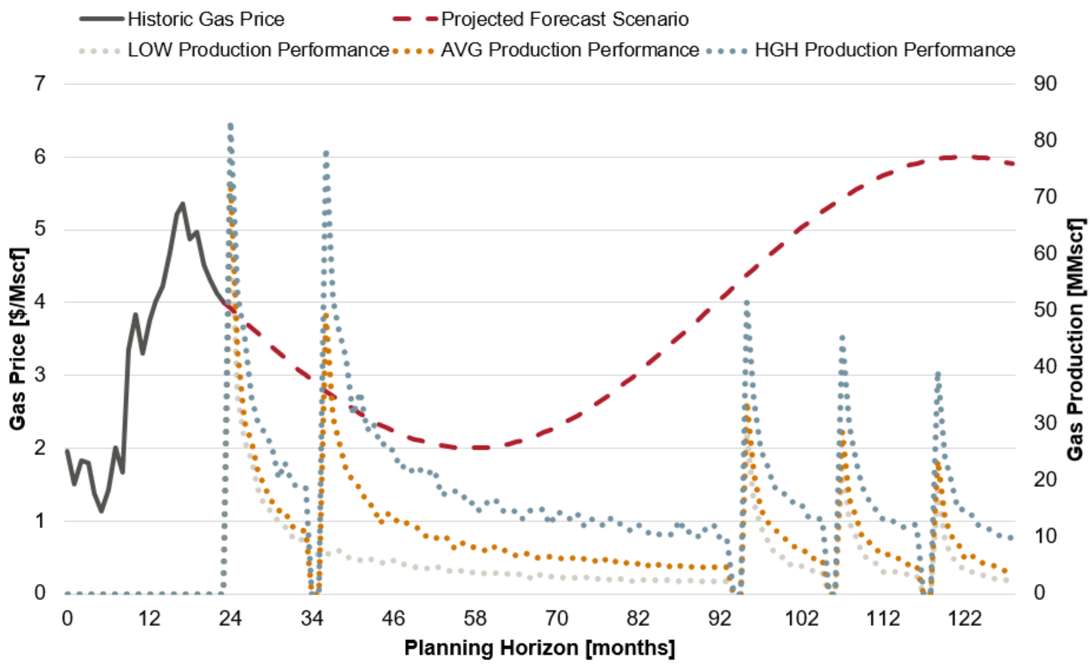

Fig. 6.7: Optimization results for year 2 of the case study given one particular price forecast scenario and all three well performance scenarios

Interestingly, for the "average" and "high" performance scenarios, the optimization proposes to refracture the well just one year after turning it in-line, even though the price is expected to decrease significantly. However, if the well's production performance turns out to be "low", then it is suggested not to recomplete. This confirms the previously stated recommendation that early refracture treatments can be justified even in low-price environments.

The results in Fig. 6.7 also show a clear trend for late-life refracture treatments. As prices are forecasted to increase, the optimization proposes to exploit the projected price peak by scheduling multiple well restimulations. This trend holds true regardless of which well performance scenario realizes. It confirms that the timing of the late-life recompletions is very sensitive to the price environment at the time.

6.11 Field-Wide Shale Development Planning Considering Refracturing Opportunities

The presented results raise the question how the proposed optimization framework could be used for field-wide shale development planning, rather than merely being applied to a single, prospective well. Given a set of prospective locations for developing new wells and a set of mature, actively producing wells, an upstream operator may have to decide how many new wells to drill, fracture and complete and/or whether existing wells should be restimulated instead. The proposed optimization framework can be embedded in field-wide development planning models such as those proposed by Drouven & Grossmann (2016) or Cafaro & Grossmann (2015). Even though we do not address the field-wide development planning problem explicitly in this work, we attempt to discuss and evaluate refracturing opportunities within mature shale development areas qualitatively. The motivation for this discussion is that in mature development areas new wells and refracturing opportunities will compete against one another; especially in light of limited resources such as development capital, fracturing crews or drilling rigs.

Conceptually, refracturing provides operators with a number of promising opportunities. For instance, Drouven & Grossmann (2016) find that the equipment utilization in shale gas gatherings systems is often poor due to the characteristically steep decline curves of unconventional wells. Operators tend to size pipelines and compressors such that they can handle the high initial production rates of shale wells.

However, within months after these wells are turned in-line, production declines dramatically and operators are left with oversized and under-utilized pipelines and compressors. To offset volumes lost to decline and to maintain constant production, operators are forced to drill and complete new shale wells in quick succession (Kotov & Freitag, 2015). As Fig. 6.9 illustrates, the impact of these development strategies on rural landscapes can be quite significant. Moreover, for every new well that is drilled an operator needs to install additional gathering equipment such as production units or well lines.

Fig. 6.8: Development of the Jonah natural gas field near Pinedale, Wyoming, illustrates the impact that shale gas development can have on rural landscapes

However, by reinvigorating existing wells through restimulations upstream operators can increase the utilization of gathering pipelines and compressor stations without constantly opening up new wells; in simple terms: refracturing can help operators keep their pipelines and compressors "full". In this way, by drilling fewer new shale wells and “reusing” existing infrastructure, operators can decrease the well count in development areas, lay out fewer gathering pipelines, and thereby reduce the overall surface disruption.

It is also worth mentioning that refracturing an existing well takes far less time than drilling and completing a new well. The process of developing a prospective shale well involves securing additional acreage, applying for permits, relocating and assembling a drilling rig, drilling the vertical and horizontal segments of the well, completing the well and installing production equipment as well as gathering pipelines. From start to finish the entire process may take several months to complete. Refracturing an existing well, on the other hand, can be done within weeks. Considering the recent, dramatic fluctuations in natural gas prices, refracturing could allow upstream operators to very quickly respond to projected price increases by ramping up field-wide production in a short period of time. From this perspective, refracturing conceptually compares to shut-in based production schemes such as those proposed by Knudsen & Foss (2013) and Knudsen et al. (2014).

Even from a water management perspective refracturing makes sense. It is well-known that hydraulic fracturing requires significant volumes of water of up to 20 million liters per well. However, over the lifespan of a shale well up to 50% of the injected water is eventually recovered at the surface again as flowback or produced water. The recovered water is generally contaminated and may not be released back into the environment unless it has undergone extensive (and therefore costly) treatment. Alternatively, operators have two options: a) dispose of the impaired water by injecting it into abandoned wells (which is strictly regulated, very expensive, and known to lead to undesirable seismic activity), or b) reuse the recovered water for future fracturing operations. Given these options, upstream operators have increasingly been reusing impaired water for hydraulic fracturing in an attempt to reduce disposal volumes and avoid costly treatment. For this purpose, however, the recovered water oftentimes needs to be transported from one well pad to another – depending on where the development activity is occurring. Transportation is usually performed with water hauling trucks, which leads to increased truck traffic, road deterioration, the potential for accidents, and added costs. These issues can be mitigated if upstream operators choose to restimulate more of their horizontal wells as part of field-wide development programs. Rather than transporting impaired water across and in between development areas, operators could temporarily store the recovered water on-site and re-use it to refracture other producing wells eventually.

Finally, it is important to note that refracturing is significantly cheaper than drilling and completing new wells. This cost advantage can be of significant importance to smaller, capital-constrained upstream operators, who do not always have access to the financial markets and therefore fresh capital. Instead of being able to drill just one new shale well, refracturing may allow these companies to reinvigorate production at up to six of their assets. By embedding the proposed optimization framework in field-wide development models, these benefits could easily be quantified and may convince operators to increasingly exploit refracturing opportunities in mature development areas.

6.12 Conclusions

In this chapter, we have presented stochastic programming models for optimal shale well development and refracturing planning under exogenous price uncertainty and endogenous well performance uncertainty. The proposed optimization framework is intended to help upstream operators decide: a) if and when a prospective shale well should be drilled and fractured, and b) how often and when the well should be refractured. In our work, we accounted for uncertain price forecasts and uncertain well performance by proposing mixed-integer linear, two-stage stochastic programming models. The endogenous nature of the well performance uncertainty was addressed through a moving horizon strategy into which the proposed models were embedded. As part of a comprehensive case study, we demonstrated how the proposed optimization framework can be used to determine when to drill and/or refracture a shale well in light of price and performance uncertainty. The case study also revealed two interesting observations: a) even if commodity prices are low, it can make economic sense to refracture active shale wells early into their lifespan, and b) late-life refracture treatments only appear justified in elevated price environments or in direct response to projected price peaks. Finally, we concluded our analysis with a qualitative discussion on refracturing opportunities for field-wide shale development planning projects.

6.13 Nomenclature

Sets

$i \in I$	Refracture treatments
$f \in F$	Price forecast scenarios
$p \in P$	Well performance scenarios
$t \in T$	Time periods

Binary variables

w^{DRILL}	Active if the well is drilled here-and-now (stage one decision variable)
x^{REFRAC}	Active if the well is refractured here-and-now (stage one decision variable)
$x_{i,t,f,p}$	Active if the well is refractured for the *i*-th time in time period t for price forecast scenario f and well performance scenario p
$y_{i,t,f,p}$	Active if in time period *t* the well has been refractured a total of *i* times for price forecast scenario f and well performance scenario p
$z_{i,t,\hat{t},f,p}$	Active if in time period *t* the well has been refractured a total of *i* times and the last refracturing occurred in time period $\hat{t}$ for price forecast scenario f and well performance scenario p
$z_{t,f}^{N}$	Active if in time period t the producing well has <u>not</u> been refractured for price forecast scenario f

Continuous variables

$P_{t,f,p}$ Gas production of the shale gas well in time period t for price forecast scenario f and well performance scenario p

Parameters

$a_{i,p}$ Production decline after i well restimulations for well performance scenario p

$b_{i,p}$ Post-refracturing decline after i well restimulations for well performance scenario p

$\beta_{i,p}$ Peak reduction factor after i well restimulations for well performance scenario p

cr Current refracturing state of the shale well

ct Current time period

d Discount rate

dt Drilling time period

DC Drilling cost

CC Completions cost

RC Refracturing cost

φ_p Realization probability for well performance scenario p

fwd Number of periods the planning horizon moves forward at every iteration

$gp_{t,f}$ Gas price in time period t for price forecast scenario f

$\tilde{\gamma}_{i,p}$ Original fracture contribution after i restimulations for well performance scenario p

k_p	Initial production peak for well performance scenario p
lt	Last refracture time period
π_f	Realization probability for price forecast scenario f
$r_{i,\hat{t},p}$	Supplemental production peak after i well restimulations when the last one occurred in time period $\hat{t}$
rc_i	Cost of i-th well restimulation
rt	Duration of refracture treatment
$Q_{i,t,\hat{t},p}$	Shale gas well production in time period t given that it has been refractured i times, and the last restimulation was performed in time period $\hat{t} \le t$ for well performance scenario p

CHAPTER 7

Conclusions

In this thesis, we have proposed a suite of mixed-integer programming models for various aspects of the general shale gas development problem. The main topics we addressed were: a) strategic, quality-sensitive shale gas development planning in chapter 2, b) impaired water management in active development areas in chapter 3, c) line pressure optimization in gas gathering systems in chapter 4, and d) planning refracture treatments for individual shale wells considering deterministic data in chapter 5 and accounting for uncertain price forecasts/well performance in chapter 6. In the following sections, we summarize the major findings of this thesis and we provide a critical review of our work.

7.1 Quality-Sensitive Shale Gas Development Planning

In chapter 2, we proposed a multi-period MINLP model to address the quality-sensitive shale gas development planning problem. This model is meant to help shale gas producers make a number of important development decisions, such as: a) where, when and how many shale wells to drill, b) where to install pipelines and compressor stations, c) how much gathering capacity to provide, and d) which delivery agreements to arrange with midstream processing companies.

Within the proposed optimization framework we explicitly considered the fact that the quality of the produced gas oftentimes varies within development areas. This can lead to serious operational challenges since upstream operators are responsible for meeting strict downstream gas quality specifications when delivering their product to the market. Our model is aimed at either: a) identifying blending strategies that avoid or minimize the need for purifying produced gas, or b) determining which processing agreements are most suitable for a selected development area.

Since the consideration of spatial gas composition variations lead to nonlinear and nonconvex model constraints, we developed a tailored solution strategy specifically for the quality-sensitive shale gas development planning problem. The solution strategy relies on an efficient initialization of the MINLP based on an approximation of the true problem, and on identifying tight bounds for all nonlinear decision variables. Yet, we emphasized that the proposed solution strategy does not necessarily guarantee convergence to the global optimum, and therefore it is possible to get trapped in suboptimal solutions. However, we demonstrated that the algorithm is capable of identifying near-global solutions to large-scale, practical problems (e.g. 59,680 binary variables, 21,707 continuous variables, 56,859 constraints and 1,008 bilinear terms) within reasonable solutions times (less than four hours).

The application of our optimization framework to two real-world case studies revealed intriguing findings. Most importantly, we verified that return-to-pad strategies, i.e., the delay of selected drilling and fracturing operations, are the key to cost-effective shale gas development strategies. Previously, return-to-pad situations were perceived as an undesirable, oftentimes unintentional "side-effect" of shale gas development that occurred whenever development operations were not properly coordinated. For the longest time the "development philosophy" of the shale industry was to simply drill as many wells as possible and turn them in-line as quickly as possible. Instead, we found that intentionally splitting the development of a pad is an ideal countermeasure against the characteristically steep decline curves of shale wells. By stacking completions jobs, one can install significantly smaller gathering equipment, maximize the utilization of pipeline systems, and ultimately improve the economics of development projects by millions of dollars. To support this claim, we performed a rigorous lookback-analysis with one shale gas producer in the Appalachian Basin and found that an optimized development strategy could have improved their profitability in one area by 133 million dollars.

7.2 Impaired Water Management in Shale Gas Development Areas

In chapter 3, we presented a multiperiod MILP for impaired water management in shale gas development areas. This model is designed to address three important issues: a) the sequencing of fracturing jobs and the corresponding completions water demand, b) the coordination of freshwater and impaired water deliveries, and c) the selection and sizing of on-site water storage solutions. Although the objective function of the model is to maximize the NPV of a development project, we primarily evaluated how water management costs could be reduced effectively. In particular, we investigated three opportunities for cost savings: a) rearranging the fracturing schedule by implementing return-to-pad operations, b) using 100% impaired water for individual fracturing jobs, and c) installing limited-capacity, temporary above-ground storage tanks on-site.

We applied the water management optimization model to a real-world case study using actual data from a shale gas producer in the Appalachian Basin. For a problem considering 9 well pads, a total of 29 completions jobs and a one year planning horizon, discretized by weeks, the corresponding MILP involved 5,304 binary variables, 31,253 continuous variables and 10,278 constraints. The optimal solution was obtained in less than 1.5 hours and allowed for a number of interesting discoveries. First, the results suggested that the optimization is primarily aiming to minimize water expenses. Rather than turning all 29 prospective wells in-line as quickly as possible and generating early gas sales revenues (which would be an entirely feasible and intuitive solution at first sight), the optimization positively leveraged the possibility of implementing return-to-pad operations to maximize impaired water reuse. In other words, we found supporting evidence that the fracturing schedule should be driven by water operations – and not the other way around, which is still common in industry.

The case study also revealed that impaired water storage capacity – provided either by permanent pits or temporary tanks – is crucial for cost-effective water management. Lastly, our findings confirmed that companies should make every effort possible to reduce impaired water disposal in order to improve the economics of their operation. In the presented case study, the optimization managed to reduce potential freshwater consumption by nearly 2.75 million barrels of water (87 million gallons) by reusing available impaired water in the development area. Altogether, less than 7,500 barrels of water had to be disposed of over a one year planning horizon. This corresponds to an effective disposal rate of 0.3% which is a significant improvement compared to the current industry standard of 10-30%.

7.3 Line Pressure Optimization in Shale Gas Gathering Systems

In chapter 4, we developed a multiperiod MINLP model for line pressure optimization specifically in shale gas gathering systems. Given an existing gas gathering network consisting of well pads, pipelines and compressor stations, this model can be used to coordinate the following decisions: a) the timing of when prospective wells are turned in-line, b) which pressure profile to establish within a gathering system, and c) how much compression power to provide at every point in time. The motivation for this work is that upstream operators often struggle with line pressure management in their gathering systems. On the one hand, it is well-known that as the line pressure within a pipeline network is raised or lowered, the production within that development area collectively decreases or increases respectively. Therefore, producers typically strive to operate their systems at low line pressures, hoping to "squeeze" as much gas as possible out of their assets. However, whenever operators bring new wells online, the line pressure in their gathering systems increases significantly, which has a negative effect on the production output of mature wells. This cause-and-effect relationship is known as the *backoff effect* and it presents a major challenge to practitioners.

The model we proposed is designed around three fundamental building blocks (all of which are nonlinear and nonconvex): a) a simplified reservoir model, b) a pressure drop model, and c) a compression model. Binary variables are introduced to determine when exactly prospective wells should be turned in-line. Since the resulting nonconvex MINLP is challenging to solve with commercial MINLP solvers, we developed a tailored solution strategy specifically designed for the line pressure optimization problem. This strategy is based on the following two steps: a) solving an approximation of the real problem by only considering existing wells (yielding a good initial solution), and b) performing a rigorous pressure bound analysis (yielding tight pressure bounds). Both, the initial solution and the pressure bounds, can be used to effectively solve the line pressure optimization problem with commercial MINLP solvers. The proposed solution strategy is not designed or guaranteed to converge to the global optimum. However, in our experience it yields near-global solutions to practically relevant problems within very reasonable solution times.

We applied the proposed model and solution strategy to a real-world line pressure optimization problem in the Appalachian Basin using actual data. Our case study was set up for a 26 week planning horizon, a gathering system containing 4 well pads, 21 existent wells, 14 prospective wells, a mature pipeline network and a single compressor station. The corresponding MINLP involved 728 binary variables, 4,499 continuous variables, 6,530 constraints and was solved in 2.5 hours. Conceptually, we found that preventive line pressure manipulations can mitigate backoff effects associated with bringing new wells online. By intentionally raising the line pressure prior to the onset of new production volumes, system backoff can be minimized. This is an important finding since it suggests that upstream operators can take an active role in preparing and "readying" their gathering systems for development operations through effective line pressure management.

7.4 Planning of Shale Gas Well Refracture Treatments

In chapters 5 and 6, we proposed multiperiod MILP models to plan refracture treatments for shale gas wells. This work was motivated by the fact that refracturing is a promising option for addressing the characteristically steep decline curves of shale wells. By restimulating the shale reservoir, operators can extract previously unrecovered hydrocarbons and reinvigorate their wells. One of the remaining key challenges to successful refracturing is the precise timing of well restimulations – especially with respect to projected natural gas price developments.

In order to address this problem, we developed an optimization framework for refracturing planning in chapter 5. Our models are based on a novel production forecast function which is capable of estimating the pre- and post-refracture well performance of a given shale well. We embedded this forecast function in different model formulations to evaluate their computational performance. Ultimately, we found that a discrete-time, multi-period MILP derived from a disjunctive model formulation performed best computationally. This model allowed us to solve the deterministic refracturing planning problem efficiently within seconds. From applying the proposed optimization framework to several case studies with different underlying price developments, we learned three things: a) shale well restimulations have the potential to increase the ultimate gas recovery by up to 25%, b) refracturing can improve the profitability of individual wells by several hundred thousand dollars, and c) under certain circumstances it can make economic sense to refracture shale wells multiple times over their expected lifespan.

In chapter 6, we extended the deterministic refracturing planning model formulation to account for two major sources of uncertainty: price forecasts and expected well performance. Moreover, we drew attention to the fact that price uncertainty can be classified as exogenous, whereas well performance uncertainty is endogenous in nature. Once a decision-maker drills and completes a shale well, its performance before and after any refracture treatment can be forecasted relatively accurately. Hence, we categorized this uncertainty as endogenous. Price uncertainty, on the other hand, is exogenous since commodity prices realize regardless of which decisions individual companies make.

Ultimately, we addressed the refracturing planning problem under uncertainty through a two-stage stochastic programming model. The stage one, here-and-now decision is concerned with whether a prospective shale well should be drilled at the present time, whereas the second stage captures scenario-dependent, wait-and-see recourse actions in terms of future well restimulations. The stochastic programming model itself was embedded in a moving horizon framework to account for the endogenous nature of the well performance uncertainty. The results of our case study in this chapter allowed for two practical insights. First, refracturing recently completed shale wells can make economic sense even in low-price environments due to the lasting impact on production. Second, restimulations of mature wells are only justified if either a) prices are elevated, or b) price peaks are imminent. Otherwise, late-life refracture treatments are unlikely to improve the economics of well development projects.

7.5 Contributions of the Thesis

The main contributions of this thesis are summarized below:

1. A multiperiod MINLP model was proposed for addressing the long-term, quality-sensitive shale gas development planning problem. The problem involves where, when, and how many shale wells to drill, where to lay out pipelines, and how much compression power to provide. The framework explicitly considers a) gas quality variations within active development areas, and b) the arrangement of complex gas delivery agreements between upstream operators and midstream processors.
2. Since the aforementioned large-scale, nonconvex MINLP models are difficult to solve with existing MINLP solvers, a tailored solution strategy was developed for the strategic development planning problem. By solving an approximation of the full

problem, the solution strategy increases the likelihood of converging to near-global solutions within reasonable solution times.

3. As part of a rigorous lookback analysis the proposed optimization framework for strategic development planning was applied to an actual gathering system operated by one of the largest shale gas producers in the Appalachian Basin. The results demonstrated significant economic potential for optimization in this domain: the NPV of the company's development strategy in one particular area could be increased by over $133 million. Furthermore, the results proved that *return-to-pad operations* are the key to cost-effective shale gas development.
4. A multiperiod MILP model was developed for impaired water management in active shale gas development areas. The model determines the optimal fracturing schedule, the coordination of water deliveries and the selection of appropriate water storage solutions such that water management costs are minimized without compromising revenues from gas sales.
5. The proposed MILP model was applied to a real-world problem based on actual data from a shale gas producer in the Appalachian Basin. The results indicated that water management based on rigorous optimization could a) drastically reduce freshwater consumption by nearly 2.75 million barrels of water (87 million gallons) in one area in just one year, and b) curtail water disposal rates from an industry average of 10-30% to merely 0.3%.
6. A multiperiod MINLP model for line pressure optimization in shale gas gathering systems was developed. The presented model determines when to turn prospective

wells in-line and how to manage line pressure such that production backoff is minimized.

7. As part of a real-world case study the proposed MINLP model was tested using actual data provided from an upstream operator in the Appalachian Basin. The results demonstrated that active line pressure manipulations can successfully mitigate backoff effects associated with turn in-line operations. These insights are expected to improve the profitability of development projects by hundreds of thousands of dollars annually.
8. A set of multiperiod MILP models for refracturing planning were developed. The models determine: a) if a given shale gas well should be refractured, b) when to restimulate the well, and c) how many recompletions to perform over the lifespan of the well.
9. The proposed deterministic refracturing planning model was extended to account for exogenous price uncertainty and endogenous well performance uncertainty. A two-stage stochastic programming model formulation embedded in a moving horizon strategy was presented to plan refracture treatments under uncertainty.
10. The refracturing planning model was applied to a comprehensive case study to demonstrate when to restimulate shale gas wells in practice – particularly in consideration of price and well performance uncertainty. The results suggested that a) refracturing can help upstream operators combat the characteristically steep production decline curves, and b) well restimulations give producers the opportunity to proactively respond to commodity price fluctuations.

Altogether, this thesis has led to the following journal publications and conference articles:

1. Drouven MG, Grossmann, IE. Multi-Period Planning, Design, and Strategic Models for Long-Term, Quality-Sensitive Shale Gas Development. *AIChE Journal*. **2016**. 62(7):2296-2323.
2. Drouven MG, Grossmann IE. Disjunctive Models for Strategic Midstream Delivery Agreements in Shale Gas Development. Proceedings of the 26th *European Symposium on Computer Aided Process Engineering* (ESCAPE), p. 931-936, June 12-16, **2016**, Portorož, Slovenia, Elsevier.
3. Drouven MG, Grossman IE. Optimization Models for Impaired Water Management in Shale Gas Development. *Journal of Petroleum Science and Engineering*. **2017**. Submitted for publication April 2017.
4. Drouven MG, Grossmann IE. Mixed-Integer Programming Models for Line Pressure Optimization in Shale Gas Gathering Systems. *Journal of Petroleum Science and Engineering*. **2017**. To be submitted April 2017.
5. Cafaro DC, Drouven MG, Grossmann IE. Optimization Models for Planning Shale Gas Well Refracture Treatments. *AIChE Journal*. **2016**. 62(12):4297-4307.
6. Drouven MG, Cafaro DC, Grossmann IE. Stochastic Programming Models for Optimal Shale Well Development and Refracturing Planning under Uncertainty. *AIChE Journal*. **2017**. Submitted for publication February 2017.

7.6 Directions for Future Work

In the following sections we summarize selected directions for future work.

7.6.1 Global Optimization Strategies for Quality-Sensitive Shale Gas Development

As outlined previously, the quality-sensitive shale gas development planning problem gives rise to large-scale, nonconvex MINLPs, which are challenging to solve. In fact, although the solution strategy proposed in chapter 2 has proven to perform very well, it does not actually guarantee convergence to the global optimum. Yet, considering the scope and potential impact of this research area, we believe that it would be of great value to practitioners if these problems could rigorously be solved to global optimality. Despite recent advances, it is unlikely that general-purpose MINLP solvers will be able to solve practically relevant development planning problems to global optimality in the near future. These problems quickly become computationally intractable. Hence, we believe that there is an opportunity to develop tailored global optimization strategies. One promising direction would be to explore a possible MILP reformulation of the nonconvex MINLP. While it is generally favorable to solve linear programs instead of nonlinear optimization problems, such a reformulation may come at the expense of adding a very large number of binary variables and constraints to the problem.

7.6.2 Quality-Sensitive Impaired Water Management

The multiperiod MILP model presented in chapter 3 distinguishes between just two water qualities, namely freshwater and impaired water. This distinction is accurate from a regulatory perspective and it is common in industry. Yet, in practice the concentration of total dissolved solids (TDS) in the impaired water – which is the prevalent measure for the "degree of water contamination" – actually varies spatially and temporally within active development areas. According to a recent expert elicitation conducted by Mauter & Palmer (2014), upstream operators currently do not believe that water quality, and high TDS in particular, represent a barrier to reusing impaired water for fracturing purposes. However, it is possible that this view will change. The shale gas industry as a whole is increasingly reusing impaired water to minimize freshwater consumption, and as a result it is likely that the average TDS concentration will increase significantly over time. Therefore, we believe that it would be interesting to extend the proposed MILP model to account for the quality of the impaired water, and possible water treatment solutions (e.g. reverse osmosis, membrane distillation). An extended, quality-sensitive model could be used to implement water blending strategies within development areas that prevent TDS concentrations and/or other water quality metrics from exceeding certain thresholds. From a mathematical programming perspective it is likely that such models will give rise to nonlinear and nonconvex problems.

7.6.3 Global Optimization Strategies for Line Pressure Management

In chapter 4 we proposed a nonlinear and nonconvex MINLP model for line pressure optimization in shale gas gathering systems. This model can give rise to suboptimal solutions. The solution strategy we presented does not necessarily guarantee convergence to the global optimum. Therefore, we believe that the investigation and development of global optimization strategies specifically for the line pressure management problem would be a promising direction for future work. The challenge here will consist of obtaining tight underestimators or convex envelopes for: a) the nonconvex shale well reservoir model, b) the nonconvex constraints governing pressure drops along pipeline segments, and c) the nonconvex compression model.

7.6.4 Refracturing Opportunities in Field-Wide Development Planning

In chapters 5 and 6, we proposed mixed-integer programming models for refracturing planning. However, the presented framework was focused on individual shale wells. We believe that it would be interesting to extend this work to consider refracturing opportunities within strategic, field-wide development planning models. In other words, given an active development area containing existing and prospective wells, the optimization could select where it wants to drill entirely new wells, and/or which mature wells it chooses to restimulate. In light of limited resources (drilling rigs, fracturing crews, development budget) upstream operators frequently have to weigh these opposing options and decide how many wells to refracture at the expense of drilling fewer new wells.

7.6.5 Multi-Stage Stochastic Programming for Refracturing Planning

In chapter 6, we presented a two-stage stochastic programming model embedded in a moving horizon framework to address the refracturing planning problem under exogenous price uncertainty and endogenous well performance uncertainty. In the past, optimization problems involving both exogenous and endogenous uncertainties have been addressed primarily through the multi-stage stochastic programming framework (Apap & Grossmann, 2016). On the one hand, this framework represents a more accurate representation of the decision-making process in practice. On the other hand, multi-stage stochastic programs generally lead to large optimization problems that can take very long to solve. Nevertheless, we believe that the refracturing planning problem under exogenous and endogenous uncertainties would make for an interesting application to contrast and compare alternative stochastic programming approaches. In particular, the question is to which extent two-stage stochastic programs embedded in moving horizon strategies can compete with multi-stage stochastic programming in terms of solution accuracy.

7.6.6 Multi-Level Shale Gas Development Planning

In this thesis, we have addressed several detailed topics within the context of shale gas development. In chapter 3, we proposed optimization models for operational impaired water management. In chapter 4, we focused on tactical line pressure optimization in shale gas gathering systems. Finally, in chapters 5 and 6, we presented models for strategic refracturing planning. In practice, the respective decisions within each of these domains are often made separately by individual business units or groups. Hence, we are confident that the proposed models will help practitioners make better and faster decisions within their domains. However, we also believe that there is significant value in coordinating individual and collective efforts in the interest of an organization as a whole. Ideally, the detailed models presented in chapters 3, 4, 5 and 6 could be coupled with the strategic development planning framework proposed in chapter 2. The ultimate goal would be to coordinate strategic, tactical and operational decisions within a multi-level shale gas development planning framework. Since it is likely that any coupled models, or even their mere coordination, will result in extremely large-scale mixed-integer optimization problems, this line of work will require the investigation of effective decomposition strategies.

REFERENCES

Achterberg T. SCIP: solving constraint integer programs. *Mathematical Programming Computation*. **2009**;1(1):1-41.

Allison D, Parker M. Refracturing extends lives of unconventional reservoirs. The *American Oil & Gas Reporter*. **2014**; January Issue.

Anderson S, Anderson D, Edwards K, Epp K, Stalgorova K. Pressure Normalized Decline Curve Analysis for Rate-Controlled Wells. SPE Hydrocarbon Economics and Evaluation Symposium. *Society of Petroleum Engineers*. **2012**.

Apap RM & Grossmann IE. Models and Computational Strategies for Multistage Stochastic Programming under Endogenous and Exogenous Uncertainties. *Computers & Chemical Engineering*. **2016**. DOI: 10.1016/j.compchemeng.2016.11.011.

Baihly J, Altman R, Malpani R, Luo F. Study assesses shale decline rates. *American Oil & Gas Reporter*. **2011**; May Issue.

Bartholomew TV, Mauter MS. Multi-Objective Optimization Model for Minimizing Cost an Environmental Impact in Shale Gas Water and Wastewater Management. *ACS Sustainable Chemistry & Engineering*. **2016**;4(7):3728-3735.

Biegler LT, Grossmann IE, Westerberg AW. Systematic Methods of Chemical Process Design. New Jersey: *Prentice Hall*, **1997**.

Birge JR & Louveaux, F. Introduction to Stochastic Programming. 2nd Edition. New York, *NY: Springer*, **2011**.

Boyan G, Ghalambor A. Natural Gas Engineering Handbook. *Elsevier*. **2014**.

Broderick J, Wood R, Gilbert P, Sharmina M, Anderson K, Footitt A, Glynn S, Nicholls F. Shale gas: an updated assessment of environmental an climate change impacts. A report commissioned by The Co-operative and undertaken by researchers at the Tyndall Centre, *University of Manchester*. **2011**.

Broderick J, Wood R, Gilbert P, Sharmina M, Anderson K, Footitt A, Glynn S, Nicholls F. Shale gas: an updated assessment of environmental an climate change impacts. A report commissioned by The Co-operative and undertaken by researchers at the Tyndall Centre. *University of Manchester*. **2011**.

Cafaro DC, Grossmann IE. Strategic planning, design, and development of the shale gas supply chain network. *AIChE Journal*. **2014**; 60:2122-2142.

Cafaro DC, Drouven MG, Grossmann IE. Optimization Models for Planning Shale Gas Well Refracture Treatments. *AIChE Journal*. **2016**;62(12): 4297-4307.

Carter RG, Rachford Jr HH. Optimizing line-pack management to hedge against future load uncertainty. *Proceedings of the 35th PSIG Annual Meeting*. Bern, Switzerland. **2003**.

Castro PM, Grossmann IE. Generalized disjunctive programming as a systematic modeling framework to derive scheduling formulations. *Industrial & Engineering Chemistry Research*. **2012**; 51:5781-5792.

CME Group, Henry Hub Natural Gas Futures Quotes. 2016; available at: http://www.cmegroup.com/trading/energy/natural-gas/natural-gas.html [last accessed January **2016**].

Cui J & Engell, S. Medium-term planning of a multiproduct batch plant under evolving multi-period multi-uncertainty by means of a moving horizon strategy. *Computers & Chemical Engineering*. **2010**; 34(5):598-619.

Damian N & Murphy B. Oxford Presents Physcial Geology Today: The Dilemma of Fracking. **2015**. http://www.oxfordpresents.com/ms/nance/the-dilemma-of-fracking/ [last accessed December 2016].

Dawson M, Howard P, Salkeld M. Improved Productivity in the Development of Unconventional Gas. *Technical Study for Productivity Alberta*. **2012**. Available at: http://www.csur.com/images/news/2012/productivityalberta.pdf [last accessed September 2015].

De Wolf D. Smeers Y. The gas transmission problem solved by an extension of the simplex algorithm. *Management Science*. **2000**. 46(11):1454-1465.

Dozier G, Elbel J, Fielder E, Hoover R, Lemp S, Reeves S, Siebrits E, Wisler D, Wolhart S. Refracturing works. *Oilfield Review*. **2003**; 10(8):38-53.

Drouven MG, Grossmann IE. Multi-Period Planning, Design and Strategic Models for Long-Term, Quality-Sensitive Shale Gas Development. *AIChE Journal*. **2016**;62(7): 2296-2323.

Duman RJ. Economic viability of shale gas production in the Marcellus shale; indicated by production rates, costs and current natural gas prices. *Michigan Technological University*. **2012**.

Duran MA, Grossmann IE. A Mixed-Integer Nonlinear Programming Algorithm for Process Systems Synthesis. *AIChE Journal*. **1986**;32(4):592-606.

Duran MA, Grossmann IE. An outer-approximation algorithm for a class of mixed-integer nonlinear programs. *Mathematical Programming*. **1986**; 36 (3):307-339.

Eshkalak MO, Aybar U, Sepehrnoori K. An Economic Evaluation on the Re-fracturing Treatment of the U.S. Shale Gas Resources, SPE Eastern Regional Meeting. *Society of Petroleum Engineers*. **2014**.

Fear, B. Refracturing – Coiled Tubing Enables Effective Horizontal Recompletions. *The American Oil & Gas Reporter*. **2016**. February 2016 Editor's Choice.

Folger PF, Tiemann M. Human-Induced Earthquakes from Deep-Well Injection: A Brief Overview. *Congressional Research Service*. **2014**.

Gao J, You, F. Optimal Design and Operations of Supply Chain Networks for Water Management in Shale Gas Production: MILFP Model and Algorithms for the Water-Energy Nexus. *AIChE Journal*. **2015**;61(4):1184-1208.

Gao J, You F. Shale gas supply chain design and operations toward better economic and life cycle environmental performance: MINLP model and global optimization algorithm. *ACS Sustainable Chemical Engineering*. **2015**; 3:1282-1291.

Goel V, Grossmann IE. A stochastic programming approach to planning of offshore gas field developments under uncertainty in reserves. *Computers and Chemical Engineering*. **2004**; 28 (8):1409-1429.

Goellner JF. Expanding the shale gas infrastructure. *Chemical Engineering Progress*. **2012**; 108 (8):49-52.

Gregory KB, Vidic RD, Dzombak DA. Water Management Challenges Associated with the Production of Shale Gas by Hydraulic Fracturing. *Elements*. **2011**;7(3):181-186.

Grossmann IE, Lee S. Generalized convex disjunctive programming: nonlinear convex hull relaxation. *Computational Optimization and Applications*. **2003**; 26:466-486.

Grossmann IE, Trespalacios F. Systematic modeling of discrete-continuous optimization models through generalized disjunctive programming. *AIChE Journal*. **2013**; 59 (9):3276-3295.

Guerra OJ, Calderon AJ, Papageorgiou LG, Siirola JJ, Reklaitis GV. An optimization framework for the integration of water management and shale gas supply chain design. *Computers and Chemical Engineering*. **2016**; 92:230-255.

Haldi J, Whitcomb D. Economies of scale in industrial plants. *The Journal of Political Economy*. **1967**; 373-385.

Iyer RR, Grossmann IE, Vasantharajan S, Cullick AS. Optimal planning and scheduling of offshore oil field infrastructure investment and operations. *Industrial & Engineering Chemistry Research*. **1998**; 37 (4):1380-1397.

Jacobs T. Renewing Mature Shale Wells Through Refracturing. *SPE News*. **2014**; May Issue.

Johnson K. Leveraging Big Data – Analytics, Dedicated Centers Enable Real-Time Optimization of Devon Energy's Operations. *The American Oil & Gas Reporter*. **2016**, July Cover Story.

Knudsen BR, Foss B. Designing shale-well proxy models for field development and production optimization problems. *Journal of Natural Gas Science and Engineering*. **2015**;27(2):504-514.

Knudsen BR, Foss B. Shut-in based production optimization of shale-gas systems. *Computers & Chemical Engineering*. **2013**; 58:54-67.

Knudsen BR, Grossmann IE, Foss B, Conn AR. Lagrangian relaxation based decomposition for well scheduling in shale-gas systems. *Computers & Chemical Engineering*. **2014**; 63:234-249.

Knudsen BR, Whitson CH, Foss B. Shale-gas scheduling for natural-gas supply in electric power production. *Energy*. **2014**; 78:165-182.

Kotov S, Freitag HC. Extending Well Life – Production Rejuvenation Poised to Transform Performance of Wells in Unconventional Plays. *The American Oil & Gas Reporter*. **2015**. July 2015 Cover Story.

Krishnaswami P, Chapman KS, Abbaspour M. Compressor station optimization for linepack maintenance. *Proceedings of the 36th PSIG Annual Meeting*. Palm Springs; October **2004**.

Lantz T, Greene D, Eberhard M, Norrid S, Pershall R. Refracture treatments proving successful in horizontal Bakken wells. *SPE Production & Operations*. **2008**; 23 (3):373-378.

Lee J, Wattenberger RA. Gas Reservoir Engineering. *Society of Petroleum Engineers*. **1996**.

Lira-Barragán LF, Ponce-Ortega JM, Guillén-Gosálbez G, El-Halwagi MM. Optimal Water Management under Uncertainty for Shale Gas Production. *Industrial and Engineering Chemistry Research*. **2016**;55:1322-1335.

Lira-Barragán LF, Ponce-Ortega JM, Serna-Gonzalez M, El-Halwagi, MM. Optimal Reuse of Flowback Wastewater in Hydraulic Fracturing Including Seasonal and Environmental Constraints. *AIChE Journal*. **2016**;62(5):1634-1645.

Martin A, Möller M. Moritz S. Mixed integer models for the stationary case of gas network optimization. *Mathematical Programming*. **2006**. 105(2-3):563-582.

Mauter MS, Alvarez PJJ, Burton GA, Cafaro DC, Chen W, Gregory KB, Jian G, Li Q, Pittock J, Reible D. Regional variation in water-related impacts of shale gas development and implications for emerging international plays. *Environmental Science & Technology*. **2014**;48(15):8298-8306.

Mauter MS, Palmer VR, Tang Y, Behrer AP. The Next Frontier in United States Shale Gas and Tight Oil Extraction: Strategic Reduction of Environmental Impacts. *Energy Technology Innovation Policy (ETIP) Research Group: Belfer Center for Science and International Affairs*. **2013**.

Mauter MS, Palmer VR. Expert Elicitation of Trends in Marcellus Oil and Gas Wastewater Management. *Journal of Environmental Engineering*. **2014**;140(5):B4014004.

McCarl BA. Expanded GAMS User Guide Version 23.6. Washington, DC: *GAMS Development Corporation*. **2011**.

Miller KD. Can Refracs Bring New Life to the Haynesville? BTU Analytics. **2015**. https://btuanalytics.com/refracs-bring-new-life/ [last accessed November 2016]

Misra S. Fisher MW, Backhaus S, Bent R, Chertkov M, Pan F. Optimal compression in natural gas networks: a geometric programming approach. *IEEE Transactions on Control of Network Systems*. **2015**;2(1):47-56.

Moore FT. Economies of scale: Some statistical evidence. *The Quarterly Journal of Economics*, **1959**; 232-125.

Pan I. Natural gas processing contracts and how they affect profits and valuation. *Market Realist*. **2013**. Available at: http://marketrealist.com/2013/01/natural-gas-processing-contracts-and-how-they-affect-profits-and-valuation/ [last accessed September 2015].

Park M, Park S, Mele FD, Grossmann IE. Modeling of purchase and sales contracts in supply chain optimization. *Industrial & Engineering Chemistry Research*. **2006**; 45 (14):5013-5026.

Quesada I, Grossmann IE. Global optimization of bilinear process networks with multicomponent flows. *Computers & Chemical Engineering*. **1995**; 19 (12):1219-1242.

Raman R, Grossmann IE. Relation between MILP modeling and logical inference for chemical process synthesis. *Computers and Chemical Engineering*. **1991**;15(2):73-84.

Ríos-Mercado RZ, Borraz-Sánchez C. Optimization Problems in natural gas transportation systems: A state-of-the-art review. *Applied Energy*. **2015**;147:536-555.

Ríos-Mercado RZ, Kim S, Boyd EA. Efficient operation of natural gas transmission systems: A network-based heuristic for cyclic structures. *Computers & Operations Research*. **2006**;3:2323-2351.

Schilling KL. Managing Water Supplies Key to Operation Strategies in Unconventional Plays. *The American Oil & Gas Reporter*. **2016**, August Cover Story.

Selot A, Kuok LK, Robinson M, Barton PI. A short-term operational planning model for natural gas production systems. *AIChE Journal*. **2008**; 54 (2):495-515.

Sharma MM. Improved Reservoir Access Through Refracture Treatments in Tight Gas Sands and Gas Shales. *Research Partnership to Secure Energy for America*. **2013**.

Sider A, Ailworth E. Oil Companies Tap New Technologies to Lower Production Costs. *Wall Street Journal*. **2013**.

Tarhan B, Grossmann IE, Goel V. Computational strategies for non-convex multistage MINLP models with decision-dependent uncertainty and gradual uncertainty resolution. *Annals of Operations Research*. **2013**; 203:141-166.

Tavallali MS, Karimi IA, Teo KM, Baxendale D, Ayatollahi S. Optimal producer well placement and production planning in an oil reservoir. *Computers & Chemical Engineering*. **2013**; 55:109-125.

Tavassoli S, Yu W, Javadpour F, Sepehrnoori K. Well screen and optimal time of refracturing: a Barnett shale well. *Journal of Petroleum Engineering*. **2013**; 2013:1-10.

Tawarmalani M, Sahinidis, NV. A polyhedral branch-and-cut approach to global optimization. *Mathematical Programming*. **2005**;103(2):225-249.

Tobin J, Shambaugh P, Mastrangelo E. Natural Gas Processing: The Crucial Link between Natural Gas Production and Its Transportation to Market. *Energy*

Information Administration, Office of Oil and Gas, **2006**. Available at: http://www.eia.gov/pub/oil_gas/natural_gas/feature_articles/2006/ngprocess/ngprocess.pdf [last accessed September 2015].

Tribe MA, Alpine RLW. Scale economies and the “0.6 rule”. *Engineering Costs and Production Economics*. **1986**; 10 (4):271-278.

U.S. Energy Information Administration (EIA). Annual Energy Outlook 2014 with projections to 2040. *U.S. Department of Energy Information. Office of Integrated and International Energy Analysis*, **2014**. Available at: www.eia.gov/forecasts/aeo/pdf/0383(2014).pdf [last accessed September 2015].

U.S. Energy Information Administration. EIA Estimates of Drilled but Uncompleted Wells (DUCs). *Drilling Productivity Report*. September **2016**.

van den Heever SA, Grossmann IE, Vasantharajan S, Edwards K. A Lagrangean decomposition heuristic for the design and planning of offshore hydrocarbon field infastructures with complex economic objectives. *Industrial & Engineering Chemistry Research*. **2001**; 40 (13):2857-2875.

van den Heever SA, Grossmann IE. An iterative aggregation/disaggregation approach for the solution of a mixed-integer nonlinear oilfield infrastructure planning model. *Industrial & Engineering Chemistry Research*. **2000**; 39 (6):1955-1971.

Vecchietti A, Lee S, Grossmann IE. Modeling of discrete/continuous optimization problems: characterization and formulation of disjunctions and their relaxations. *Computers & Chemical Engineering*. **2003**; 27:433-448.

Viswanathan J, Grossmann IE. A combined penalty function and outer approximation method for MINLP optimization. *Computers & Chemical Engineering*. **1990**; 14:769-782.

Westerlund T, Pettersson F. An extended cutting plane method for solving convex MINLP problems. *Computers & Chemical Engineering*. **1995**. 19:131-136.

Weymouth, TR. Problems in Natural Gas Engineering. Transactions of the American *Society of Mechanical Engineers*. **1912**;34(1349):185-231.

WorldOil - Upstream News. Refracing fever sweeps across shale industry after oil collapse. http://www.worldoil.com/news/2015/7/07/refracing-fever-sweeps-across-shale-industry-after-oil-collapse (July **2015**).

Wu S, Ríos-Mercado RZ, Boyd EA, Scott LR. Model Relaxations for the Fuel Cost Minimization of Steady-State Gas Pipeline Networks. *Mathematical and Computer Modeling*. **2000**;31:197-220.

Yang L, Grossmann IE, Manno J. Optimization models for shale gas water management. *AIChE Journal*. **2014**; 60 (10):3490-3501.

Yang L, Grossmann IE, Mauter MS, Dilmore RM. Investment Optimization Model for Freshwater Acquisition and Wastewater Handling in Shale Gas Production. *AIChE Journal*. **2015**;61(6):1770-1782.

Zamarripa M, Marchetti PA, Grossmann IE, Singh T. Lotero I, Gopalakrishnan A, Besancon B, Ande, J. Rolling Horizon Approach for Production-Distribution Coordination of Industrial Gases Supply Chains. *Industrial & Engineering Chemistry Research*. **2016**; 55:2646-2660.

Zavala VM. Stochastic optimal control model for natural gas networks. *Computers & Chemical Engineering*. **2014**. 64:103-13.

APPENDICES

Appendix A: Pipeline Sizing Guidelines for Strategic Development Planning

As outlined in section 2.5.1 Model Formulation: Single Delivery Node Problem we size gathering lines based on fluid velocity. As a rule of thumb operators strive to ensure that the fluid velocity in gas lines does not exceed 20 m/s to minimize noise emissions and allow for corrosion inhibition. We rely on this design specification for preliminary pipeline sizing purposes. The necessary pipeline diameter $\delta_{j,q}$ is calculated using Eq. (A.1).

$$\delta_{j,q}^2 \quad \geq \quad \underbrace{\frac{60 \cdot T \cdot z}{v_g \cdot p_l}}_{= \ k^P} \quad \cdot \quad F_{j,q,t}^{JQ} \qquad \forall (j,q) \in \mathcal{JQA}, t \in \mathcal{T} \qquad \text{(A.1)}$$

In Eq. (A.1), T is the gas temperature in K, z is the gas compressibility factor ($z = 1$ due to the ideal gas assumption), v_g is the maximum gas velocity set to 20 m/s, and p_l is the line pressure MPa. For simplicity, we define the pipeline coefficient k^P as seen in Eq. (A.1) and use it for pipeline sizing purposes. For a given gas flow $F_{j,q,t}^{JQ}$ in 10^6 m^3/day and an unknown pipeline diameter $\delta_{j,q}$ in inches the pipeline coefficient is $k^P = 0.0026716$.

We note that once the gathering system has been sized using the proposed approach we generally advise to use standard gas flow equations such as the Weymouth or Panhandle equations to calculate the explicit pressure drops along individual pipeline segments. When evaluating pressure drops rigorously along pipelines installed in parallel, we advise to perform these calculations separately for each line, considering the individual flowrate through each line at every point in time. If these calculations reveal pressure drops beyond tolerable specifications, a larger diameter pipeline may be selected. In our experience, however, the sizing procedure based on gas velocity provides a sufficiently good estimate of the required pipeline size and, generally, the calculated pressure drops are reasonably small due to the relatively low line pressure and short lengths of the pipeline segments.

Appendix B: Compact Hull-Reformulation (Introduction)

Disjunctions are usually reformulated using either a Big-M (BM) or a Hull Reformulation (HR) formulation. Given disjunction (2.12) its HR is as follows.

$$F_{j,q,t}^{JQ} = \sum_{d \in D_0} F_{d,j,q,t}^{DJQ} \qquad \forall (j,q) \in \mathcal{JQA}, t \in \mathcal{T} \tag{A.2}$$

$$k^P \cdot F_{d,j,q,t}^{DJQ} = \left(\left(\delta_{j,q}^0 \right)^2 + \delta_d^2 \right) \cdot z_{d,j,q,t}^{PIPE} \qquad \forall d \in \mathcal{D}_0, (j,q) \in \mathcal{JQA}, t \in \mathcal{T} \tag{A.3}$$

$$F_{j,q,t}^{JQ,LOW} \cdot z_{d,j,q,t}^{PIPE} \le F_{d,j,q,t}^{DJQ} \le F_{j,q,t}^{JQ,UP} \cdot z_{d,j,q,t}^{PIPE} \qquad \forall d \in \mathcal{D}_0, (j,q) \in \mathcal{JQA}, t \in \mathcal{T} \tag{A.4}$$

$$\sum_{d \in \mathcal{D}_0} z_{d,j,q,t}^{PIPE} = 1 \qquad \forall (j,q) \in \mathcal{JQA}, t \in \mathcal{T} \tag{A.5}$$

Compared to its alternative – the Big-M formulation – the HR requires the introduction of the disaggregated variables $F_{d,j,q,t}^{DJQ}$, the corresponding constraints as seen in Eq. (A.2), as well as two constraints for each disaggregated variable (to impose lower and upper bounds on these variables) as captured by Eq. (A.4). Therefore, the HR generally requires more variables and constraints than the BM. This increase in model size oftentimes adds to the computational effort of solving the respective problems. At the same time Grossmann and Lee (2003) show that the continuous relaxation of the HR formulation is as least as tight as and generally tighter than the BM when the discrete domain is relaxed.

In the particular case of disjunction (2.12), however, it is possible to derive a *compact* HR: if, for a given $(j,q) \in \mathcal{JQA}$ and $t \in \mathcal{T}$, we sum up the inequality constraint (A.3) over all $d \in \mathcal{D}_0$ then we get:

$$\sum_{d \in \mathcal{D}_0} k^P \cdot F_{d,j,q,t}^{DJQ} = \sum_{d \in \mathcal{D}_0} \left(\left(\delta_{j,q}^0 \right)^2 + \delta_d^2 \right) \cdot z_{d,j,q,t}^{PIPE} \qquad \forall (j,q) \in \mathcal{JQA}, t \in \mathcal{T} \quad \text{(A.6)}$$

Next, we can replace the summation of the disaggregated variables $F_{d,j,q,t}^{DJQ}$ on the left-hand side of Eq. (A.6) with their initial definition in Eq. (A.2) as shown below.

$$k^P \cdot F_{j,q,t}^{JQ} = \left(\delta_{j,q}^0 \right)^2 + \sum_{d \in \mathcal{D}_0} \delta_d^2 \cdot z_{d,j,q,t}^{PIPE} \qquad \forall (j,q) \in \mathcal{JQA}, t \in \mathcal{T} \quad \text{(A.7)}$$

Since Eq. (A.7) no longer involves any disaggregated variables, we can now drop Eqs. (A.2) and (A.4) from the reformulation of the disjunction and merely impose regular bounds on the flow variables. Hence, the compact HR is as follows.

$$k^P \cdot F_{j,q,t}^{JQ} \le \left(\delta_{j,q}^0 \right)^2 + \sum_{d \in \mathcal{D}_0} \delta_d^2 \cdot z_{d,j,q,t}^{PIPE} \qquad \forall (j,q) \in \mathcal{JQA}, t \in \mathcal{T} \quad \text{(A.8)}$$

$$\sum_{d \in \mathcal{D}_0} z_{d,j,q,t}^{PIPE} = 1 \qquad \forall (j,q) \in \mathcal{JQA}, t \in \mathcal{T} \quad \text{(A.9)}$$

As highlighted by Castro and Grossmann (2012), the noteworthy property of the compact HR is that it combines the advantages of the HR and the BM without introducing their respective shortcomings.

Appendix C: Compressor Sizing Guidelines for Strategic Development Planning

The size of a compressor is determined in terms of its maximum power requirement. For this purpose we assume adiabatic compression and a fixed compression ratio, i.e., suction and discharge pressure specifications Pd_q and Ps_j are fixed. Given these assumptions the power requirement $\Lambda^C_{j,q}$ is linearly proportional to the gas flow $F^{JQ}_{j,q,t}$ as seen below.

$$\Lambda^C_{j,q} \geq \underbrace{\left[\frac{(4.0426 \cdot T \cdot \gamma)}{(\gamma - 1) \cdot \eta}\right] \cdot \left[\left(\frac{Pd_q}{Ps_j}\right)^{\frac{z \cdot (\gamma - 1)}{\gamma}}\right]}_{= \ k^C} \cdot F^{JQ}_{j,q,t} \qquad \forall (j,q) \in \mathcal{DSR}, t \in \mathcal{T}$$

(A.10)

In Eq. (A.10) above T is the gas temperature at suction conditions in K (typically $T = 298.15K$), γ represents the heat capacity ratio (typically $\gamma = 1.26$), η stands for the compressor efficiency (we assume $\eta = 0.9$), and finally z is the gas compressibility factor which we set to $z = 1$ due to the ideal gas assumption. For simplicity, we define the compression coefficient k^C as seen in Eq. (A.10) and use it for compressor sizing purposes. For a given gas flow $F^{JQ}_{j,q,t}$ in 10^6 m^3/day and unknown compression power $\Lambda^C_{j,q}$ in kW the compression coefficient is $k^C = 0.0023813$.

Appendix D: Compressor Sizing Reformulation

The previously introduced binary variables $y^{COMPR}_{c,j,q,t}$ and $z^{COMPR}_{c,j,q,t}$ correspond directly to their counterpart Boolean variables $Y^{COMPR}_{c,j,q,t}$ and $Z^{COMPR}_{c,j,q,t}$. Here, too, the introduction of disaggregated variables and the corresponding constraints can be avoided as shown in Appendix B: Compact Hull Reformulation. Thus Eq. (A.11) represents the *compact* Hull Reformulation of disjunction (2.19). Since disjunction (2.19) is exclusive, we add Eq. (A.12) and transform the logic constraint into the mixed-integer linear constraint (A.13) using propositional logic.

$$k^C \cdot F_{j,q,t}^{JQ} \leq \lambda_{j,q}^0 + \sum_{c \in \mathcal{C}_0} \lambda_c \cdot z_{c,j,q,t}^{COMPR} \qquad \forall (j,q) \in \mathcal{DSR}, t \in \mathcal{T} \quad \text{(A.11)}$$

$$\sum_{c \in C_0} z_{c,j,q,t}^{COMPR} = 1 \qquad \forall (j,q) \in DSR, t \in T \quad \text{(A.12)}$$

$$\sum_{\tau=1}^{t-\tau_c} y_{c,j,q,\tau}^{COMPR} = z_{c,j,q,t}^{COMPR} \qquad \forall c \in C, (j,q) \in DSR, t \in T \quad \text{(A.13)}$$

Appendix E: Delivery Agreements for Strategic Development Planning

Fee-based processing agreements (index $da = FB$) are the most common arrangements between upstream operators and midstream processors. Under these, operators pay a *service fee* α_{FB}^A to the processor based on how much gas is processed in terms of throughput volumes. Eq. (A.14) captures the processing expenses $PRE_{j,q,t}$ under such a fee-based agreement. In return, the processor receives all pipeline-quality gas and any natural gas liquids extracted from the raw gas stream to the operator who markets these. Eq. (A.15) shows the operator's revenue function.

$$\alpha_{FB}^A \cdot \left(F_{j,q,t}^{JQ} + F_{j,q,t}^S \right) - PRE_{j,q,t} \leq m_{\mathrm{FB},j,q}^{PRE} \cdot \left(1 - y_{FB,j,q}^{AGR} \right) \quad \forall (j,q) \in \mathcal{JQA}, t \in \mathcal{T} \quad \text{(A.14)}$$

$$REV_{j,q,t} - \sum_{k \in \mathcal{K}} F_{k,j,q,t}^{KJQ} \cdot p_{q,k,t} \leq m_{\mathrm{FB},j,q}^{REV} \cdot \left(1 - y_{FB,j,q}^{AGR} \right) \qquad \forall (j,q) \in \mathcal{JQA}, t \in \mathcal{T} \quad \text{(A.15)}$$

Under fee-based processing contracts the processor's revenues are primarily related to the quantity and not the quality of the gas that is delivered. To the operators, on the other hand, who market the gas and liquids exclusively, these arrangements are highly quality-sensitive; when NGL prices are high, processing can increase the operator's overall revenues, whereas low NGL prices favor other alternative agreements or blending strategies to reduce or avoid the need for processing.

Under *percent-of-proceeds* contracts (index $da = PP$) processors will generally only charge a small servicing fee α_{PP}^{A} for their processing service depending on how much gas is received. These processing expenses are captured by Eq. (A.16). In addition, however, the processors are entitled to receive an agreed upon percentage γ_{PP} of the proceeds from all natural gas and NGLs sales[19]. Hence, upstream operators and midstream processors split the overall revenues. Therefore, the operator's revenues are given by Eq. (A.17). Under percent-of-proceeds arrangements both parties, the operators and the processor, share commodity risks.

$$\alpha_{PP}^{A} \cdot \left(F_{j,q,t}^{JQ} + F_{j,q,t}^{S}\right) - PRE_{j,q,t} \leq m_{\mathrm{PP},j,q}^{PRE} \cdot \left(1 - y_{PP,j,q}^{AGR}\right) \quad \forall (j,q) \in \mathcal{JQA}, t \in \mathcal{T} \tag{A.16}$$

$$REV_{j,q,t} - \left(1 - \gamma_{PP}\right) \cdot \sum_{k \in \mathcal{K}} F_{k,j,q,t}^{KJQ} \cdot p_{q,k,t} \leq m_{\mathrm{PP},j,q}^{REV} \cdot \left(1 - y_{PP,j,q}^{AGR}\right) \quad \forall (j,q) \in \mathcal{JQA}, t \in \mathcal{T} \tag{A.17}$$

Under *keep-whole* arrangements (index $da = KW$) the midstream processor is compensated for the processing service by retaining title to any NGLs recovered from the raw gas stream. In return, the upstream operator receives an identical amount of pipeline-quality gas that equals the heating value of the original raw gas stream. Thus, the operator is "kept whole" on a heating value basis. Since the processors market the

NGLs exclusively under keep-whole agreements, they are directly exposed to NGL price fluctuations, which presents a severe strategic risk. However, when NGL prices are high, midstream processors can generate substantial revenues from these contracts. The corresponding constraints are as follows:

$$\alpha_{KW}^{A} \cdot \left(F_{j,q,t}^{JQ} + F_{j,q,t}^{S}\right) - PRE_{j,q,t} \leq m_{\mathrm{KW},j,q}^{PRE} \cdot \left(1 - y_{KW,j,q}^{AGR}\right) \quad \forall (j,q) \in \mathcal{JQA}, t \in \mathcal{T} \quad \text{(A.18)}$$

$$REV_{j,q,t} - \sum_{k \in \mathcal{K}} F_{k,j,q,t}^{KJQ} \frac{H_k}{H_{CH4}} \cdot p_{q,CH4,t} \leq m_{\mathrm{KW},j,q}^{REV} \cdot \left(1 - y_{KW,j,q}^{AGR}\right) \forall (j,q) \in \mathcal{JQA}, t \in \mathcal{T} \quad \text{(A.19)}$$

Direct deliveries contracts (index $da = DD$) generally do not imply significant processing expenses, and hence, the processing cost coefficient α_{DD}^{A} in Eq. (A.20) is usually set to zero. In rare cases, though, transmission companies may impose a minimum fee for dehydrating the received gas. Either way, the operator gets to market all gas and natural gas liquids sales individually as depicted in Eq. (A.21).

$$\alpha_{DD}^{A} \cdot \left(F_{j,q,t}^{JQ} + F_{j,q,t}^{S}\right) - PRE_{j,q,t} \leq m_{\mathrm{DD},j,q}^{PRE} \cdot \left(1 - y_{DD,j,q}^{AGR}\right) \quad \forall (j,q) \in \mathcal{JQA}, t \in \mathcal{T} \quad \text{(A.20)}$$

$$REV_{j,q,t} - \sum_{k \in \mathcal{K}} F_{k,j,q,t}^{KJQ} \cdot p_{q,CH4,t} \leq m_{\mathrm{DD},j,q}^{REV} \cdot \left(1 - y_{DD,j,q}^{AGR}\right) \quad \forall (j,q) \in \mathcal{JQA}, t \in \mathcal{T} \quad \text{(A.21)}$$

Appendix F: Reformulation Multiple Delivery Nodes Disjunction

Disjunction (2.72) is reformulated using big-M constraints. Eqs. (A.22)-(A.23) show the reformulation of those constraints that determine which processing expenses are incurred and how revenues are generated.

$$\alpha_{FB}^{A} \cdot \left(F_{j,q,t}^{JQ} + F_{j,q,t}^{S}\right) - PRE_{j,q,t} \leq m_{\mathrm{FB},j,q}^{PRE} \cdot \left(1 - y_{FB,j,q}^{AGR}\right) \quad \forall (j,q) \in \mathcal{JQA}, t \in \mathcal{T} \quad \text{(A.22)}$$

$$REV_{j,q,t} - \sum_{k \in \mathcal{K}} F_{k,j,q,t}^{KJQ} \cdot p_{q,k,t} \leq m_{\mathrm{FB},j,q}^{REV} \cdot \left(1 - y_{FB,j,q}^{AGR}\right) \quad \forall (j,q) \in \mathcal{JQA}, t \in \mathcal{T} \quad \text{(A.23)}$$

Eqs. (A.24)-(A.25) address minimum delivery requirements and maximum delivery capacities.

$$F_{j,q,t}^{JQ} - \sigma_{dc,da,j,q} \le m_{dc,da,j,q}^{\sigma} \cdot \left(1 - z_{dc,da,j,q,t}^{CPTY}\right) \quad \forall dc \in \mathcal{DC}, da \in \mathcal{DA}, (j,q) \in \mathcal{JQA}, t \in \mathcal{T} \tag{A.24}$$

$$\varphi_{dc,da,j,q} - \left(F_{j,q,t}^{JQ} + F_{j,q,t}^{S}\right) \le m_{dc,da,j,q}^{\varphi} \cdot \left(1 - z_{dc,da,j,q,t}^{CPTY}\right) \quad \forall dc \in \mathcal{DC}, da \in \mathcal{DA}, (j,q) \in \mathcal{JQA}, t \in \mathcal{T} \tag{A.25}$$

Gas quality specifications that may be imposed along with particular delivery agreements are governed by Eqs. (A.26)-(A.27).

$$F_{j,q,t}^{JQ} \cdot h_{dc,da,\mathrm{j,q}}^{\min} - \sum_{k \in \mathcal{K}} F_{k,j,q,t}^{KJQ} \cdot h_k \le m_{dc,da,j,q}^{h^{min}} \cdot \left(1 - z_{dc,da,j,q,t}^{CPTY}\right) \quad \forall dc \in \mathcal{DC}, da \in \mathcal{DA}, (j,q) \in \mathcal{JQA}, t \in \mathcal{T} \tag{A.26}$$

$$\sum_{k \in \mathcal{K}} F_{k,j,q,t}^{KJQ} \cdot h_k - F_{j,q,t}^{JQ} \cdot h_{dc,da,\mathrm{j,q}}^{\max} \le m_{dc,da,j,q}^{h^{max}} \cdot \left(1 - z_{dc,da,j,q,t}^{CPTY}\right) \quad \forall dc \in \mathcal{DC}, da \in \mathcal{DA}, (j,q) \in \mathcal{JQA}, t \in \mathcal{T} \tag{A.27}$$

Since disjunction (2.72) is exclusive, we add Eq. (A.28) and transform the logic constraints (2.73)-(2.78) into the mixed-integer linear constraints (A.29)-(A.34) using propositional logic.

$$\sum_{da \in \mathcal{DA}} y_{da,j,q}^{AGR} = 1 \qquad \forall (j,q) \in \mathcal{JQA} \tag{A.28}$$

$$\sum_{pa \in \mathcal{PA}} y_{pa,j,q}^{AGR} = 1 \qquad \forall (j,q) \in \mathcal{PSR} \tag{A.29}$$

$$\sum_{ta \in \mathcal{TA}} y_{ta,j,q}^{AGR} = 1 \qquad \forall (j,q) \in \mathcal{DSR} \tag{A.30}$$

$$y_{da,j,q}^{AGR} = \sum_{dc \in \mathcal{DC}} z_{dc,da,j,q,t}^{CPTY} \qquad \forall da \in \mathcal{DA}, (j,q) \in \mathcal{JQA}, t \in \mathcal{T} \tag{A.31}$$

$$y_{pa,j,q}^{AGR} = \sum_{pc \in \mathcal{PC}} z_{pc,pa,j,q,t}^{CPTY} \qquad \forall pa \in \mathcal{PA}, (j,q) \in \mathcal{PSR}, t \in \mathcal{T} \tag{A.32}$$

$$y_{ta,j,q}^{AGR} = \sum_{tc \in \mathcal{TC}} z_{tc,ta,j,q,t}^{CPTY} \qquad \forall ta \in \mathcal{TA}, (j,q) \in \mathcal{DSR}, t \in \mathcal{T} \qquad \text{(A.33)}$$

$$\sum_{\tau = t - \tau_{da,da}^{A}}^{t} y_{dc,da,j,q,\tau}^{CPTY} = z_{dc,da,j,q,t}^{CPTY} \qquad \forall dc \in \mathcal{DC}, da \in \mathcal{DA}, (j,q) \in \mathcal{JQA}, t \in \mathcal{T} \qquad \text{(A.34)}$$

Appendix G: Compact Hull-Reformulation (Tradeoffs)

In this section we study the Compact Hull Reformulation (CHR) in more detail, in an attempt to clarify: (a) when a CHR may generally be applied, and (b) what advantages and disadvantages it entails compared to alternative reformulations.

First, we assume that a given optimization problem involves a set of disjunctions $k \in K$ as shown in Eq. (A.35). Each of these disjunctions includes $j \in J_k$ disjunctive terms, all of which are linked by the logic OR-operator ($\vee$). Each disjunctive term is associated with a Boolean variable $Y_{jk} \in \{True, False\}$, which controls which disjunctive term is active, i.e., which constraints $A_{jk}x \le b_{jk}$ are enforced. We note that Eq. (A.35) is restricted to the linear case, i.e., all constraints $A_{jk}x \le b_{jk}$ involved in the disjunction are linear. Lastly, Eq. (A.36) ensures that no more than one disjunctive term $j \in J_k$ may be active for every disjunction $k \in K$.

$$\bigvee_{j \in J_k} \begin{bmatrix} Y_{jk} \\ A_{jk}x \le b_{jk} \end{bmatrix} \qquad \forall k \in K \qquad \text{(A.35)}$$

$$\underline{\bigvee}_{j \in J_k} \quad Y_{jk} \qquad \forall k \in K \qquad \text{(A.36)}$$

The set of disjunctions in Eq. (A.35) may generally be transformed into mixed-integer constraints using a Big-M reformulation (BM), as shown in Eqs. (A.37)-(A.38), by introducing large parameters M_{jk}.

$$A_{jk}x \le b_{jk} + M_{jk}\left(1 - y_{jk}\right) \qquad \forall k \in K, j \in J_k \tag{A.37}$$

$$\sum_{j \in J_k} y_{jk} = 1 \qquad \forall k \in K \tag{A.38}$$

Alternatively, the set of disjunctions in Eq. (A.35) can be transformed using a Hull-Reformulation (HR), as displayed in Eqs. (A.39)-(A.41), by introducing a set of disaggregated variables ν_{jk} for every disjunctive term.

$$x = \sum_{j \in J_k} v_{jk} \qquad \forall k \in K \tag{A.39}$$

$$A_{jk}v_{jk} \le b_{jk}y_{jk} \qquad \forall k \in K, j \in J_k \tag{A.40}$$

$$\sum_{j \in J_k} y_{jk} = 1 \qquad \forall k \in K \tag{A.41}$$

In general terms, the HR involves more variables and constraints than the BM, but its continuous relaxation is as least as tight as and generally tighter than the BM – as shown by Vecchietti, Lee and Grossmann (2003). For more details regarding Generalized Disjunctive Programming and a comparison of reformulations, we refer to the work by Grossmann and Trespalacios (2013).

Given the set of disjunctions in Eq. (A.35) we argue that a Compact Hull-Reformulation (CHR) can only be applied if the coefficient matrix A_{jk} involved in the linear constraints $A_{jk}x \le b_{jk}$ is independent of the set of disjunctive terms $j \in J_k$, i.e., in this particular case $A_{jk} = A_k$. The CHR of the set of disjunctions in Eq. (A.35) is given by Eqs. (A.42)-(A.43).

$$A_k x \le \sum_{j \in J_k} b_{jk}y_{jk} \qquad \forall k \in K \tag{A.42}$$

$$\sum_{j \in J_k} y_{jk} = 1 \qquad \forall k \in K \tag{A.43}$$

A noteworthy property of the CHR is that – compared to the standard Hull-Reformulation – it involves $|J_k| \times |K|$ fewer variables and $|J_k| \times |K|$ less constraints. However, it is important to note that the CHR is a "surrogate formulation", since the right-hand side of Eq. (A.42) is made up of aggregated constraints. Hence, it can be proven that the continuous relaxation of the standard HR is generally tighter than the continuous relaxation of the CHR. Yet, the significant reduction of the model size achieved by the CHR – both in terms of decision variables and model constraints – generally aids the performance of mixed-integer programming solvers such as CPLEX or Gurobi. Moreover, in direct comparison with the BM reformulation, we highlight the fact that the CHR does not require the specification of any big-M parameters.